Feasibility Study for an Aquatic Ecosystem Earth Observing System

Feasibility Study for an Aquatic Ecosystem Earth Observing System

Version 2.0
March 2018

Version 2.0   March 2018

CEOS

Feasibility Study for an Aquatic Ecosystem Earth Observing System

Committee on Earth Observation Satellites (CEOS)

Compiled & edited by: Arnold G. Dekker (CSIRO) and Nicole Pinnel (DLR)

Contributing Authors

Arnold G. Dekker
Commonwealth Scientific and Industrial Research Organisation (CSIRO, Australia)

Nicole Pinnel
German Aerospace Center (DLR, Germany)

Peter Gege
German Aerospace Center (DLR, Germany)

Xavier Briottet
French aeronautics, space and defense research lab (ONERA, France)

Andy Court
Netherlands Organisation for Applied Scientific Research (TNO, The Netherlands)

Steef Peters
Water Insight (The Netherlands)

Kevin R. Turpie
National Aeronautics and Space Administration (NASA, USA)

Sindy Sterckx
Flemish Institute for Technological Research (VITO, Belgium)

Maycira Costa
University of Victoria (UVIC, Canada)

Claudia Giardino
Italian research Council (CNR, Italy)

Vittorio E. Brando
Italian Research Council (CNR-ISAC, Italy)

Federica Braga
Italian Research Council (CNR, Italy)

Martin Bergeron
(CSA, Canada)

Thomas Heege
Eomap (Germany)

Bringfried Pflug
German Aerospace Center (DLR, Germany)

CONTENTS 1

Abstract

Many Earth observing sensors have been designed, built and launched with primary objectives of either terrestrial or ocean remote sensing applications. Often the data from these sensors are also used for freshwater, estuarine and coastal water quality observations, bathymetry and benthic mapping. However, such land and ocean specific sensors are not designed for these complex aquatic environments and consequently are not likely to perform as well as a dedicated sensor would. As a CEOS action, CSIRO and DLR have taken the lead on a feasibility assessment to determine the benefits and technological difficulties of designing an Earth observing satellite mission focused on the biogeochemistry of inland, estuarine, deltaic and near coastal waters as well as mapping macrophytes, macro-algae, sea grasses and coral reefs. These environments need higher spatial resolution than current and planned ocean colour sensors and need higher spectral resolution than current and planned land Earth observing sensors offer (with the exception of several R&D type imaging spectrometry satellite missions). The results indicate that a dedicated sensor of (non-oceanic) aquatic ecosystems could be a multispectral sensor with ~26 bands in the 380-780 nm wavelength range for retrieving the aquatic ecosystem variables as well as another 15 spectral bands between 360-380 nm and 780-1400 nm for removing atmospheric and air-water interface effects. These requirements are very close to defining an imaging spectrometer with spectral bands between 360 and 1000 nm (suitable for Si based detectors), possibly augmented by a SWIR imaging spectrometer. In that case the spectral bands would ideally have 5 nm spacing and Full Width Half Maximum (FWHM), although it may be necessary to go to 8 nm wide spectral bands (between 380 to 780nm where the fine spectral features occur -mainly due to photosynthetic or accessory pigments) to obtain enough signal to noise. The spatial resolution of such a global mapping mission would be between ~17 and ~33 m enabling imaging of the vast majority of water bodies (lakes, reservoirs, lagoons, estuaries etc.) larger than 0.2 ha and ~25 % of river reaches globally (at ~17 m resolution) whilst maintaining sufficient radiometric resolution.

Keywords: (Earth observation, aquatic ecosystems, multispectral remote sensing, imaging spectrometry, optical sensor specifications, environmental applications)

Executive summary

Initially this work had a more limited scope to focus on inland waters only. It started as a Committee on Earth Observation Satellites (CEOS) response to the Group on Earth Observations System of Systems (GEOSS) Water Strategy developed under the auspices of the Water Strategy Implementation Study Team that was endorsed by CEOS at the CEOS 2015 Plenary. As one of the actions, CSIRO took the lead on recommendation C.10: A feasibility assessment to determine the benefits and technological difficulties of designing a hyperspectral satellite mission focused on water quality measurements. This inland water focus was considered as being of too limited scope as there has never been a dedicated published study to assess the requirements for an aquatic ecosystem imaging spectrometer or multispectral sensor (excluding ocean requirements).

We performed a feasibility assessment of the benefits and technological challenges of designing a passive multispectral or hyperspectral satellite sensor system focused on biogeochemistry of inland, estuarine, deltaic and near coastal waters - as well as mapping macrophytes, macro-algae, seagrasses, coral reefs and shallow water bathymetry. Compared to any existing sensors, this sensor shall need to have a significantly higher spatial resolution than 250 m, which is the maximum spatial resolution of dedicated current aquatic sensors such as Sentinel-3 as well as future planned aquatic sensors such as the Coastal Ocean Color Imager (COCI) at 100 m spatial resolution. Further, the GEOSS Aquawatch suggested that alternative approaches, involving augmenting designs of near future planned spaceborne sensors for terrestrial and ocean colour applications to allow improved inland, near coastal waters and benthic applications, could offer an alternative pathway. Accordingly, this study also analyses the benefits of this option as part of this feasibility study.

The approach was to follow a science and applications traceability approach of required aquatic ecosystem variables to be measured, the level of accuracy required, the level of temporal, spatial, spectral and radiometric resolution required. Although we were aware of current bounds of what was technically feasible, we did believe that the requirements should lead this study and therefore may not (yet) be technically feasible.

Because there are global pressures (e.g., growing human exploitation of coastal and inland resources and changing climate), we need to study effects on global scales. A global observation system is thus an appropriate and invaluable tool to assess the impact at all spatial and temporal scales. In many countries, field-based monitoring efforts are currently insufficient or even absent to provide national-scale assessments of aquatic ecosystems. In improving the design of such assessments using Earth observation, key considerations include:

1) Temporal sampling to i) represent the dynamics of water quality, benthic, coral reef and water depth change and the range of conditions that can occur over diurnal, seasonal, and annual cycles (e.g., droughts and flooding), ii) develop time series for understanding phenology and trend analysis, including the effects of climate change, iii) retrospective processing of satellite archives of relevant data, which date back to the early 1980's, may also reveal temporal changes, trends, and anomalies across inland water and near-coastal waters to coral reef systems.
2) Spatial sampling that is representative of the processes and dynamics in these non-oceanic aquatic ecosystems to provide understanding of system processes, such as for water bodies:

heterogeneity, environmental flows, interrelationships between water bodies, and catchment runoff effects, global climate change effects including acidification; and for benthic ecosystems the effects of these flows as well as predation, smothering, trophic state and global warming effects such as water temperature changes, increasing acidification, and coral bleaching. End-user requirements should determine the optimal spatial and temporal sampling scheme, but logistical, operational, and financial constraints usually prevent the optimal sampling scheme from being realised *in situ*. Extensive distances and remoteness, for instance, may make capturing the spatial distribution of measurements using field-based methods infeasible. Earth observation (EO)-derived aquatic ecosystem information, albeit on a more limited set of parameters, may be used to overcome the challenges in sampling schemes based solely on field-based approaches.

3) Capability building should focus on the integration of EO data and field-based observations, integration of observations with modelling (biogeochemical and hydrodynamic) and the development of early-warning tools such as for algal blooms and coral bleaching.

We analysed past existing and upcoming satellite sensor systems of relevance for aquatic ecosystem assessment. While policy, legislative, environmental, and climate change drivers should steer the development of a global, operational system for aquatic ecosystem monitoring, the ideal satellite sensor system does not yet exist. Different satellite systems show different trade-offs between the temporal frequency (once a day to once a year), spatial resolution (1.0 m to 1.2 km pixels), spectral resolution and range (and the related issue of more aquatic ecosystem variables at higher confidence level), radiometric resolution (how accurate and how many levels of reflectance are measureable as well as the dynamic range measureable), and the costs of unprocessed satellite data acquisition (ranging from publicly available to commercially available very high spatial resolution data at ~30 USD per km^2 for the most expensive type of single scene acquisition). These trade-offs also influence the usefulness for aquatic ecosystem assessment.

Spatial resolution (the size of the area being measured on the ground) has consequences for imaging (i) small water bodies such as small- or medium-width river systems or small lakes. In such situations, high spatial-resolution imagery (with pixel sizes of 1 to 10 m) may be the only option, possibly leading to significant data-acquisition and processing costs. A similar argument exists for mapping habitats in coastal and ocean waters formed by foundational species, including submerged plants such as macrophytes (in inland waters) and seagrasses; kelp; corals; sponges; and benthic micro-algae, and environments such as rock reefs and various bottom substrates. However, for a global mapping mission, spatial resolution between 10 and 30 m may be suitable and effective.

Spectral resolution and range (the number, width, and location of spectral bands) determines the amount and accuracy of aquatic ecosystem variables that are discernible from a water body. Sensors with few broad VIS-NIR bands (usually a blue, a green, a red and a nearby infrared spectral band) may only be used to detect those variables that have a broad spectral response: TSM, K_d, Secchi disk transparency, turbidity, and CDOM as water column variables and presence –absence of underwater flora and fauna (e.g. corals). Algal pigments such as chlorophyll-a and cyanobacterial pigments such as cyanophycoerythrin and cyanophycocyanin may also be detected if the broad spectral bands happen to be located appropriately. However, at low concentrations, accuracy will be low, as broad spectral bands cannot discriminate narrow pigment spectral absorption features from other

absorbing and backscattering materials in the water column or benthos. As the number of narrower and more suitably positioned spectral bands increases (e.g., for the coarse spatial resolution ocean colour sensors MODIS, MERIS, OLCI, and OCM-2), chlorophyll-a becomes a more accurately measureable variable, and other cyanobacterial pigments may become detectable.

Radiometric resolution determines the lowest interval of radiance or reflectance that the sensor can reliably detect and discriminate per spectral band. As the spectral and spatial resolution increase, the useful signal relative to noise in the data decreases (as less photons are captured). This trade-off in spectral, spatial, and radiometric resolution is countered by improvements in instrument design and technology, for example, detectors (e.g. CMOS) which have much better performance than older sensors. An added complexity is that the water leaving signal at the satellite sensor (typically at an altitude between 450 and 800 km for polar orbiting Low Earth Orbit (LEO)) is a small part of the total measured signal, composed of the water leaving signal plus the reflections at the air-water interface plus the signal from reflected sun and skylight in the atmosphere, hence radiometric resolution should be sufficient to detect relevant levels of aquatic ecosystem variables through a set of atmospheric and air water interface conditions and solar angles. In addition, temporal radiometric stability is a key requirement to ensure generations of consistent water quality products like TSM, chlorophyll, cyanobacterial pigments, K_d, Secchi disk transparency, turbidity, and CDOM as well as consistency in water depth and benthic mapping.

We considered three approaches to determine the specifications for an aquatic ecosystem Earth observing sensor: i) a literature study with a focus on quantitative research including end user requirements as well as the sensor specifications required to be able to detect and assess aquatic ecosystem variables, ii) a simulation of bottom of atmosphere (or water leaving) radiance and reflectance for inland, coastal and coral reef waters with different depths, coupled with spectral libraries of substratum types such as sands, seagrasses, macro-algae and corals using the WASI-2D software package augmented by non-algal particulate matter absorption and phytoplankton backscattering inputs, and iii) the identification of the requirements of various types of algorithms for retrieving these variables. Often in literature one of these aspects is considered but seldom has a study considered all three aspects simultaneously.

An important distinction to be made is between those water bodies where the incoming sun- and skylight does not reach the bottom at all or where the bottom reflectance does not leave the water; these are the optically deep waters. Optically shallow waters are those waters where there is a measurable amount of reflected light from the bottom passing through the water column and reaching the Earth observing sensor.

As a result of the above mentioned three approaches, we identified that the following requirements should determine a comprehensive aquatic ecosystem Earth observing capability: i) ability to estimate algal pigment concentrations of chlorophyll-a, accessory pigments, cyanobacteria pigments (cyano-phycoerythrin and cyano-phycocyanin especially) as well as other wavelengths relevant for phytoplankton functional types research, ii) algal fluorescence (especially chlorophyll-a fluorescence at 684 nm), iii) ability to measure suspended matter, possibly split up into organic and mineral matter, iv) ability to measure coloured dissolved organic matter and discriminate terrestrial from marine CDOM, v) spectral light absorption and backscattering of the optically active components, vi) measures of transparency of water such as Secchi disk transparency, vertical attenuation of light and

turbidity. For optically shallow waters also: vii) estimates of the water column depth (bathymetry) and viii) estimates of substratum type and cover (e.g. muds, sands, coral rubble, seagrasses, macro-algae, corals, etc.) as well as plants floating at or just above the water surface. For residual sun glint correction (if sun glint mitigation measures are insufficient) and for estimating the atmospheric composition it is also required to have spectral bands to measure O_3, NO_2, water vapour and aerosols as well as have some bands in the nearby infrared and/or SWIR for sun glint correction.

The results indicate that a dedicated sensor of (non-oceanic) aquatic ecosystems could be a multispectral sensor with ~26 bands in the 380-780 nm wavelength range for retrieving the aquatic ecosystem variables as well as another 15 spectral bands between 360-380 nm and 780-1400 nm for removing atmospheric and air-water interface effects. These requirements are very close to defining an imaging spectrometer with spectral bands between 360 and 1000 nm (suitable for Si based detectors), possibly augmented by a SWIR imaging spectrometer. In that case the spectral bands would ideally have 5 nm spacing and FWHM, although it may be necessary to go to 8 nm wide spectral bands (between 380 to 780nm where the fine spectral features occur -mainly due to photosynthetic or accessory pigments) to obtain enough signal to noise. The spatial resolution of such a global mapping mission would be between ~17 and ~33 m enabling imaging of the vast majority of water bodies (lakes, reservoirs, lagoons, estuaries etc.) larger than 0.2 ha and ~25 % of river reaches globally (at ~17 m resolution) whilst maintaining sufficient radiometric resolution.

A cost-effective alternative solution of obtaining improved data over aquatic ecosystems could be to augment near future planned terrestrial Earth observing sensors to make them significantly more useful for aquatic ecosystem Earth observation. Two spectral bands (one between 615-625 nm) and one between 670-680 nm) would greatly enhance the capability of these terrestrial focused sensors to determine two important aspects of water quality and benthic composition or cover in inland, coastal and coral reef ecosystems: respectively, cyanobacterial (or blue-green algal) concentration and overall abundance of algae via the main photosynthesis pigment of chlorophyll-a.

As spectral and spatial resolution are the core sensor priorities, the radiometric resolution and range and temporal resolution need to be as high as is technologically and financially possible. A high temporal resolution could be obtained by a constellation of Earth observing sensors e.g. in various low Earth orbits augmented by high spatial resolution geostationary sensors.

1 Background

ARNOLD G. DEKKER, NICOLE PINNEL, KEVIN R. TURPIE, MAYCIRA COSTA, CLAUDIA GIARDINO

1.1 Introduction to remote sensing of aquatic ecosystems

This report is a high-level feasibility assessment of the benefits and technological challenges of designing a multispectral or hyperspectral satellite sensor system focused on biogeochemistry of inland, estuarine, deltaic and near coastal waters - as well as mapping macrophytes, macro-algae, seagrasses, coral reefs and shallow water bathymetry. Compared to any existing sensors this sensor shall need to have a significantly higher spatial resolution than 250 m, which is the maximum spatial resolution of dedicated current aquatic sensors such as Sentinel-3, and future planned aquatic sensors such as the Coastal Ocean Color Imager (COCI – 100 m res). Further, the GEO Community of Practice AquaWatch suggested that alternative approaches, involving augmenting designs of spaceborne sensors for terrestrial and ocean colour applications to allow improved inland, near coastal waters and benthic applications, could offer an alternative pathway to addressing the same underlying science questions. Accordingly, this study also analyses the benefits and technological difficulties of this option as part of the high-level feasibility study.

Initially this work had a more limited scope to focus on inland waters only. It started as a Committee on Earth Observation Satellites (CEOS) response to the Group on Earth Observations System of Systems (GEOSS) Water Strategy developed under the auspices of the Water Strategy Implementation Study Team that was endorsed by CEOS at the 2015 Plenary. As one of the actions, CSIRO initially took the lead on recommendation C.10: A feasibility assessment to determine the benefits and technological difficulties of designing a hyperspectral satellite mission focused on water quality measurements. This was considered a too limited scope, as there has never been dedicated study to assess the requirements for an aquatic ecosystem imaging spectrometer or multispectral sensor (excluding ocean requirements).

The approach is to create a science traceability of required aquatic ecosystem variables to be measured, the level of accuracy required, the level of temporal, spatial, spectral and radiometric resolution required. Although we are aware of current bounds of what is technically feasible, we did believe that the requirements should lead this study and therefore may not (yet) be technically feasible We examine the potential of establishing threshold and baseline observation requirements for sensors suitable aquatic ecosystem applications. This information will inform CEOS Agencies when considering the potential to adapt their sensors to add this globally important application area to their mission designs.

The writing team is composed of experts in:

- Earth observation of inland and near coastal waters, macrophytes, macro-algae, seagrasses and corals, bathymetry.
- Optical sensors with preference for imaging spectrometry focus: to discuss feasibility of what is maximally possible with the trade-offs of signal to noise/radiometric , spectral, temporal and spatial resolution.
- Atmospheric correction and air-water interface.

- In water and substratum algorithm with expertise in radiative transfer and/or bio-optical modelling.
- Designing, building and launching satellite sensors with hyperspectral capabilities.

CEOS notes that funding for dedicated missions, or for enhancing or adapting mission designs, is a decision for individual agencies and governments. CEOS recommends that it is key to define inland and near-coastal and benthic habitat essential variables for water quality including an assessment of relative priority, linked to defined economic, social and environmental benefits. This information would be of great value in informing investment decisions.

In many countries, field-based water quality monitoring efforts are currently insufficient or even absent to provide national-scale assessments of aquatic ecosystems. In improving the design of such assessments using Earth observation, key considerations include:

Temporal sampling to represent the dynamics of water quality, benthic and water depth change and the range of conditions that can occur over diurnal, seasonal, and annual cycles (e.g., droughts and flooding) as well as to develop time series for understanding phenology and trend analysis, including the effects of climate change. Retrospective processing of satellite images, archives of relevant data which date back to the early 80's, may also reveal temporal changes, trends, and anomalies across inland water and near-coastal water systems.

Spatial sampling that is representative of the processes and dynamics in aquatic ecosystems under consideration to provide understanding of system processes, such as for water bodies: heterogeneity, environmental flows, interrelationships between water bodies, and catchment runoff effects, global climate change effects; and for benthic ecosystems the effects of these flows as well as predation, smothering, trophic state and global warming effects such as water temperature changes, increasing acidification, coral bleaching. End-user requirements should determine the optimal spatial sampling scheme, but logistical, operational, and financial constraints usually prevent the optimal sampling scheme from being realised. Extensive distances and remoteness, for instance, may make capturing the spatial distribution of measurements using field-based methods infeasible. EO-derived aquatic ecosystem information, albeit on a more limited set of parameters, may be used to overcome the challenges in sampling schemes based solely on field-based approaches.

Capacity building should focus on the integration of EO data and field-based observations, where possible augmented by biogeochemical and hydrodynamic modelling, and the development of early-warning tools such as for algal blooms and coral bleaching.

Table 2.7 provides an overview of past existing and upcoming satellite sensor systems of relevance for aquatic ecosystem assessment (see science and applications traceability (See Appendix 1) for what is needed). While policy, legislative, environmental, and climate change drivers should steer the development of an operational system for aquatic ecosystem monitoring, the ideal satellite sensor system does not yet exist; there are trade-offs between spatial, temporal, spectral, and radiometric characteristics. Thus, the available satellite sensors for retrospective, current, and planned future systems for aquatic ecosystems detection and monitoring are boundary conditions for developing regional, national, and transboundary monitoring systems using EO.

Satellite systems require trade-offs between the temporal frequency (once a day to once a year), spatial resolution (2.0 m to 1.2 km pixels), spectral resolution (and the related issue of more aquatic ecosystem variables at higher confidence level), radiometric resolution (how accurate and how many levels of reflectance are measureable), and the costs of unprocessed satellite data acquisition (ranging from 0 to ~30 USD per km2). This also influences their usefulness for aquatic ecosystem assessment

Spatial resolution (the size of the area being measured on the ground) has consequences for imaging (i) small water bodies such as small- or medium-width river systems or small lakes. In such situations, commercial high spatial-resolution imagery (with pixel sizes of 1 to 5 to 10 m) may be the only option, possibly leading to significant data-acquisition costs. A similar argument exists for mapping submerged plants such as macrophytes (in inland waters) and seagrasses, kelp, corals, sponges, rocky reefs, benthic micro-algae in coastal and ocean waters.

Spectral resolution (the number, width, and placing of spectral bands) ultimately determines the amount and accuracy of aquatic ecosystem variables that are discernible from a water body. Sensors with few bands (usually a blue, a green, a red and a nearby infrared spectral band) may only be used to detect those variables that have a broad spectral response: TSM, K_d, Secchi disk transparency, turbidity, and CDOM as water column variables and presence –absence of underwater flora and fauna (e.g. corals). Algal pigments such as chlorophyll-a and cyanobacterial pigments such as cyanophycocyanin may also be detected. However, at low concentrations, accuracy will be low, as broad spectral bands cannot discriminate the more narrow pigment spectral absorption features from other absorbing and backscattering materials in the water column or benthos. As the number of narrower and more suitably positioned spectral bands increases (e.g., from MODIS, VIIRS, OCM-2, MERIS, Sentinel-3 OLCI, and PACE), chlorophyll becomes an accurately measureable variable, and other cyanobacterial pigments may become detectable.

Radiometric resolution determines the lowest level and interval of radiance or reflectance that the sensor can reliably detect and discriminate per spectral band. As the spectral and spatial resolution increases, the useful signal relative to noise in the data decreases. This trade-off in spectral, spatial, and radiometric resolution is countered by improvements in detector technology where, in general, more modern sensors have a higher radiometric sensitivity than older sensors. An added complexity is that the water leaving signal at the satellite sensor (typically at an altitude between 450 and 800 km) is small part of the total measured signal, composed of the water leaving signal plus the reflections at the air-water interface plus the signal from reflected sun and skylight in the atmosphere, hence radiometric resolution should be sufficient to detect relevant levels of aquatic ecosystem variables through a set of atmospheric and air water interface conditions and solar angles.

1.2 Strategic direction for detection, monitoring and assessment of inland, coastal and coral reef waters, including benthos and shallow water bathymetry

The strategic direction for a dedicated satellite sensor designed for (non-oceanic) aquatic ecosystems shall follow the hypothesis that such a system can provide significant added value in comparison to other existing and planned satellite systems, and serve relevant requirements.

Aspects of added value are addressed in this report, including benefits to the society and social impacts as outlined in section 1.5, and benefits to relevant science questions as outlined in section 2.2. The required public funded investments of such a mission shall be in balance with the expected socio-economic relevance and values generated out of the system. The system shall not conflict with actual or foreseeable commercial investments into comparable satellite systems. It shall support the self-sustainable and demand driven market development of value added Earth observations (EO) services, and investments in complementary commercial systems and services, by closing data gaps. Therefore, a collaboration and alignment with related investment activities of the private sector needs to be considered.

We illustrate these concepts with some examples: The spectral resolution is expected to go beyond those of Worldview-3 or Sentinel-2, if the evaluation proves significant added value (e.g. providing increased reliability or further water quality and benthos related products of relevance). The spatial resolution shall be lower than those of the very high spatial resolution sensors to avoid competition with commercial sensors, but still suitable to resolve spatial structures in smaller inland and estuarine waters and heterogeneous benthic ecosystems whilst enabling a global mapping effort. The radiometric sensitivity should go beyond upcoming state-of-the art hyperspectral missions such as ENMAP, in order to reduce uncertainties of products over dark water targets and support a full exploitation of the spectral resolution. The revisit rate and data provision capacities may need to be suitable and reliable enough to serve scientific purposes, environmental monitoring and management, economic data exploitation and commercial investments into Intellectual property, market integration and application development.

1.2.1 Remote sensing of inland water ecosystems

Inland waters play a major role in water, sediment, carbon, nitrogen, and phosphorous cycles between the catchments and the receiving inland waters that (except for inland saline lakes and salt lakes) ultimately flow to the coastal waters. After Guerschman et al.,(2016) 'inland waters' are defined as inland surface waters including rivers, lakes, artificial reservoirs and estuaries, and their associated wetlands. 'Water quality' refers to the physical, chemical, and biological content of water, and may vary geographically and seasonally, irrespective of the presence of specific pollution sources. Many factors affect water quality. No single measure exists that constitutes good water quality and, as such, the term 'water quality' does not describe an absolute condition but rather a condition relative to the use or purpose of the water (e.g., for drinking, irrigation, industrial, recreational, or environmental purposes); water that is suitable for irrigation, for instance, may not meet drinking water standards. Thus, 'water quality' refers to the overall natural state of water bodies and to their responses to a combination of stressors such as changes in land use; nutrient inputs; contamination from farming practices, industrial activity, and urbanization; and changes in hydrology, flow regimes, and climate.

Figure 1.1 Different colours of water (images courtesy of CSIRO) depending on their concentration of optical water quality variables

EO can be used to directly assess a subset of water quality variables, often referred to as optical water-quality variables, including concentrations of (Figure 1.1):

- Chlorophyll-a (CHL, mg m-3): an indicator of phytoplankton biomass, trophic, and nutrient status; the most widely used index of water quality and nutrient status globally;
- Cyano-phycocyanin (CPC, mg m-3) and cyano-phycoerythrin (CPE, mg m-3): indicators of cyanobacterial presence and biomass common in potentially harmful algal blooms;
- Coloured Dissolved Organic Matter (CDOM, m^{-1} absorption at 440 nm): the optically measureable component of dissolved organic matter in the water column, sometimes used as an indicator of organic matter and aquatic carbon;
- Total Suspended Matter (TSM, mg m-3) and Non-Algal pigmented Particulate matter (NAP): important for assessing the quality of drinking water, the amount of sediment in suspension and being transported and often controlling the light characteristic of aquatic environments.

Together with pure water light absorption and scattering, it is possible to estimate the following variables that are a consequence of the optical water quality variables:

Vertical light attenuation (K_d, m^{-1}), Secchi disk transparency and turbidity: measurements of the underwater light field that are important to assess the degree of light limitation, rates of primary production, species composition, and other ecosystem responses;

Emergent and submerged macrophytes: down to depth visibility, important indicators of wetland and aquatic ecosystem health and function (Figure 1.2);

Bathymetry (m): if the bottom or bottom cover of a water body reflects a measureable amount of light through the water column to above the surface, the water depth can be estimated from which the bathymetry can be derived.

EO cannot directly assess water quality parameters that do not have a direct expression in the optical response of the water body. These parameters include many chemical compounds such as nutrients. However, in some cases, non-optical products may be estimated through inference, proxy relationships, or data-assimilation with remotely-sensed optical properties of products such as nitrogen, phosphate, organic and inorganic micro-pollutants, and dissolved oxygen. However, these relationships are empirical, may not be causal, and may have a limited validity range. By making use of the combined information in directly measurable optical properties, it is possible to derive information about trophic state, environmental flows (e.g. inorganic and organic sediment fluxes), and carbon and primary productivity.
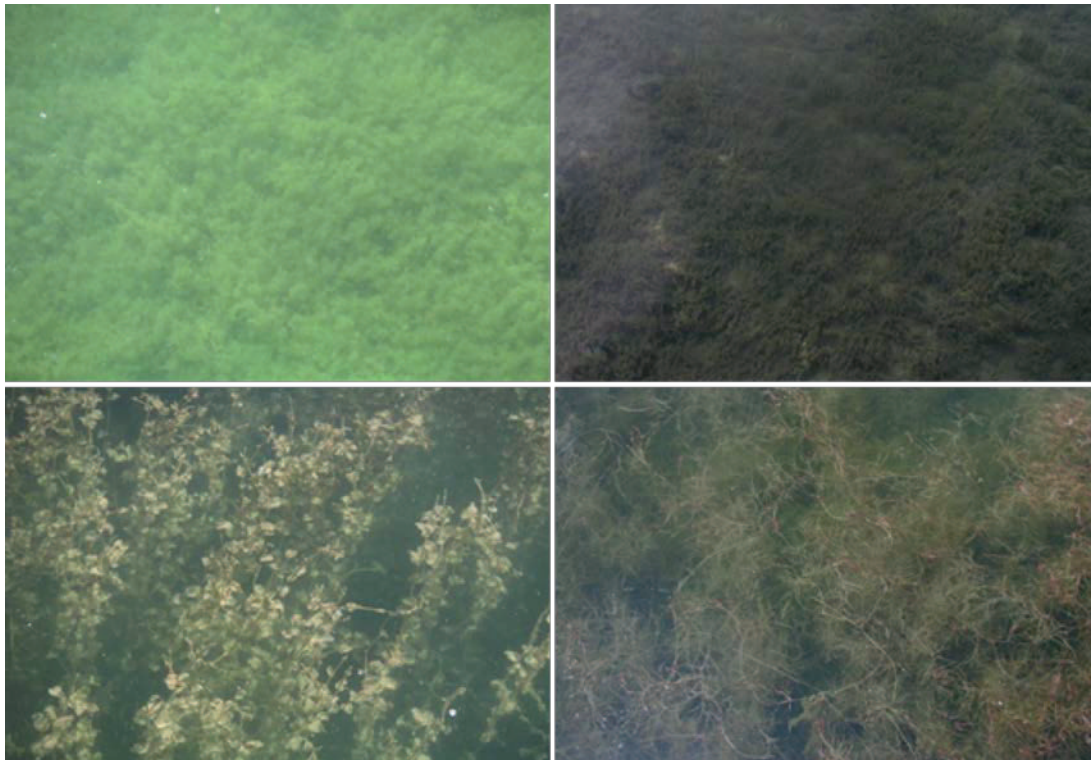
Figure 1.2 Macrophyte substrates: from left (*Chara tomentosa* (Lake Constance), *Chara contraria* (Lake Starnberg), *Potamogeton perfoliatus* (Lake Starnberg), *Potamogeton pectinatus* (Lake Starnberg) (Images courtesy of N. Pinnel, DLR).

1.2.2 Coastal waters, benthos and shallow water bathymetry

Coastal ecosystems are among the most productive ecosystems in the world, playing a major role in water, carbon, nitrogen, and phosphorous cycles between land and sea (Turpie et al., 2015). Furthermore, coastal regions are home to about two thirds of the world's population (Cracknell 1999). The social and economic wellbeing of human communities living in these regions depends significantly on the health of the surrounding coastal ecosystem. Studies of coastal and inland aquatic ecosystems including water quality are critical to understanding and protecting these valuable resources. These marginal regions between land and sea support valuable ecotones that are highly vulnerable to shifts in the environment, whether from climate change and its consequences (e.g., sea level rise), human activities (e.g., eutrophication or changes to existing watershed hydrology), or natural disturbances (e.g., storms or tsunamis). Coral reefs are a specific case of coastal as well as oceanic ecosystems functioning as high biodiversity ecosystems with a high sensitivity to climate change e.g. in the form of coral bleaching, ocean acidification and cyclone

damage. As these drivers of change can occur on large scales or even globally, spaceborne remote sensing is a key tool for systematically studying these environments. EO can be used to directly assess a subset of coastal and coral reef water quality variables as well as water column depth and substratum composition. The water column variables are the same as for inland waters: chlorophyll a (CHL), cyano-phycocyanin (CPC), cyano-phycoerythrin (CP), coloured dissolved organic matter (CDOM), total suspended matter (TSM), non-algal pigmented particulate matter (NAP), vertical light attenuation (K_d), Secchi disk transparency and turbidity. The water column depth and substratum composition variables are seagrasses (Figure 1.3), macro-algae (such as kelp), benthic micro-algae, sands, silts, muds, coral ecosystem variables (Figure 1.4) (all down to depth visibility)- important indicators of d aquatic ecosystem health and function.

Figure 1.3 Seagrass substrates: from left *Zostera spp.* (Baltic sea), *Heterozostera tasmanica* and *Ulva* (South Australia), *Posidonia sinuosa* (South Australia), *Heterozostera spp.* (South Australia). (Images courtesy of CSIRO)
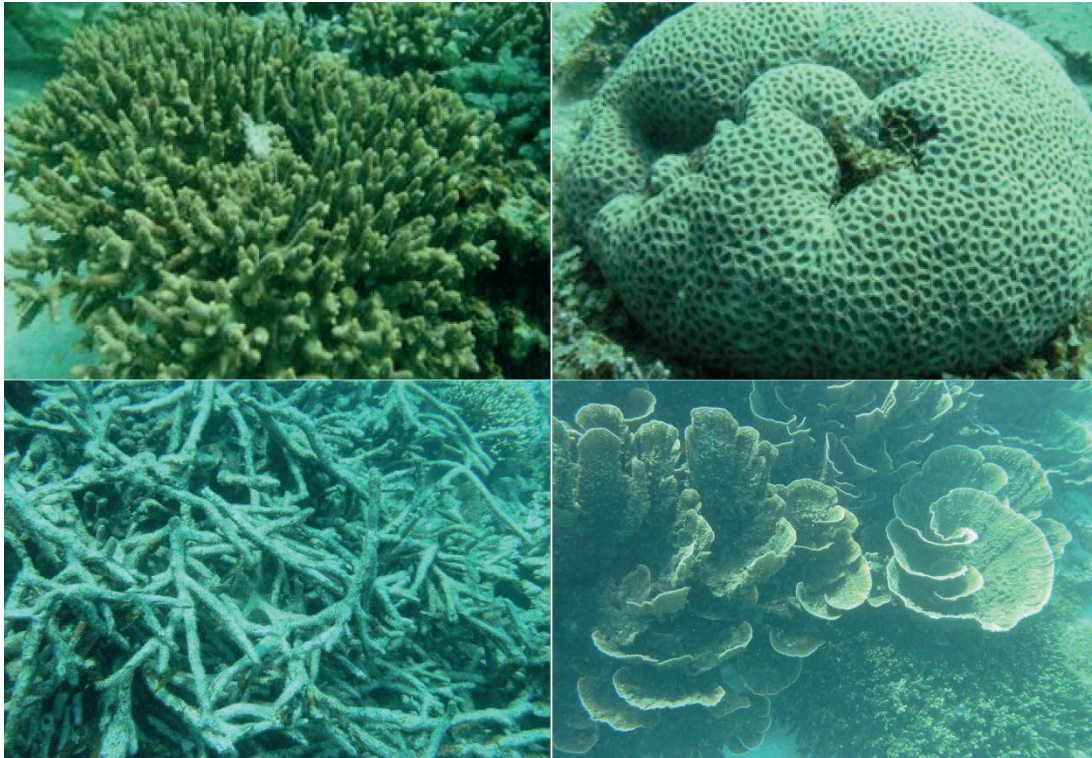
Figure 1.4 Coral reef substrates: branching coral, massive coral, dead coral, tabulate coral in Ningaloo (Western Australia). (Images courtesy of N. Pinnel, DLR).

1.3 Introduction to physics of remote sensing for aquatic ecosystems

In order to define Earth observation sensor characteristics for an aquatic ecosystem sensor it is necessary to understand the physics of visible and nearby infrared sun light and sky light interactions with the atmosphere, the air-water interface, the water column and the benthos. Here we provide a brief introduction. In Chapter 2 a more thorough description of the physics is presented for modelling water leaving spectra, transmitted from the benthos, through the water column, through the air-water interface and atmosphere to simulate an at-satellite sensor signal (also referred to as Top of Atmosphere –TOA-signal.

Earth observation of the optical water-quality and benthic parameters is achieved through optical means in the VIS/NIR spectral region (~400–900 nm). The light reaching the surface of a water body consists of direct sunlight and diffuse skylight after scattering and absorption interactions in the atmosphere (see Figure 1.5). At the water surface, this light is either reflected by the surface or refracted, as it passes across the air/water interface. Within the water column, the water itself and different particulate and dissolved water column constituents transform the light by transmitting, absorbing, or scattering the down-welling light. Of the light that is scattered, a proportion may be backscattered in an upward direction and pass across the water/air interface at the right angle to be observed by satellite sensors once it has again passed through the atmosphere.
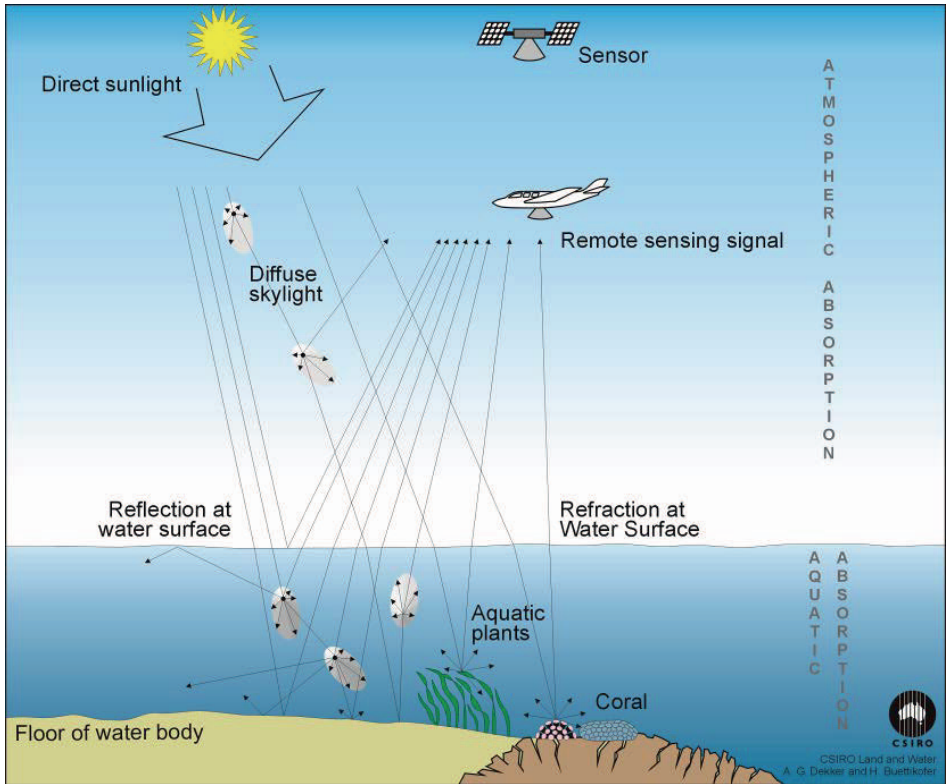
Figure 1.5 Schematic of the light Interactions that drive optical EO involving the air, water, and substrate

In the visible spectrum (~400-900 nm), light interaction with sediments, chlorophyll, and coloured dissolved organic matter modify the shape and amount of the spectrally reflected signal (Kirk, 2011); it is these variations in the 'shape' of spectral reflectance that RS water quality algorithms largely take advantage of (see Figure 1.6). In wavelengths longer than 900 nm, water itself is such a strong absorber that very little radiation is reflected from water bodies, except for high turbid waters (see Figure 1.7).

When an aquatic ecosystem is optically shallow it means that a measureable signal has passed through the water column to the bottom (the benthos) and has been reflected from the benthos is sufficient quantity to pass through the water column, through the air –water interface and through the atmosphere to be measurable at the satellite sensor. The benthos may be composed of benthic micro-algae in and just on top of clay, silt, sand or coral rubble, of seagrasses and macro-algae, rocky reefs and coral reefs with corals, coralline encrusting algae, sponges etc., (see Figure 1.8).
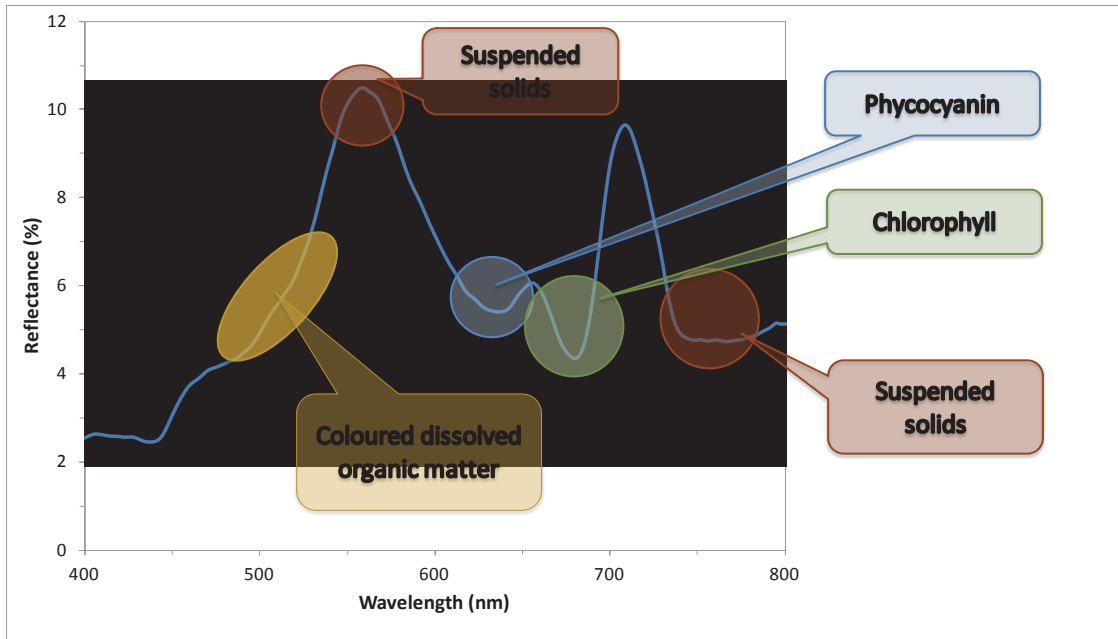
Figure 1.6 Typical reflectance spectrum from a eutrophic inland water body and the regions in which different water-quality parameters influence the shape of that spectrum (source T. Malthus, CSIRO, Australia)
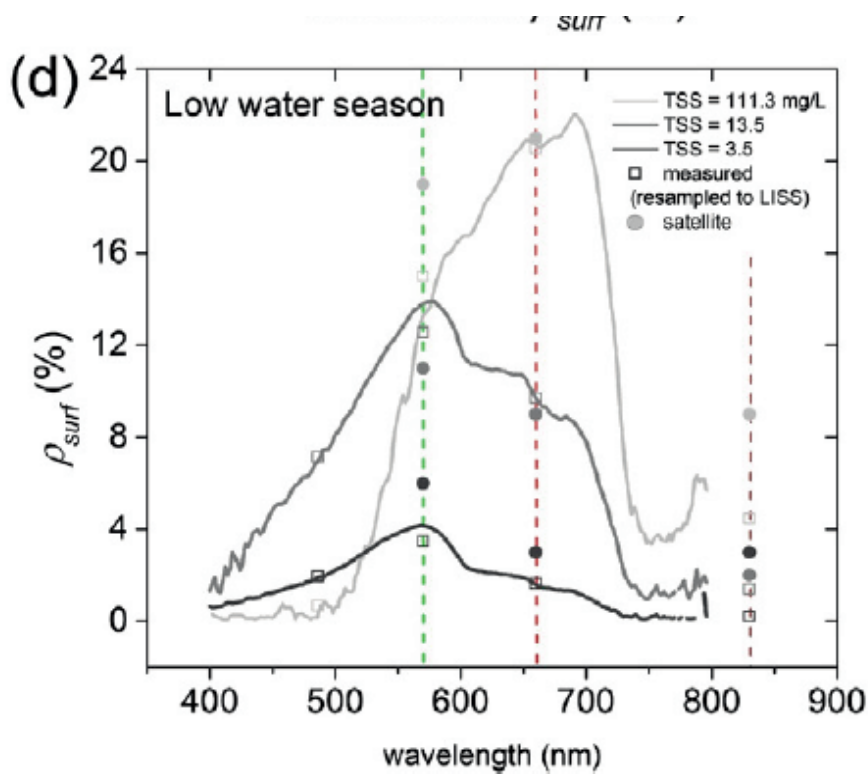
Figure 1.7   Reflectance spectrum from a turbid inland water body, Amazonian rivers (Lobo et al., 2015)
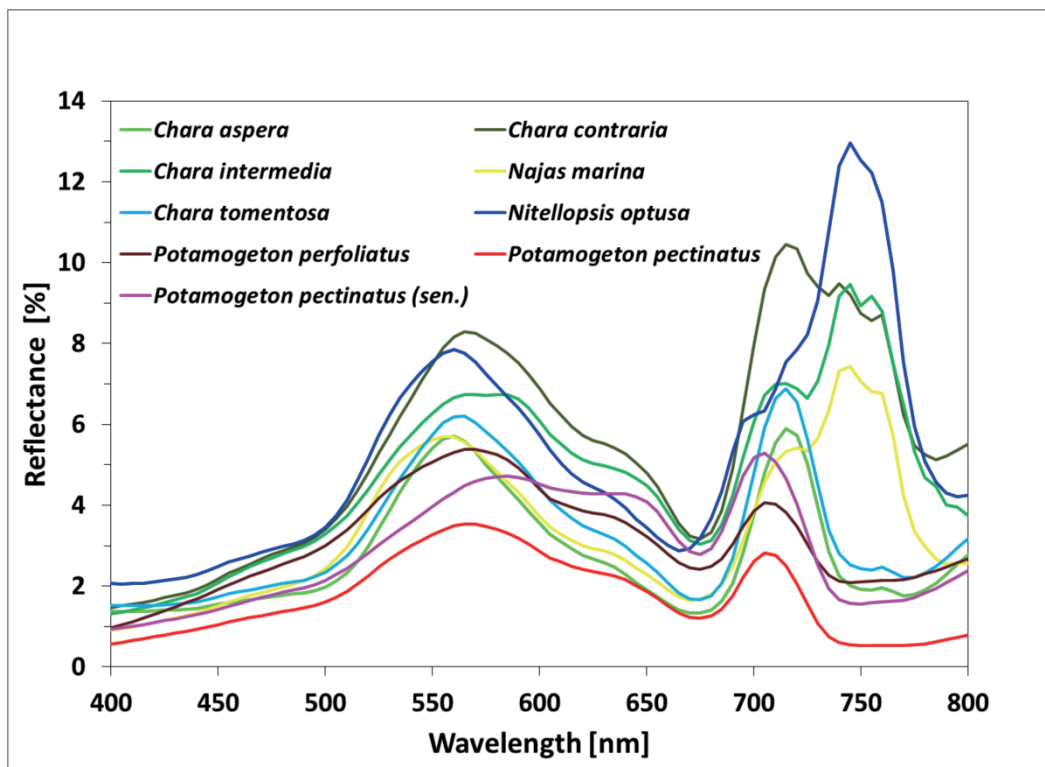
Figure 1.8 Typical bottom reflectance spectra of macrophytes in Lake Starnberg and Lake Constance, Germany ranging from 0.5 to 3.5 m water depth (Pinnel, 2007).

1.4 Introduction to algorithms to derive information from remote sensing data over aquatic ecosystems

In order to create maps of a water quality or benthic variable or a characteristic such as bathymetry from Earth observing data we need algorithms that can translate the photon counts per spectral band imaged at the satellite sensor to the required relevant water body information: these are the remote sensing or Earth observation algorithms.

There are several approaches to algorithms. The first distinction to be made is between algorithms that presume an atmospheric correction and air-water interface effect correction have already been performed so that the algorithm only has to deal with translating the remote sensing reflectance or water leaving radiance signal to an aquatic ecosystem variable. The other approach is to infer an aquatic ecosystem variable from the Top of Atmosphere signal measured at the satellite sensor.

The algorithms for translating the measured spectral reflectance from a water body to water-quality variables range from: (i) empirical approaches (See reviews by Matthews et al., 2012 and Tyler et al., 2016); (ii) semi-empirical approaches (Gons, 1999, Härmä et al., 2001); (iii) physics-based, semi-analytical spectral inversion methods (Lee et al., 1998; Brando et al., 2012; a review by Odermatt et al., 2012)) to (iv) Artificial Neural Network and Machine Learning Methods and (v) Object Based Image Analysis methods. Increasingly use is made of several of these techniques together: e.g. performing atmosphere correction using a ANN approach and then performing a semi-analytical

inversion on the remote sensing reflectance or water leaving radiance at the surface (Brando et al., 2012) or using a radiative transfer based atmospheric correction and then applying OBIA etc.

These methods are outlined below and subsequently compared in terms of their need for field measurements, as well as their reliability, accuracy, maturity, and complexity.

Empirical approaches statistically relate field samples of the optical water-quality or benthic variables to radiance or reflectance values measured by a satellite. While there is no need to understand the underlying physical relationships in such algorithms (such as atmospheric and underwater light processes), they do require coincident field measurements to calibrate the relationships for specific water bodies and, as such, struggle when water column constituents or benthic properties lie outside the range upon which the pertinent statistical relationship was based (in both space and time) and are not easily adapted to new satellite sensors. Empirical methods are also less reliable when undertaking retrospective monitoring, especially when water-quality or benthic characteristics may change and end up outside the range of those upon which the empirical relationship is based.

Semi-empirical algorithms improve over pure empirical approaches by choosing the most appropriate single or spectral band combination to estimate the water column or benthic constituent. They can also partly annul some of the atmospheric and water surface effects. Semi-empirical algorithms, however, also suffer from extrapolation errors beyond the range of constituents observed; the requirement to establish new, semi-empirical algorithms when switching sensors or water bodies; less reliability in retrospective monitoring when water-quality or benthic characteristics change, compared with fully empirical methods.

The water-quality variables retrieved using empirical and semi-empirical algorithms include total suspended matter, suspended inorganic matter, CDOM, turbidity, transparency, chlorophyll and cyano-phycocyanin pigments (Matthews, 2011). With few exceptions (e.g., Minnesota lakes in the USA, Olmanson et al., 2011), neither approach offers significant confidence for application in a national monitoring system (Dekker and Hestir, 2012). The Minnesota lakes method worked because it is supported by a vast, citizens' science-based field measurements effort. The benthic variables are water column depth, benthic type and benthic cover type. In addition floating or submerged macrophytes can be estimated.

Semi-analytical inversion algorithms are built around knowledge of the underlying physics of light transfer in waters, and use the inversion of predictions of light reflecting from a water body, generated by forward radiative transfer models, to simultaneously estimate key water-quality and benthic constituents. Such approaches show improved accuracy for estimating water-column composition (Dekker et al., 2001), and are capable of assessing the error in the estimation of water-quality constituents, are repeatable over time and space, are transferable to new water bodies and other sensors, and can be retrospectively applied to image archives (Dekker at al., 2006, Odermatt et al., 2012). This means that retrospective monitoring of optical water-quality changes is possible to assess the impacts and mitigation of various stressors to the system. In Dekker et al., (2011) a summary is presented of applying semi-analytical algorithm approaches to estimating water column composition, depth and benthic composition in optically shallow waters.

Artificial intelligence (AI) methods such as an Artificial Neural Network (ANN) and machine learning methods are becoming more powerful as computing power increases. ANN and machine learning methods can be trained using a radiative transfer model or using a bio-optical semi-analytical model or they can be trained using large amounts of in situ data.

OBIA makes use of the pattern, texture and spectral information in a remote sensing image, it requires initial rule creation by an expert image and domain knowledge expert, but can then be rerun automatically on images of the same area. OBIA is not useful for water quality extraction but highly applicable to benthic vegetation and benthic substratum mapping.

Recommended pathways for longer-term operational use is to develop robust inversion methods for application globally. The most likely globally valid methods for use in areas where there may be little or no in situ data for verification or for dealing with the vast range of possible types of waters are the methods that are based on understanding and simulating the physics of light interaction in the atmosphere, the air-water interface, the water column and the benthos.

Semi-empirical methods can be used in the interim, as they often are reasonably robust for one variable for a category of water types and for a single EO sensor system. Empirical approaches are only useful as proof of concept but, in general, are not recommended if all optically active substances (Chl, CDOM, TSS, CPC, CPE and resulting physical properties of turbidity, Secchi Disk depth, and vertical light attenuation) as well as, in the case of optically shallow water systems, water column depth and benthic composition need to be determined.

In situ data (field or laboratory measured data) is often referred to as "ground truth". It is more proper to refer to these measures as field measurements as they are prone to uncertainty and inconsistencies. There are many different protocols and variations on protocols for measuring e.g. Chlorophyll-a (HPLC, spectrophotometrically or by fluorescence). Inter-lab variability is significant (REVAMP report; GLaSS protocols report www.glass-project.eu). Extraction before measurement and then measurement of the blue green algae pigment cyanophycocyanin is even more difficult. Recent additions of algal and CDOM fluorescence measurements have only increased the uncertainty of in-situ measurements. E.g. when field samples are taken and the same sample is distributed across multiple laboratories for measuring concentrations a variability of 50 % to 100 % and sometimes higher are encountered. Thus when comparing earth observation derived aquatic ecosystem measurements with field and laboratory measured samples, issues of validity and confidence must be addressed for both types of measurements.

1.5   Benefits to society / societal impact

Water and life – no two features more completely define planet Earth, and no two are more inextricably intertwined. Biology thrives particularly where water and land come together. Inland waters flow into coastal waters via creeks, rivers, reservoirs, dams, floodplains , estuaries and delta's, except for saline and salt lakes which evaporate the incoming waters. In the transition zone from freshwater to salt water mixing takes place often driven by river flow and tidal action. In most cases there is no clear divide between freshwater and ocean water. Here we discuss inland and coastal waters including coral reefs, seagrasses, macro-algae and other benthic habitat components from a perspective of using earth observation to detect, monitor and assess these waters.

Access to clean, safe drinking water is a key determinant of quality of life, as it is directly linked to human health. Depending on the use to which the water is put, polluted or contaminated water may not be regarded as a useable resource. Similarly, as contaminant concentration is often related to water volume and flow, water quality is ultimately linked to water quantity.

Inland waters have important functions in the environment (Dörnhöfer and Oppelt, 2016): they provide habitat for a wide range of species and form essential components in hydrological, nutrient and carbon cycles (Moss, 2012). Other usages encompass energy production, transportation, fishery and recreational purposes (Stendera et al., 2012; Carvalho et al., 2013a).

The quality of water is affected by a number of stressors including urbanization, population growth, land use change, deforestation, eutrophication, inorganic and organic contaminants, morphological alterations and climate change effects such as acidification or increasing water temperatures , farming needs, overexploitation, and contamination from extractive industries in the mining and energy sectors (Kuenzer and Renaud, 2012). As such, the relevance of water quality issues will change in different settings and its impact will ultimately depend on the water's intended use.

Therefore water quality detection, monitoring and assessment is key for ensuring that both human and ecosystem health are not compromised and for determining its suitability for other purposes (irrigation, industry, etc., Kuenzer et al., 2011).

Coastal zones encompass less than 10 % of Earth's land surface, yet over 70 % of the human population lives near a coast, estuary, wetland, or coral reef. These zones host the most significant and diverse bacterial, algal, plant, and animal populations of the planet; more than 100,000 animal species, with over 80 % of all marine fish species and over 20 % of bird species live in or migrate through these areas. The economic, environmental, and social benefits of coastal zones is now estimated at US$56 trillion (Barbier et al., 2011; Keddy 2010; MEA,2005; Costanza et al., 2014). By 2025, the world's population will have grown by one more billion people. By then, the risk that over 70 % of humanity will have lost benefits derived from coastal zones and wetlands, including good water and living resources like fish, is 'high' (UNEP, 2012).

Nation states require water quality information to inform key policy and legislative requirements that may include assessments against water quality guidelines and targets, national water quality management strategies, water resources assessments, state of the environment reporting, and strategies formulating adaptive responses to climate change. However, even in developed countries (e.g., USA and Australia), no nationally coordinated water quality monitoring programs may exist, and the authorities may instead rely on individual states to provide such information; moreover, frameworks for the dissemination of such information are often lacking or poorly developed (Dekker and Hestir, 2012). The IOCCG report (in prep) on earth observation of global water quality provides an overview of national and international directives that address these problems and aim to improve the ecological state of inland and coastal waters. A common target of these directives is to improve water quality by identifying stressors and by implementing sustainable management strategies supported by a more or less frequent monitoring. Currently, most monitoring programmes are field based even if sampling and analysis are labour, cost and time intensive (Schaeffer et al., 2013). It should be noted that providing information on species level, single measurements or unevenly distributed sampling points are problematic and may result in erroneous water quality classifications (Bresciani et al., 2011; van Puijenbroek et al., 2015). Moreover, in situ measurements hardly capture

the temporal and spatial variability of phenomena such as short-living cyanobacterial or phytoplankton blooms (Reyjol et al., 2014) or significant river inflow (lakes and reservoirs) and outflow events (from lakes and reservoirs to rivers and from rivers to coastal water).

In summary, the evaluation of inland and coastal water systems lacks historic and actual information. Information gaps are of high ecological and economical relevance, e.g. the impact of dams and related economic/ecologic changes in the whole watershed down to the coast. Remote sensing based maps, time series, products and services can significantly contribute to close data gaps. Water supply and sanitation are thus essential components of any integrated approach to malnutrition and poverty reduction, and water quality is a key related challenge in sustainable development.

Despite international efforts at monitoring global inland and coastal water quality, existing data are scarce and declining, have poor geographic and temporal coverage, may lack quality assurance and control, and thus be of questionable accuracy (Strebotnjak et al., 2012). The international coordinating group, the Group on Earth Observations (GEO), recognizes the value of EO for improving understanding of global water quality, as well as its hotspots and trends; for ensuring food and energy security; for facilitating poverty reduction; for protecting the health of humans and ecosystems; and for maintaining biodiversity. In 2007 GEO formed the Inland and Near-Coastal Water Quality Remote Sensing Working Group within the GEO Water Task with the objective to promote the development of improved optical water-quality products (GEO, 2007). Sine 2016 this GEO inland water activity has progressed into AquaWatch, a GEO Initiative for 2017 onwards. The coastal waters and coastal zone are part of the GEO initiative Blue Planet.

Shallow benthic ecosystems are a subset of aquatic ecosystems that can be assessed using earth observation. It is possible to map benthic micro-algae, seagrasses, macro-algae (e.g. kelp), coral reefs and other shallow water ecosystems from space if the bottom is visible at the water surface. Water depth can be estimated as well as the water column composition. These shallow water ecosystems are essential for environmental, food and recreational purposes and are under pressure from navigation needs (ports, harbours), receiving waste water, overfishing, ocean acidification, temperature increases etc.

The recently established United Nations Sustainable Development Goals have three SDG's that relate to aquatic ecosystems that are the subject of this study: they are SDG 6: "Clean Water and Sanitation" focusing on inland waters; SDG 14: " Life below water" focusing on coastal and ocean ecosystems and SDG 15: " Life on Land:" where for the purpose of this study the wetlands are a key target. Earth observation can play a key role in monitoring and assessing progress for all UN countries on those variables that are measureable from space (GEO, 2017).

Through the provision of synoptic, consistent, and comparable data, EO has the opportunity to overcome some of the gaps and deficiencies that exist in current, field-based water quality monitoring efforts. Sufficient archives of EO data now exist to monitor global trends of some relevant variables in aquatic ecosystems for several decades and to develop suitable reports to address specific questions raised by decision and policy makers. Still there is so far no specific satellite sensor designed for supporting information extraction requirements over inland, coastal waters and coral reefs preventing more effective applications

1.6   What we propose to do

In Chapter 2, the focus is on determining the satellite sensor requirements for inland, coastal and benthic ecosystems. We look at the science and application requirements and what can be measured using visible and nearby-infrared imagery. The science and applications traceability (See Appendix A.1) summarises these requirements into one table. The science questions cover topics of inland, estuarine, deltaic and lagoonal waters, transitioning into coastal and coral reef waters. It also includes shallow water bathymetry as well as the benthic types found. A science and applications traceability matrix is represented which condenses a significant amount of information required. With this information a series of simulations of what an earth observing sensor would see in space over a large variety of often occurring aquatic ecosystem permutations is performed that predict the spectrum as measured just above the water surface as well as in space. The full results of these simulations are presented in the Appendix A.2 that belongs to chapter 2. From these results sensor requirements are determined for spectral, radiometric, spatial and temporal resolution of a dedicated aquatic ecosystem sensor. We also discuss issues of atmospheric, adjacency effect and air-water interface correction. Adjacency effect is where photons reflected from bright targets (sand beaches or vegetation) are scattered in the atmosphere so that it seems they come from dark targets such as deep water or a dense seagrass bed leading to erroneous interpretation. With all this knowledge it then becomes possible to assess the relevance of the sensor specifications of past (archival data), present and near future planned relevant satellite sensor missions. We are able to then determine what the specifications should be for a dedicated aquatic ecosystem earth observing satellite sensor, keeping in mind that a trade-off between spectral, spatial, radiometric and temporal resolution has to be made. In addition we can also recommend proposed modifications to planned future sensors to make them more suitable for (non-oceanic) aquatic ecosystems.

Chapter 3 focuses on instrument, platform and mission design aspects. We discuss the merits and drawbacks of low earth polar orbiting satellite systems versus geostationary systems. Next we tackle the issues of how to correct the satellite signal for atmospheric constituents, light effects (e.g. polarization) instrument artefacts (stray light, striping, linear responses etc.), platform stability etc. An important and often underappreciated issue is that of pre-launch and post-launch calibration of the sensor measured signal - an important issue as water bodies generally reflect low levels of incoming light and thus a high level of accuracy is required. All these requirements are summarized in the proposed schematic outline of what an end to end simulator of such a dedicated aquatic ecosystem sensor should look like if the recommendations of this report are taken up.

Chapter 4 considers what would need to be done once we do have a dedicated aquatic ecosystem earth observing satellite mission (which may be composed of multiple satellite sensors). Chapter 4 focuses on the relevant earth observation enabling activities such as water quality, bathymetry and benthic mapping methods and algorithms; the various corrections that need to be applied to TOA data from satellites; the required in situ instruments for parameterizing the algorithms, as well as validating the earth observation derived aquatic ecosystem variables. A general discussion on sources of uncertainties, recommended field campaigns and a brief discussion of interdisciplinary science and application studies that can be performed once the earth observing data has been processed to its most definitive informative state.

Chapter 5 provided a succinct summary of the recommendations for a dedicated (suite of) aquatic ecosystem satellite sensor(s). Chapter 6 provides the literature references.

2 Science and applications driving sensor specifications

Xavier Briottet, Peter Gege, Kevin R. Turpie, Arnold G. Dekker, Nicole Pinnel, Sindy Sterckx, Thomas Heege, Maycira Costa, Vittorio E. Brando, Claudia Giardino, Federica Braga and Steef Peters

2.1 Introduction to the science and applications questions

In Chapter 1 we introduced the necessity for society to be able to detect, monitor and assess the biogeochemistry of inland, estuarine, deltaic and near coastal aquatic ecosystems as well as to map macrophytes, macro-algae, seagrasses, coral reefs and shallow water bathymetry.

To understand and evaluate the anthropogenic and natural effects on aquatic ecosystems, it is of importance to improve our knowledge on a local to regional to global scale. Due to the large diversity of such systems, their large extension and their rapid temporal evolution, remote sensing may be an efficient tool for improving our understanding of coastal and inland aquatic processes through detection and quantification of aquatic environmental variables and their change. Together with process based understanding of these environments or habitats it may become possible to link these changes to causes providing management relevant information.

For Earth observation to be able to play this role, the following general science questions provide guidance towards these goals (modified after Turpie et al., 2015):

SQ-1. What are the distribution, abundance, function, and state of biodiversity for coastal and inland aquatic ecosystems on regional and global scales? At what rate are theses quantities changing and what factors are driving their change?

SQ-2. What are the biogeochemical fluxes across the boundaries between land, water, and air; how are they changing? What are the reasons for these changes?

SQ-3. How are these changes interconnected? What are the consequences to important ecological resources, e.g., fish stocks and water quality and availability?

For each of these questions, Earth observation needs to provide information for:

Continental (fresh water) habitats: inland waters (lakes, reservoirs, rivers, ponds, wetlands etc.) with phytoplankton and aquatic macrophytes, benthic and pelagic fauna.

Coastal (brackish – salt water) habitats: estuarine, deltaic and lagoon waters with phytoplankton, seagrasses and coral reefs, kelp, benthic flora and benthic and pelagic fauna (bathymetry is an important variable in shallow waters).

For successful remote sensing of aquatic ecosystems it is important to realise that the atmosphere and water interface are part of the measured signal and thus need to be characterised, to be able to correct for these effects.

§ 2.2 will discuss the scientific and application questions related to each of the above applications. The essential variables to be estimated from space remote sensing will be listed in the science and applications traceability matrix (see Appendix A.1). The method to measure these essential variables are then described in § 2.3 including mission requirements in terms of spectral range, intervals and spectral resolution, radiometric sensitivity, spatial resolution and geometric (geolocation, swath width etc.) specifications and temporal resolution requirements. To adequately correct for the aforementioned atmospheric (including adjacency) effects and the air-water interface the space sensor also needs to address specific requirements. In § 2.4 a suitability assessment of past, current and near-future earth observing sensors is presented in table format to provide a quick overview of where current and planned and funded future sensors do and do not meet the requirements set in the previous sections. Although a dedicated (suite of) aquatic ecosystem multispectral or imaging spectrometers is a desirable outcome, it is also practical to see whether modest changes to planned future multispectral sensor systems for land and for ocean could provide partial solutions to improved assessment of aquatic ecosystems. Therefore § 2.5 includes modifications to planned ocean and coastal colour sensors.

2.2 Science and applications questions per aquatic ecosystem

This section describes the essential variables which can be estimated from remote sensing to characterize each application for non-oceanic aquatic ecosystems.

2.2.1 Inland waters ecosystems

From a societal point of view, inland water bodies are vital for recreation, food supply, commerce, human health, urbanization, tourism, transportation, industry, fish farming and drinking water supply whilst environmentally they support habitats for a large floral and faunal diversity. Currently, these ecosystems experience high pressure from increasing social and economic human activities as well as climate change. As sinks for pollutants, freshwater ecosystems are among the most sensitive indicators of environmental impacts related to human activities (UNEP, 2012). For example, a major global ecological problem is the increasing eutrophication, pollution and loading with sediments of inland water bodies caused by fluvially transported substances such as phosphate and nitrogen compounds as well as eroded soil and creek and gully embankments which derive from intensified agricultural and industrial activities, including mining. Monitoring and managing the water quality of freshwater habitats is therefore necessary. E.g. according to the EU Water Framework directive 2000, specified biological, hydro-morphological and physio-chemical parameters of water bodies should be monitored on a regular basis. Similar requirements exist across the globe.

The global abundance and size distribution of lakes was recently reported by Verpoorter et al., (2014) using analysis based on Landsat imagery. This work quantified the number and surface areas of the world lakes larger than 0.002 km² (0.2 ha). Andreadis et al., (2013) reported estimates of global river width, depth and discharge using a combination of Landsat image analysis and hydrologic modelling. Using these datasets, an estimate is derived for the total number of lakes and rivers that are globally resolvable by different sensor spatial resolutions, where a lake is resolved if a 3 x 3 contiguous array of lake pixels, not affected by any land spectra, can be collected. The majority of lakes globally occur in size classes less than 1 km^2. While there are fewer number of lakes in size classes greater than 1 km^2, they contribute a substantial portion of the total surface area covered by lakes. Therefore, in theory, about 60 % of the world's surface lake area can be resolved with a sensor

ground sampling size (pixel size) GSD of ~333 m (Table 2.4). This is the equivalent of a sensor with MERIS/S3-OLCI/OCM/SGLI-type resolution. If smaller lake classes are included, nearly 80 % of the global lake surface area be viewed with a sensor with a GSD of 105 m, whereas 100 % of the global lake area of lakes 0.2 ha or larger can be resolved with 15 m spatial resolution (e.g., Sentinel-2 type sensor resolution which has 10m, 20m and 60 m bands). Thus, we estimate that a Landsat resolution sensor (30 m multispectral bands and 15 m panchromatic) available since 1984 can detect approximately 27 million lakes worldwide, or more than 90 % of the global lake (larger than 0.2 ha) surface area. See paragraph 2.3.3 for more detailed information.

Whereas conventional monitoring approaches tend to be limited in terms of spatial coverage and temporal frequency, remote sensing has the potential to provide an invaluable complementary source of spatial data at local to global scales. Furthermore, as sensors, methodologies, data availability and the network of researchers and engaged stakeholders in this field develop, increasingly widespread use of remote sensing for operational monitoring of inland waters can be envisaged (Palmer et al.,2015). Systematic examples of truly operational monitoring of inland water quality beyond that applied to single water bodies are sparse, reflecting the challenges in applying simpler empirical and semi-empirical algorithms. Olmanson et al., (2008) compiled a comprehensive water clarity database assembled from Landsat imagery over 1985–2005 for over 10,500 Minnesota lakes larger than 8 ha in surface area, on the basis of empirical methods using citizen science approaches. This study highlighted the geographic patterns in clarity at both individual lake and eco-region level linked to land use. Such an approach requires significant interaction and investment with the local communities.

Several researchers have developed algorithms to quantify various optical water quality parameters, including chlorophyll-a, suspended matter, coloured dissolved organic matter, dissolved organic carbon concentration and water transparency measures such as vertical attenuation of light, Secchi disk transparency and turbidity (Dekker et al.,, 2001; Park and Latrubesse, 2014; Gilerson et al., 2010; Giardino et al., 2007; Gitelson et al., 2007; Kallio et al., 2001). Moreover, phytoplankton taxonomic groups can be identified, which provide indications for the occurrence of harmful algal blooms, e.g. cyanobacteria (Simis et al., 2007; Bracher et al., 2009; Duan et al., 2014). Chlorophyll-a as one of the important water quality parameters is often used as a measure of the level of water eutrophication and can be used as a proxy for phytoplankton biomass in aquatic ecosystems (Giardino et al., 2001; Zhang et al., 2012). Accurate estimates of algal pigment concentration from remotely sensed data for inland and near-coastal waters however are challenging due to their optical complexity and there being many smaller or narrower water bodies requiring smaller pixel sizes.

Algorithm development to allow application beyond single inland water bodies is predominantly being addressed in research projects targeting larger lakes using low spatial resolution ocean colour sensors (e.g., GLaSS and GloboLakes projects) and smaller lakes using terrestrial sensors such as Landsat and Sentinel-2 (Lymburner et al., 2016).

2.2.2 Wetlands ecosystems: macrophytes

Apart from water quality wetland ecosystems are important for their macrophytes. Macrophytes link the sediment with the overlying water. They are beneficial to lakes because they provide habitat for fish and substrate for aquatic invertebrates, offering protection against both currents and predators.

Macrophytes also produce oxygen via photosynthesis, which assists with overall lake functioning, and are an important food resource for some fish and other wildlife (Jeppesen et al., 1998). Lakes with water plants thus have high ecological value. Because of specific growth requirements, macrophyte species tend to reflect the physical and chemical (nutrient) conditions of the lake in which they occur (Sondergaard et al., 2010). Thus, the composition of macrophyte species in a water body makes it possible to draw conclusions about local chemical and physical conditions. Aquatic macrophytes have several advantages which make them attractive as limnological indicators, as opposed to other algae (diatoms) or macroinvertebrates. They are especially sensitive to changes (increases) in nutrient concentrations (notably phosphorus and ammonium) and to organic pollutants and can be used as long-term indicators, as they change slowly and progressively. Secondly, submerged macrophytes are rooted; therefore, they reflect the nutrient status of their immediate habitat by their presence/absence and abundance. Thus, they can indicate patterns of nutrient concentration, e.g. caused by natural or artificial inflows. An additional advantage which makes them attractive to remote sensing applications is that they can generally be seen and identified to the species level at the sampling site.

Macrophytes may be separated into three remotely measured groups, based upon their principal growth habits—submersed, floating-leaved, and emergent. The mapping of species by growth habit using both airborne and satellite data can be done reasonably accurately (Malthus and George, 1997; Hunter et al., 2010; Tian et al., 2010, Pinnel 2007). Routine mapping of the biophysical parameters of macrophytes will have value in assessing cover and the effectiveness of management practices for controlling excessive aquatic plant growth.

Several remote sensing techniques are used to characterize macrophyte habitats: Synthetic Aperture Radar (SAR), passive optical and nearby infrared data and LIDAR. SAR has been used to map wetland extent and emergent vegetation (Evans et al., 2010; Costa 2004) but due to the lack of penetration of microwaves, is not able to detect submersed macrophytes species. Further, because wetlands are highly spatially heterogeneous, the coarse spatial resolution provided by most publicly available SAR systems also limits their ability to successfully discriminate wetland plant species from space. Table 2.7 highlights the abilities of current and future optical sensors for differentiation of the different macrophyte growth habits. In addition to providing valuable habitat to multiple freshwater ecosystem species, emergent wetland vegetation has extremely high rates of net primary production and evapotranspiration (ET), drives a large portion of wetland carbon formation and storage, and plays an important role in wetland sediment stability and accretion (Byrd et al., 2014; Zhou and Zhou, 2009). Floating and submerged plants provide important structuring for freshwater ecosystems, influencing the physical and chemical environment and food web (Liu et al., 2013; Meerhoff et al., 2003; Santos et al., 2011; Vanderstukken et al., 2014).

With respect to satellite data, the high spatial heterogeneity of macrophytes and their presence in relatively small water bodies and wetland areas needs to be monitored at a spatial resolution which is not supported by most high temporal frequency and low spatial resolution sensors (300–1000 m) used for terrestrial vegetation applications at global scale (e.g. Hmimina et al., 2013). Medium resolution EO data (10–30 m ground resolution) are the best option. A good potential for developing applications to map macrophytes has been shown by exploiting multi-temporal information. This is done largely based on reflectance values in NIR wavebands, which are much stronger from emergent and floating-leaved species than from the surrounding water. The straight forwardness of spectral

vegetation indices has long demonstrated its advantages for large scale mapping of aquatic vegetation (e.g. Hu et al., 2010). Villa et al., (2015) showed capabilities and performance of temporal series of vegetation indices in mapping wetland vegetation groups on a functional basis beyond the local scale.

Hyperspectral data can differentiate several aquatic plant associations (Tian et al., 2010) and be used to detect submersed aquatic species, even in highly turbid environments (e.g., Hestir et al., 2008; 2012, Santos et al., 2012), as can the use of LiDAR and textural analysis of image data (e.g., Proctor et al., 2013; Verrelst et al., 2009). The differentiation of species, however, currently poses a greater challenge. Because of the high spatial and phenological variability of aquatic macrophytes, improved resolution (e.g. spectral, spatial, temporal) data are needed to adequately discriminate communities (Klemas, 2013) and to measure biogeochemical features needed for species discrimination and physiological function (Ustin et al., 2004, and Santos et al., 2012).

Although not referred to often, inland waters can be optically shallow too and then, in principle water depth and benthic composition can be mapped. Most likely this has not yet been done extensively as the water bodies with bottom visibility tend to be small or narrow and thus require high spatial resolution sensors.

2.2.3 Transitional ecosystems: estuarine, deltaic and lagoon waters

Transitional waters, as estuaries, deltas and lagoons, are situated at the land-ocean boundary. Depending on the tidal influence from coastal waters, but also on the freshwater influence from upstream, transitional waters are highly dynamic and often characterized by a typical flora and fauna. The transition from freshwater to marine conditions influences the distribution of suspended and dissolved matter, varying their concentration, size and physical–chemical composition. These transitional waters are important to mankind because many industrial, commercial, and recreational activities are concentrated in these regions (Brondizio et al., 1994; Razinkovas et al., 2008). These waters historically have been degraded by pollution from urban, industrial and agricultural areas and by land reclamation for sea defenses, building and agriculture. Management of these requires an understanding of the processes occurring in these water bodies (Elliott and Quintino, 2007). The transitional waters, due to their hydromorphology, respond rapidly to changes in forcing and are therefore characterized by wide temporal and spatial fluctuations in environmental variables (Newton and Mudge, 2005; Viaroli et al., 2007; Tagliapietra et al., 2009; Kuenzer et al., 2017).

Remote sensing can be a relevant, effective way of monitoring coastal transitional environments: the derived geospatial products typically include the same water column constituents as for inland waters but with the addition of water depth and benthic composition in the case of optically shallow waters. The new generation of high spatial resolution satellites (e.g. Landsat 8 and Sentinel 2) is providing a relevant contribution for coastal, inland and estuarine water applications (Concha and Schott, 2016; Toming et al., 2016; Brando et al., 2016). Moreover, modern experimental space-borne hyperspectral sensors along with airborne imaging spectrometry show an increasing capability for assessing optical properties and water components of transitional and coastal waters quality (Braga et al., 2013; Dekker et al., 2011; Gitelson et al., 2011; Lee et al., 2007; Santini et al., 2010) and for preliminary testing to design satellite-based systems (e.g., PRISMA, EnMAP, HyspIRI) (Hestir et al., 2015). Most of the applications were derived with physics-based (bio-optical model) inversion techniques or semi-empirical algorithms. For the physics-based inversion methods and for training

ANN and ML methods, a comprehensive bio-optical data set of the regional and temporal variability in optical properties and biogeochemical quantities is recommended (Aurin et al., 2010; Blondeau-Patissier et al., 2009; Brando et al., 2012).

2.2.4 Shallow coastal ecosystems: seagrasses and coral reefs, macro-algae

In shallow coastal waters, corals, seagrass and macro-algae habitats (e.g. kelp) provide important ecosystem services, both individually and through their functional linkages. Coral reefs are widely recognized as a valuable resource for tourism, fisheries and local economies but are susceptible to large-scale processes, such as rising ocean temperatures, acidification, changes in ocean water biogeochemistry, anthropogenic effects and competition by invasive species (LeDrew et al., 2000; Riegl et al., 2009).

Seagrass meadows play an important role in providing nursing and feeding habitats for many commercially and recreationally important fish species (Short et al., 1999; Ferwerda et al., 2007). These plants regulate the water quality of the water column as well as stabilize the bottom sediments. Changes in the distribution and structure of seagrass communities have impact on local and regional biodiversity, nearshore geomorphology and biochemical cycles. Canopy forming kelp beds play vital roles as a source of diet, shelter, and recruitment for multiple species including fish and invertebrates (Bennett and Wernberg, 2014) as well as ecosystem services such as carbon fixation and nutrient production and baffling currents and protecting the shoreline from erosion (Schaefer et al., 2015). At local scales, seagrass abundance and distribution loss happens due to overgrazing by sea urchins or severe storms (Byrnes et al., 2011), but are more likely to occur on a broad scale due to anthropogenic pressures such as pollution, nutrient overload, heavy suspended sedimentation, coastal development, and warming and acidifying waters caused by climate change.

In this context, remote sensing can obtain unique spatial and temporal information about these habitats (Dekker et al., 2006). Providing baseline estimates of the current extent, diversity and condition of seagrass meadows and coral reefs will enable the establishment of monitoring programs designed to detect disturbances at an early stage.

Medium spatial resolution Landsat imagery has been used to support shallow-tropical benthic habitat mapping both at the local scale (e.g. Marsa Shagra in the central Egyptian Red Sea, Purkis et al., 2004) and at a wider region scale (e.g. the Caribbean see Wabnitz et al., 2008). Similarly, medium resolution SPOT imagery (Cavanaugh et al., 2010; Casal et al., 2011) and high spatial resolution WorldView 2 and SPOT 6 imagery (O'Neill and Costa, 2015) have been successfully used for locally mapping giant kelp and bull kelp beds, respectively.

Seagrass and corals have been estimated from remote sensing with a variety of techniques, which includes classification techniques (Leiper et al., 2014), spectral inversion of bio-optical modelling (Dekker et al., 2011), and an assemblage of those methods (Purkis et al., 2004). Dekker et al., (2011) provided a comparative study of spectral inversion methods applied to airborne hyperspectral data for a Caribbean coral reef area and an Australian embayment. The results overall provided moderately accurate simultaneous retrievals of bathymetry, water column inherent optical properties and benthic reflectance in waters less than 13 m deep with homogeneous to heterogeneous benthic/substrate covers.

The spectral and spatial resolution of a sensor will determine which aspects of a habitat can be mapped (Mumby and Harborne, 1999). A coarse spectral/spatial resolution may be sufficient to differentiate coral reefs from seagrass beds while finer resolution may be needed to differentiate coral species and seagrass densities (e.g. Mumby et al., 1997). Multispectral satellite data has been used to produce maps of coral reef systems (Purkis et al., 2004; Yamano and Tamura 2004) and seagrass meadows (Dekker et al., 2005; Wabnitz et al., 2008). However, the spatial resolution of the sensor plays a key role in classification accuracies achieved for highly heterogeneous coral reef environments (Andrefouët et al., 2003). To accurately map changing coral cover over time, hyperspectral and very high spatial resolution sensors are required (Kutser et al., 2003; Hochberg et al., 2003; Phinn et al., 2008; Lim et al., 2009, Leiper et al., 2012).

An optical sensor's ability to identify floating kelp beds relies on the high near-infrared reflectance from the floating kelp, due to the interaction of light within the internal cellular structure of floating bulbs and fronds, in contrast with the very low NIR reflectance due to light absorption by the surrounding waters. The visible spectra also play an important role in the detection of kelp as a result of the characteristic reflectance peak in the green and red wavelengths due to the presence of chlorophyll-a and fucoxanthin, respectively (Cavanaugh et al., 2010; O'Neill and Costa, 2015). Submerged macro-algae can also be mapped from space using Landsat TM data as illustrated in Dekker et al., (2005).

2.2.5 Shallow water bathymetry

Bottom visibility provides challenges and opportunities to remote sensing of optically shallow waters. Fine scale data to determine near coast or coral reef bathymetric characteristics, especially at depths less than 20 m, are often required for a variety of uses (science, ship navigation and resource management). However, when mapped with traditional ship based methods using echo sounding, water depth measurements are costly and time consuming and might not be practicable at very shallow conditions. Moreover, in coastal and inland areas the variation of depth in time and space can be quite high and need regular updating; for instance, the seasonal strength of longshore currents often alters sediment movement, storms and currents may increase erosion, resuspension or sedimentation processes, and heavy rain events can increase drastically the input of sediments from rivers and lead to a short-time redistribution of the sediment bed of estuaries. Earth quakes can cause significant changes in shallow water bathymetry.

Remote sensing therefore provides an opportunity for gap filling (Gao, 2009; Pleskachevsky et al., 2011) or remote area mapping of water depth. Three methods exist for mapping bathymetry from airborne or spaceborne platforms: non-imaging LiDAR that uses timing to measure a laser based return signal from the air water interface versus the return signal from the bottom to calculate depth; imaging SAR that images surface wave patterns and infers bottom geomorphology from current driven changes and passive optical multi or hyperspectral imaging that analyses the light spectrum modification as it passes through the water body to the benthos and back again. Satellite based imaging represents a reasonably accurate and cost effective technology for fine scale mapping of near coast or reef bathymetric characteristics. Multi-spectral (e.g. Landsat-8; Sentinel-2) and commercial very high spatial resolution multispectral sensors (e.g. WorldView 2 and 3, RapidEye that measure the entire spectrum from ~ 400 to 800 nm in broad contiguous bands) offer an operational alternative for regional scale water depth mapping. Hyperspectral remote sensing provides improved estimates of water depth because water attenuates the signal from the bottom with a

strong wavelength dependency. Moreover, the signal from heterogeneous substrates might be spectrally complex and hyperspectral data provide more information for decoupling the remotely sensed signal from shallow waters (Lee et al., 2005, Botha et al., 2013) and down to greater depth (Botha et al., 2013).

2.2.6 Atmospheric and water interface

The signal measured by a satellite sensor is, the sum of the signal coming from a water area corresponding to a pixel, which has been attenuated by the atmosphere (through loss of photons due to absorption and scattering) and an additive radiative component due to the atmospheric scattering from adjacent areas into the field of view of that pixel. The total sensor-reaching radiance is mostly comprised of the atmospheric signal, i.e., > 90 % for low reflecting water bodies, which makes the removal of this signal a crucial step for the retrieval of biogeochemical properties (Gordon 1997). This relative atmospheric contribution in the blue significantly increases over CDOM-rich and organic matter rich but mineral suspended matter poor waters, i.e., boreal aquatic systems (Wang 2010), as CDOM and organic particulate matter absorb light significantly in the blue decreasing towards the green and yellow wavelengths. The atmospheric effects along the total path sun-atmosphere-target-atmosphere sensor are due to light absorption and (back) scattering. The absorption by gases induces strong absorption bands caused by the type of gas. As shown in Figure 2.1, the main absorbing gas is water vapour and then by order of importance ozone and dioxygen. It has been recently shown that industry or urban areas can produce nitrogen which has to be taken into account as well. As an example, at 0.4µm, the NO_2 transmission ranges from 0.985 to 0.995, inducing a possible error of 10-20 % on the retrieved water reflectance at some wavelengths. The strength of the absorption depends on the gas concentration. Gas also attenuates the radiation along the path by scattering.
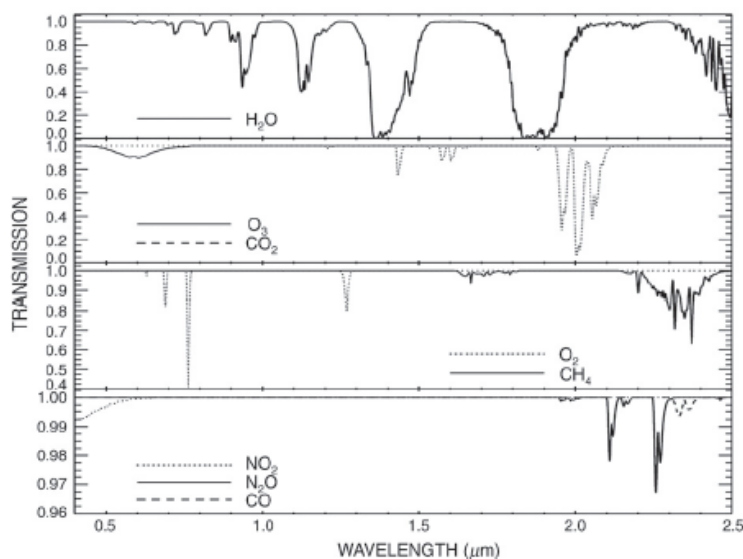
Figure 2.1 Transmissions of atmosphere gas (from Gao et al., 2009) Note that the wavelengths of interest for this study occur in the 0.38 to 1.00 micron area (380 to 1000 nm)

In addition to gaseous absorption, air molecules contribute to a significant amount of scattering, increasing the total measured signal across the spectrum in particular towards the blue and ultra-violet regions. Its impact within the blue portion of the spectrum follows a λ^{-4} law. Aerosols can absorb but also scatter a signal along its path. Its attenuation will depend on the aerosol type and its

abundance. Aerosols exhibit strong variations in time and space (Remer et al., 2005) especially over land-water boundaries. The removal of the aerosol scattering contribution (see Ch. 4) present over inland, coastal and coral reef waters remain one of the most challenging tasks in the atmospheric correction process.

Another challenge is quantifying the reflected signal contributions from surrounding non-water areas, i.e., land (vegetation, soils, beaches, coral islands) or ice. Due to their proximity to water surfaces, land or ice masses contribute to the total radiance budget reaching the sensor, especially if the scattered light from these high reflecting non-water targets change direction and seem to be coming from the water pixels. These contributions, called adjacency effects, cannot be neglected over a water body, particularly when an aquatic target pixel is adjacent to highly reflective pixels often associated with significant topographic features. The additive radiative component has several origins, where their relative contributions depend on the atmosphere composition, the spectral range and the environment of the targeted (water) and adjacent (vegetated or bare land, white sands or coral sands or ice) surfaces. They are the atmospheric upwelling radiance, the environment upwelling radiance and the surface-atmosphere coupling radiance referred to as adjacency effect. The relative contribution of these two last components cannot be neglected over water and needs careful estimation (Santer and Schmechtig, 2000; Bulgarelli et al., 2014).

To achieve a proper retrieval of the aquatic ecosystem surface reflectance (R_{rs}), it is thus necessary to measure or estimate the surrounding terrestrial reflectance as well as the atmospheric composition. § 2.3 explores the specific measurement requirements in more detail.

2.3   Measurement requirements (based on bio-optical or RTF based forward models)

A sensor system on a satellite platform for aquatic applications has to provide, in summary, data for environmental baseline reporting (environmental status), monitoring extreme events (algal blooms, river plumes, oil spills, floods) and providing time series of environmental information for assessing environmental condition and trend. These measurements provide management relevant information. These measurements from space will often be under sub-optimal conditions due to atmospheric composition, air-water interface effects, polarization, clouds and related shadows etc.

The accuracy at which an unknown parameter can be determined from a multi- or hyperspectral image depends on sensor properties, illumination conditions and optical properties of the environment, and the retrieval algorithm. For HICO, the first experimental spaceborne hyperspectral sensor (on board of ISS) designed specifically for coastal systems, the impact of sensor noise on the accuracy of chlorophyll-a, total suspended matter and CDOM concentration has been studied by Moses et al., (2012) for lake-typical concentrations and three retrieval algorithms. Assuming a perfectly calibrated instrument and an error-free atmospheric correction, they found that just sensor noise can introduce errors as high as 80 % in optically complex waters. A subsequent study (Moses et al., 2015) indicated that these errors might be reduced by 50 to 92 % by increasing instrument sensitivity by changing the objective's F-number from 3.5 (HICO) to 1.0 (fictive sensor). Such direct back-tracing of instrument requirements to the accuracy of constituent retrieval can be done for a limited number of cases (as in Appendix A.2.), but it cannot cover the entire range of water types, error sources and retrieval algorithms.

As there exist numerous retrieval algorithms and strategies to handle ill-posed problems caused by the non-uniqueness of the optical properties, and as it is difficult to assess propagation of systematic errors arising from calibration and atmosphere correction, an alternate strategy is chosen here to derive measurement requirements of optically complex waters. Using bio-optical modelling we simulated the changes of remote sensing reflectance induced by an altered optical water quality variable, benthic variable or water column depth of interest for a wide range of environmental aquatic ecosystem conditions. We then translated these reflectance changes to space borne sensor requirements such as spectral intervals and spectral resolution and radiometric sensitivity. The remote sensing reflectance or radiance (=reflectance or radiance emanating from the water body) needs to be transported through the atmosphere to the satellite sensor providing top of atmosphere simulations, thereby adding spectral and radiometric requirements. Together these simulations will provide the required signal to noise ratio (SNR) of the sensor. SNRs are however dependent on the ambient light field (e.g. low sun angles early in the morning and/or at high latitudes versus high sun angles at noon or at low latitudes) and we therefore also discuss the noise equivalent radiance differences (NEΔL) and noise equivalent reflectance differences (NEΔR) (see Wettle et al., 2004 for definitions) as they are more relevant for designing an appropriate sensor.

After determining these spectral and radiometric specifications we focus on the spatial resolution and geometric accuracy requirements; temporal resolution requirements and the atmospheric, adjacency effect and air-water interface correction requirements.

2.3.1 Bio-optical simulations of remote sensing reflectance and water leaving radiance

2.3.1.1 Theory

WASI-2D (Gege, 2014) is an image processing software for multi-and hyperspectral data from deep and shallow waters. It has been developed for inverse modelling of atmospherically corrected data from airborne sensors and satellite instruments and supports radiance as well as reflectance spectra. The executable program including user manual can be downloaded from the IOCCG website (IOCCG, 2013a), the source code can be obtained from the author on request. As WASI has been designed for accurate analysis of regional data by experienced users, but not for automated processing of large datasets covering a wide variety of optical properties, it is intended primarily for research and educational purposes. For the purpose of this study WASI was reparametrized with more detailed bio-optical variables.

The reflectance of water depends on the spectral absorption coefficient, $a(\lambda)$, and spectral backscattering coefficient, $b_b(\lambda)$, of the water layer. The most relevant components contributing to $a(\lambda)$ and $b_b(\lambda)$ are: pure water (index "W"), phytoplankton (index "p"), coloured dissolved organic matter (index "CDOM") and non-algal pigmented particles (index "NAP"). Their absorption and backscattering coefficients are so-called inherent optical properties (IOPs), which are additive:

$$a(\lambda) = a_w(\lambda) + C_p \cdot a_p(\lambda) + C_{CDOM} \cdot a_{CDOM}(\lambda) + C_{NAP} \cdot a_{NAP}(\lambda), \tag{1}$$

$$b_b(\lambda) = b_{b,w}(\lambda) + C_p \cdot b_{b,p}(\lambda) + C_{NAP} \cdot b_{b,NAP}(555) \cdot \left(\frac{\lambda}{555}\right)^{-n}. \tag{2}$$

The C's are the concentrations, and the star symbol indicates normalization to concentration (for phytoplankton and NAP) or wavelength (for CDOM). The normalized IOPs are called specific inherent optical properties (SIOPs).

All calculations are made with the software WASI 2-D. These simulate measurements of remote sensing reflectance R_{rs}, which is the ratio of upwelling radiance to downwelling irradiance, both above the water surface and excluding specular reflections at the surface. The model of Albert (Albert and Mobley 2003, Albert 2004) is used for the simulations, which expresses R_{rs} as a polynomial of fourth order of the quantity

$$u(\lambda) = \frac{b_b(\lambda)}{a(\lambda) + b_b(\lambda)}$$

(3)

The model can be used for optically deep and shallow waters and accounts for the sun zenith angle and the viewing angle. Its coefficients have been derived using Hydrolight (Mobley, 1994) simulations covering wide ranges of environmental parameters, including most of the high concentrations observed in inland waters.

More details are given in Chapter 2

2.3.1.2 Radiometric sensitivity (NEΔR, NEΔL and SNR)

There are 3 ways to describe the required or measured sensitivity of an earth observing sensor (Wettle et al., 2004): the noise equivalent reflectance difference (NEΔR), the noise equivalent radiance difference (NEΔR) and the signal to noise ratio (SNR). The exact definitions are presented in the Ch2 Appendix. From a sensor design point of view the NEΔL is the most important as that value is translatable to the amount of photons at a specific wavelength that the sensor optical device registers. NEΔL of a sensor is independent of the ambient light field. NEΔR is the noise equivalent reflectance (usually remote sensing reflectance, occasionally subsurface irradiance reflectance). The attractiveness of the NEΔR approach is that once an image or a suite of images or an entire archive of images is processed to remote sensing reflectance values a single algorithm can be applied giving consistent results (as there are no variations due to sun angle, atmospheric condition, sensor look angle etc.). However if we take the example of a northern hemisphere boreal lake at 60° latitude in winter or a tropical lake at 0° in spring the radiance (L) returning from each water body will be vastly different (much less photons impinging on the water body and thus being reflected from within the water body) whereas (if the optically active constituent concentrations are the same) the reflectance will be the same.

In a similar fashion the signal to noise (SNR) ratio is often used to depict the sensitivity of a sensor. However SNR is dependent on several definitions needing to be specified such as: the saturating signal, and a 30 % or 5 % bottom albedo in combination with a certain sun zenith angle and atmosphere condition, and a given TOA radiance spectrum. Another key issue is what the amount of radiance is that the sensor collects: in the case of the boreal lake in winter the amount of radiance (photons) is much lower than from the tropical lake. In this example the relationship for the SNR will be approximately related to the cosines of the sun angles.

In fact NEΔL or NEΔR are a science requirement used by industry to design the earth observing instrument and the initial data processing. In other words, if we want to discriminate two spectra characterized by NEΔL, the sensor (characterized by its SNR) and the processing need to have a total noise less than NEΔL (factor 2 is a minimum). It is the ratio NEΔL/L that is related to different scenarios (discrimination of spectra, different atmosphere conditions, during the year and at different latitudes…thus several sun zenith angles) that is key to understanding an optical and nearby infrared earth observing sensor's performance. Thus, although it is preferable to discuss sensor performance in terms of NEΔL, we also present results in NEΔR and SNR as that allows comparison with most of the literature on this subject.

It should be noted that the SNR is frequently used in a confusing way. Since the SNR depends on the signal and the measurement noise, it specifies the quality of a measurement, but not of a sensor. Confusion is caused by the fact that it is common practice to use the SNR for comparing or specifying optical sensors, even though no common definition of the underlying signal exists. To mention a few, the saturating signal (usually 100 %) is sometimes taken, sometimes a 30 % or 5 % bottom albedo in combination with a certain sun zenith angle and atmosphere condition, and sometimes a given TOA radiance spectrum. This inconsistent usage of SNR makes the comparison of sensors difficult (see Hu et al., 2012 for a method to compare sensors with varying SNR definitions).

Figure 2.2 illustrates the changes induced to R_{rs} by altering TSM from 0.2 to 10 mg/l (panel A), CHL from 0.2 to 5 μg/l (panel B) and the lope of the CDOM absorption SCDOM from 0.010 to 0.020 nm^{-1} (panel C). A shallow water simulation is in Panel D, illustrating the changes of the reflectance spectrum when the bottom substrate "Posidonia australis" is submerged in water of different depth ranging from 1 mm to 50 cm. In each case, the altered parameter was changed in 50 equidistant steps, while all other parameters were kept constant.

The largest changes in the amplitudes of R_{rs} are obviously introduced by changes of TSM (panel A) and water depth (panel D), but the spectral changes are difficult to recognize in this kind of representation. The spectral changes are better visible after normalization. Figure 2.11 shows the spectral R_{rs} normalized in the range from 400 to 900 nm. This normalization has least effect in the chlorophyll change graph (panel B) as at 550 nm chlorophyll changes have almost no effect.
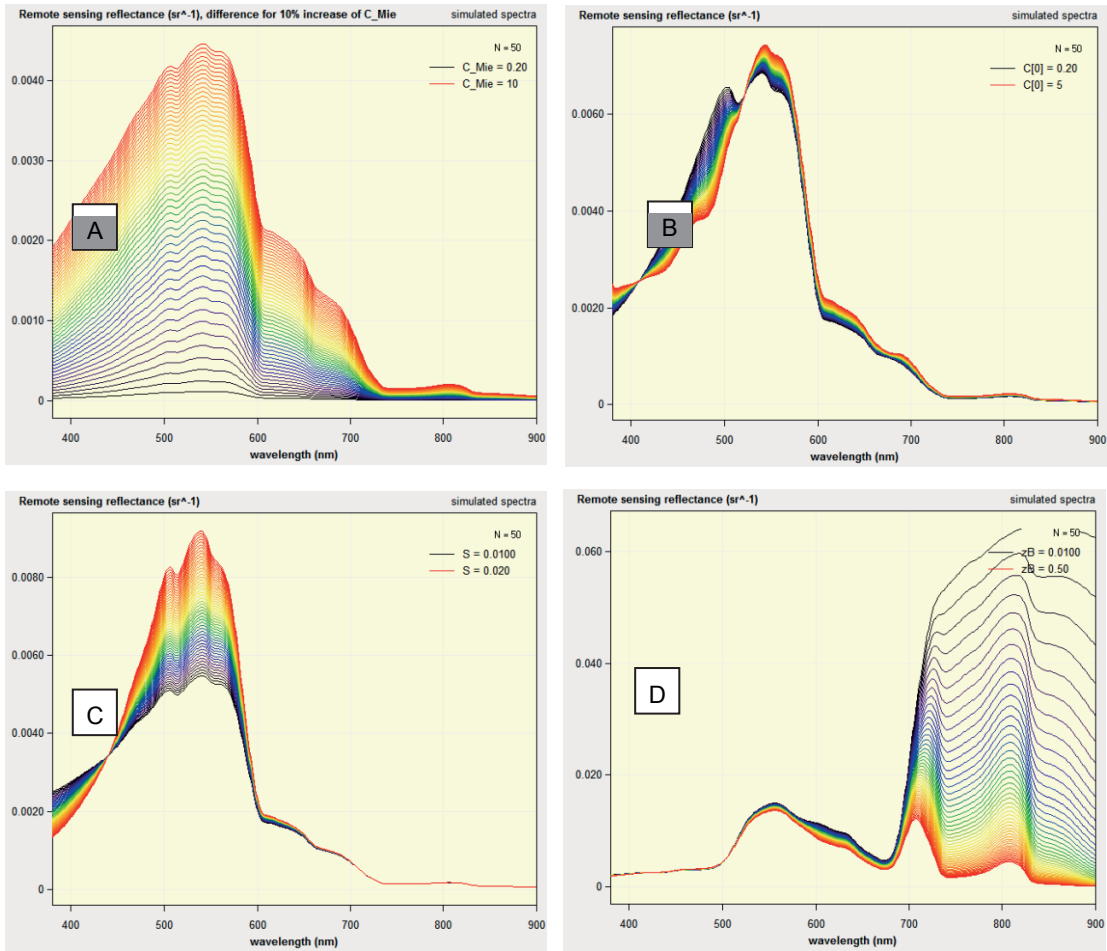
Figure 2.2 Remote sensing reflectance changes for (A) TSM range 0.2 - 10 mg/l, (B) CHL range 0.2 – 5 µg/l, (C) SCDOM range 0.010 – 0.020 nm^{-1}, (D) depth range 0.01 – 0.5 m with Posidonia cover of substratum
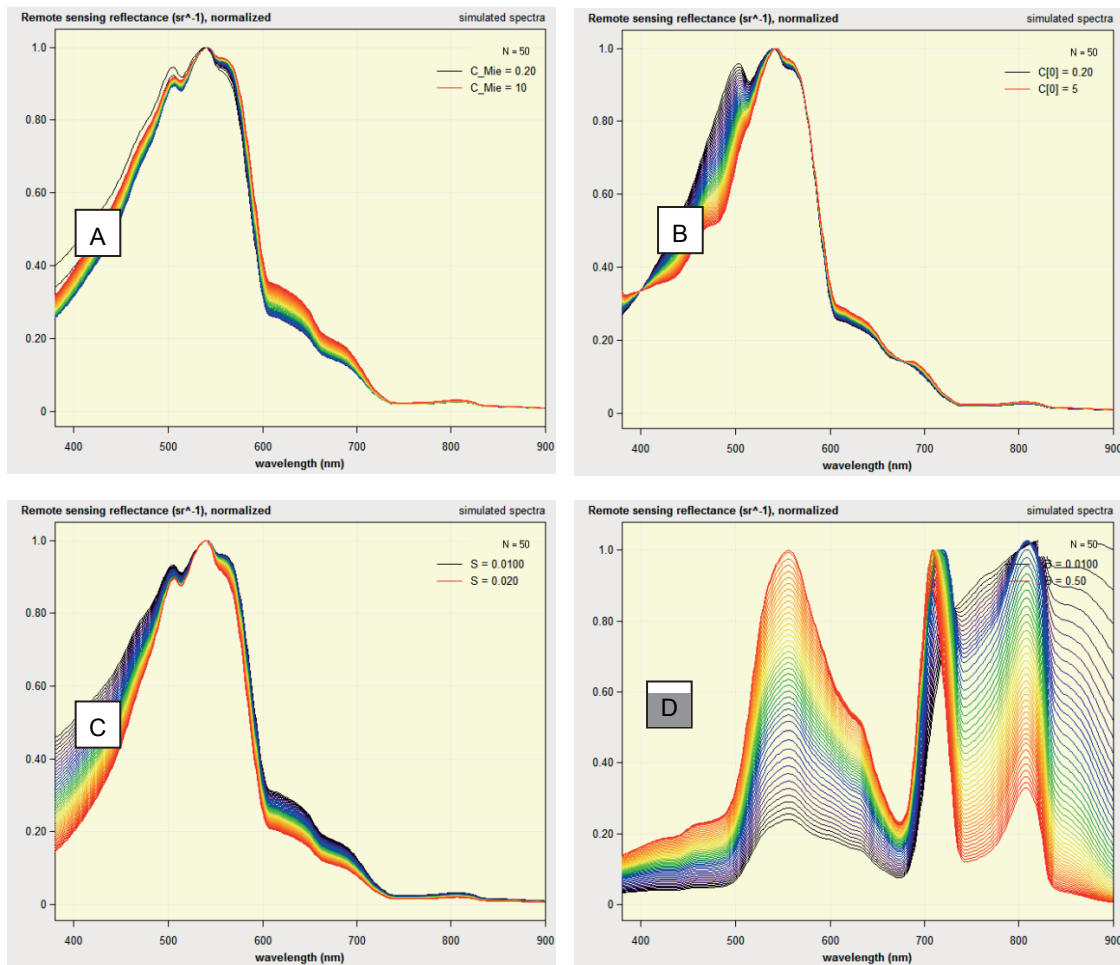
Figure 2.3 Normalized remote sensing reflectance changes for (A) TSM range 0.2 - 10 mg/l, (B) CHL range 0.2 – 5 µg/l, (C) S_{CDOM} range 0.010 – 0.020 nm^{-1}, (D) depth range 0.01 – 0.5 m with Posidonia cover of substratum.

For deep water (panels A, B, C), the normalized spectra show much less variability than R_{rs}, and variability is now more pronounced for changes of SCDOM (panel C) and CHL (panel B) than for changes of TSM (panel A). The reflectance maximum remains near 540 nm for all studied conditions, but the spectral shape undergoes systematic modifications.

For shallow water, Panel D illustrates the large spectral changes of remote sensing reflectance for water layer thicknesses between 1 mm (black) and 50 cm (red). The 1 mm case represents almost no water (a water depth of zero cannot be simulated for several reasons). The difference between any two curves corresponds to a water layer difference of 1 cm. The water not only decreases the amplitude of R_{rs} (panel D of Figure 2.2), but also changes the spectral shape markedly, which leads at certain spectral regions to a shift of the minima and maxima of the R_{rs} spectra.

Better suited for comparing or specifying optical sensors is the noise-equivalent radiance difference NEΔL which is a sensor property. The summary of the results is in section 2.3.6 and the full results in Appendix A.2.

Of particular relevance for defining sensor requirements are the extreme cases of the measurements of interest; if a sensor is suitable for the extremes, it will provide even better data in-between. This

concept of extremes is chosen to define the scenarios. The choice of extreme values for optically deep water (Table 2.1) is based on the lakes selected for the GLaSS project as these cover a wide range of conditions (Peters et al., 2015). Each scenario represents an extreme concentration of total suspended matter (TSM), coloured dissolved organic matter (CDOM) or chlorophyll-a (CHL) chosen close to a minimum or maximum of Table 2.1 in Peters et al., (2015). TSM and CHL are defined in units of concentration (g m^{-3}, mg m^{-3}), while CDOM is expressed in terms of absorption at 440 nm, aCDOM (m^{-1}).

Table 2.1 Scenarios for optically deep water. A scenario is defined by the extreme value of a parameter marked as bold. The other parameters are specified by a representative value and a representative range (min-max).

Scenario	X-	X+	Y-	Y+	C-	C+
Extreme for	low TSM	high TSM	low aCDOM	high aCDOM	low CHL	high CHL
Example	Lake Garda	Lake Taihu	Lake Garda	Finnish lakes	Italian lakes	Lake Taihu
TSM [g m^{-3}]	0.1	300	1(0.2-20)	2(0.5-5.0)	1(0.2-20.0)	50(10-300)
aCDOM [m^{-1}]	0.1(0.04-2.00)	1(0.2-3.0)	0.04	10	0.1(0.04-2.00)	1(0.2-3.00)
CHL [mg m^{-3}]	1(0.1-10.0)	20(1-1000)	1(0.1-10.0)	5(1-10)	0.2	1000
S [nm^{-1}]	0.014 (0.01-0.02)	0.014 (0.01-0.02)	0.014 (0.01-0.02)	0.014 (0.01-0.02)	0.014 (0.01-0.02)	0.014 (0.01-0.02)

The simulations for a scenario keep the extreme value constant and change a number of relevant model parameters within a range that is considered realistic for that scenario. As the concentrations of water constituents are not completely independent from each other (e.g. high CHL prevents very low aCDOM values as CDOM is a degradation product of phytoplankton), the parameter ranges were chosen with regard to the scenario-relevant lakes. The iterated model parameters include TSM, aCDOM, CHL, and the slope of CDOM absorption (S).

The following settings were chosen for the simulations:

- Phytoplankton absorption spectrum of green algae from the WASI database
- TSM absorption is approximated by an exponential equation (typical for detritus) with slope 0.0123 nm^{-1} and specific absorption coefficient 0.027 m^2 g^{-1} (Babin et al., 2003)
- The differences ΔR_{rs} x are calculated for $\Delta x = 0.1x$, i.e. they show the change of R_{rs} for a 10 % increase of the parameter x.
- The normalized differences $[\Delta R_{rs} x]N$ are calculated by dividing ΔR_{rs} (ΔRx) with the maximum of $| \Delta R_{rs} x|$ in the range 400 – 800 nm.

The scenarios of shallow water are defined by the irradiance reflectance spectra of bottom substrate. The water is represented by the low concentrations scenario representing relatively clear water. The bottom substrate spectra used are from a range of aquatic ecosystems such as inland water macrophytes, seagrass, macro-algae, corals and various substratum types:

0	Chara contraria (macrophyte)
1	Potamogeton perfoliatus (macrophyte)
2	Rock
3	Bleached coral
4	Dark silt
5	Bright sand
6	Yellow porites sp. (coral)
7	Purple encrusting coralline algae
8	Brown porites sp. (coral)
9	Posidonia australis (seagrass)
10	Detritus (sea-grass wrack)
11	Ecklonia radiata (a form of kelp)
12	Coarse coral rubble
13	Dark sand

The plots and results of all these simulations are shown in the Appendix A.2.

2.3.1.3 Spectral range and resolution requirements

A sensitivity analysis has been performed for a wide range of aquatic ecosystems (see Appendix A.2.) to determine the spectral range and resolution required to extract relevant information for optically deep and optically shallow waters from remote sensing reflectance spectra. According to these simulations, the ideal sensor is a hyperspectral instrument covering the range from 380 to 730 nm at a spectral resolution of 5 nm or better, and the range from 730 to 860 nm at a spectral resolution around 15 nm.

Only a hyperspectral sensor catches the high spectral variability in the visible with the capacity to discriminate the spectrally interacting water constituents and, in addition in optically shallow areas, water column depth and bottom substratum composition and cover types. Since the infrared region above ~730 nm is spectrally only influenced by particulate backscattering in the water and pure water absorption, the sensor could be multispectral in the infrared beyond ~730 nm.

The minimum spectral requirements for a multispectral sensor are summarized in Table 2.2. They combine the recommendations of IOCCG (2012) for ocean and coastal colour satellites with the results of derivative analysis and sensitivity analysis from the Appendix A.2., as well as some detailed a priori knowledge on spectral pigment absorption features. Multispectral sensors, through their reduced spectral coverage, limit the separability and quantification of water constituents and bottom substrates. Nevertheless multispectral satellites may be a cost-effective way for providing significantly improved capabilities by modifying existing terrestrial focused systems such as Landsat and Sentinel-2 that have adequate spatial resolution.

Table 2.2 Recommended minimum set of spectral bands for extracting information from remote sensing reflectance spectra of optically deep and shallow waters. The Table doesn't include bands required for monitoring of terrestrial surfaces or emerged vegetation or for correcting disturbing environmental influences (e.g. atmosphere, reflections at the water surface, cloud shadows-see Table 2.5). All these bands are suitable for assessing benthic composition, shallow water bathymetry, AOPs, IOPs and SIOPs. Note that for the algal pigment absorption maxima we have included reference bands for the 3 band pigment absorption line height approaches. Physics based spectral inversion methods do not specifically need these pigment reference bands but do need spectral bands where the pigments absorption effects are measureable.

Centre	FWHM	Water quality and benthic characterisation related application	
[nm]	[nm]		
+/-380	15	CDOM (Mannino et al., 2014) ; NAP; PFT (Wolanin et al., 2016); mycosporin-like amino acids (Dupuoy et al., (2008)	1
+/-412	5 to 8	CDOM (Mannino et al., 2014); PFT (Wolanin et al., 2016)	2
+/-425	5 to 8	CDOM ; Blue Chl-a absorption reference band ; NAP; PFT (Wolanin et al., 2016)	3
+/-440	5 to 8	CDOM (Mannino et al., 2014); Blue Chl-a absorption maximum; PFT (Wolanin et al., 2016)	4
467	5 to 8	Band required to separate Pheaocystis from diatoms (Astoreca et al., 2009); Blue Chl-a absorption band reference band; Accessory pigments	5
+/-475	5 to 8	Accessory pigments ; Blue Chl-a absorption band reference band ; PFT (Wolanin et al., 2016), NAP;	6
+/-490	5 to 8	Blue Chl band-ratio algorithm; PFT (Wolanin et al., 2016), Accessory pigments	7
+/-510	5 to 8	Blue Chl band-ratio algorithm ; NAP ;	8
+/-532	5 to 8	PFT & carotenoids (Wolanin et al., 2016); NAP	9
+/-542	5 to 8	NAP	10
555	5 to 8	NAP (as most algal pigments absorptions are low); Cyanophycoerythrin reference band PFT (Wolanin et al., 2016)	11
565	5 to 8	CPE in vivo absorption maximum and possibly fluorescence (Dierssen et al., 2015)	12
+/-583	5 to 8	CPE and CPC reference band; chlorophylls a,b and c (Johnsen et al., 1994); CPE fluorescence (Dierssen et al., 2015)	13
+/-594	5 to 8	PFT (Wolanin et al., 2016)	14
+/-615	5 to 8	CPC in vivo absorption maximum (Hunter et al., 2010)-avoiding chlorophyll- c	15
624	5 to 8	CPC in vivo absorption maximum (Dekker, 1993; Simis 2007), suspended sediment, PFT(Wolanin et al., 2016); chlorophyll c (Johnsen et al., 1994)	16
631	5 to 8	PFT (Wolanin et al., 2016)	17
+/-640	5 to 8	NAP, CPC reference band	18
649	5 to 8	Chl-b in vivo absorption maximum (Johnsen et al., 1994)	19
665	5 to 8	FLH baseline (Gower et al., 1999; Gilerson et al., 2008)	20
676	5 to 8	Red Chl-a in vivo absorption maximum (Johnsen et al., 1994)	21
683	5	Chlorophyll fluorescence (FLH) band (Gower et al., 1999; Gilerson et al., 2008)	22

+/-700	5 to 8	HABs detection; NAP in highly turbid water; reference band for 2 or 3 band Chl-a algorithms	23
+/-710	5 to 8	FLH baseline (Gower et al., 2005); HABs detection; NAP in highly turbid water; reference band for 2 or 3 band Chl-a algorithms	24
+/-748	15	NAP in highly turbid water (Ruddick et al., 2006) ; FLH baseline band (Gilerson et al., 2008)	25
+/- 775	15	NAP in highly turbid water (Ruddick et al., 2006);	26
		See table on atmospheric characterization bands for NAP relevant bands beyond the O_2 absorption feature at 761 nm.	

[1]Notes: CPC= Cyanophycocyanin; CPE= Cyanophycoerythrin; CDOM=Coloured dissolved organic matter; NAP= non algal pigmented particulate matter; Chl= chlorophyll; PFT=phytoplankton functional type; FLH = fluorescence line height; Note: NAP, blue and red chlorophyll absorption maxima and related reference bands and HABs detection do not have literature references as they are ubiquitous in literature. NAP scatters and absorbs light decreasing with increasing wavelength and thus does not need a specific band –although 3 bands without too much algal pigment or CDOM absorption are useful; The blue chlorophyll absorption band is centred around 438-443 nm in vivo; the red chlorophyll band around 676 nm in vivo. HAB's need estimation of Chlorophyll, CPE, CPC and any other accessory pigments where possible.

The wavelength positions in are a compromise between desired NEΔL, NEΔR, SNR, required spectral bandwidth as well as being able to have adjacent spectral bands suitable for distinguishing one or more variables that do not overlap.

In Lee et al., (2014) a study was performed for ocean and coastal water colour that used 5 nm contiguous bands over 400 to 700 nm to estimate whether a multispectral band set could sufficiently represent this full spectral band set. Their analyses found that 15 spectral bands of ~ 10 nm wide is sufficient for a chlorophyll range of ~0.02 to >100 mg m^{-3}, bottom depths from ~1 m to >1000 m (note by editors: simulating to 1000 m deep is irrelevant as the maximum depth from which a signal is retrieved in natural waters is about 40 m in the clearest oceanic waters), and bottom substrates including sand, coral reef, and seagrass. These authors do state that these results apply: 'provided that the focus of remote sensing is the primary variables instead of subtle spectral features'. Sun et al., (2015) repeated the Lee et al., (2014) study for set of optically deep hypertrophic lakes and reached similar conclusions with the exception of chlorophyll fluorescence contributing to the relatively lower spectral interdependence near 700 nm than at other visible wavelengths. They suggest that for sensor design, more spectral bands are required around 700 nm than in other visible wavelengths.

A FWHM for all bands could also be 5 nm as recommended from our simulations and by Vandermeulen et al., (2017), however, that reduction from 8 nm to 5 nm would also reduce the sensitivity by approximately 38 %. Vandermeulen et al., (2017) obtained spectra from a variety of water types (turbid river filaments, coastal waters, shelf waters, a dense Microcystis bloom, and oligotrophic waters), as well as individual and mixed phytoplankton functional types (PFTs; diatoms, eustigmatophytes, cyanobacteria, coccolithophores). Results show that a continuous spectrum of 5 to 7 nm spectral resolution is optimal to resolve the variability across mixed reflectance and absorbance spectra.

Research by Wolanin et al., (2016) on assessing Phytoplankton Functional Types (PFT's across diatoms, coccolithophores, dinoflagellates, chrysophytes, prasinophytes and cyanobacteria) showed that compared to multispectral bands, the continuous hyperspectral data usually yielded the best results. They also found that a small improvement was obtained for increasing the resolution of

hyperspectral from 10 nm to 5 nm, but no significant improvement was obtained for increasing resolution from 5 nm to 1 nm. For Trichodesmium Dupouy et al., (2008) determined a specific suite of pigment absorption linked to the Trichodesmium pigmentation: at 380 nm (MAA's =mycosporin-like amino acids, 438 nm (CHL), 470 nm (carotenoids), 495 nm (phycourobilin, PU), 547 nm (phycoerythrobilin, PE), 620 nm phycocyanin, PC) and 677 nm (CHL). These values are close to but not exactly the same as the bands proposed here. Astoreca et al., (2009) identified the need for a 467 nm centred band to detect and discriminate phaeocystis species. From a volume scattering function perspective Robertson Lain et al.,(2017) determined that the 709 nm region (carrying critical biomass and assemblage-related signal) is sensitive to the use of the comparative phase. They also confirm that the 550 to 650 nm bands contain absorption features of diagnostic accessory pigments useful in resolving for example, trophic status and the presence of diagnostic features of cyanobacteria, including phycocyanin pigment, and have previously been identified as sensitive to size-related assemblage variability as well. Information in these critical spectral regions is vital for PFT algorithm development including inversions and the retrieval of IOPs.

In summary, the requirements from literature and from our simulations indicate that 5 nm is an optimal spectral bandwidth from a spectral perspective but that 8 to 10 nm is required for increased signal levels. As several features of atmospheric or pigment spectral absorption lie close together spectrally it seems that 8 nm is reasonable compromise between these conflicting requirements (with 10 nm width there would be overlap in many areas between spectral features that need to be separately determined).

For the <380 and >748 bands a width 15 nm was chosen as there are no neighbouring essential bands and the sensor sensitivity in those ranges is lower due to silicon based detectors having lower sensitivity towards the deep blue and UV and towards the mid NIR.

In Turpie et al., (2015) the case is made that for detecting invasive (macrophyte) species in wetlands hyperspectral data is required as there is no a priori knowledge of the distinguishing spectral features.

This line of reasoning is also true for new algal species occurring due to eutrophication, coastal water acidification or water temperature changes. Another example of no a priori knowledge of the distinguishing spectral features feature is that of extreme waters such as acidic mining pit lakes (Glaser et al., 2011) , sugar mill ponds, sewage ponds etc., where water colours can vary from bright to dark: blue, to blue green, to green, yellow, orange, pink, red and deep red and many variations thereof.

Spectral requirements

Hyperspectral from aquatic ecosystems: 5 to 8 nm wide bands between 400 and 730 nm, with 15 nm wide bands from 380 -400 and from 730 to 1000 if limiting to the VIS-NIR range. See section 2.4.5.6. for atmospheric and air-water interface requirements; if multispectral then: 26 bands between 380 and 800 nm between 5 to 8 nm wide.

2.3.1.4 Radiometric Sensitivity Requirements (SNR and NEΔL and NEΔR)

The radiometric sensitivity requirement for a sensor is driven by dark waters that reflect little light due to low concentration of light scattering particles (TSM) or high concentration of light absorbing

matter (CDOM or NAP with high organic matter contents). Note that phytoplankton have both algal pigments that lower the reflectance (E.g., Chl-a absorption peaks at 443 and 676 nm as well as several cyanobacterial pigment absorption peaks between 490 and 630 nm) and algal biomass that increases the reflectance (and significantly so when containing gas vacuoles such as some cyanobacteria or coccolithopores). Absorbing water types can have remote sensing reflectance (R_{rs}) maxima below 0.005 sr^{-1} and R_{rs} minima in the order of 10-4 sr^{-1}, and 10 % concentration changes of chlorophyll-a can affect R_{rs} as little as 10-6 sr^{-1} and even below, which seems impossible to resolve by current spaceborne instrument at a fine spatial resolution.

A sensitivity analysis was made to derive recommendations concerning radiometric sensitivity (see Appendix A.2.). It is based on simulations of R_{rs} for a wide range of water types and uses two different approaches. The first approach investigates the radiometric sensitivity required to resolve the spectral signature of reflectance spectra between 400 and 800 nm at a SNR of 100:1, and the second approach investigates the maximum changes of R_{rs} in the range from 400 to 800 nm induced by 10 % concentration changes of chlorophyll-a, TSM (~ NAP) and CDOM. Both approaches lead to the conclusion that most challenging is the detection of algal pigments as CHL and CPC and CPE in dark water types. That means, the requirements concerning pigment detection determines the sensor requirements. Although it needs to be said that detecting any substance in a spectral area where reflectance is very low (e.g. measuring CDOM in a clear water body) will be challenging. Determining cyanobacterial pigments with the same accuracy as CHL will require higher radiometric sensitivity than for CHL as the concentration specific absorption is lower than for chlorophyll (Dekker, 1993). We did not simulate separate CPE and CPC SIOPs in these simulations; instead we used one cyanobacterial algal pigment spectrum that also contained these pigments.
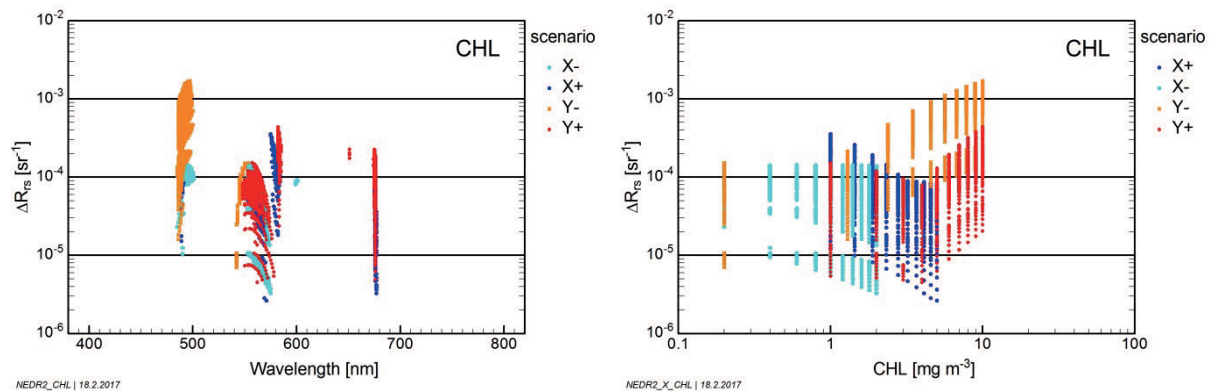
Figure 2.4 Maximum R_{rs} differences (ΔR_{rs}) induced in the range from 400 to 800 nm by 10 % changes of chlorophyll-a concentration (CHL) for typical water types ("scenarios"). The variability within a scenario reflects typical concentration ranges of CDOM and TSM. Left: ΔR_{rs} as a function of wavelength. Right: ΔR_{rs} as a function of CHL. See Table 2.1 for scenario description X and Y.

Figure 2.4 illustrates the impact of CHL changes on R_{rs} under typical conditions (see Appendix A.2. for definition of scenarios). The Figure shows that a sensor should be capable of resolving R_{rs} differences of about $1 \times 10\text{-}5$ sr^{-1}. This allows detection of CHL differences in the order of 10 % for most of the considered water types and concentration ranges, but not for all. A dedicated EO sensor, that is sensitive to CHL change detection even under difficult conditions, should resolve ΔR_{rs} of ~$3 \times 10\text{-}6$ sr^{-1}. Detection of TSM and CDOM is less critical, i.e. resolving R_{rs} differences of $1 \times 10\text{-}5$ sr^{-1} is

sufficient for most conditions. However CDOM detection in absence of enough scattering material in the water is also unlikely as there is no signal to work with.

2.3.2 Top of atmosphere simulations (SNR and NEΔL and NEΔR)

To derive sensor recommendations in terms of radiometric sensitivity, top of atmosphere (TOA) spectral radiance was simulated for 27 water types covering a wide range of optically deep waters, excluding extremely dark and extremely bright waters. These 27 reflectance spectra were obtained by combining 3 TSM concentrations (0.5, 1.6, 5 g m^{-3}), 3 CHL concentrations (1, 10, 100 mg m^{-3}), and 3 aCDOM values (1.0, 3.2, 10.0 m^{-1}). One SIOP parameterisation was used. TOA radiances were calculated for 2 sun zenith angles (10°, 70°) and 2 visibilities (10, 80 km) in the simulation a maritime aerosol and the U.S. Standard Atmosphere 1976 profile was used. The simulation were done for a nadir viewing geometry. For each parameter combination, the radiance differences were calculated for 5 relative changes of CHL (10 %, 20 %, 30 %, 40 %, and 50 %). Figure 2.5. illustrates these simulations for the darkest considered water type (TSM = 0.5 g m^{-3}, aCDOM = 10 m^{-1}, CHL = 100 mg m^{-3}).
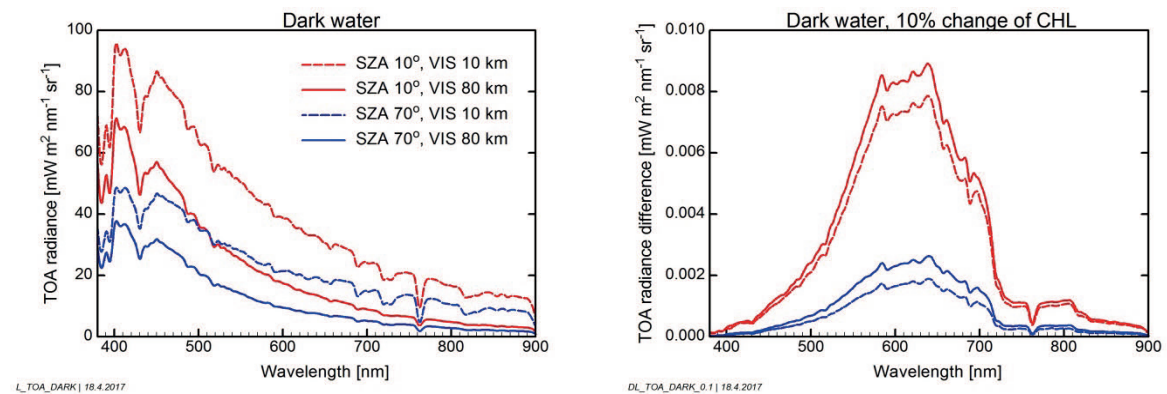
Figure 2.5 Left: TOA radiances of dark water for different sun zenith angles and visibilities. Right: Corresponding TOA radiance differences induced by changing CHL by 10%.

The TOA radiance spectra (LTOA) for the darkest water type and the 4 environmental conditions are shown in Figure 2.5 left. The corresponding radiance differences (ΔLTOA) induced by changing CHL by 10 % are shown in Figure 2.5 right. While LTOA depends strongly on sun zenith angle and visibility, ΔLTOA is mainly affected by SZA and only little by VIS. ΔLTOA is by several orders of magnitude lower than LTOA and has a completely different spectral shape. In this example it is a peaked function with maximum near 600 nm and a width around 170 nm. Since the highest sensitivity of a radiance measurement to CHL is at the maximum of ΔLTOA (λ), the ΔLTOA maxima are taken to specify the sensor requirement for radiometric sensitivity. The wavelengths and induced radiance differences of these maxima are shown in Figure 2.6 for 10 % and 50 % changes of CHL. For comparison the sensitivity of MERIS is also shown in Figure 2.6.
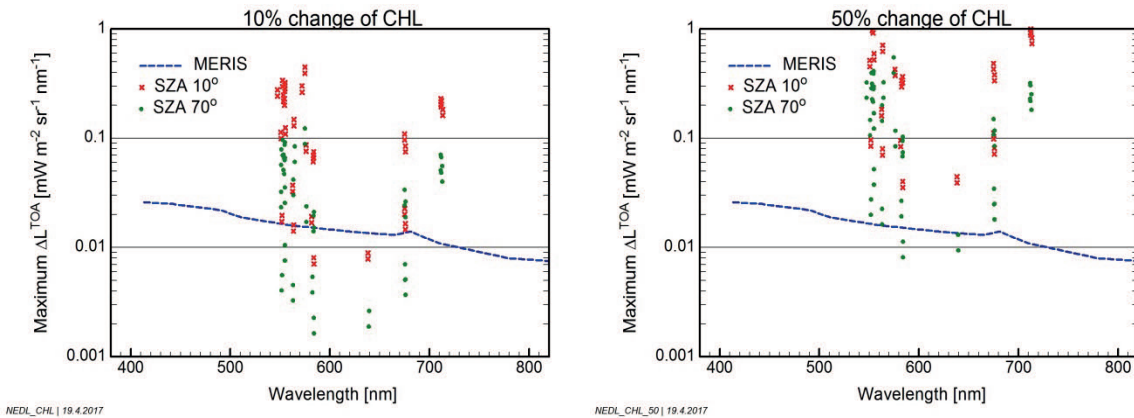
Figure 2.6 Maximum radiance differences induced at TOA by 10 % (left) and 50% (right) CHL changes, and sensitivity of MERIS for comparison.

Low sun elevation (green dots) produces lower radiance differences than high elevation (red crosses). The sensitivity of MERIS prevents detection of 10 % changes of CHL in many water types for low sun elevation, but makes it possible in most cases at high sun elevation. A 50 % change of CHL is detectable by MERIS in most water types even at low sun elevation. As a conclusion from the results presented in Figure 2.6 and Figure 2.7 (see Appendix A.2. for details) we recommend a sensitivity of NEΔL = 0.010 mW m^{-2} sr^{-1} nm^{-1} (minimum requirement) which is slightly more sensitive than MERIS in the visible. It induces a sensor signal for 82 % of the studied cases when CHL changes by 10 %, but already for 92 % of the cases for 20 % CHL changes, and 98 % for 50 % CHL changes.

The sensitivity to concentration is proportional to the radiometric sensitivity of the sensor. The optimal sensitivity is 0.005 mW m^{-2} sr^{-1} nm^{-1} or higher, which leads in 92 % of the studied cases to a detectable signal for CHL changes of 10 %, and in 100 % for CHL changes above 30 %.The radiance range for which such high sensitivity is required is illustrated in Figure 2.6. To cover the studied range of water types and environmental conditions, the sensor should not saturate up to radiances of 100 mW m^{-2} sr^{-1} nm^{-1} in the blue and 20 mW m^{-2} sr^{-1} nm^{-1} in the red and near infrared.

In addition to the analyses presented here, the SNR requirements for a mission with ocean colour capabilities have been well documented in Del Castillo (2012). The document calls for SNRs ranging from 600 to 2000 within the UV, visible, and the NIR parts of the spectrum.

Radiometric requirements

Maximum radiances over dark water bodies: 100 mW m^{-2} sr^{-1} nm^{-1} in the blue and 20 mW m^{-2} sr^{-1} nm^{-1} in the red.

Maximum radiances for monitoring extremely turbid waters, bleached corals, and shallow waters with bright sand: 400 mW m^{-2} sr^{-1} nm^{-1} in the blue and 200 mW m^{-2} sr^{-1} nm^{-1} in the red.

Radiometric sensitivity NEΔL: in the range 0.005 mW m^{-2} sr^{-1} nm^{-1} (optimal) and 0.010 mW m^{-2} sr^{-1} nm^{-1}.

2.3.3 Spatial resolution and geometric accuracy requirements

The requirements for spatial resolution across all aquatic ecosystems are quite complex. They vary from microscale (10's of cms) for e.g. highly biodiverse coral reefs through to kilometre scale for the largest inland lakes with surface areas of 1000's of square kilometres. For a global mapping mission

it is important to strike the right balance between spatial, spectral radiometric and temporal scale as well as data rates for direct broadcast and image processing capacity. If, as determined above we need high spectral (5 to 8 nm on average) and radiometric resolution as high priorities, whilst requiring to resolve spatial features of relevance at a global scale, it seems that the inland water requirements could be taken as a lead requirement applicable the other estuarine, lagoonal, coastal, seagrass, macro-algal and coral reef requirements.

 For freshwater ecosystems spatial resolution is one of the primary limiting factors in the application of satellite remote sensing (Ozesmi and Bauer, 2002). When considering spatial resolution requirements for inland water systems, the determining factor is the pixel size of the sensor system relative to the size of ecosystem of interest. This will vary depending on the type of system, the particular geometry of the feature, and the geography of the target region.

Coastal and inland aquatic targets are composed of three primary habitat levels types: at or above the water's surface (e.g., floating biota, emergent or terrestrial vegetation), the water column composition and the benthic environment. The dominant feature for the macrophytes, seagrasses, macro-algae and corals are habitats formed by key species, which require a pixel size finer than for water column composition of optically active constituents. These water column features (plumes, eddies, blooms) typically have larger scaled features, albeit much more transient (thus requiring finer temporal resolution). A hard limiting factor is the size of the water body of course. If it is impossible to fit 3 by 3 or 4 by 4 pixels within the coast line of a water body- there will likely not be one valid pixel available. Commercially available satellite data can now provide from 5 m down to 0.34 m (panchromatic) and 1.3 m (multispectral data) e.g. Worldview 3. Therefore this study looks at spatial resolution of 10 m or more (because we also need high NEΔL and high spectral resolution of 5 to 8 nm).

The ability to resolve rivers from space requires much higher GSD than lakes. The vast majority of global river reaches are less than 10 m wide, requiring a sensor resolution of ~3 m (Table 2.3). Less than 1 % of total river reaches are resolvable at the MERIS/OLCI sensor type resolution of 300 m pixels, and only 12 % of all river reaches are resolvable using Landsat sensor type resolution of 30 m pixels. Encouragingly, more than one quarter of global river reaches are wide enough to be resolved from sensors (> 17 m GSD). As this study already decided that 5 to 8 nm is the desired spectral bandwidth and we intend to have spatial resolution greater than 10 m as well as wanting to image as many water bodies as possible with sufficient radiometric sensitivity, aiming for the ~17 m spatial resolution seems to be the best compromise. This 17 m spatial resolution is indicative and not an absolute value. For an actual specific sensor design it is recommended to do a more detailed end-user requirements analysis to determine the required spatial resolution. Although we will be using the 17 and 33 m spatial resolution as baseline and threshold levels respectively they are meant to be approximately ~17m and ~ 33 m, where e.g. technological advance may allow a spatial resolution of 10 m pixels to be possible for a global mapping mission with sufficient spectral and radiometric resolution.

Due to shoreline complexity of water bodies and cloud cover, the actual number and area of lakes and river widths resolvable in each size class will likely be less than the estimates provided herein. For example Sayers et al., (2015) determined that MODIS 4-km product would be expected to retrieve CHL values for approximately 1000 lakes worldwide (Verpoorter et al., 2014). The use of 1

km MODIS imagery provides information on a substantially larger number of lakes, approximately 19,000 worldwide; the 300 m resolution Sentinel-3 OLCI and previous MERIS data have the potential to map CHL distribution for lakes ≥ ~1 km², numbering approximately 170,000 in the Global Lakes and Wetlands Database (GLWD). Similarly, using an analysis of polygons, Hestir et al., (2015) determined that MERIS FR 300 m resolution is capable of observing more than 50 % of the area of inland waters in Europe. However, MERIS observed only a few percent of Australia's water bodies, where a 30 m resolution sensor resolved less than 50 % of the area due to differences in topography and water body geometry.

This demonstrates that spatial resolution requirements may differ substantially based on geography. However, global requirements should be prioritized over local ones in the design of an aquatic ecosystem earth observing sensor.

To illustrate the importance of spatial resolution in observing tidal wetlands, a pixel size or GSD simulation was applied to a wetland mask to derive the percentage of pixel mixing as a function of resolution for a large marsh system (Turpie et al., 2015). Figure 2.8 shows the fraction of the wetland type that remains unmixed as the pixel size increases. Generally, 30 meters (the fourth circle) is where significant degradation begins to occur and beyond 60 meters the loss is substantial. Therefore, 60 m or coarser resolution sensors are less appropriate for mapping, assessing, or monitoring marshes, mangroves or similar wetland systems globally.

Table 2.3 Ground sampling distance requirements showing the resolvable river width class and cumulative number of total river reaches of the world's rivers based on spatial analysis by Erin Hestir using the Pavelsky et al., (2012) dataset .

River Reach Size Class (width)	Required GSD*	Total number of reaches	Percent of total reaches
≥ 1.5 km	500	2,877	< 0.1%
≥ 1 km	333	8,483	<1%
≥ 0.5 km	167	35,420	1%
≥ 0.1 km	33	382,466	12%
≥ 0.05 km	17	766,303	24%
≥ 0.01 km	3	2,576,452	81%
*Calculated using a box of 3 x 1 pixels sufficient to resolve the width of the river reach			

Table 2.4 Ground sampling distance requirements showing resolvable size class and total cumulative number and area coverage of the world's lakes larger than 0.2 ha (The lake spatial analysis was conducted by Mark Matthews based on assumptions using the Verpoorter et al., (2014) dataset).

Size Class	Required GSD*	% Total Area	Total number
≥ 10 km²	1054 m	44	25,976
≥ 1 km²	333 m	60	353,552
≥ 0.1 km²	105 m	80	4,123,552
≥ 0.01 km²	33 m	90	27,523,552
≥ 0.002 km²	15 m	100	117,423,552
*Calculated using a box of 3 x 3 pixels sufficient to resolve the specified lake size			
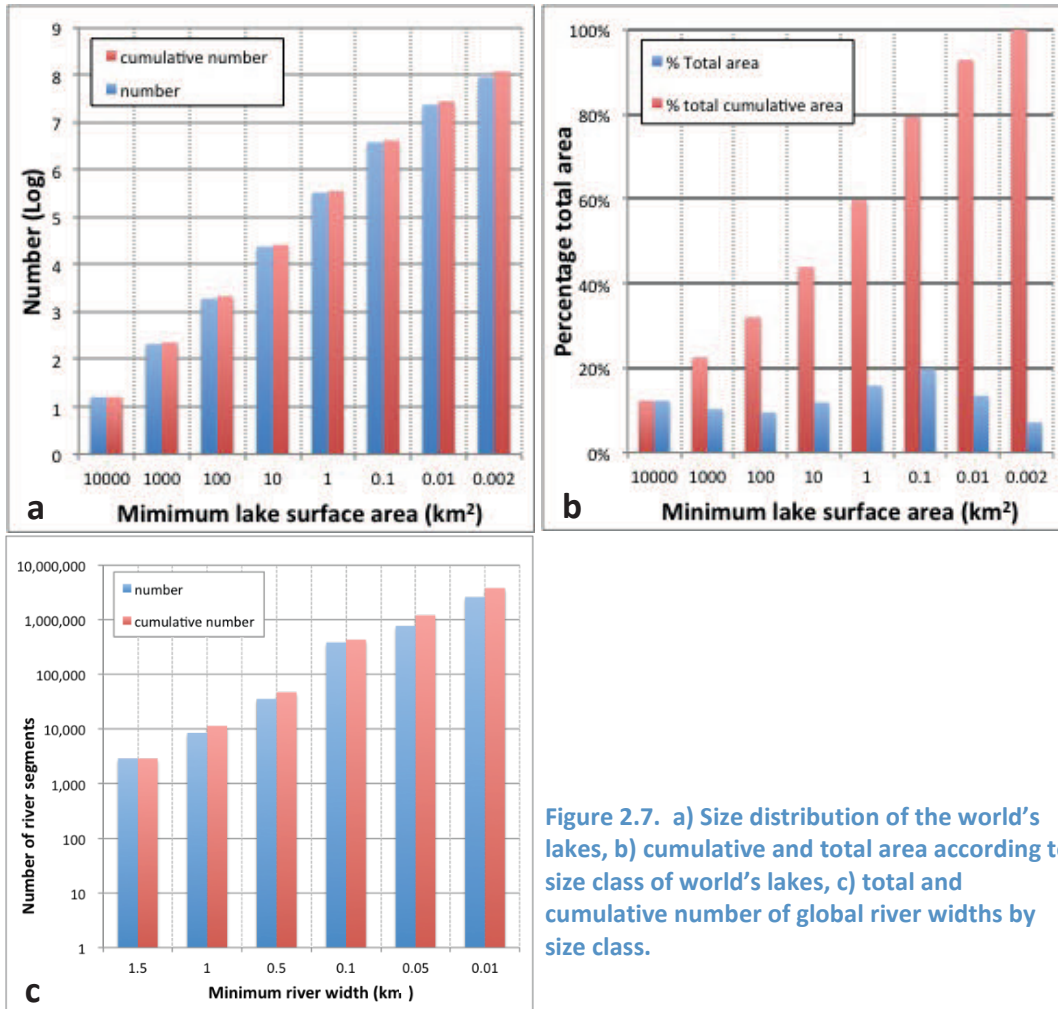
Figure 2.7. a) Size distribution of the world's lakes, b) cumulative and total area according to size class of world's lakes, c) total and cumulative number of global river widths by size class.
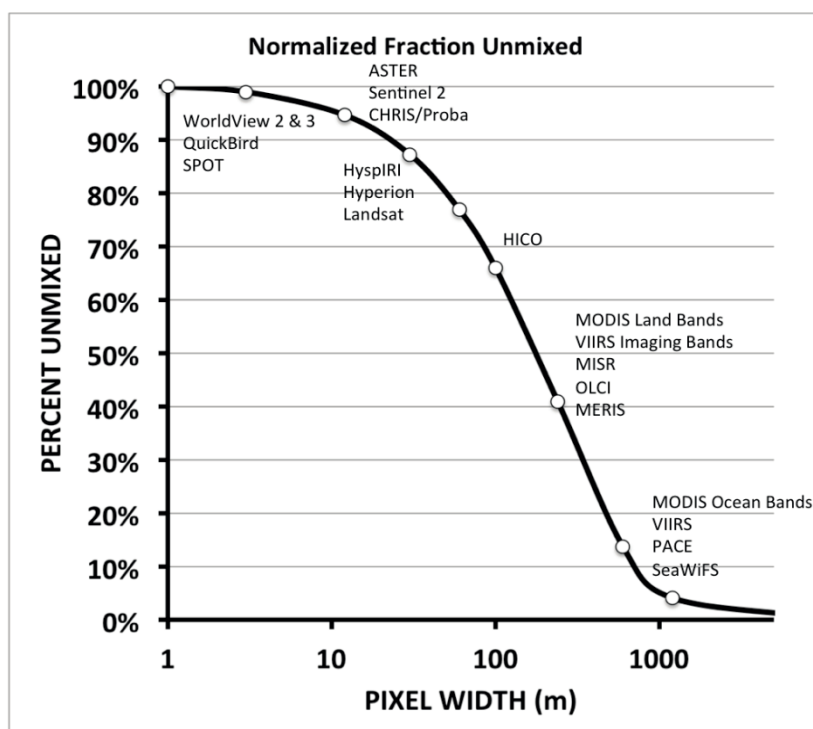
Figure 2.8 Effects of increasingly coarser resolution on pixel mixing over an example wetland. Shown fraction of the estuarine and marine wetland (simulated at one-meter resolution) that remains unmixed as a function of pixel size.

The maximum coverage necessary for a coral, coastal and inland water observatory is significantly less than global as the ocean waters are not included, but it is spread across most of the Earth's landmasses and waters near their margins (see Figure 2.9) with some corals also present in deep ocean environments.

A search for estimating global surface area for inland waters, wetlands, estuaries, coastal waters, seagrass and coral reef extent was found to be more difficult than anticipated as definitions vary, may overlap or have gaps. A very approximate estimate of the worlds land and ocean area is that wetlands are between 1.9 to 2.3 % (Lehner and Dohl, 2014), broadly defined including ~1 % inland waters (Downing et al., 2006, Gong et al., 2013 and Verpoorter et al., 2014), estuaries about ~0.2 % , seagrasses and corals less than ~0.1 % each and coastal waters (up to 20 km offshore) are 1.4 % to 2.4% global surface (this large variance is due to the length of coastlines being subject to the level of detail used for tracing a coastline). Importantly it seems that the combined surface area % of these non-oceanic aquatic ecosystems is about ~11.1 to ~15 % of the Earth's land surface (or 3.7 to 5.1 % of the total earth's surface) equal to about 19 to 26 million km^2. We emphasize that this assessment is very approximate and should be verified in future. This maximum of ~ 15% of land surface area also means that a dedicated aquatic ecosystem medium to high spatial and high spectral resolution mission as proposed here in the threshold situation would only need to image and process this amount of surface area; in a baseline for this sensor system all terrestrial and aquatic ecosystems

could be imaged as this sensor would also be highly suitable for terrestrial Earth observation applications.
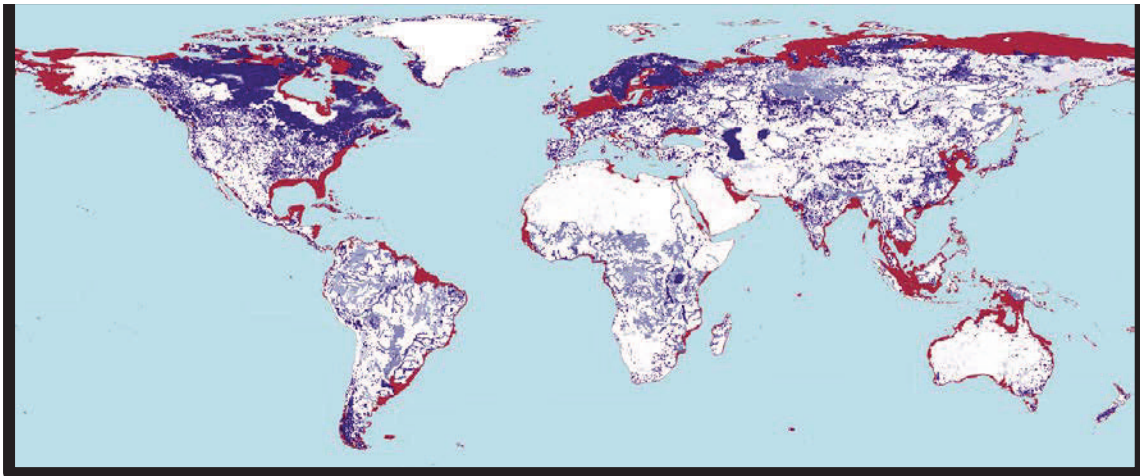
Figure 2.9 Global distributions of coastal and inland aquatic ecosystems. Red indicates regions where water depth is less than 50 m and where land elevation is less than 50 m. Light to dark violent gives the concentration of inland wetlands, lakes, rivers and other aquatic systems. Increased darkness means greater percentage of areal coverage for inland aquatic ecosystems (UNEP-WCMC, 2005 a & b).

Spatial requirements

Global coverage: all inland wetland, estuarine, deltaic, agonal, coastal and coral reef waters with water depths less than ~30 m and larger than ~0.002 ha.

Spatial resolution: ~17 m (baseline) to ~33 m (threshold).

The geo-location accuracy may be determined by direct observation of geographic features in images coupled to the geometric knowledge of the instrument orientation mounted on the platform with respect to on board attitude control systems and pointing knowledge of the platform. A normal target range to be set is that the geo-location knowledge should be better than 0.5 pixels (as else pixel locations get confused and post flight geometric correction would always need to be applied) and thus preferably (Threshold) in the order of 0.4 pixels or less in along and across track directions. Which equates to 0.4 * 33 = ~ 13 m for the coarser spatial resolution and to 0.4 * 17 m =~ 7 m for the finer spatial resolution. Baseline requirement is 0.2 pixels or less in along and across track directions.

Geometric requirements

Georeferencing: Threshold is 0.4 pixels in along and across track directions; baseline is 0.2 pixels in along and across track directions.

2.3.4 Temporal resolution requirements

For time dimension, the range is the duration over which observations are made, during a single mission or series of missions and resolution is the temporal sampling rate. For LEO missions, this is defined by the revisit period for a single satellite or constellation of satellites and swath width of an imager. For LEO polar orbiters sun synchronicity is possible: passing over the same area at the same time during the day. Other LEO orbits (such as the International Space Station) pass over the equator

multiple times day in an inclined orbit that reaches about 53° North and South maximally-this orbit is not sun-synchronous. For GEO orbits with the sensor stationary above fixed location on the equator, the temporal sampling is determined by the image collection rate. In either case, the cloud cover frequency and duration set a lower limit for effective sampling. Temporal sampling duration and resolution are important in determining whether a sensor will observe seasonal, inter-annual, or inter-decadal variation (i.e., tending toward studies of responses to climate change and increasing anthropogenic pressures or providing the ability to distinguish between periodic and secular trends).

Episodic changes and diurnal cycles in the environment, including variation in light, temperature, atmospheric aerosol and cloud formation, absorbing trace gas fluxes, surface wind, mixing depth, current, and precipitation and watershed hydrology could influence observations of coral reef, coastal and inland aquatic environments. Coastal tidal waters and wetlands can be subject to a variation with tides, which can periodically change the flux of optically active constituents in the water column. LEO, sun-synchronous polar orbits used for global mapping of environments would sample these processes at the same time of day, only providing one point in diurnal cycles and aliasing the tidal signal. Either long-term time series are needs to wash out these effects or an ~hourly observation strategy must be put into effect. Some regions near coasts will form clouds during the same time of day (e.g., tropics), seasonally, or over most of the year (see Figure 2.10), obscuring observation of all or the same interval of diurnal responses in coastal and inland aquatic environments. The use of models and auxiliary observations from SAR imagers (e.g., Sentinel-1) or surface measurements could help fill in the gaps caused by a persistently or periodically opaque atmospheric in the visible region of the electromagnetic spectrum but only for vegetation or related material that is at the surface or above the surface.

Monitoring phytoplankton blooms or the effects of episodic river discharges requires temporal sampling of a few days or less. Conversely, long-term secular changes in static characteristics of habitats formed by foundational species (e.g., wetland and submerged aquatic vegetation and corals) could be satisfied with less frequent observations, provided tidal, periodic or episodic changes are considered. Temporal sampling of these changes can be as coarse as monthly or seasonal, provide they are observed under consistent conditions. However, changes in phenology would require several observations over short periods of time during the key phases of the growth cycle. Elmendorf et al., (2016) proposed that graminoïd (marshes) and trees (swamps and mangroves) should be sampled as frequently as once every couple of days during key stages during the growth cycle as part of the design work for observing phenology for the National Ecological Observatory Network (NEON). Thus, observing change in phenological patterns in more stationary communities require higher temporal observations than observing changes in distribution and extent.

Preferences about the temporal frequency of information delivery can change with the aquatic ecosystem parameter considered and its periodic cycle if present (e.g. recurrences of algae blooms with seasonal conditions or growing circles of macrophytes). Conversely, preferences can be imposed by the possible presence of unknown and unpredictable events during periods with particular exploitation pressure of the water resource (e.g. bathing season, water capitation during the drought season, coral bleaching events).
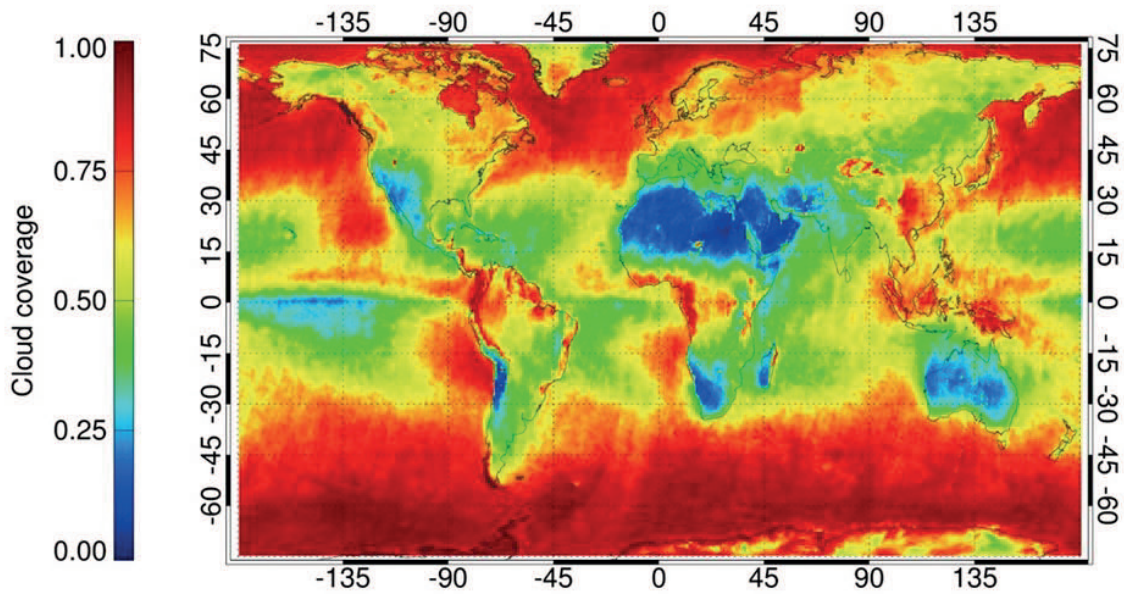
Figure 2.10 Global annual mean cloud cover derived from three years (2007–09) of Envisat data. The map shows areas with little to no cloud coverage (blue) as well as areas that are almost always cloudy (red). West coasts of most landmasses and open water regions at high latitudes are prone to cloudiness around the year. Data from both the MERIS and AATSR instruments on Envisat were used. Credits: ESA/Cloud–CCIs http://www.esa.int/Our_Activities/Observing_the_Earth/Space_for_our_climate/Highlights/Cloud_cover (on 6 November 2016).
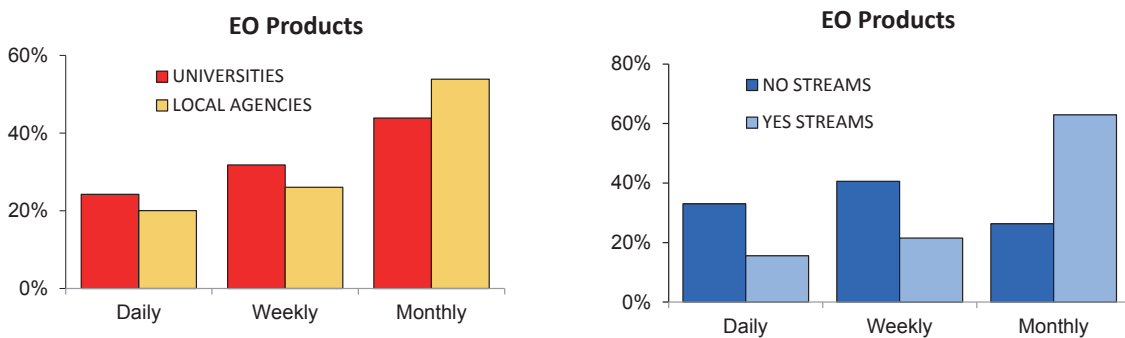
Figure 2.11 Bar charts showing the temporal frequencies preferred by end-users subdivided in groups (left: not working or working on streams and rivers, right: working in Universities/Research Institutions or Local Agencies (Source: C. Giardino, CNR, Italy, from INFORM Project, www.copernicus-inform.eu).

For the temporal frequencies the inland water end-users answers have been analysed dividing them in different representative groups (Figure 2.11). Comparing the two categories of products it can be seen that for the EO derived products there is a general tendency in preferring the monthly temporal frequency, especially end-users working also on streams and rivers. End-use that requires at least one product per month, will need much more frequent coverage taking into account the risk of sun glint (avoidable by proper sensor and platform geometry design), wave foam, clouds, fog, smoke and haze etc.

With respect to the time of the day a single sun synchronous acquisitions might be insufficient to capture phenomena with a high degree of change, such as re-suspension of suspended matter due to tides or storms or cyanobacterial blooming. Geostationary platforms with suitable earth observing sensors may provide relevant high frequency data, although spatial resolution will be lower indicating that GEO sensors would be used mainly for medium to large aquatic ecosystem areas.

Due to this large variation in end-user requirements and the priority for spatial resolution between ~17 to ~33 m with fine spectral bands with sufficient radiometric resolution the temporal requirement is as high as is technologically possible and affordable. An absolute minimum would be Landsat frequency as that would deliver seasonal data, whilst the dual sensor Sentinel-2 frequency is preferable (once every five days). But essentially the revisit should be as high as possible (baseline one overpass per day and threshold one overpass once every 3 to 5 days) as especially the water quality characteristics change rapidly. However, larger water bodies (in excess of 1 by 1 km) can be imaged more regularly by the ocean colour sensors such as Sentinel-3. For substratum measurements and bathymetry these requirements are more relaxed as only one cloud free image per season is required, unless there is an extreme event such as coral bleaching, cyclone/hurricane, tsunami or man-induced damage such as dredging or pollution events that need to be monitored. A mix of LEO sensors in polar orbit, complemented by sensors on board of e.g. the international space station (or LEO sensors) covering the mid and lower latitudes complemented by highest spatial resolution possible geostationary sensors would be the optimum configuration.

> **Temporal requirements**
>
> The temporal requirement is as high as is technologically possible and affordable. An absolute minimum would be Landsat frequency whilst once every one to five days is much better. But essentially the revisit should be as high as possible as especially the water quality characteristics change rapidly. For substratum measurements and bathymetry these requirements are more relaxed as only one cloud free image per season is required, unless there is an extreme event such as coral bleaching, cyclone/hurricane, tsunami or man-induced damage such as dredging or pollution events that need to be monitored.

2.3.5 Atmospheric, adjacency effect and air-water interface measurement requirements

As we presented in 2.2.6 the proposed sensor or sensor system (flying in tandem with atmosphere capable sensors) will need to have the capability to also measure relevant atmospheric composition components such as aerosols, the atmospheric gases and water vapour that affect the measured aquatic ecosystem reflectance spectrum at the top of atmosphere including the atmospheric adjacency effect. To correct for the atmospheric adjacency effect it is essential to have (for all the spectral bands) non-saturated data over the land pixels. The requirements for air water interface corrections, specifically sun glint and sky glint of water surface that may be affected by multiple wave types (capillary waves, refractive waves, wind induced waves, current affected waves and swell) are different as they occur across the measured spectrum and are by definition the colour of the blue sky (diffuse irradiance reflected at surface = sky glint) or of the sun.

2.3.5.1 Ozone absorption

Absorption by ozone impacts the radiance mainly between 500 nm and 700 nm and has to be corrected for based on the ozone concentration. The total columnar ozone is normally taken from external data sources (such as TOMS, OMI, ECMWF, GOME (Bracher et al., 2005)), although some algorithms are being developed to retrieve columnar ozone from the image through a spectral fitting method applied to the Chappuis absorption band between 400 and 650 nm with maxima around 577 and 605 nm (Gorshelev et al., 2014).

2.3.5.2 NO$_2$ absorption

Nitrogen dioxide (NO$_2$) absorbs at wavelengths lower than 600 nm with a peak in the blue region around 412 nm. In the atmospheric correction, the importance of NO$_2$ absorption has often been neglected or assumed to be constant in time and space. However near urban or industrial areas the NO$_2$ concentrations can be significant. Gao et al., (2009) indicated that neglecting NO$_2$ absorption in the atmospheric correction process can lead to errors in the order of 10 to 20 % in the retrieved reflectance at ~400 nm over dark targets as coastal waters. We therefore recommend taking into account the NO$_2$ amount in the atmospheric correction. NO$_2$ amounts are retrieved from satellites missions such as SCIAMACHY, GOME-2 and OMI and other future atmospheric composition focused missions.

2.3.5.3 Water vapour

Water vapour is the gas having the most important radiative impact in the spectral areas considered for aquatic ecosystems. It may have high spatial and temporal variability. All methods to estimate water vapour require the presence of a measurement band in the water vapour absorption feature centred at 820 nm and/or 940 nm (for SWIR at 1130 nm) and two reference bands at about 770 nm and 870 nm for the 820 nm feature; at about 870 and 1020 nm for the 940 nm feature, and at about 1050 and 1135 nm for the 1130 nm feature. Some more recent methods use first and second derivatives of a full spectrum (Miesch et al., 2015 and Rodgers et al., 2001) leading to a sensor hyperspectral requirement.

2.3.5.4 Aerosols

Measuring aerosols requires separating three areas of application: estimating aerosols over land, over dark water bodies and over bright water bodies

• Aerosol information from nearby land pixels – these require the same spectral bands as determined previously for aquatic ecosystem variables augmented by the bands required for dark and bright water bodies.

• Aerosol retrieval over dark waters including clear ocean waters - Vanhellemont and Ruddick (2015) give an excellent review of the various approaches for aerosol retrievals. Open ocean atmospheric correction schemes typically assume that the water–leaving radiance reflectance in NIR bands is zero. Therefore, at NIR bands the total radiance reaching the sensor is of atmospheric origin. The signal in the NIR bands can thus be employed for the aerosol abundance estimation (Gordon and Wang, 1994). The assumption, referred to as NIR black pixel assumption, holds for waters with low chlorophyll concentration and where phytoplankton or CDOM is the only optically significant water column contributor. To retrieve both the aerosol type and aerosol optical depth at least two NIR bands are used (Gordon and Wang, 1994). These are located around 778 nm and 865 nm.

• Aerosol retrieval over bright waters where the NIR black pixel assumption no longer holds - Coastal waters, lakes and rivers may contain low to moderate to very high concentrations of particulate matter. The water leaving radiance in the NIR is no longer negligible for these turbid waters. In chapter 4 information is provided on manners to retrieve aerosol information over bright water, here we summarize the required bands: 520, 620, 709, 775 and 865 nm.

Instead of using NIR bands for quantifying the aerosol contribution one can switch to longer short-wave infrared (SWIR) bands (Vanhellemont and Ruddick 2015) which have the advantage that no assumptions have to be made on the water optical properties. First, the spectral ratio of Rayleigh-corrected reflectances at two SWIR bands is used to deduce the aerosol model or aerosol spectral shape. Once the aerosol model is determined, the aerosol optical thickness (AOT) can be derived, from the aerosol reflectance in a single SWIR band. Uncertainties in the SWIR black pixel atmospheric correction mainly arise from the relative high noise in the SWIR bands and the spectral distance across which the retrieved aerosol properties are extrapolated. This latter is particularly a significant issue when absorbing aerosols are present. Therefore constraining the SWIR-based aerosol model retrieval using reflectance from a very short visible band (e.g. a 412 nm band) or preferable an UV band is recommended. The inclusion of one or two bands in UV, around 360 and 368 nm, will help to improve the atmospheric correction in various turbid waters. In highly productive waters with high CDOM and detritus the water reflectance in the UV can be assumed to be quasi-black allowing to detect the presence of absorbing aerosols.

Spectral matching or neural network techniques (Goyens et al., 2013) that simultaneously retrieve atmospheric and water components indicate the need for hyperspectral data. The parameters of the aerosol and bio-optical models are retrieved simultaneously and therefore the use of hyperspectral data will reduce the ambiguity in the retrieval of the different parameters.

2.3.5.5 Cirrus clouds

Cirrus clouds and aircraft contrails strongly affect images degrading the quality of the atmospheric correction. Cirrus clouds are semi-transparent and therefore difficult to detect except around 1380 nm. At this wavelength water vapour absorbs all the light reflected by the earth. As cirrus clouds are high in the atmosphere, they are much less affected by water vapour absorption and as consequence they give a clear signal at 1380 nm. In the spectral range from 0.4 to 1.0 µm, the spectral reflectance of the cirrus is close to one. This enables us to assume (Richter et al., 2011) that the cirrus reflectance in the VNIR is linearly related to the cirrus reflectance at 1380 nm. Thus, it is possible to correct these bands from the presence of cirrus. In the SWIR range, the cirrus can absorb and scatter the radiation, and at present no efficient correction method is available but empirical correction method exists as proposed by Richter et al., 2011.

2.3.5.6 Air-water interface

For water targets the 'non-lambertian' or non-flat air-water interface is an extra complication. Only photons which have penetrated the air-water interface and been scattered or absorbed by the water or benthos itself contain useful information. Photons which are reflected by the air-water interface have not interacted with the water and its constituents and thus represent an unwanted signal. A correction for the air-water interface reflection is required in order to derive the water leaving reflectance or radiance from hyperspectral imaging data. The air-interface correction includes correction for sun glint, sky glint and reflection from white caps.

In open-oceans a Cox-Munk (Cox and Munk, 1954) probability distribution formulism is commonly used to predict and correct for glint contamination for ocean colour sensors with sufficiently coarse spatial resolution that individual wave facets or wave trains cannot be distinguished. This formulism is however often not justified for shallow waters, estuaries, lagoons, rivers, lakes and reservoirs where local wind effects due to topography and refraction against shorelines affect the resultant wave height and patterns. Moreover when the spatial resolution of the sensor (e.g. the recommended resolution proposed here of 17 m or finer spatial resolution such as Sentinel-2 at 10 m, or commercial satellites with multispectral bands and pixels of 1 to 5 m) are in the same range as the wave facets or wave crest trough distances, the stochastic approach can no longer be used.

Because of this finer spatial resolution issue image-driven glint correction approaches are being developed. Kutser et al., (1999) developed a glint correction method applicable to a high spectral resolution sensor. The method uses the information available in the oxygen absorption feature at 760 nm and two bands, at 739 and 860nm, outside the oxygen feature to estimate the amount of glint and to correct for it.

Table 2.5 Atmospheric and air-water interface characterisation spectral bands. The greyed spectral bands already occur in Table 2.2..

centre	FWHM	Atmospheric characterisation and air-water interface effect removal bands	
[nm]	[nm]		
+/- 360	8	To constrain the SWIR-based aerosol model over turbid waters	1
+/- 368	8	To constrain the SWIR-based aerosol model over turbid waters	2
+/-412	8	NO2	
+/-520	8	Aerosol retrieval	3
+/-575	8	Chappuis band for O3 absorption(Gorshelev et al., (2014)	4
+/-605	8	Chappuis band for O3 absorption (Gorshelev et al., (2014)	5
+/-620	8	Aerosol retrieval	
+/-709	8	Aerosol retrieval	
+/-740	8	Sun glint removal	
+/- 761	3	Sun glint removal	6
+/-775	16	Aerosol retrieval; water vapour reference band	7
+/-820	16	Water vapour absorption	8
+/-865	16	Aerosol retrieval; water vapour reference band; sun glint removal; (Dogliotti et al., 2015)	9
+/-940	16	Water vapour absorption	10
+/-1020	16	water vapour reference band	11
+/-1050	16	water vapour reference band	12
+/-1130	16	Water vapour absorption	13
+/-1135	16	Water vapour reference band	14
+/- 1380	16	Cirrus clouds	15

In general it is useful to have two NIR spectral bands beyond 730 nm that can be sacrificed for sun and sky glint correction. It is a requirement that these bands are registered simultaneously with the other VIS-NIR bands as wave glint varies almost instantly when taking into account capillary and refractive waves and a sensor flying in LEO orbit at ~ 30000 km/hr.

2.3.6 Summary of sensor specifications

The following order of priority applies to defining the optimal requirements for an aquatic ecosystem earth observing sensor:

- Priority 1: Spatial resolution: as a water body cannot be measured if the pixels are too large, and a requirement for heterogeneous macrophytes, seagrasses, macro-algae and coral.
- Priority 2: Spectral resolution: as aquatic ecosystems variables need to be identified through their spectral signature (be it spectral absorption, spectral backscattering or spectral reflectance as well as fluorescence).
- Priority 3: Radiometric resolution: This determines to what level of accuracy a variable can be detected if priorities 1 and 2 are adequately addressed. Radiometric range is also relevant as the proposed sensor system will need to be able to cater for very low reflecting targets next to very high reflecting targets.
- Priority 4: Temporal resolution: Once priorities 1 through to 3 are adequately addressed of course temporal resolution becomes the most important factor as it will determine how often suitable images of aquatic ecosystem areas will be revisited. However this will be a factor of cost mainly: many permutations (sensors in multiple orbits and orbit types) exist to solve this issue which will be further detailed in chapter 3.

The minimum and optimal measurement requirements for reliable monitoring of aquatic ecosystem are summarised here leading to the following sensor recommendations: Regarding spectral resolution for water quality, macrophytes, bathymetry and benthic substratum measurements a hyperspectral sensor is recommended covering the spectral range from 380 to 730 nm with a spectral resolution around 5 to 8 nm. Over clear dark water bodies the instrument should not saturate up to radiances of more than 100 mW m^{-2} sr^{-1} nm^{-1} in the blue and 20 mW m^{-2} sr^{-1} nm^{-1} in the red, and its radiometric sensitivity (NEΔL) should be between 0.005 mW m^{-2} sr^{-1} nm^{-1} (optimal) and 0.010 mW m^{-2} sr^{-1} nm^{-1}, which is comparable to the sensitivity of MERIS (with 300 m pixels, whereas this report recommends ~17 to ~33 m pixels). Such a sensor provides information about water constituents for many coastal waters and the majority of inland waters, many of which are located at high latitudes and monitored at low sun elevation.

When monitoring bright targets like extremely turbid waters, bleached corals, and shallow waters with bright sand, the instrument must be able to measure radiances up to 400 mW m^{-2} sr^{-1} nm^{-1} in the blue and 200 mW m^{-2} sr^{-1} nm^{-1} in the red. Thus this becomes the core requirement.

If a more cost-effective solution is considered such as dedicated fixed band multispectral sensors, we propose the 26 bands in Table 2.2. possibly augmented by the 15 atmospheric and air water interface correction bands of Table 2.5., although a solution of flying in tandem with existing atmospheric capable sensors is an option too.

Table 2.6 Summary of sensor requirements

Requirements	Values
Spatial	
Spectral	Spectral range from 380 to 730 nm with a spectral resolution around 5 to 8 nm and reduced spectral requirements from 380-400 and from 730 to 1000 nm; a multispectral band set of ~26 bands (between 380 and 780 nm) is an alternative. Ancillary bands (in total 15) from 360 to 380 and 760 to 1340 are advised for atmospheric correction, and a band at 1380 for cirrus cloud detection.
Radiometric	Saturated radiances: more than 400 mW m^{-2} sr^{-1} nm^{-1} in the blue and 200 mW m^{-2} sr^{-1} nm^{-1} in the red Maximum radiances: radiances up to 400 mW m^{-2} sr^{-1} nm^{-1} in the blue and 200 mW m^{-2} sr^{-1} nm^{-1} in the red NEΔL: between 0.005 mW m^{-2} sr^{-1} nm^{-1} (optimal) and 0.010 mW m^{-2} sr^{-1} nm^{-1}
Temporal	As high as feasible. A threshold would be one image globally once every 16 days; preferable would be one image globally per day; a mix of high spatial resolution LEO and lower spatial but high temporal resolution GEO (allowing images once every 10 minutes) could be a valuable combination
Geometric	Registration: Threshold is 0.4 pixels in along and across track directions; baseline is 0.2 pixels in along and across track directions

If a more cost-effective solution is considered such as dedicated fixed band multispectral sensors, we propose the 26 bands in Table 2.2, possibly augmented by the 15 atmospheric and air water interface correction bands of Table 2.5.

Applications requiring temperature make a separate instrument necessary, i.e. a thermal sensor.

Correction of sun and sky glint, atmospheric and adjacency effects and masking of clouds and cloud shadows drive contradictory spatial sensor requirements. Correction of sun and sky light reflections at the water surface requires at least three channels in the near infrared (730 to 860 nm) with a spectral resolution around 15 nm. While these data must be acquired simultaneously and geometrically identical to the hyperspectral images, correction of atmospheric and adjacency effects can be done at reduced geometric resolution and should cover a much larger field of view to capture also the terrestrial surroundings of the aquatic ecosystem being targeted. Flying an aquatic ecosystem dedicated sensor in tandem with atmospheric capable sensors is of course a cost-effective solution to this issue. Cloud and cloud shadow corrections should ideally be done at the highest spatial resolution. If it is acceptable to lose some information around the clouds and cloud shadows a coarser spatial resolution is possible-similar to that sufficient for atmospheric and adjacency effects.

2.4 Suitability assessment of past, current and near-future earth observing sensors

Table 2.7 resents an overview of past, present and future relevant sensors and their suitability for use in aquatic ecosystems. The scoring has been done against the threshold and baseline sensor specification presented. It is evident that none of the existing sensors meet all requirements at baseline or threshold level.

The ocean-coastal sensors are too low in spatial resolution and the land and land-coast sensors do not have sufficient spectral bands and/or SNR, NEΔL and NEΔR mainly. Some commercial sensors score quite high on spatial resolution and revisit time (if their capability for pointing at angles up to 40 degree of nadir are taken into consideration) but lack in (number of or fine resolution in) spectral bands and SNR, NEΔL and NEΔR. Moreover the data costs can be become prohibitive for large areas and frequent monitoring.

Within the section of the table on future sensors it is evident that the planned R&D hyperspectral satellite sensors are all highly suitable except for radiometric sensitivity and only being able to image and direct broadcast (or store on board) small parts of the earth during one orbit. The most recent HyspIRI configuration proposal would be very suitable as a threshold mission with 30 m pixels except for its revisit time.

For the purpose of testing the recommendations of this report the upcoming experimental hyperspectral satellite and ISS missions are highly suitable.

Table 2.7 Overview of past, present and future relevant sensors and their suitability for use in aquatic ecosystems

Legend:
- Meets baseline requirements
- Meets threshold requirements
- Suitable for some applications - but does not meet one or more requirements
- Commercial data costs
- Unsuitable

- ❶ Highly suited
- ❷ Suitable
- ❸ Potential
- ❹ Not suitable

Data currency	Sensor functional type	Sensor name	Spatial resolution (= Pixel size)	Spectral bands from 360-1000 nm	SNR	Revisit frequency (once every x days)	Raw data cost/km² [USD]	Launch date	End date	CHL	CYP	TSM	CDOM	Kd	Turb SD	Emergent	Floating-leaved	Submersed	Shallow water bathymetry
Archival	Ocean-coastal	MERIS	1.2 km	15		2 days	Free	2002	2012	1	1	1	1	1	1	1	1	1	1
	Ocean-coastal	MERIS	0.3 km	15		2 days	Free	2002	2012	1	1	1	1	1	1	1	1	1	1
Archival	Land	Hyperion	30 m	60		16 days (by pointing orbit <51 degrees N and S = a 3 to 5 days cadence	Free	2000	2017	1	1	1	1	1	1	1	1	1	1
Archival	Coastal	HICO	90 m	100		orbit <51 degrees N and S = a 3 to 5 days cadence	Free	2009	2014	1	1	1	1	1	1	1	1	1	1
Archival	Land	LANDSAT 4 to 7	30 m	4		16 days)	Free	1984	2017	3	Surface bloom	2	2	2	2	2	3	3	2
Current	Ocean-coastal	MODIS-A&T	1 km	9		daily	Free	2000		2	3	1	1	1	1	2	2	2	2
	Land	MODIS-A&T	500 m	2		daily	Free	2000		4	4	2	2	2	2	4	3	3	3
	Land	MODIS-A&T	250 m	2		daily	Free	2000		2	4	2	4	2	2	3	3	3	3
	Ocean-coastal	OCM-2	300 m	15		2-3 days	Free	2009		1	1	1	1	1	1	2	2	2	2
	Ocean-coastal	Sentinel-3	300 m	21		Daily (with 2 satellites)	Free	2016		1	1	1	1	1	1	1	1	1	1
	Ocean-coastal	Suomi-VIIRS	750 (375) m	7 (3)		daily	Free	2012		2	3	1	1	1	1	2	2	2	2
	Ocean-coastal	SGLI	250 m	11		2 days	Free	2018		2	4	1	1	1	1	2	2	2	2
Current	Geostationary	SEVIRI on MSG	1 km	2		96 per 24 hours	Free	2002		3	4	2	4	2	2	3	3	3	4
		GOCI	500 m	8		Hourly	Free	2010		1	3	1	2	1	1	2	2	2	2
		Himawari-8&9	500 m – 2 km	4		10 min possible	Free	2014		3	4	1	3	2	1	3	3	3	3
		GOES-R	500 m – 2 km	4		10 min possible	Free	2017		3	4	1	3	2	1	3	3	3	3
Future		GOCI-II	250 m - 1 km	12		Hourly	Free	2019		1	3	1	1	1	1	2	2	2	2
Current	Hyper-spectral	CHRIS-PROBA	17 or 34 m	19 or 63		7 by pointing	Free	2001		1	1	1	1	1	1	1	1	1	1
Current	Land -coast	LANDSAT 8	30 m	5		16 days	Free	2013		2	Surface bloom	1	2	1	1	2	2	2	2
	Land	SENTINEL-2	10 m	4		5 days with 2 S-2's	Free	2014		2	Surface bloom	1	2	1	1	2	2	2	2
	Land	SENTINEL-2	20 m	4		5 days with 2 S-2's	Free	2014		2	Surface bloom	1	2	1	1	2	2	2	2
	Land	SENTINEL-2	60 m	2		5 days with 2 S-2's	Free	2014		2	Surface bloom	1	2	1	1	2	2	2	2
	Land	IKONOS, QuickBird, SPOT-5, 6 GeoEye etc.	2 – 4 m	3 to 4		Programmable: 60 days to 2–3 days	5 to 15	1999 onwards		3	Surface bloom	1	3	1	1	2	2	2	2
	Land	RapidEye	6.5 m	5		Daily	1.5	2005		3	Surface bloom	1	3	1	1	2	2	2	2
	Land -coast	WORLDVIEW-2	2 m spectral 0.5 m B&W	8		Programmable: 60 days to 1 day	30	2009		2	2	1	2	1	1	1	1	1	2
	Land -coast	WORLDVIEW-3	1.24 m spectral 0.34 m B&W	8		Programmable: 60 days to 1 days	30	2014		2	2	1	2	1	1	1	1	1	2
Future	Ocean-coastal	JPSS-1, -2, ….	750 (375)	7 (3)		daily	Free	2017, 2022,…		2	3	1	1	1	1	2	2	2	2
Future	Hyper-spectral	EnMap	30 m	90		Programmable once per 4 days	Free	2020		1	1	1	1	1	1	1	1	1	1
		PRISMA	20 m spectral 2.5 m B&W	66		25 days pointing-7 days	Free	2018		1	1	1	1	1	1	1	1	1	1
		HyspIRI	30	60		16	Free	2022		1	1	1	1	1	1	1	1	1	1
Future	Hyper-spectral ISS	HISUI	20 * 30 m pixels	60		orbit <51 degrees N and S = a 3 to 5 days cadence	Free	2018		1	1	1	1	1	1	1	1	1	1
Future	Hyper-spectral ISS	DESIS	30 m	235		orbit <51 degrees N and S = a 3 to 5 days cadence	Free	2018		1	1	1	1	1	1	1	1	1	1
CEOS FS																			
Baseline	Hyper-spectral	CEOS FS AE-Baseline	~17 m	75 to 120		daily	Free	a.s.a.p.		1	1	1	1	1	1	1	1	1	1
Threshold	Hyper-spectral	CEOS FS AE-Threshold	~33 m	75		3 to 5 days	Free	a.s.a.p.		1	1	1	1	1	1	1	1	1	1
CEOS FS																			
Baseline	Multi-spectral	CEOS FS AE-Baseline	~17 m	41		daily	Free	a.s.a.p.		1	1	1	1	1	1	1	1	1	1
Threshold	Multi-spectral	CEOS FS AE-Threshold	~33 m	41		3 to 5 days	Free	a.s.a.p.		1	1	1	1	1	1	1	1	1	1

Water-quality variables (freshwater, coastal and ocean): Note based on spectral capability only; Macrophytes, macro-algae, seagrasses and corals Note based on spectral capability only; Shallow water bathymetry Note based on spectral capability only

2.5 Proposed modifications to planned future sensors to make them more suitable for (non-oceanic) aquatic ecosystems

2.5.1 Modifications to planned land sensors

Many publicly available land sensors have sufficient spatial resolution (such as Landsat 8 and Sentinel-2) to be relevant for earth observation of aquatic ecosystems. However their spectral bands are often too broad and miss essential areas for aquatic ecosystems. We discuss two systems for which future missions are highly likely and can still be modified: Landsat 10 and the Sentinel-2-E and 2-F satellite sensors.

By adding 2 spectral bands of no more than 15 nm width: one centered at 620-624 nm (the in vivo absorption maximum of cyanophycocyanin) and one centred at 676 nm (the in vivo red wavelength absorption maximum of chlorophyll –a) these systems would become significantly more useful for aquatic ecosystems. In the case of Sentinel-2 making all 13 bands in the 400 to 1000 nm range 10 m spatial resolution (instead of the current 10, 20 and 60 m band configuration) would already be of major benefit. By adding two more bands as stated (620 -624 and 676 nm) Landsat and Sentinel-2 would become significantly more relevant for aquatic ecosystems.

Given the rapid advances in sensor technology it may be more cost-effective to make these systems hyperspectral as that would assure continuity with past systems (as the hyperspectral bands can be convoluted or binned to match the previously used multispectral bands of the Landsat and Sentinel-2 series)) and suitable for all current and future applications.

2.5.2 Modifications to planned ocean and coastal colour sensors

Most ocean sensors are spectrally and radiometrically suitable for aquatic ecosystems (specifically Sentinel-3's OLCI sensor), except for their spatial resolution. Adaptation of these sensors so they image at higher spatial resolution near coasts, estuaries, lagoons, rivers, lake and reservoirs is recommended. Alternatively it could be considered to add (piggyback) hyperspectral sensors with higher spatial resolution (e.g. ~17 to ~30 m) to future ocean-coastal sensors.

3 Platform requirements and mission design

ANDY COURT, XAVIER BRIOTTET, SINDY STERCKX, MARTIN BERGERON, ARNOLD G. DEKKER , KEVIN R. TURPIE, CLAUDIA GIARDINO, VITTORIO E. BRANDO AND PETER GEGE

3.1 General considerations

In previous chapters we identified that the following order of priorities applies to an aquatic ecosystem earth observing sensor:

- Priority 1 Spatial resolution: as a water body cannot be measured if the pixels are too large for heterogeneous macrophyte, seagrass, macro-algae, coral and other benthic covers
- Priority 2 Spectral resolution: as aquatic ecosystems variables need to be identified through their spectral signature (including spectral absorption and spectral backscattering in the water column or spectral reflectance of floating or submerged macrophytes, of the substratum and is cover); atmospheric and air-water interface effects removal require specific spectral bands too
- Priority 3 Radiometric resolution and range: Coastal and inland water and adjacent terrestrial targets cover a large radiance range, with many dark to bright surfaces of interest. Such an environment requires a sensor that can make radiometric measurements that cover this range while accurately resolving variation in dark targets. This determines to what level of accuracy a variable can be detected if priorities 1 and 2 are adequately addressed
- Priority 4 Temporal resolution: Once priorities 1 through to 3 are adequately addressed, temporal resolution becomes the most important factor as it determines how often the aquatic ecosystem areas will be revisited. This is mainly a cost driver as many permutations exits to solve this issue.

In chapter 2 the case is made for either a 26 band multispectral sensor or a hyperspectral sensor focusing on the range of 380 to 1000 nm with potential additional SWIR bands up to 1380 nm for atmospheric correction facilitation. The spatial resolution required is equal to or less than ~17 m for the baseline mission and equal to or less than ~33 m for the threshold mission. The radiometric sensitivity needs to be as high as possible given the spatial and spectral design criteria. The temporal resolution needs to be as high as possible as aquatic ecosystem variables can change:

1. Within hours such as algal blooms, flood events with associated influxes of high nutrient, high coloured dissolved organic matter and suspended sediment loads into reservoirs, estuaries or coastal seas or with tidal or wind driven events.
2. Within days such as pollution events, dredging effects etc.
3. Within weeks such as coral bleaching events.
4. Seasonally to yearly to longer term such as successions of phytoplankton functional types or emergence, florescence and decay of macrophytes.

At the same time the atmospheric and air-water interface contribution to signals measured from space must also be taken into account. Combining all these criteria means that for persistent and accurate measurements covering all applications a range of earth observing sensors and platforms may be required (ideally) whether for scientific, environmental or management relevant monitoring.

Many ancillary measurements may be able to be obtained from other earth observing sensors such as dedicated atmospheric missions. Whilst satellites can fulfil the majority of the measurements other systems are also likely to be needed, for example on or within the waterbody or on aircraft, drones or high altitude platforms, in order to provide specific coverage when needed.

First we will discuss the pro's and con's of LEO and GEO satellite platforms. Next we discuss platform and mission design considerations such as scanning time and coverage, sun glint avoidance and mitigation strategies, and polarization. Following on we discuss instrument characteristics and response functions such as spectral, radiometric and polarization responses, optical and electronic crosstalk, striping and -detector uniformity, near-field response, stray light rejection and band to band registration issues. In the following section on calibration and validation we present consideration for pre-launch calibration and characterization and for post launch calibration and validation. We then discuss some additional platform requirements such as geometric stability, possible pointing function and ancillary data requirements. At the end of this chapter we present a conceptual framework for an end-to-end simulator as an activity to be recommended when actually designing and building a complete aquatic ecosystem Earth observing senor satellite system.

3.2   Orbit sensors

A generic straw-man concept for the required instruments will be described to a level that allows a (rough) estimation of mass, volume, data rate, etc. Possible orbital configurations, e.g. sun-synchronous, drifting, will be described with pros and cons with respect to the science requirements.

3.2.1 Low Earth Orbit (LEO) satellites.

LEO satellites fly between approximately 400 km and 800 km above the Earth and can have a variety of orbits to provide different measurements, for example in a Sun synchronous orbit to observe a specific time of day on the ground, or in inclined orbits to optimize revisit times or specific geographic coverage. LEO satellites with a sufficient wide swath allow the full globe to be observed with a uniform and high spatial ground resolution. The major issue for current and planned medium to high spatial and spectral resolution LEO satellites is that they have a limited swath which limits ground coverage per orbit, this is to maintain reasonable instrument dimensions (mass, volume) and also to limit the required data bandwidth for data transmission – high resolution and hyperspectral imaging require high transmission data rates. The transmission of data may only occur to ground stations at particular geographic locations where the satellite is in contact for only a few minutes during which all acquired data must be transmitted to the receiving station, which creates a data volume limitation for observations. The European Space Agency makes use of data relay satellites in geostationary orbit as an alternative way to buffer data allowing greater data volumes to be transmitted to ground stations. The increasing amount of ground stations globally also increases this satellite to ground data down links capacity.

As well as measurement of the aquatic ecosystem variables, the atmospheric conditions at the time of measurement must also be taken into account, to date this is largely achieved through atmospheric models (e.g. Modtran) assuming certain prevailing conditions. In the foreseeable future, near real time measurements of the atmospheric gases and aerosols can be provided by missions such as the Copernicus Sentinel 4, 5, 5P, the NASA/NOAA (GOES, JPSS)and the Japanese Himawari series of GEO satellites. Compact instruments are in development for measurement of

specific atmospheric gases and aerosols respectively, which could also share the same platform as any dedicated water mission instrument.

Table 2.7 summarizes all relevant archival, current and planned missions that can meet some of the requirements for assessing aquatic ecosystems from ocean via coast and coral reef to inland water measurements. Currently not one instrument meets all the desired criteria. Therefore the last rows in Table 2.7 contain the specifications of this feasibility study. We identified in chapter 2 that a dedicated aquatic ecosystem earth observing sensor would require 5 to 8 nm wide bands, a spatial resolution of ~17 to ~33 m ground resolution with high radiometric accuracy. These requirements are challenging and requires special optics and/or detector configurations which then also impact system resources such as downlink and on-board data storage and data transmission speeds.

Noise in an earth observing sensor is the square root of the sum of the shot noise, and of instrumental noise such as dark noise, readout noise and digitization noise. Note that photon noise is a function of the square root of the entrance radiance. Assuming an ideal instrument, the maximum theoretical SNR is limited by the shot noise.

In order to understand what the current technical limitations are on the 3 constraints that interact with respect to spatial, spectral and radiometric resolution we calculated a theoretical maximal SNR for an imaging spectrometry Earth observing sensor with pixel size of 17 and 33 m, spectral sampling interval of 8 nm with a lens aperture of 300 mm in a 400 km orbit.

Figure 3.1 shows the results. The following variables will change the SNR linearly: increasing the aperture to e.g. 600 mm will double the SNR, increasing the altitude to 800 km will decrease the SNR by half, decreasing the spectral sampling interval from 8 to 4 nm will decrease the SNR by a square root function. An increase in spatial resolution from e.g. 17 to 34 m increases the SNR by a square root function of pixel size.

It is useful to discriminate three main sources of noise in an earth observed image: i) the instrument noise (discussed above) and ii) the environmental noise that is caused by spatially variable atmosphere and air-water interface effects that we cannot fully correct for (Wettle et al., 2004) and iii) by the algorithm and it's parameterisation used to retrieve the variable to be estimated.

In this chapter we focus on key instrument design considerations such as SNR (from which NEΔR and NEΔL can be estimated if all relevant information is presented such as in Figure 3.1.), polarization and stray light.

It is evident that the level of specifications that are needed, to estimate optically active water constituents in high latitudes or over very dark waters or to classify benthic materials through an almost optically deep water column, cannot be met by current LEO sensor technology given a pixel size of 17 to 33 m. The main variables that can be influenced (at a cost increase as the size and weight of the instrument increases) are the optics (increasing the aperture width and the focal length). Also, there are technological developments possible (see e.g. the CHRIS-PROBA experimental sensor) such as pointing the sensor on a fixed position for a longer time (dwelling such as ground motion compensation) to increase the SNR. However, over water bodies this will be less effective as the water surface variability (with its often occurring wind ripples and waves and, varying surface Fresnel reflectance with sun and sensor look angle), may enhance the environmental

noise effects. Detector technology is also rapidly improving allowing more sensitive detector types which could also increase the SNR.

For a more detailed discussion on SNR we refer to Moses et al., (2012) that analyse the effects of SNR for retrieving optical water quality variables using the HICO sensor over turbid inland waters.

**Maximum theoretical SNR:
aperture 300 mm; altitude 400 km;
spectral sampling interval 8 nm**
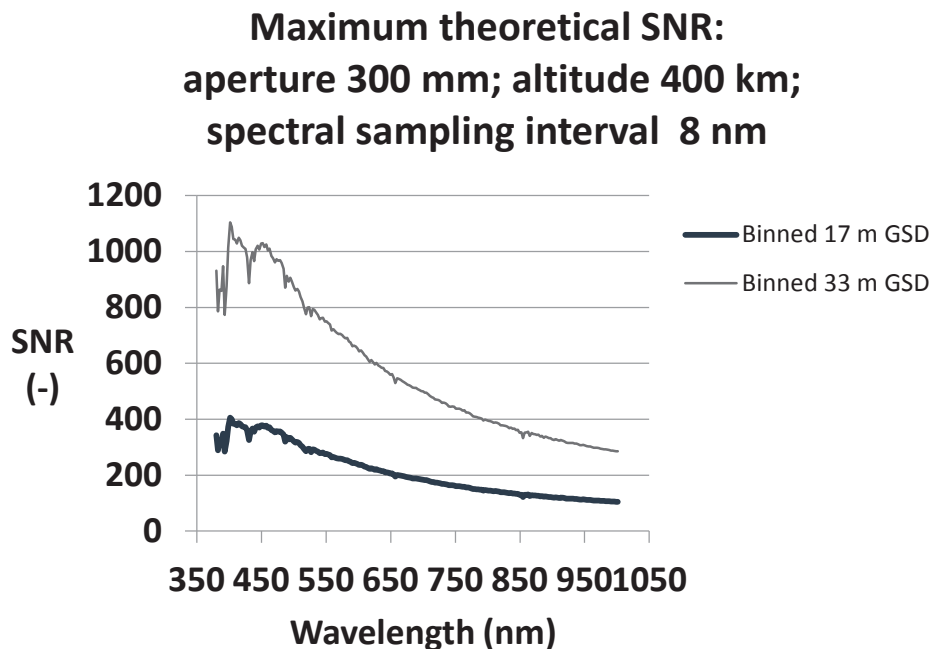
Figure 3.1.Theoretical maximal SNR for an imaging spectrometry earth observing sensor with pixel size of 17 and 33 m, spectral sampling interval of 8 nm with a lens aperture of 300 mm in a 400 km orbit. The radiance was calculated using Ahmad (2010) with a sun zenith angle of 42°. Typical radiance from PACE Ocean Color Instrument (Meister et al., 2011)

Looking to the future some of these limitations for instruments in LEO satellites can be overcome:

- Improved detector systems will allow greater flexibility in targeted data acquisition over specific water systems, while ignoring unwanted areas in the same field of view (i.e. programmed CMOS pixel windowing across the detector), this will allow more specific data to be acquired during each orbit.
- Optical systems will become more compact through new techniques such as free form optics, allowing instrument performances to be increased while maintaining, or reducing, current volumes and masses.
- On-board processing can be implemented to carry out Level 0 to 1b processing of raw data, which again will allow larger regions to be observed, while maintaining current data rates.
- Optical telecommunication terminals will become available for smaller satellites allowing much higher data transmission rates (up to 10 Gb/sec), which again helps to overcome the data bottleneck.

3.2.2 Geostationary orbit sensors

Geostationary satellites are becoming increasingly useful for monitoring aquatic ecosystems. The main focus would be looking at events which occur at timescales of minutes to hours. In addition the

fact that geostationary sensors image continuously also means that the probability of obtaining cloud free or sun glint free images increases. Some of these events relevant to aquatic ecosystem include (potentially harmful) algal blooms, the extent of river plumes after heavy rainfall in the catchment, coral reef spawning events, effects of tides and eddies, oil slicks etc., and dust storms as they can transport and deposit large amounts of dust that acts as a fertilizer for oligotrophic waters.

Advances in technology now allow higher spatial resolution: between 500 m pixels (Himawari 8 and GOES-R series of satellites and future GOCI-II) to 192 m resolution for multi and hyperspectral data for the Indian GISAT-1 satellite and 50 m pixels for the Chinese GF-4 broad band multispectral sensor; higher spectral resolution in the visible and nearby infrared spectral range (Landsat similar bands for Himawari and GF-4, eight ocean colour bands for GOCI-I). The temporal resolution varies from one image every hour (GOCI-I) to one image very ten minutes (Himawari-8 and onwards-with 2 minute resolution for the Japan area), to once every 20 seconds for the GF-4 focusing on an area of 400 by 400 km.

Several proposals are under consideration for geostationary satellites with enhanced spectral and spatial resolution that would focus on oceans and coastal waters (US: GEO-CAPE). Therefore it makes sense to consider the requirements for geostationary sensors in addition to LEO sensors. In an ideal case it would be a constellation of LEO and GEO sensors that could be truly innovative in being able to look events and processes that occur at a timescale of a few minute intervals to those that occur at seasonal intervals. Within CEOS there is an ad-hoc working group on the non-meteorological use of meteorological geostationary satellites. This working group studied the merits of simultaneous use of Himawari-8 and MODIS and VIIRS data, showing that although at lower spectral resolution and SNR, the addition of geostationary data to LEO ocean colour data does enhance the amount of pixels for a given coastal-ocean area significantly.

For a global extent from geostationary satellites it is most likely that an aquatic ecosystem sensor placed on four geostationary satellites would be required for continuous global coverage at sufficiently low grazing angles. In theory two geostationary satellites could cover the Earth's surface but of course the slant angles at the extreme edges would come close to 90 degrees. A disadvantage of geostationary satellites is for imaging the higher south and north latitudes where the slant angles cannot be avoided unless a highly elliptical orbit (HEO) is considered.

For 99.5 % of the inland water bodies where 300 m pixels would not suffice (see Table 2.3 and Table 2.4) as well as similar sized estuarine, lagoonal and near coastal waters finer resolution will increase the amount of these types of waters to be imaged. From a radiometric SNR perspective geostationary sensors can, in principle, have much longer integration times thereby creasing the SNR. From the temporal and spectral resolution perspective geostationary sensors are only limited by the amount of data that needs to be recorded, stored and direct broadcast. At this altitude however, the spatial resolution is constrained by the diffraction limit which requires a relatively large aperture for the highest spatial resolutions (e.g. an aperture of at least 80 cm at 900 nm if a 50 m GSD is desired). Combined modes of operation are also of course possible where the full disk is e.g. imaged once very hour at a resolution of 500 m and targeted areas at much higher spatial resolution down to 50 m resolution as for GF-4.

In summary it is relevant to consider the synergy between LEO and GEO sensors, to advocate the use of the existing and confirmed near future systems and to propose what a dedicated aquatic ecosystem GEO sensor (or a modified land, ocean or atmosphere GEO sensor) should be able to do in future to complement LEO sensors.

3.3   Platform and mission design considerations

3.3.1 Scanning time and coverage

For LEO sensor systems there are several factors to consider when determining an optimum for overpass time and the spatial coverage per orbit:

- Overpass time at the same time each day or multiple times per day?
- In the tropics early in the morning is preferred as clouds have not yet developed
- But, depending on season, sun glint needs to be avoided which is most severe at tropical latitudes.
- At high latitudes solar noon is the best overpass time to get as much signal from the water bodies as possible.
- How many sensor platforms are being considered? One or 2 or 5 or 100+?
- Near polar orbit or also considering an International space station type quasi-circum-equatorial orbit?
- Will the sensor be pointable in space (see 3.6)?

Some sort of compromise will be need to be achieved between all of these variables. A coral reef focused imaging system (also suitable for all tropical aquatic ecosystems) would focus on an early morning overpass time, but a high latitude boreal lake sensor system would focus on a solar noon overpass time guaranteeing highest possible sun zenith angle.

For GEO sensor systems these issues do not apply as the sensor is fixed over a fixed position on the equator (but with higher slant angles at high North and South latitudes). However the distance of a GEO stationary satellite has significant consequences for lens aperture, the imaging detector array, data transmission etc.

3.3.2 Sun glint avoidance and mitigation strategies

Here we discuss sun glint avoidance and sensor based mitigation strategies, whereas the post launch image based sun and sky glint removal strategies will be discussed in chapter 4.

Currently, the presence of sun glint during the acquisitions depends on the characteristics of the platform: swath, time of overpass, orbit inclination, depointing capabilities, spatial sampling, etc. Thus, before the platform and its orbit are defined, recommendations have to be to maximise avoidance of sun glint.

Earth observation sensors that have been designed for use over water bodies have opted for either tilt or roll for sun glint avoidance to increase the fraction of glint free acquisitions. For example, OLCI has a 12 degrees westward roll to avoid sun glint. For wide swath sensors however, across track glint avoidance is limited by the incidence angle threshold for accurate retrievals of water-leaving radiance (MODIS uses a 55 degrees upper limit for sun zenith and 75 for sensor zenith angles [MODIS Level 3 Data User Guide, 2014]). Excessive roll also exacerbates the issue of Earth curvature.

As with SeaWIFS and OCTS, PACE is proposing a ± 20 degrees aft (Northern hemisphere on the descending node) and forward (Southern hemisphere) pitch in order to minimize sun glint (PACE Mission SDT Report, 2012). This implies that the instrument is tilted as it comes over the sub-solar point with a staggered pattern to ensure data is acquired over the tilting latitudes (generally, the equator) to avoid a gap using off-nadir data from adjacent orbits. Alternative approaches can also achieve equivalent glint avoidance (Gregg and Patt, 1994). Sensors that neither roll nor tilt, such as MERIS (operated from 2003 to 2012), were affected by a considerable fraction of sun glint (Steinmetz et al., 2011).
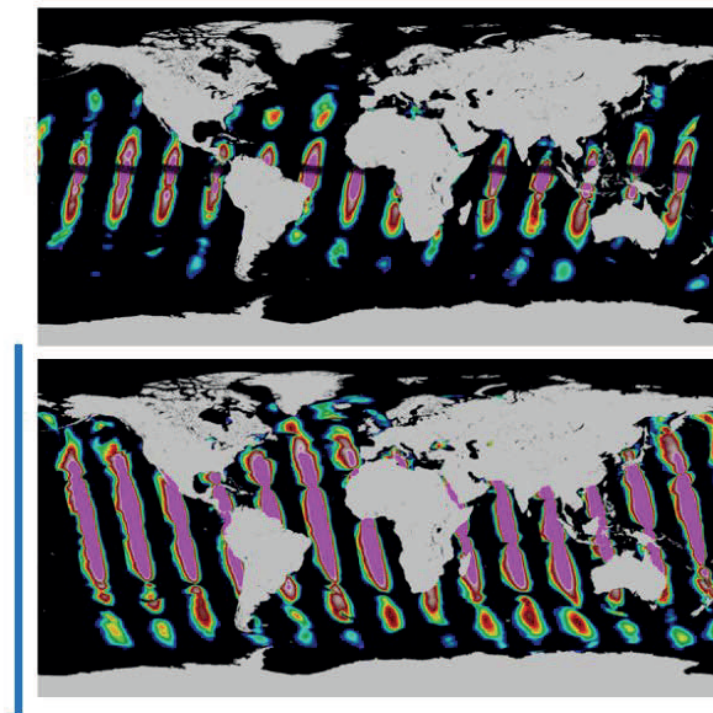
Figure 3.2 (after Meister et al., 2011) Illustration of how choosing sensor tilt (for SeaWiFS) significantly decreases the sun glint effects in the imagery. Global map of SeaWiFS (top) and MODIS Aqua (bottom) glint coefficients for March 22nd 2006. MODIS is not tilted. Glint coefficients larger than 0.005 in reflectance terms) are classified as high glint in NASA ocean colour processing and coloured pink in the images. Glint coefficients from 0.001 to 0.005 are classified as moderate glint and coloured red to white. The tilting of the SeaWiFS sensor significantly decreases the amount of data affected by sun glint.

The LEO sensor we are considering key for aquatic ecosystem processes will need to be carefully designed to avoid sun glint as much as possible given that low latitudes earth observation will be a crucial component of this sensor mission with its abundance of shallow water tropical ecosystems such as coral reefs, tropical seagrasses etc. Sun glint avoidance thus will be a combination of (for polar orbiting LEO) overpass time and tilt of the sensor. In the case of orbits such as that of the ISS (from about 51.6 ° N to 51.6 ° S with a 3 to 5 day cadence and associated varying overpass times) this becomes more intricate to solve.

3.3.3 Polarization

Accurate knowledge of polarization sensitivity prior to launch is critical. Top of atmosphere radiances can have a high degree of linear polarization of up to 75 % (Takashima and Masuda, 1985),

but tend to be less than 50 % (Meister et al., 2011). This linear polarization primarily arises from atmospheric Rayleigh single scattering with a maximum perpendicular to the direction of light propagation and at longer wavelengths (Chandrasekhar, 1961). Light reflected by water is horizontally polarized and maximum at the Brewster angle (53.1°) while the upwelling light tends to be vertically polarized (Sabbah and Shashar, 2007). Hence, coastal imagers have demanding polarization sensitivity requirements coming from the high spatial heterogeneity, high contrast and significant water and atmospheric polarization (Van Gorp et al., 2010).

The impact of polarization on retrieved geophysical parameters is a result of the convolution of the top of atmosphere radiance polarisation with the instrument polarization sensitivity, which for water colour sensors typically ranges by design from 1 to 4 %. Most of this sensitivity can be attributed to polarization sensitive instrument components such as gratings, specular reflectance on optical surfaces at high incidence angles and dichroics. Such low polarization sensitivity can still lead to errors in the atmospheric correction resulting in significant errors (as much as 10 % at 443 nm) in the retrieved water leaving radiance (Gordon et al., 1997).

HICO's design-level polarization sensitivity was for example estimated at 4 % @900 nm, 2 % @450-650 nm and higher around 350 nm (Lucke et al., 2011). The polarization sensitivity of MERIS was about 3 % without a depolarization scrambler but reduced to only 0.25 % when one was introduced (Qian, 2016). The PACE upper limit for polarization sensitivity is 1 % while it is recommended that it be characterized to within 0.2 % to reduce the uncertainty in TOA radiances due to polarization to less than 0.1 % for a large majority of global ocean cases (Meister et al., 2011). Ocean colour instruments, such as CZCS, SeaWiFS and MERIS all opted for polarization scramblers in order sufficiently reduce polarization sensitivity. Polarization scramblers, such as the dual Babinet, however have a negative impact on the spatial resolution and, to a lesser extent, on signal to noise ratio (Collett, 2005, Caron et al., 2012).

Thus for the proposed aquatic ecosystem Earth observation sensor we are selecting the PACE requirements of an upper limit for polarization sensitivity of 1 % while it is recommended that it be characterised to within 0.2 % to reduce the uncertainty in TOA radiances due to polarization to less than 0.1 % for a large majority of water bodies. Regardless of the polarization response, it is generally accepted that this instrument behaviour should be characterized to 0.5 % uncertainty and that characterization should be applied on-orbit to remove the effects of response to polarization.

3.4   Instrument characteristics & response functions

Numerous instrument artefacts contribute to the uncertainties in the at-sensor radiance and, thus, to errors in retrieved geophysical parameters. Instrument artefacts include diverse effects such as striping, response linearity, polarization sensitivity, stray light, out-of-band responses, electronic cross-talk, etc. Minimizing the uncertainties associated with such artefacts is especially important for inland and coastal imagers given the high contrast between dark water and bright clouds, ice on water and/or adjacent land areas with high reflecting vegetation or soils and sands.
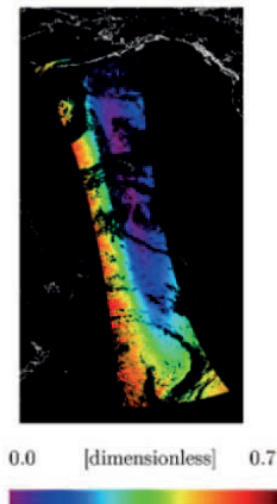
Figure 3.3 (after Meister et al., 2011) Degree of linear polarization (a dimensionless quantity from 0 to 1, where 0 is unpolarised light and 1 is completely linear polarised light) of the TOA radiances for an orbit of MODIS Aqua data over the Pacific Ocean for August 14, 2000. MODIS Aqua equator crossing time is 13:30; for a sensor with a noon crossing time a more symmetric distribution around nadir is expected.

Experience with heritage sensors indicates that instrument artefacts can be reduced to <0.5 % of TOA radiances, given an effective approach for characterizing the performance and degradation of all detectors (e.g., SeaWiFS), although this success has not been realized for most heritage instruments. The requirement for the planned PACE mission is that the total uncertainty for a given observation of TOA total radiance be less than 0.5 % of the typical top-of-atmosphere clear sky ocean radiances (Ltyp) after vicarious calibration (assuming a perfect vicarious calibration). (PACE Mission SDT Report, 2012). Assuming that these artefacts are uncorrelated, the total radiance retrieval uncertainty caused by instrument artefacts is equal to the root mean of squares of each individual artefact. Hence, given such a demanding requirement, artefacts need be minimized both at the instrument design level and through a stringent pre-launch characterization for best post-processing correction. For some artefacts, post-launch characterization can and/or need also be done given performance degradation over time.

3.4.1 Spectral response function

Spectral calibration includes the determination of the centre wavelength, the spectral response curves and spectral distortions (also known as smile and keystone). For this, the instrument needs to be illuminated with a monochromator. As the spectral response is likely to change as function of position across track (smile effect), the whole FOV needs to be characterized. This is done for discrete positions across the swath by tuning the wavelength in small steps (typically 1/10 of spectral bandwidth) across the spectral range of the instrument. The centre wavelengths should be determined at an uncertainty <0.5 nm.

 Spectral smile is a systematic variation in the band centre across detectors and needs to be assessed accurately.

3.4.2 Radiometric response

Absolute radiometric calibration: Absolute radiometric calibration is required to convert sensor digital read out (DN) to radiance in physical units. The instrument needs to be illuminated by an absolute calibrated light source that is SI (International System of Units) traceable to standards from a National Metrology Institute. An uncertainty of ~5 % is sufficient if the instrument is equipped for on-orbit radiometric calibration or vicarious calibration is performed. Absolute radiometric calibration is also performed at different temperature regimes to characterize the change in the instrument response to variation in instrument temperature, which can occur on-orbit.

Relative radiometric calibration: The variation of responsivity over all pixels in the array which needs to be established in order to get a spatially and spectrally homogeneous image. The relative radiometric calibration uncertainty should be <0.5 %. On board flat fielding methods exist using an on-board uniform reference. Measurements at detector level are required to obtain the intrinsic variation of responsivity of the different detector pixels, called Photo Response Non-Uniformity (PRNU). Furthermore measurements at the integrated instrument level are required to quantify the variations over the FOV due to slit width variations and optical vignetting.

Dark current and bias determination: Even when no photon falls on the detector, a current will be produced. These electrons are thermally generated and will contribute to the overall signal obtained in a regular measurement. The detector electronics generates an offset signal called bias to avoid conversion of negative signals in the A/D converter. This bias level can be obtained by extrapolating dark current measurements at different integration times to a 0 sec integration measurement. The uncertainty should be below ± 2 DN for the sum of dark current and bias.

Linearity characterization: Ideally, the measured signal increases linearly with increasing input radiance and increasing integration time. This signal gain is called response. It depends on wavelength, temperature, detector size, doping etc. and can show deviations from linearity, in particular at low radiance levels and close to detector saturation. Nonlinearity should be measured at an accuracy which allows determining the response at an accuracy of 1 %.

Developments with optical detectors that have a designed non-linear response may become a solution allowing fine resolution at lower radiance levels and less fine resolution at higher radiance levels.

3.4.3 Polarisation response

It is important to derive the degree of polarisation sensitivity as function of wavelength and spatial position. As mentioned before for the proposed aquatic ecosystem earth observation sensor we are selecting the PACE requirements of an upper limit for polarization sensitivity is 1 % while it is recommended that it be characterized to within 0.2 % to reduce the uncertainty in TOA radiances due to polarization to less than 0.1 % for a large majority of water bodies

3.4.4 Optical and electronic crosstalk (After Oudrari et al., 2010):

Electronic and optical crosstalks are radiometric challenges that often exist in the focal plane design in many sensors. Crosstalk is a response in any detector when a single detector (or band) is illuminated. For the NPP VIIRS instrument, optical crosstalk caused by light scatter with the instrument's filter array, was shown to be dependent not only on the source wavelength, but also its

polarization and spatial characteristics (e.g. angular scatter). The new generation of environmental satellites will be required to develop a comprehensive specification definition for both optical and electronic crosstalk, as well as reliable test procedures to collect appropriate data in the pre-launch phase. Crosstalk Influence Coefficients (CICs) derived from prelaunch spectral measurements will be the foundation of this methodology to assess crosstalk impact on MODIS-like sensor radiance, and associated geophysical algorithms. Analysis of crosstalk contaminated products will indicate potential problems, and help to determine if a hardware fix and/or on orbit mitigation plan is necessary. The Oudrari et al., (2010) proposed method uses crosstalk characterization data sets from newly designed sensors in conjunction with heritage space based data to assess the crosstalk impact on the data measurement, and the higher level products. It is also important to separate band-to-band optical crosstalk from Out-of-Band (OOB) contamination, and to include crosstalk polarization and measurement uncertainties. OOB sensitivity is a non-zero response outside the nominal band width and usually occurs when filters are used for spectral band separation as the filters may not filter out all light beyond the intended wavelength range.

3.4.5 Striping and detector to detector response

With more than two decades with ocean and coastal waters imaging, it is well recognized that striping and detector to detector artefacts (i.e. non-uniformity) can result in large variability across uniform water bodies. The impact is, in general, more appreciable over dark waters. The use of large detector arrays, i.e., pushbroom or 2D frames, complicates the design and pre-launch activities in characterizing the uniformity. Some examples are MERIS, MODIS, OLI, IKONOS, QuickBird, Worlview-2 and -3 and Landsat-8 for which such artefacts are pronounced. For these reasons, the PACE mission has considered designing a single-detector imager to avoid/minimize striping/banding effects.

3.4.6 Stray light and stray light rejection

Stray light can be defined as radiant energy that reaches a detector element from a wavelength or a direction other than those intended in the nominal design. This includes scattering, diffraction, self-emission (at longer wavelengths only), diffuse and specular reflection from surfaces (the later resulting in spatial and spectral ghosts) whose overall effect is the contamination of the at-sensor radiance. Stray light can be minimized using instrument outer and inner baffles, coatings or anodization, enclosures and careful design, manufacturing and cleanliness of the optical components (Fest, 2013). Minimizing stray light also helps improve the utility of high contrast imagery such as with adjacent land, cloud or ice on water contamination, especially in the infrared where water leaving radiance is much smaller than that of contaminating sources. For MODIS, as much as half of the ocean pixels are found to be within the Aqua stray light mask (5x7 pixels), which significantly reduces the useful data available (Meister and McClain, 2010). For all these reasons, careful stray light design and correction is needed for an aquatic ecosystem imager.

Legacy spaceborne instruments such as HICO, with a stray light requirement of <1.0 %, and MERIS, with an achieved performance for stray light <1.4 %, certainly provide guidelines for an achievable requirement. For PACE, the stray light contamination for the instrument is required to be less than 0.2% of the typical radiance 3 pixels away from a cloud (PACE Mission SDT Report, 2012). Such demanding requirements cannot be achieved solely with careful instrument design and post-processing is required to correct for stray light. Correction algorithms to reduce the stray light

induced errors have been developed and used (Bourg et al., 2012 and Yeh et al., 1997). However, when stray light contamination is relatively large at the instrument level, such as with SeaWiFS, correction does not suffice to meet the most demanding requirements (Barnes et al., 1995).

Spectral stray light assessment: stray light or light from different spectral orders which will contribute light outside the designated spectral band. The measurement of the spectral response with the collimated monochromator or tuneable laser can be used to search for light outside the spectral bandwidth corresponding to the wavelength of the transmitted light. This will be especially useful to look for spectral 'ghosts' giving line emissions and which is easier to pick up from the measurement with the spectral source. For faint stray light spread over a larger wavelength region, the laser or monochromator measurement is likely to be insufficient. An alternative method, is to use a panchromatic light source with a sufficient and stable intensity and spectrum in combination with well-known band pass filters that block parts of the wavelength range.

Spatial stray light assessment: Through reflections (internal or external to the instrument) light can fall outside the intended light path on the detector. Two types of spatial stray light are considered: one coming from a light source inside the FOV (i.e. in-field stray light) and the other from outside (i.e. out-of-field stray light). Stray light will affect the radiometric accuracy and will also limit the detection of faint structures (i.e. reduced contrast). It is difficult to quantify stray light through test measurements and it needs to be carefully analysed through optical modelling.

3.4.7 Band to band registration

Depending on the way an earth observation scene is imaged (in both a spatial and spectral dimension) the band to band registration needs to be as accurate as possible. There are another two dimensions of relevance here: the geospatial dimension and the time dimension. The geospatial dimension is when identical features have identical geolocation in all bands. Another important and often ignored dimension is that of having all spectral bands image the same target area at the same time or as close as possible to this ideal situation. The main reason for this high time synchronization requirement is that sun glint from capillary waves, refractive waves, , wind waves and facets and swell at the surface of water bodies can vary quickly. Sun and sky glint removal algorithms rely on simultaneous imaging of e.g. VIS and NIR bands used to correct for sun and sky glint of visible bands.

3.5   Calibration and validation

3.5.1 Pre-launch calibration and characterization

Careful pre-flight calibration and characterization under operating environmental conditions, such as space based temperature and vacuum, and the full range of possible viewing conditions, are essential to ensure that mission requirements are met over the sensor's range of operating conditions, to determine all the influencing parameters on the sensor response and to accurately initialize the different parameters of the sensor model. Previously we discussed the spectral, radiometric and polarisation responses. Here we add some details to the geometric and radiometric pre-launch calibration and characterisation.

The goal of geometric calibration of an optical sensor system is to model the line-of-sight for each pixel element of the imaging system. This is usually performed pre-flight in laboratory conditions where precise measurements enable to characterize the various aspects of the system. These

measurements should include: The determination of the line of sight vector of each detector of the hyperspectral sensor; the determination of the boresight angles of the camera (angle x, angle y, angle z in degree) for calculating the transformation between the body fixed frame and the spectral imager frame and the characterisation of the spatial distortions over the FOV (i.e. keystone or band-to-band misregistration).

Radiometric pre-flight calibration. As discussed before the sensor needs to be illuminated by an absolute calibrated light source that is SI (International System of Units) traceable to standards from a National Metrology Institute. An uncertainty of ~5 % is sufficient if the instrument is equipped for on-orbit radiometric calibration. The following calibrations need to be done: relative radiometric calibration; dark current and bias determination and linearity characterization.

It is becoming apparent to the calibration community that drift in the spectral response is possible, and needs to be deconvolved from the radiometric response change across all bands simultaneously.

3.5.2 Post-launch calibration and validation

Variations in the characteristics of the instrument are likely to occur in orbit due to outgassing phenomena during launch, aging of the optical parts, thermal stresses and cosmic ray damage. This makes it necessary to perform post-launch calibration and validation to guarantee that both spectral, radiometric and geometric requirements are met.

Different factors such as the launch shock and gravity release might reduce the post-launch sensor geo-pointing accuracy. Therefore in-flight geometric calibration is required to estimate and monitor on a regular basis the exterior orientation (i.e. boresight misalignment angles) and interior orientation deformations at different conditions. In-flight geometric calibration can be performed, depending on the spatial resolution, through GCP (Ground Control Point) matching using reference datasets from other missions e.g. the Landsat Global Landsat Survey GLS 2010 dataset. For a decametric GSD the geometric calibration can be based on existing databases of geometric reference sites as already being used for high resolution missions as SPOT or Pléiades .

After launch, the calibration process will be based on both on-board calibration facilities and vicarious methods (based on sensing a reference target a the earth's surface). In fact, as these methods are using independent facilities, a statistical processing is usually achieved to deliver an accurate estimation of the calibration. Usually, two main families are distinguished: one using on board facilities and the second one based on sensing reference targets (vicarious calibration).

For the calibration of the reflective band on-board lamps and solar diffusers are often used. The diffuser plates are not perfectly Lambertian and therefore the Bi-directional Reflectance Distribution Function (BRDF) of the diffusers has to be determined with pre-launch measurements. As solar diffusers might degrade over time, their stability should be monitored through on-board solar diffuser stability monitoring devices or using a second diffuser and/or the use of vicarious calibration approaches.

In the absence of on-board calibration devices, a series of approaches exist based on vicarious methods that use specific terrestrial or space targets, considered as secondary references. Vicarious calibration methods will enable the monitoring, through sensor independent means, of the calibration evolution of the instrument during its life. Close to absolute calibration can be achieved

based on acquisitions over some sites, recommended by the CEOS IVOS group, with synchronous ground and/or aircraft measurements-although the atmospheric contribution to this signal will always introduce some additional uncertainties. To ease access to data from Land Equipped Sites, RadCalNet, a Radiometric Calibration Network of Automated Instruments, is currently being established by a dedicated working group with members from different international (space) organizations. AERONET-OC (Ocean Colour) sites record both sun and sky irradiance as well as water leaving radiance autonomously and therefore allows for validation at low radiances. Absolute calibration can be complemented through the use of the Rayleigh scattering over deep ocean oligotrophic sites to calibrate the VIS spectral range. Inter-band calibration can be verified through observations over sun glint or deep convective clouds. The temporal drift can be estimated using continuous acquisitions over temporally stable sites such as dedicated ocean deep water sites with low reflectance such as the MOBY (near Hawaii) and BOUSSOLE (near Villefranche, France) optical buoys, deserts or through lunar calibration which allows to perform stability monitoring with sub-percent per year precision. Lunar calibration requires a platform manoeuvre to observe the moon. Inter-instrument calibration can be achieved with quasi simultaneous acquisitions of different sensors with similar spectral bands.

In-flight spectral calibration, i.e. retrieving the shifts in the centre wavelengths of on-orbit imaging spectrometers, can be performed through on-board spectral calibration mechanisms such as monochromatic light sources such as LED's, lasers, rare earth-doped diffusers, solar diffusers or Fraunhofer lines on a white diffuser. In the absence of on-board spectral calibration devices a series of approaches exist based on solar or terrestrial atmospheric features (for example the oxygen absorption feature centred at 762 nm) in the measured data.

3.6   Platform requirements including geometric stability

Earth observation sensors are becoming more and more versatile. Initially most global earth observing sensors had a fixed look angle in a near polar orbit enabling creation of a multi-decade acquisition of sun synchronous images suitable for trend detection. Most of these EO sensors were relatively large and heavy. With the advent of SeaWiFS in 1997 platform sensor combinations were enabled to turn upside down in space in order to perform a moon surface radiometric and spectral calibration (as the earth observing sensor-optics was then pointed at the moon). In the late nineties very high spatial resolution sensors commencing with IKONOS followed in the 2000's by Quickbird, WorldView and many more, had increasingly sophisticated and versatile pointing capabilities. These pointing capabilities allowed these narrow swath, high spatial resolution sensors, with a nominal nadir looking repeat cycle of e.g. one image every 60 days, to increase this to one image every day, albeit with significant pointing variability: up to 40 degrees in any direction. The advantages are clear: despite having only one or a few sensors with very high spatial resolution it becomes possible to image a selected area of interest much more often. It also becomes possible to obtain stereo pairs of images in quick succession. The drawback is that the images are no longer sun-synchronous, the look angles between successive images may vary significantly in both across and along track direction with the ensuing variations in radiance path length, atmospheric scattering, atmospheric and water body polarization, water surface incidence angle affecting Fresnel reflection etc. Moreover it becomes more difficult to build a time series of areas that are not imaged due to the sensor pointing at another target.

This pointing capability of course does offer the option of pointing away from the sun thereby avoiding sun glint (although the opposite is true too).

Whether a proposed aquatic ecosystem earth observing sensor should have a fixed nadir or sun avoiding off-nadir tilt angle or whether it should have flexible pointing capabilities will depend on the degree to which certain end-user requirements need to be met. This will also depend on chosen solutions for achieving both high spatial, spectral, radiometric and temporal requirements. E.g. a suite of satellite sensor-platforms could all be looking at fixed angle off-nadir for sun glint avoidance whereas a single sensor-platform may need pointing capability to e.g. be able to image an extreme event such as a flood, a river flood plume or an algal bloom or a coral bleaching event. A combination of LEO and GEO sensors would also be able to solve these often conflicting requirements.

The geo-location calibration is of paramount importance over aquatic ecosystem targets such as freshwater macrophytes, optically shallow water seagrass, macro-algae, benthic micro-algae and coral reef sites to detect change. It needs to be less than 0.4 of the pixel size and preferably smaller (e.g. 0.1 of the pixel size). In many cases in coastal waters and over coral reef there are much less well characterised GCP's available.

3.7   End to end simulator

To demonstrate the feasibility of a mission, modelling tools are necessary. Two ways are developed depending on the scene type given as inputs: either a synthetic aquatic ecosystem with an adjacent landscape or a scene acquired from an airborne or spaceborne hyperspectral sensor. The resulting tools are described below.

Several end to end simulators already exist like the EnMAP simulator or the Comanche-Cochise one (Miesch et al., 2005) used for the SPECTRA (Schaepmann et al., 2004) and HYPXIM (Briottet et al., 2011) hyperspectral missions. A general flowchart of such a simulator is proposed in Figure 3.4.

As inputs, such a simulator has to consider scenarios of various complexities:

- **Hyperspectral airborne or spaceborne** acquisition expressed in radiance unit. To have a good estimation of the ranges of upwelling environment radiances, the at sensor radiance needs to be atmospherically corrected to retrieve the surface reflectance R_{rs}, and then this is used to simulate the corresponding signal at TOA sensor level. Such a procedure allows simulation of multiple environmental water surface state and atmospheric conditions.
- **Spectral reflectances from existing data bases** such as SEABASS or MERMAID for coastal waters and oceans or LIMNADES for lakes. A dedicated macrophytes, seagrass, macro-algae, coral reef and associated benthic cover types does not yet exist but is advised (see e.g. Dekker, 2006).
- **Synthetic spectral reflectance** simulated from radiative transfer tools like Hydrolight (Mobley) or WASI (used for the simulations in chapter 2 and the Appendix A.2.). Such tools can simulate the bottom of atmosphere spectral reflectance from an accurate description of the aquatic ecosystem and its corresponding geo-physical variables.

We note that for heterogeneous ecosystems like coastal zone or inlands water, the radiative contribution of the environment is crucial. The Comanche-MODTRAN tool uses a Mont Carlo kernel

to deliver a good estimation of the Earth atmosphere coupling irradiance and the environment upwelling radiance. Although the exo-atmospheric solar irradiance is not polarized, the photons crossing the atmosphere and reflected by the Earth are polarized; it is possible to estimate the polarized TOA radiance by using MODTRAN-P radiative tool or OSOAA (Chami et al., 2015). Further, different atmospheres, aerosols (type and abundance) and acquisitions geometry can be considered using e.g. Multi-Angle Implementation of Atmospheric Correction (MAIAC) products.

Thus, the top of atmosphere (TOA) radiance is estimated from these inputs and a radiative transfer code such as: MODTRAN, DISORT or three atmospheric correction codes used by Martin et al., (2017) for Brazilian rivers and floodplains, or Second Simulation of a Satellite Signal in the Solar Spectrum (6SV), or ACOLITE and Sen2Cor with the highest spectral resolution. Note that the 6SV code is not suited for hyperspectral simulations, its spectral resolution (2.5 nm) is not sufficient to model the TOA signal for 5 to 8 nm bandwidth. To estimate the resulting signal collected by the hyperspectral camera at the output of the electronic chain (expressed in digital count units) several contributions have to be taken into account such as:

- **Spatial module:** to simulate the corresponding spatial resolution of the sensor and taking into account its Modulation Transfer Function (MTF) able to simulate various spatial aberrations caused by, e.g. the telescope optics, the double slit and the curved prisms (e.g. EnMap simulator).
- **Spectral module:** to perform the spectral resampling, taking into account the spectral response functions in all spectral bands, non-uniformities in the spectral domain such as smile, polarization, and an optional spectrometer shift in the spectral dimension (e. g. EnMap)
- **Electronic module:** to convert the radiance in digital count by taking into account the artefact of the electronic detection chain (noises, temporal shift…)

The resulting digital output signal needs several pre-processing steps to overcome the deterministic artefacts introduced by the instrument itself.

From a radiometric and geometric modelling of the camera, a pre-processing is necessary which depend on its design such as dark current correction, inter-detector sensitivity correction, smile etc. The resulting signal is then converted into output radiance taking into accounts the calibration accuracy. From the output radiance, atmospheric compensation has to be achieved to retrieve the bottom surface reflectance as follows: estimation of the atmospheric state: using the image itself (estimation of the water vapour content, aerosol type and abundance…) or from externally obtained data (atmospheric profiles, AERONET and AERONET-OC data, RAdCalNet data and similar data sources). Using this information, the TOA signal is corrected to retrieve the bottom of atmosphere (BOA) surface reflectance R_{rs}. The resulting BOA reflectance image can be georeferenced or not. At this level, biophysical parameters can be retrieved following the approach outlined in 4.1.
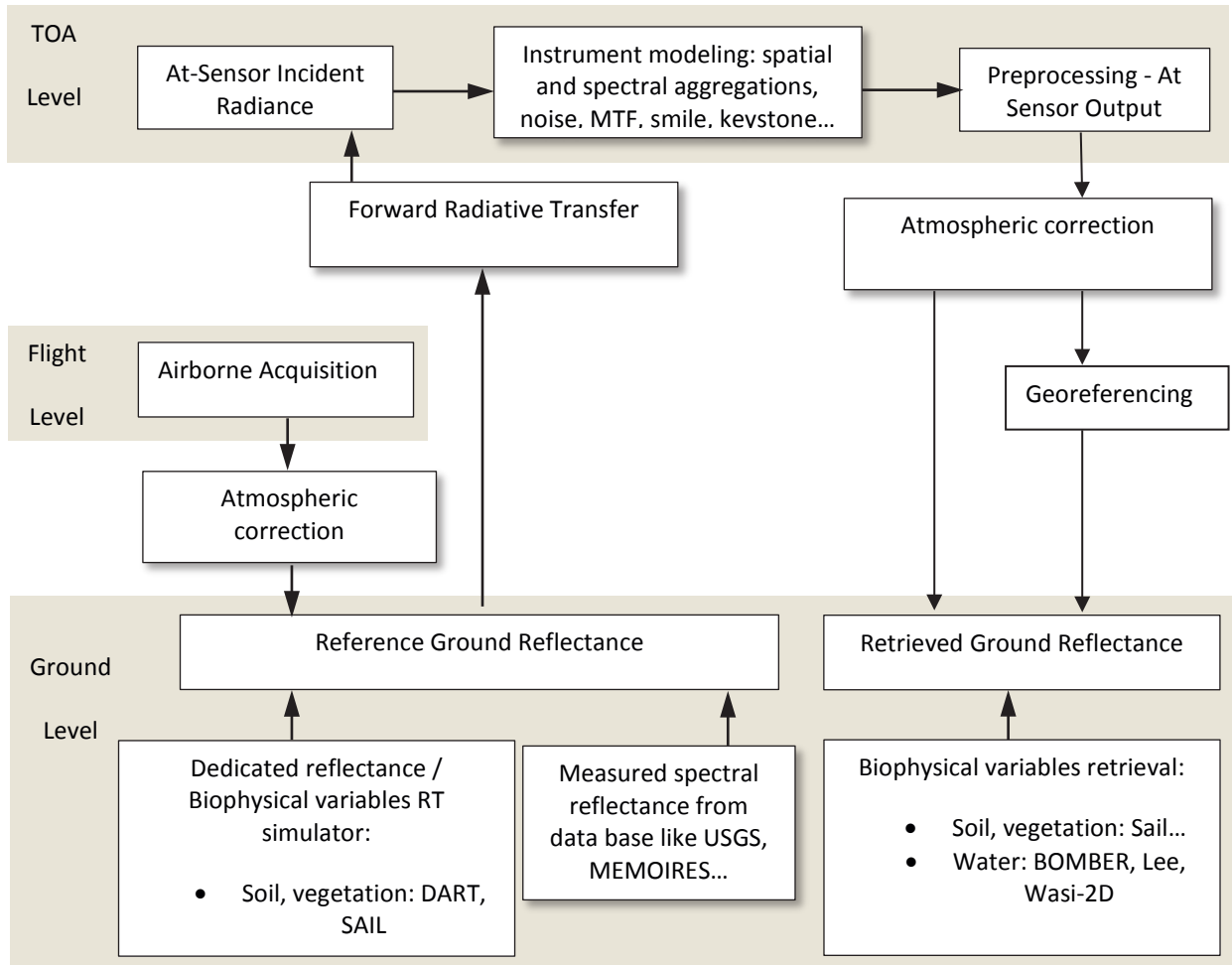
Figure 3.4 General flowchart of an End-to-End simulator

4 Aquatic ecosystem earth observation enabling activities

Steef Peters, Kevin R. Turpie, Sindy Sterckx, Peter Gege, Xavier Briottet, Martin Bergeron, Nicole Pinnel, Arnold G. Dekker, Claudia Giardino, Vittorio E. Brando and Bringfried Pflug.

4.1 Introduction

In previous chapters we defined why and what an aquatic ecosystem satellite sensor should be able to measure, and determined the satellite platform capabilities to ensure that the right type of measurements over aquatic ecosystems from space can be achieved; the final component are the enabling activities. Enabling activities take place mostly after launch, although preparatory activities are possible before launch. These activities vary from ensuring the top of atmosphere (TOA) radiance is measured in a well-characterized way, the satellite sensors' degradation can be monitored during time, the atmospheric correction methods are robust, the air water interface mitigation measures and corrections (sky glint, sun glint and whitecaps) function well and the in situ instruments provide proper vicarious calibration and validation data. By performing these enabling activities the quality of the input data to the algorithms that extract the desired aquatic ecosystem information (see chapters 1 and 2) is assured. Chapter 4 provides a condensed overview of steps and methods to do this. In general, the following steps are required after an earth observation image is acquired:

1. Decide if a pixel offers an unobstructed view at surface water (so filter out effects of clouds, cloud shadows, land, objects etc., in the pixel).
2. Decide if a direct calculation of water parameters can be done on the TOA reflectance
3. If not, obtain the Bottom of Atmosphere reflectance by correcting for atmospheric influences.
4. Since the BOA water leaving radiance or reflectance signal will often contain additional reflections (sun- and sky glint) at the water surface, apply a correction for this additional reflectance.
5. The transport of light through the air-water interface alters the signal so a correction should be applied to arrive at the desired quantity: i.e. water leaving radiance or reflectance directly above or below the air-water interface.
6. To obtain a measure of aquatic ecosystems variables from the water leaving reflectance, water quality, bathymetry or emerse, submerged or benthic mapping algorithms are used.
7. Establish the quality of the product by validation or uncertainty (propagation) analysis.

Each step can be implemented as a calculation recipe (algorithm) containing simplified or extensive physical descriptions of the radiative transport processes involved. This chapter focusses on the main categories involved, namely:

4.2 Atmospheric correction methods.
4.3 Corrections at the air-water interface.
4.4 How to estimate aquatic ecosystem variables from water leaving radiance or reflectance using in-water algorithms (optically deep and optically shallow waters).
4.5 Sources of uncertainties in the obtained quantities.

4.5 In-situ measurements for algorithm development and calibration designed to make optimal use of the proposed sensor(s).

4.6 Instrumentation and campaign requirements for validation.

4.2   Atmospheric correction methods

Atmospheric correction is the inversion of radiative transport models that characterise the atmospheric optical properties in various degrees of detail. This correction is necessary to obtain the bottom of atmosphere (BOA) or surface reflectance or water leaving radiance of imaged water pixels. Pixels that are contaminated by dense smoke, fog, clouds or cloud shadows need to be filtered out prior to atmospheric correction. As seen in Chapter 2 of this report, the aquatic ecosystem main radiative transport processes are influenced by the aquatic optical active components, the substratum or benthic vegetation reflectances and pure water itself. In the case of floating plants or floating algae their reflectance is the sought after parameter. The atmosphere needs characterising as follows:

- Absorption by absorbing aerosols and gasses (O_2, O_3, NO_2 and H_2O)
- Rayleigh scattering by small molecules of non-absorbing atmospheric gasses (CO, N_2O, CH_4 and CO_2)
- Mie scattering by larger molecules (aerosols and water vapour)
- Polarization effects

In addition to this, scattering by ice crystals in partially transparent cirrus clouds and aircraft contrails, lens effects at cloud edges and "the adjacency effect" have an influence of the observed TOA signal of a water pixel. Depending on location, time and topographical height, different mixtures of atmospheric optical active components and variable path lengths lead to different effects on radiative transfer. To estimate the true water leaving radiance from the TOA radiance it is necessary to remove the reflection at the water surface by sun- and sky glint and whitecaps. A good introduction to the underlying physics is given by Mobley et al., 2016.

Note that as the number of spectral bands and their resolution increases (e.g. from a few multispectral bands to through to imaging spectrometry) it becomes increasingly feasible to use the satellite sensor spectral data itself to perform the required corrections to estimate the atmospheric parameters from the image itself. Alternatively, by flying our proposed sensor(s) in tandem with atmospheric characterisation satellites, the required atmosphere parameterisation data can be obtained.

The steps that need to be considered to assess the BOA (water leaving radiance or reflectance at or just below water level) are as follows:

1. Select pixels that are in the water, not obscured by clouds, cloud shadows, smoke, fog, aircraft contrails etc., and not affected by reflectance of floating objects and emerging vegetation.
2. Identify pixels that are affected by sun/sky glint and whitecaps reflection and either discard them or correct for this additional reflectance source.
3. Correct the observed signal for gaseous absorption using assumed values or external data sources for O_2, O_3, and NO_2 etc.

4. Correct the observed signal for Rayleigh scattering using knowledge about topographical location, height (water bodies exist from -430 m to in excess of 5900 m altitude) and time.
5. Estimate the amount of water vapour and aerosol scattering per pixel (or per image) and correct the signal for water vapour and aerosol absorption and scattering.
6. Correct for contamination of the pixel reflectance from nearby, high reflecting targets (adjacency effect).
7. (Optional) Couple the atmospheric correction to an in-water model to solve the RTE for the total water-atmosphere system and obtain optical closure.

There are several types of approaches to estimate the true water leaving radiance or reflectance from the compound signal measured at TOA. Overviews of such approaches have been published by e.g. (Goyens et al., 2013; Muller et al., 2015; Minu and Shetty, 2015; Emberton, 2016 etc.). All authors conclude that there is currently not a single suitable method for all situations. Situations that need further development include (very) turbid waters and conditions with strongly absorbing aerosols. Adjacency correction methods need to be addressed properly. A method to pre-select a suitable inland waters atmospheric correction based on optical water type classification was recently proposed by Eleveld et al., 2017. It is desirable, however, to have one generic method for atmospheric correction over inland, coastal and coral reef waters.

Based on inquiries amongst participating scientists the GLaSS project (www.glass-project.eu) made a list of scientific and operational criteria that may help to select an appropriate atmospheric correction scheme for inland waters. These include:

- Adaptable to a multitude of sensors (legacy missions, Sentinel-2, Sentinel-3, L8, future missions).
- Preferably open access, well documented, no other commercial software required, future maintenance assured.
- Wide range of AOT and atmospheric models.
- With adjacency correction (possibility).
- Configurable for optical properties of atmosphere and water.
- Configurable for ancillary data (e.g. O_3, NO_2), site elevation
- Suitable physical range of the underlying radiative transfer model
- Pixel wise retrievals of AOT and H_2O vapour

Here we briefly discuss three approaches to atmospheric correction:

1. Methods inherited from ocean colour remote sensing:

These include methods based on more or less analytical solutions to the RTE (Gordon & Wang, 1994, Ruddick et al., 2000, etc., see Goyens et al., 2013). They start with assuming that there is no water leaving signal in the NIR and derive aerosol optical properties from that assumption. For turbid waters the zero reflectance in the NIR is not true, which lead to approaches deriving aerosol optical properties from SWIR bands where the water absorption is so high it overwhelms any backscattering by suspended matter (e.g. Vanhellemont and Ruddick, 2015; Moore and Lavender, 2011; Mazeran et al., (2011)). An alternative approach is to derive aerosol concentrations from nearby land pixels (Guanter et al., ;2010, Pons et al., 2014 and Xu et al., 2016).

2. Methods that invert RT codes (LOWTRAN, MODTRAN, 5S, 6S):

These methods were often applied for atmospheric correction of airborne remote sensing over inland and coastal waters. A recent review was given by Minu and Shetty, 2015. Additional studies evaluating such approaches are e.g. Sterckx and Debruyn (2004); Montes and Gao (2004); Adler-Golden et al., (2005); Brando and Dekker (2003); Giardino et al., (2007); Guanter et al., (2010); Knaeps et al., (2012); Sterckx et al., (2015); Bagheri et al., (2004) and Peters et al., (2008). Although the advantage is that the radiative transport is well described by the standard code, one must pre-select an appropriate atmosphere and aerosol type which is subsequently kept constant over the image.

3. Methods that simultaneously retrieve atmospheric and water components:

Several spectral matching or neural network techniques (Doerffer and Schiller (2007); Schroeder et al., (2007),; Heege et al., (2005); Steinmetz et al.,(2011); Kuchinke et al., (2009) and Xu et al., (2016)) which simultaneously retrieve atmospheric and water components have been developed. These algorithms can manage optically complex waters from inland to coastal. It should be noted that because the parameters of the atmosphere, the air-water interface and the water body are retrieved simultaneously an error in the coefficients of any parameter will impact the retrieval of all parameters, whereby some effect may cancel each other out and some effects may exacerbate errors.

The use of hyperspectral data will reduce the ambiguity in the retrieval of the different parameters. Alternatively use can be made of other satellite sensors that are designed to measure these atmospheric variables- of course there needs to be near simultaneous measurement by this suite of sensors. Extension of the wavelength range either into the ultraviolet or into the SWIR will improve the removal of atmospheric effects.

4.3 Air-water interface correction

For water targets the 'non-lambertian' air-water interface is an extra complication. Only photons which have penetrated the air-water interface and been backscattered or absorbed by the water or have reached the benthos and are reflected upwards to the water surface contain useful information. Photons from the sun and sky immediately reflected by the air-water interface represent an unwanted component of the water leaving reflectance or radiance. Therefore a correction for the air-water interface reflection is required. The air-interface correction includes correction for sun glint, sky glint and reflection from white caps. Of course it is preferable to avoid sun glint as much as possible by appropriately tilting the sensor and planning the orbit inclination and overpass time (see chapter 3).

A number of methods have been developed to correct the sun glint signal over water bodies. The underlying algorithms fall into two categories: geometric models based on the statistics of the slope distribution of waves in the open ocean (Cox and Munk, 1954), and radiometric or image (pixel) driven models based on the spectral distribution of the light reflected at the water surface.

The first approach is applicable to open ocean imagery based on a probability distribution formulism with pixel resolutions well beyond that of wave facets and wave slopes in the order of $100 - 1000$ m, while the second one is used for images with a higher resolution resolving individual waves and

wave facets and for coastal and inland waters where local wind fields make the wind-wave-statistics of the open ocean unreliable. As this study recommends a maximum spatial resolution of ~33 m with preferable spatial resolution of less than ~17 m the only methods applicable are those that can work on a pixel by pixels basis with possibly highly varying contributions of sky and sun glint.

A review of both approaches is given by Kay et al., (2009), see Figure 4.1. All available correction methods for coastal and inland waters contain some residual effects in the water leaving radiance or reflectance products (Kay et al., 2009; Martinez-Vicente et al., 2013). Groetsch et al., (2017) provide a detailed discussion of required corrections for in situ above water spectroradiometric measurements which are akin to a one pixel measurement from an earth observing imager.

For optically shallow waters care must be taken to avoid using spectral bands that have a measurable substratum or benthic vegetation signal at the surface as the sun and sky glint removal method may also remove some of this desired benthic signal. Use of NIR wavelength for sun and sky glint correction is recommended.

It may be useful to define threshold levels for acceptable residual tolerable sun glint levels. For example the MODIS quality flag defines a threshold contribution of 0.005 reflectance as a 'high' glint and 0.001 as a 'Moderate' one. Specifications for glint tolerance also imply that the fraction of such contaminated pixels within a given scene be defined which is usually set at 5%. Finally, it has been shown that while sun glint contamination can be well corrected for retrieved ocean colour products, the effect of sun glint on retrieved atmospheric products, e.g. aerosol optical thickness, can still be significant (Wang and Bailey, 2001).
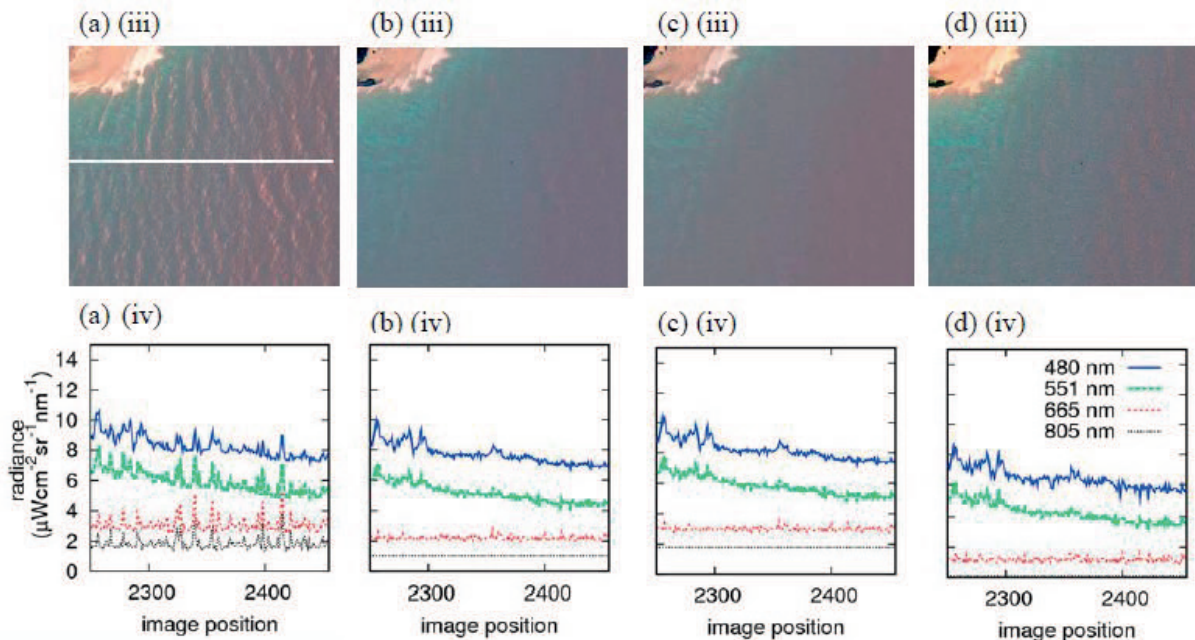
Figure 4.1 IKONOS images of Glover's Reef, Belize, showing effects of different glint correction tools. (a) Image with no glint correction, showing regions used for correction and analysis. Image corrected using the method of Hedley et al.,2005 (c) Lyzenga et al., 2006 , (d) Goodman et al., 2007 In each case (iii) is a pseudo-true colour representation (blue = 445-516 nm, green = 506-595 nm, red = 632-698 nm), (iv shows four wavebands for the line in (a) (iii) Source: Parts of Figure in Kay et al., 2009.

4.4 How to estimate aquatic ecosystem variables from water leaving radiance or reflectance

The aim of the proposed earth observing sensor is to be able to assess the state, condition and trend of inland, estuarine, deltaic and near coastal waters - as well as mapping macrophytes, macro-algae, seagrasses, coral reefs and shallow water bathymetry.

From the optical signal, one can derive optically active water quality parameters including concentrations of phytoplankton (by its proxy chlorophyll-a) as an indicator of the trophic state, concentration of cyanobacteria (by the proxy pigment cyanophycocyanin or cyano-phycoerythrin), dissolved coloured organic components, suspended matter as tracer for transport of pollutants and optical properties like turbidity, vertical attenuation, Secchi depth and euphotic depth. Some parameters serve direct monitoring requirements (e.g., chlorophyll-a, transparency and the ratio green algae / blue green algae are required for the European Water Framework Directive). The water reflectance itself is a recently established essential climate variable (GCOS, 2016).

Recent studies indicate furthermore the possibility to resolve inherent optical properties (total spectral absorption and backscattering, possibly separated into absorption and backscattering of each of the optically active substances) and to classify the spectral optical water type. With increasing spectral resolution such as proposed here it will also become possible to determine particle size distributions of the suspended matter, to establish sources of CDOM (terrestrial or aquatic origin), fractions of organic to mineral composition of suspended matter and functional phytoplankton types (e.g. how different types assimilate carbon or nitrogen etc.)

In optically shallow areas, in addition to the water column optical active constituents and the resulting light absorption and backscattering properties, the bottom type can be classified, the state, condition and trend of the benthic vegetation cover and corals can be determined and the water depth can be determined from the optical measurement.

Earth observation cannot directly assess water quality parameters that do not have a direct expression in the optical response of the water body. These parameters include many chemical compounds such as nutrients. However, in some cases, non-optical products may be estimated through inference, proxy relationships, or data-assimilation with remotely-sensed optical properties of products such as nitrogen, phosphate, organic and inorganic micro-pollutants, and dissolved oxygen. However, these relationships are empirical, may not be causal, and may have a limited validity range. By making use of the combined information in directly measurable optical properties, it is possible to derive management relevant information about trophic state, environmental flows (e.g. inorganic and organic sediment fluxes), and carbon and primary productivity.

Since different optical active water constituents as well as living materials at the surface in the water column or on the benthic substratum have different effects on the reflectance spectrum, it is possible to retrieve their concentrations from the shape and amplitude of the spectrum. Algorithms for these calculations have been designed in various degrees of complexity discussed next.

In Chapter 1 we discussed the types of algorithmic approaches for translating the measured spectral reflectance from a water body to water-quality variables; and these range from: (i) empirical approaches; (ii) semi-empirical approaches; (iii) physics-based, semi-analytical spectral inversion

methods to (iv) Artificial Neural Network (ANN) and Machine Learning Methods and finally (v) Object Based Image Analysis (OBIA) methods. Increasingly use is made of several of these techniques together: e.g. performing atmosphere correction using a ANN approach and then performing a semi-analytical inversion on the remote sensing reflectance or water leaving radiance at the surface (Brando et al., 2012) or using a radiative transfer based atmospheric correction for a seagrass or coral reef environment and then applying OBIA to map and classify the benthic habitat etc.

Most algorithms use the atmospherically corrected water leaving radiance or water leaving reflectance as input. These algorithms always use the result of an (inherently imperfect) atmospheric correction as input. An alternative approach is to use the Top of Atmosphere (TOA) signal that is (in general) more than 90% (in the blue) to less than 50% (in NIR) determined by atmospheric optical contributions. Recently Bottom of Rayleigh (BOR) atmospheric correction has been proposed which at a minimum corrects the signal for different heights of the atmospheric column. All three approaches start with a level of uncertainty in the input signal.

Most algorithms that use TOA reflectance to derive water parameters rely on using spectral band ratios or differences that focus on specific spectral absorption or fluorescence features such algal pigment absorption or fluorescence, whereby the exact spectral band that does contain a pigment absorption or fluorescence feature is divided or subtracted by a baseline created using 2 or 3 spectral bands that do not contain the pigment absorption or fluorescence signal. These methods are usually semi-empirical (although they may be parametrised using RT or semi-analytical models), reasonable robust but may be affected by strongly varying atmospheric and surface conditions. Matthews et al., (2012), Odermatt et al., (2012) and Gower et al., (2007) provide overviews of many aquatic ecosystem algorithms including pigment absorption and pigment fluorescence algorithms.

All algorithms and specifically algorithms that use water leaving reflectance or radiance are dependent on the quality of the input spectrum (see section on atmospheric correction). Depending on available parametrization, calibration and validation data and application requirements (e.g. local application vs regional or global application) the algorithms are designed to use the full spectrum, spectral subsets, retrieve single or multiple parameters and have a variety of solution methods.

Empirical approaches statistically relate field samples of one water-quality parameter of interest to reflectance values measured by a satellite or airborne sensor. While there is no need to understand the underlying physical relationships in such algorithms (such as atmospheric and underwater light processes), they do require coincident field measurements to calibrate the relationships for specific water bodies. The empirical algorithms struggle when water column constituents lie outside the range upon which the pertinent statistical relationship was based (in both space and time) and are not easily adapted to new satellite sensors. Empirical methods are also less reliable when undertaking retrospective monitoring, especially when lake water-quality characteristics may change. Empirical algorithms for optically shallow waters often cannot unravel the water column depth and optically active constituents from the substratum reflectance. Empirical algorithms require in situ measurements (preferably) concurrent with the overpass of the sensor. The in situ measurements have to be those that will be derived from the imagery: in most cases for optically deep waters this will be chlorophyll a, cyanobacterial pigments, other algal pigments, CDOM, TSS (often as NAP), Secchi Disk transparency, vertical attenuation of light and turbidity. For optically

shallow waters the in situ measurements additionally focus on water column depth, macrophytes and substratum composition.

Semi-empirical methods are generally used to estimate a single water constituent, based on the causal relation between the signals captured by optical remote sensing instruments and parameter variations. These relations are included in the statistical analysis by focusing on well-chosen wavebands or wavebands combinations, which correlates with the optically active water quality variable of interest (i.e. CHL, TSS, CPE, CPC, CDOM) or a transparency based variable (Secchi Disk transparency, K_d or turbidity). By design these algorithms can sometimes partly annul some of the atmospheric and water surface effects. Semi-empirical algorithms, however, also suffer from (i) extrapolation errors beyond the range of constituents observed; (i) the requirement to establish new, semi-empirical algorithms when switching sensors or applying the algorithm to new water bodies; less reliability in retrospective monitoring when lake water-quality characteristics change.

Physics-based, semi-analytical spectral inversion methods require proper parameterisation of the bio-optical model or radiative transfer computation method representative of the aquatic ecosystem imaged. These inversion methods can cope better with varying water concentrations, varying sources of optical active water constituents and are highly suitable for retrospective analysis. For physics based inversion methods applied to optically shallow waters it is also essential to have a representative spectral library of the freshwater macrophytes, the seagrasses, macro-algae, and corals and associated benthic cover and benthic composition materials.

Both semi-empirical (to a lesser degree) and physics based inversion methods require representative parameterisation: the field or laboratory based water column light absorption and backscattering properties (inherent optical properties (IOPs) of the phytoplankton, the CDOM, the TSS (as NAP) as well as the field-based measurements of total spectral absorption and backscattering properties in combination with the concentrations of algal pigments, CDOM and TSS (as NAP). By dividing the light absorption and backscattering of each constituent with its concentration we can obtain the concentration specific inherent optical properties (SIOPs) which are the essential input into physics based inversion methods.

In principle it is possible to calculate K_d, Secchi Disk transparency and turbidity from these spectral absorption and backscattering measurements. It is important to realize that if a water body (optically shallow or optically deep) is parameterised well there is no longer any requirement for in situ measurements except for validation purposes.

In chapter 2 (+ Appendix A.2.) we present examples of all these variables and parameterizations as they were used for the spectral simulations using the WASI 2D model.

The most important aspects that determine the robustness, accuracy, complexity and optical closure of spectral inversion are:

1. The (forward) bio-optical model formulation. Increasing computer capabilities lead to increased possibilities to approach the problem with complicated models. But the first models (e.g. Dekker, 1993) used simplifications of the RTE in water (Gordon, 1975, first term only). Later approaches (Brando et al., 2003, 2009) use the polynomial optical models published by Lee (1998), Albert and Mobley (2003) or Park and Ruddick (2005). A fast

version of the Hydrolight code was produced recently to facilitate future direct inversion using this complicated model (Mobley, 2011). From an extensive algorithm comparison experiment for more extreme variations of water quality, the main conclusion was that approaches that include a more complete optical model, perform more successfully (Nechad, 2015).

2. The formulation of the total absorption and backscattering terms. Although this seems trivial and standardized, there are variations of the SIOP models where some variables are considered together e.g. the NAP absorption with the CDOM absorption (Doerffer et al., 2007), or variables are omitted (e.g. the spectral variation of the phycocyanin absorption (Simis, 2005, Simis and Kauko, 2012)). For optically shallow waters, additionally the water column depth and bottom reflectance need to be assessed.

3. The model inversion approach and optical closure criterion. Most spectral fitting algorithms use some form of the X^2 parameter to determine the fit of modelled to measured spectrum (e.g. van der Woerd and Pasterkamp, (2008), Brando et al., (2012)). Iterative approaches use convergence of a parameter as stopping criterion which is not necessarily an indication of optimal optical closure (Yang et al., 2011). Mobley (2005) used a look-up-table approach where least-squares minimization was used as closure criterion. Dekker et al., (2011) provide an overview of inversion models for optically shallow waters that detail many of these approaches.

4. The knowledge on SIOPs and their variability. Some algorithms assume constant SIOPs over the image (e.g. Van der Woerd and Pasterkamp, 2008), others permutate over possible sets of SIOPs to make sure that a pixel is treated with its own optical properties (e.g. Brando et al., 2012.,; Tilstone et al., 2012).

4.4.1 How to discriminate between optically deep and optically shallow waters

Lodhi and Rundquist (2001) define that Optical Deep Waters (ODSs) are waters where the depth of the water is no less than three times the observed Secchi disk depth (SDD), as the bottom effect on the upwelling spectral signal may then be considered insignificant. Otherwise it is taken as Optical Shallow Waters (OWS), as the water leaving signals are influenced by either the bottom or submerged aquatic plants. Brando et al., (2009) extended this concept based on imaging spectrometry by defining OSWs as waters where the signal from the substratum is directly measurable at the surface and the substratum signal at the surface is higher than a threshold based on the noise properties of the hyperspectral data, while in ODWs no signal from the substratum is measurable. The waters where the contribution from the substratum is measurable but the substratum signal at the surface is close to or lower than the threshold are identified as "quasi-optically deep waters" (Brando et al., 2009).

4.4.2 Optical deep waters

A procedure of semi-analytical modelling for optically deep waters is firstly to use R_{rs} data at multiple bands to deduce the IOPs (inherent optical properties) of water, then based on the relationships between IOPs and water components, to establish and solve a series of linear or nonlinear equations to obtain water constituents concentrations (Lee et al., 1998, Carder et al., 2004). Lee et al., (2002) also developed a multiband quasi-analytical algorithm for ODWs to derive inherent optical properties, which is based on remote sensing reflectance derived from the radiative transfer

equation, and values of total absorption and backscattering coefficients that are analytically calculated from values of R_{rs}.

In case bio-optical models can be written as a linear equation system fast matrix inversion methods have been successfully applied in inland waters (Hoogenboom and Dekker, 1998, Keller, 2001, Giardino et al., 2007) and coastal waters (Brando et al., 2003, Brando et al., 2012).

Advanced spectral inversion procedures are typically built on matching spectral measurements with bio-optical forward models derived spectra by means of different inversion techniques. For example, Mobley (2005) used a look-up-table approach where least-squares minimization is used to found the closest match between the image spectrum and a database of remote sensing reflectance constructed with the radiative transfer numerical model Hydrolight (Mobley, 1994). Other inversion techniques such as iterative non-linear optimization (or curve-fitting) methods were used (e.g. Lee et al., 1999; Zhang et al., 2008) to provide an estimation of the parameters iteratively, when the gradient of a figure merit (e.g. the root mean square error) reached the minimum. The inversion can also be based on a neural-network inversion scheme that was for instance used by Doerffer and Schiller (2007) and Vilas et al., (2011) for retrieval of water quality parameters in optically complex waters.

All these inversion procedures can retrieve multiple optical water quality properties at once from a single optical reflectance spectrum (Keller, 2001) and are based on the inversion of a physically based model describing the relationship between the reflectance, optical properties of water components and constituent concentrations (e.g. Brando and Dekker, 2003). Semi-analytical approaches and especially spectral fitting methods show improved accuracy for estimating water-column composition (Dekker et al., 2001), are capable of assessing the error in the estimation of water-quality constituents, are repeatable over time and space, are transferable to new water bodies and other sensors, and can be retrospectively applied to image archives (Dekker at al., 2006, Odermatt et al., 2012). This means that retrospective monitoring of optical water-quality changes is possible, by processing the satellite image archives going back 40 years, to assess the impacts and mitigation of various stressors to the system.

4.4.3 Optically shallow waters

Algorithm approaches for OSWs in principle can be based on the same spectral fitting procedures as for ODWs but the signal of the substrate with certain attenuation in the water column has to be taken into account additionally. Substrate types and depth in shallow water habitats have been estimated with a variety of techniques, which includes classification techniques (e.g. Leiper et al., 2014), spectral inversion of bio-optical modelling (e.g. Dekker et al., 2011) and an assemblage of those methods (e.g. Purkis and Pasterkamp, 2004).

Theoretically, spectral inversion techniques allow water constituents, bottom depth and fractional cover of up to three substrates types per pixel to be simultaneously retrieved. As illustrated in the review by Dekker et al., (2011) most physics-based spectral inversion methods are based on the initial simplified semi-analytical model for shallow water remote sensing developed by Lee et al., (1999; 1998), which is based on the analytical model proposed by Maritorena et al., (1994). The inversion scheme can be using either look-up tables or iterative optimization.

Lee et al., (1999; 2001) used an inversion- optimization approach to simultaneously derive water depth and water column properties from hyperspectral data in coastal waters. The method developed by Lee et al., (1999; 2001) has been extend by incorporating linear un-mixing of the benthic cover. Albert and Gege (2006) and Giardino et al., (2007) used multiple substrate classes (bare sand and submerged macrophytes) in littoral zones of lakes, Goodman and Ustin (2007) and Klonowski et al., (2007) integrated a semi-analytical inversion model with a linear un-mixing of three substratum types for coral reef environments.

For the look-up table approach (Louchard et al., 2003 ; Mobley et al., 2005 ; Hedley et al., 2009), the radiative transfer model is used in forward mode in order to build a pre-computed database of spectra corresponding to different combinations of depth, concentrations, and bottom type. Most of these methods are pixel based. Jay and Guillaume (2014) recently developed a hybrid method, in which estimates of water column parameters are retrieved by maximizing the likelihood function based on a statistical sample and a radiative transfer model.

Practically, a combination of sensor characteristics (e.g., multi-spectral or hyper-spectral resolutions), water column properties (e.g., turbid or clear waters) and substrate types (e.g., clear sand, green, yellow or brown macro-algae; seagrasses, corals) determine the possibilities to obtain accurate estimates (e.g. Botha et al., 2013, Hedley et al., 2012) for all parameters. Botha et al., (2013) clearly demonstrated that by going from multispectral to hyperspectral sensing greater depth penetration and improved benthic classification is achieved.

In optically shallow waters the two extreme cases (a very thin clear water column in optically shallow waters or an almost optical deep water column) lead to either poor water column composition estimation (as the reflected signal from the water column is very small) or poor bathymetry retrieval (as the substratum reflected signal is very faint at the surface) and high uncertainty and substratum discernibility (e.g. Brando et al., 2009; Botha et al., 2013).

4.4.4 Towards global algorithms

A recommended pathway for longer-term operational use is to develop a robust, semi-analytical inversion method for application globally based on having access to relevant spectral bands (see recommendations in chapter 2 with enhanced bands for near future planned missions, or preferably 26 spectral bands for aquatic ecosystem variable estimation, augmented by 15 spectral bands for atmospheric and air-water interface corrections, or imaging spectrometer measurements). Artifical Intelligence (ANN and MLM) and Bayesian statistics approaches can be used to enable smart parametrisation of these inversion models. Semi-empirical methods can be used in the interim, as they often are reasonably robust for a category of water types and for a single EO sensor system and for a single variable such as e.g. chlorophyll a. Empirical approaches are only useful as proof of concept but, in general, are not recommended if all optically active substances (Chl, CDOM, TSS, CPC, CPE and resulting physical properties of turbidity, Secchi Disk depth and K_d) as well as emerse, submerged macrophytes or benthic substratum cover and types need to be determined. Object Based Image Analysis (OBIA) approaches are being used increasingly for benthic mapping, but are usually developed for a specific region with a specific habitat incorporating expert knowledge about the geomorphology, habitat and the species interrelationships. How these OBIA methods extrapolate to other areas is unclear.

4.4.5 Scientific algorithm development challenges

When progressing from multispectral sensors with selected broad bands at key wavelengths to hyperspectral systems with sufficiently fine resolution narrow spectral bands, globally valid algorithm development could focus on advanced hyperspectral algorithms. With full spectral information each curve and slope will be an expression of the combined influence of all optical active constituents. Combining that information with representative spectral measurements of IOPS and SIOPs over the whole spectral and water constituent concentration range as well as spectral substratum measurements will allow for more accurate or more differential algorithms. Effectively this amounts to inverting forward simulation models (see chapter 2 Appendix) that e.g., underpins the results in chapter 2.

In future the potential to map small shifts in the spectrum caused by variable depths in the water column (due to the increasing pure water absorption beyond the orange to red wavelengths), as well as multiple look angles from the EO sensor, if detectable, may enable depth discrimination within the water column of optically active substances bridging the gap between detailed three dimensional aquatic hydrodynamic and ecological models and remote sensing.

With increasing spectral resolution it will also become possible to determine particle size distributions of the suspended matter, to establish sources of CDOM (terrestrial or aquatic origin), fractions of organic to mineral composition of suspended matter and functional phytoplankton types (e.g. how different types assimilate carbon or nitrogen etc.).

4.5 Sources of uncertainties in the obtained quantities

Besides the uncertainty in the TOA measurement of reflectance (and therefore the compromise between spatial, spectral and radiometric resolution (see Ch.2) as well as platform and instrument capabilities (Ch. 3)), the uncertainty in the retrieved water quality parameter depends on the parameterisation of the algorithm as well as the choices made for the various algorithms for atmospheric correction, air-water interface corrections and in-water algorithms. All aspects of the algorithms lead to uncertainties, which include the mathematical formulation of the algorithm, its sensitivity to uncertainties to variables such as atmospheric, its parameterisation with laboratory and field based (concentration specific) inherent optical properties and representativeness of the substratum spectral library. Recent publications about the topic include Lee et al., 2010, Melin et al., 2016, Salama, 2012. The IOCCG report "Uncertainties in Ocean Colour Remote Sensing" will contribute to the discussion and understanding of all involved uncertainties. In general, it has been concluded that ultimately, the uncertainty in the (S)IOPs of air and water will remain the main potential source of error in water quality products. Therefore more spectral information (at higher resolution with higher sensitivity) is required.

4.6 In-situ measurements for algorithm parameterisation, validation and calibration designed to make optimal use of the proposed sensor(s)

4.6.1 IOP and concentration measurements

Algorithm development for future satellite sensors requires in situ instrumentation with dedicated spectral and radiometric capabilities. Based on the simulation studies in chapter 2 of this report it

may be concluded that any spectral measurement should have a spectral resolution around 5 nm or better. Pigment absorption characteristics (e.g. Stomp et al., 2007, Simis and Kauko, 2012) combined with spectral shifts caused by the depth of the water column (simulations in Ch2 and Appendix) requires sensitive well calibrated (spectral and radiometric) in-situ and laboratory equipment.

Table 4.1 Measurements for bio-optical forward and inverse model parameterisation and optical closure measurements (Dekker & Hestir, 2012)

		water quality variables							
		HPLC	Spectro-Photometer	Cell ID & count	LISST-100	HS-6/bb9	ac-s	SD	Spectro-radiometer
		Lab-based sample analysis			In situ submerged supervised				Above/ in water
Algal pigment related measurements (concentration and in-vivo absorption spectrum)	CHL	● (Highly Suited)	● (Highly Suited)	● (partial)	N/A	● (partial)	● (Suitable)	● (partial)	● (Suitable)
	CPC	● (Highly Suited)	● (Suitable)	● (partial)	N/A	● (partial)	● (Suitable)	● (partial)	● (Suitable)
	CPE	● (Highly Suited)	● (Potential)	● (partial)	N/A	● (partial)	● (Suitable)	● (partial)	● (Suitable)
Algal cells	Cell counts	N/A	N/A	● (Potential)	● (partial)	● (partial)	● (partial)	● (partial)	● (Suitable)
Dissolved organic matter related measurements	CDOM	N/A	● (Highly Suited)	N/A	N/A	N/A	● (Suitable)	● (partial)	● (Suitable)
Particulate matter related measurements	Particle size distribution	● (partial)	● (partial)	Algal cells only	● (Highly Suited)	● (Suitable)	● (Potential)	● (partial)	● (Potential)
	NAP	N/A	● (Highly Suited)	N/A	● (Potential)	● (Potential)	● (Potential)	● (partial)	● (Suitable)
	TSM	N/A	● (Highly Suited)	● (partial)	● (Potential)	● (Potential)	● (Potential)	● (partial)	● (Suitable)
Light related measurements	K_d	N/A	Calc	● (partial)	● (partial)	● (partial)	Calc	● (Suitable)	● (Highly Suited)
	Turbidity	N/A	Calc	● (partial)	● (partial)	● (partial)	Calc	● (Suitable)	● (Suitable)
	SD	● (partial)	Calc	● (partial)	● (partial)	● (partial)	Calc	● (Highly Suited)	● (Suitable)

● **Highly Suited**   ● Suitable   ● Potential   ● Not Suitable   ● Variable has a partial effect but cannot be used directly

CHL=chlorophyll; CPC=cyano-phycocyanin; CPE=cyano-phycoerythrin; CDOM =coloured dissolved organic matter; TSM=total suspended matter; NAP = Non-algal particulates; K_d= vertical attenuation of light coefficient; HPLC=high performance liquid chromatography; SD=Secchi disk transparency, Calc=calculated. Other instruments are available from other manufacturers. LISST-100 is a submersible laser scattering instrument that measures concentration and particle size spectra, pressure and temperature. HS-6 is a backscatterometer at 6 wavelengths and BB9 is a backscatterometer at 9 wavelengths. AC-S is a hyperspectral light absorption and beam attenuation meter. Note that the instruments in this table are meant as example instruments only- this report does not endorse any make of instrument.

To further our understanding of optical transfer in the whole space-atmosphere-water system and to improve algorithm approaches, one should consider moving to a more rigorous framework of optical closure. This means that an in-water bio-optical model (coupled with an air-water interface

transfer model) should simulate the same remote sensing reflectance as observed just above the surface (or modelled and observed just above the atmosphere). Optical closure indicates that all the in situ measurements of concentrations and inherent optical properties (and/or assumed model parameters, see Table 4.1.) are in accordance with the measured apparent optical properties. A rigorous hyperspectral optical closure approach requires information on concentrations and knowledge of optical properties of optical active components in water and atmosphere at preferably at minimally double the spectral resolution than the satellite sensor.

In the application field of inland waters, progress towards generic algorithms is hampered by the large diversity of in-situ instrumentation and protocols for the parameters that are measured (e.g. chlorophyll-a, cyanobacterial pigments, CDOM and suspended sediments: see GLaSS protocols report at www.glass-project.eu). Since there are many different ways to measure an optical parameter or optical property, with many different protocols it is important to ensure optical closure for each measurement set, to reduce uncertainty. Quality control is especially necessary for the measurement of algal pigments as there are many steps involved before this pigment can be measured accurately (be it spectrophotometric, fluorometric or by HPLC). Examples of currently available instruments for the measurement of optical properties and concentration are given in 1. In general one can comment that the higher the expected spectral variability is in the optical property, the better the spectral resolution should be of the measurement. Pigment absorption characteristics (e.g. Stomp et al., 2007; Simis & Kauko, 2012) combined with spectral shifts caused by the depth of the water column (simulations in Ch2 and Appendix A.2.) necessitate highly sensitive (spectral and radiometric) in-situ equipment. Going to full optical closure, it is advised to measure absorption, (back)scattering and apparent optical properties (AOPs) with the same high spectral resolution.

With future global fine multispectral or hyperspectral capability, the challenge is to move from local applications to regional and global applications while maintaining a high quality. This requires a high degree of standardization of protocols and the design of data collection methods that work on the regional to global scale. One can think of automated reflectance and IOP collection along transects: see e.g. the protocols project, examples of automated absorption measurements using a flow through Point Source Integrating Cavity Absorption Meter (Wollschläger, 2013).

There is a structural lack of regular in-situ measurements of K_d, SD, turbidity, CDOM absorption, Suspended matter (as NAP), chlorophyll-a and other accessory pigments and backscattering, absorption and cell counts of identified species (groups) such as cyanobacteria. A challenge will be to overcome this lack of systematic in-situ data using new automated sensor types (e.g. DNA identification, flow through absorption meters, flow cytometers with optical characterisation capabilities) and harmonize existing measurements by inter-comparison exercises (of protocols, calibrations and instruments). Costs for automated measurements should be reduced to allow larger scale data collection.

Table 4.2 Water measurements that can be routinely done by water quality management agencies

water quality variables									
	Spectro CHL	Spectro CDOM	Gravi-metric	Fluoro meters	Cell ID & count	K_d/PAR	single λ laser NTU	Multi-λ laser NTU	Spectro-radio
Lab-based sample analysis						In situ submerged supervised			Above/in water
CHL	Highly Suited	Not Suitable	Partial effect	Potential	Partial effect	Partial effect	Not Suitable	Not Suitable	Suitable
CPC	Partial effect	Not Suitable	Partial effect	Potential	Partial effect	Partial effect	Not Suitable	Not Suitable	Suitable
CPE	Partial effect	Not Suitable	Partial effect	Potential	Partial effect	Partial effect	Not Suitable	Not Suitable	Partial effect
Algal cell counts	Partial effect	Not Suitable	Partial effect	Not Suitable	Potential	Partial effect	Partial effect	Partial effect	Not Suitable
CDOM	Not Suitable	Highly Suited	Not Suitable	Potential	Not Suitable	Partial effect	Not Suitable	Not Suitable	Suitable
NAP	Not Suitable	Not Suitable	Highly Suited	Not Suitable	Not Suitable	Partial effect	Not Suitable	Partial effect	Suitable
TSM	Not Suitable	Not Suitable	Highly Suited	Not Suitable	Not Suitable	Partial effect	Potential	Suitable	Suitable
Particle size distribution	Partial effect	Not Suitable	Not Suitable	Not Suitable	Algal cells only	Partial effect	Potential	Suitable	Suitable
K_d	Partial effect	Partial effect	Partial effect	Not Suitable	Not Suitable	Highly Suited	Potential	Suitable	Suitable
Turbidity (NTU)	Partial effect	Partial effect	Partial effect	Not Suitable	Not Suitable	Suitable	Suitable	Not Suitable	Suitable
Secchi Disk Transparency	Partial effect	Partial effect	Partial effect	Not Suitable	Not Suitable	Suitable	Suitable	Suitable	Suitable

● Highly Suited ● Suitable ● Potential ● Not Suitable ● Variable has a partial effect but cannot be used directly

SPECTRO=spectrophotometric; CHL=chlorophyll; CPC=cyano-phycocyanin; CPE=cyano-phycoerythrin; CDOM =coloured dissolved organic matter; TSM=total suspended matter; NAP = non-algal particulates; Kd= vertical attenuation of light coefficient; HPLC=high performance liquid chromatography; SD=Secchi disk transparency; NTU=nephelometric turbidity units.

4.6.2 Measurements for model/algorithm verification and validation

Routine in situ measurements by inland, coastal and coral reef management agencies are useful for parameterizing (semi)empirical methods as well as for verifying/validating aquatic ecosystem algorithms. Many water authorities are showing an interest in aquatic ecosystem remote sensing, to fill in spatial and temporal gaps in in situ measurement programs and because of potential and

health, safety and environmental considerations. These authorities should be stimulated to engage in further (regional-global) protocol standardization and start collecting simultaneous supportive measurements. Table 4.2. provides an overview routine in situ measurements and recommended autonomous in situ sensors for deployment by aquatic ecosystem management authorities.

For further operationalization of earth observation for inland to coastal to coral reef parameters some developments of in-situ and laboratory water quality measurements may be of use or are required. Increasingly relevant management authorities are experimenting with, or deploying operationally, in situ autonomous high frequency sensor such as algal pigment- and CDOM fluorometers. Some near future development suggestions could be:

1. *In situ* measurements of reflectance should be introduced widely and move to high frequency automated sampling above and/or below the water surface to enable frequent match-ups with satellite data as well as provide diurnal reflectance variability assessments of the water studied.
2. Next generation cheap and accurate sensors (preferably autonomous, high frequency observing systems) are required: bio-optical measurements (flow-through absorption and scattering meters) for forward and inverse physics-based retrieval model parameterization and validation as well as DNA probes for fast organism identification.
3. Data collection from autonomous platforms should be encouraged: such as floating and airborne drones, gliders, UAV's etc. Protocols for such applications need to be defined.
4. The collection of low cost low quality high volume "citizen observatory" type of instruments should be encouraged with a requirement for strict protocols to ensure data quality standards.

4.6.3 Reflectance measurements

Reflectance measurements are a crucial part of in-situ data collection for vicarious calibration of the TOA radiance, algorithm parameterisation (e.g. via substratum and substratum cover types such as seagrasses, macro-algae, benthic micro-algae coralline algae and corals) design, validation and testing. Having many multispectral bands or hyperspectral reflectance observations (see Ch. 2 recommendations) from satellites will contribute to achieving optical closure, since the knowledge of the continuous shape of spectra will:

- track the TOA radiance measurement performance of the sensor leading to minimised per spectral band errors
- allow to have information on the spectral slopes of absorption and reflectance peaks while filling in spectral regions that are normally not measured but contain reference information
- allow to assess accuracy/deviations in the error-prone regions in the blue (large ambiguities between optical properties of water and air optical components)
- allow improved substratum classification to deeper depths (Botha et al., 2013)
- allow improved water depth estimation for bathymetry purposes
- etc.

Large sets of well characterised reflectance measurements over large areas open up new ways to do algorithm development e.g. by means of understanding different types of water (possibly leading to optical classification (Eleveld et al., 2017). Water reflectance measurements are also the only way to

directly validate atmospheric correction schemes, although the use of nearby land based or floating pseudo invariant reflectance targets can also be used.

Continuously measuring surface radiance or reflectance instruments can be mounted on any type of superstructure (bridge, tower etc.) and do not suffer from biofouling (although they do need cleaning from dust and protection from insects, e.g. spider webs). At locations where there is a larger public interest in water quality (e.g. swimming water locations with potential infestations of cyanobacteria) the continuous measurements can be combined with local (citizen) observations to identify e.g. the presence of floating layers. Subsurface measurements of benthic materials (or taking the benthic materials to the surface and measuring them under controlled irradiance conditions) are also key inputs to optically shallow water algorithms.

The quality of reflectance measurements is dependent on the physical properties of the device and the quality of the calibration, e.g. spectroradiometer intercomparisons (e.g. (Hommersom, 2012; Zibordi et al., 2012)). The reason why intercomparisons are necessary is that instruments with different technical specifications are on the market with various forms of calibrations. Especially in the more challenging dark waters (high spectral absorption) or very turbid waters (high spectral backscattering), measurement uncertainty becomes an issue, as these processes attenuate light thereby reducing photon counts.

By involving aquatic ecosystem management authorities in making above (and below) water in situ spectroradiometer measurements, especially as continuously measuring instruments, they get accustomed to optical water quality measurements using spectral information (similar to measuring reflectance from space) as well as providing high temporal frequency information (e.g. leading to better understanding of diurnal variability).

4.6.4 Atmosphere characterisation measurements

Retrieval of water constituents, water properties or benthic cover requires accurate correction of atmospheric effects in the imagery. Therefore an important part of all validation activities is performing measurements for characterization of the atmosphere. AERONET (a fully automated spectrometer) provides long-term, globally distributed observations of spectral aerosol optical thickness (AOT), inversion products, and precipitable water column (Holben, 1998). For oceans, coastal waters and inland water bodies the AERONET-OC systems measure water leaving radiance systematically as well. The inversion products from AERONET and AERONET-OC systems cover optical, microphysical and radiative properties useful for validation of atmospheric correction algorithms and satellite measurements. A new system is being created called RadCalNet which will focus initially on land based fiducial reference measurements. Whilst AERONET systems provide globally distributed observations from fixed positions, localized field campaigns will require more flexible instrumentation. A good choice for mobile use are handheld sun photometers like the Microtops instruments. Coupled analysis of Microtops sunphotometer and ozonometer measurements give vertical column precipitable water content, vertical column ozone content and vertical column AOT-spectra. AOT spectra are used for computation of the Ångstroem-Exponent, which gives an indication of the aerosol type (Pflug, 2013).

4.7 Instrumentation, protocols and data collection strategies for validation

4.7.1 Towards fiducial reference measurements

Currently the Ocean Colour community is attempting to achieve a high quality standard in in-situ reflectance measurements for satellite validation. This is addressed in the ESA project Fiducial Reference Measurements for Ocean Colour. The objective of this ESA FRM4SOC project is to establish and maintain SI traceability of Fiducial Reference Measurements (FRM) for satellite ocean colour. It implements some of the CEOS Ocean Colour-Virtual Constellation INSITU-Ocean Colour Radiometry white paper recommendations.

Activities in the FRM4SOC project are to:

1. Develop and implement an instrument laboratory and field inter-comparison experiment for FRM radiometers (round robin) with mandatory participation of National Metrology Institution(s).
2. Foster and enhance international Ocean Colour validation activities.
3. Study what is required in terms of infrastructure for vicarious calibration and validation for Europe for the next 20 years leading to firm recommendations on the way forward for the next generation of European Ocean Colour vicarious calibration/verification infrastructure.

We strongly recommend a similar activity for non-oceanic aquatic ecosystems involving inland waters, coastal waters and optically shallow waters (e.g. seagrasses, macro-algae and coral reef environments).

4.7.2 Requirements for next generation field radiometer systems for validation purposes

Depending on the mode of application and the specific purpose, researchers and users should be able to choose between fixed position stations, handheld radiometers and radiometers on floating and flying platforms (buoys and airplanes/drones). Important factors are:

1. Instrument stability, sensitivity to environmental factors and calibration drift should be reduced by smart instrument design.
2. The prescribed viewing geometry should be strictly observed and known.
3. The calibration of the instrument is valid and performed properly, preferably with some form of certification.
4. For high quality (FRM) satellite validation measurements, the SI traceability and the instrument characterization are essential (sensitivity, stray light, thermal drift, etc.).
5. For validation and under-flight studies the spectrometer should have equal or a significantly higher spectral resolution than the satellite/aircraft/drone.
6. For application in challenging environments (high sediment concentration, studies of bottom vegetation etc.) a combination of submergibility, high sensitivity and extended spectral range is required (e.g. observation capability at NIR with relative high sensitivity).
7. To maximize the chance for satellite and in situ match-ups autonomous fixed position instruments are essential (but can be systematically deployed from boats).

8. Managing sub-optimal measurements (e.g. Brando et al., (2009)) and correction of unwanted artefacts by sun glint, sky glint and whitecaps should be investigated and implemented. Such methods should lead to preferred or even standardized approaches.

9. To prevent data loss, connection to the internet and automated upload of the measurements is recommended. For satellite cal/val it would be beneficial if databases would provide an interface to specific Cal/Val databases.

10. Instrument handling (especially for handheld systems) and data processing should be easy enough to allow deployment by non-specialists.

11. Although low cost high frequency citizen observations is seen as a means to increase the number and spatial spread of observations, significant attention will need to be spent on making these measurements robust, effective and systematic by developing strict and easy to use protocols.

4.7.3 Data collection strategies and priorities for calibration/validation research

Data quality is of critical importance for Earth observation applications. Calibration, vicarious calibration and validation (often referred as Cal/Val) correspond to the process of updating and validating on-board and on-ground configuration parameters and algorithms to ensure that the product data quality requirements are met. To meet the baseline product quality requirements, a well-defined Cal/Val plan will be systematically applied. In complement, the operational monitoring of the resulting product-quality is ensured through well-defined Quality Assurance and Quality Control (QA-QC) procedures. The challenge is to ensure that measurements and methods yield consistent and accurate geophysical parameters even though measurements are often made with a variety of different instruments, under different observational conditions, and using different methodologies.

Satellite missions are typically accompanied by a high-level description of all the validation and (vicarious) calibration activities sought for the different levels of data delivery (from Level-1 to Level-2A). The documentation typically includes a list of reference test sites for performing calibration and validation activities during the lifetime of the mission. In many cases field and airborne campaigns are part of the Cal/Val plan in support of the satellite mission specification and implementation.

Therefore, a smart set up of field campaigns and priorities for Cal/Val purposes is briefly presented for supporting this aquatic ecosystem earth observing sensor. Cal/Val items regard every data level (e.g. geometric and radiometric accuracy of Level- 1B data) encompassing prelaunch calibration, post-launch on-board vicarious calibrations and ground-reference methods. In this document, we focus on field data gathering and priorities for Cal/Val of Level-2A data of inland and coastal waters. Considering that these waters show an extremely high variability in aquatic optics, a generally low water leaving signal and a high degree of change during time, the design of a Cal/Val plan in support of this aquatic ecosystem earth observation sensor mission is challenging. A post-launch validation plan based on three approaches is proposed:

1. Autonomous ship based systems provide a suitable platform to collect spatially temporally diverse continuous field reference data for addressing a minimum required number of spectral matchups for validating satellite imagery corrections. A set of hyperspectral radiometer sensors that measure sea surface, sky radiance and total irradiance have been successfully mounted to gather reference remote sensing reflectance for validating ocean colour sensors (e.g. Brando et

al., 2016; Costa et al., 2016; Simis and Olsson, 2013). In many cases the ship based systems include probes for gathering water quality measures (e.g. fluorometry, turbidimetry and thermometers) relevant for satellite products validation.

2. Permanent fixed platforms and moorings supported by dedicated calibration and maintenance regimes provide the best quality observations for long-term calibration data. Prime example is given by the NASA initiated AERONET – Ocean Colour (AERONET-OC), which provides the additional capability of measuring water-leaving radiance in seven channels with CE-318 sun-photometers (used in AERONET) installed on offshore platforms like jetties, lighthouses, oceanographic and oil towers. It is strongly recommended to equip such systems with hyperspectral sensors in order to cater to the increasing amount of multispectral and hyperspectral sensors planned and proposed. Continuous autonomous hyperspectral measurements have been used to obtain intra- and inter-daily data in very productive waters (Bresciani et al., 2013). In many cases the fixed platforms include probes for gathering water quality measures (e.g. CDOM and algal pigment fluorometry, turbidity and thermal measurements) relevant for satellite products validation (Zappalà et al., 2004).

3. Field campaigns carried out during the sensor overpass aimed at the EO-product validation have been largely used to collect reference and validation data. Such type of campaigns are specifically designed to account for the spectral variability on water types at the local scale, and they provide support for vicarious calibration, data processing and validation of image analysis. Validation campaigns usually present an opportunity to collect water optical measurements concurrently with water quality and ancillary data to support satellite validation activities. In some cases project activities provide a database or data warehouse of field campaign results (e.g., SEABASS, LIMNADES, MERMAID and GLEON).

Whatever the approach a Cal/Val plan in support of the multi or hyperspectral mission in inland and coastal waters and over coral reefs should provide field observations which are accurate and statistically representative of the variability of these targets (from high absorbing to high scattering, from sea level to alpine mountains, from small ponds to large lakes, from optically shallow mid ocean coral reefs to optically deep) as well as on data processing issues (e.g. water targets suffer from the presence of the adjacent land surface and new approaches to correct for this type of contamination are still under development and require validation (Kiselev et al., 2015)).

4.8 Conclusion and recommendation

Enabling activities are in summary: atmospheric correction methods; corrections at the air-water interface; estimating aquatic ecosystem variables from water leaving radiance or reflectance using in-water algorithms for optically deep and optically shallow waters; identifying and quantifying sources of uncertainties in the obtained quantities; obtaining in-situ measurements for algorithm development, calibration and validation designed to make optimal use of the proposed sensor(s).

The enabling activities summarised in this chapter are an essential part of making all the investments in earth observing sensors worthwhile as the aim is to provide scientific, environmental and resource information for aquatic ecosystems of relevance to society. It is essential that a balance of funding is assured for all stages of an aquatic ecosystem dedicated mission. In the past, too often, funds reserved for the enabling activities were used to counter cost overruns in the Earth observing sensor and platform production testing, launch and commissioning. We recommend that in the case of an

approved and funded aquatic ecosystem mission funds are reserved for the enabling activities that are quarantined from the sensors production testing, launch and commissioning. There are many examples where the enabling activities could not be funded after launch after which it took years to adequately characterise the TOA data and the BOA data and the applied algorithms before the earth observed data were of sufficient quality to be relevant for assessing the state and condition of the aquatic ecosystem and enabling assessment of trends.

5   Summary of recommendations

Arnold G. Dekker

In summary we identified that the following requirements should determine a comprehensive aquatic ecosystem Earth observing capability:

i)   ability to estimate algal pigment concentrations of chlorophyll-a, accessory pigments, cyanobacteria pigments (cyanophycoerythrin and cyanophycocyanin especially) as well as other wavelengths relevant for phytoplankton functional types research,

ii)   algal fluorescence (especially chlorophyll-a fluorescence at 684 nm),

iii)   ability to measure suspended matter, possibly split up into organic and mineral matter,

iv)   ability to measure coloured dissolved organic matter and discriminate terrestrial from marine CDOM,

v)   spectral light absorption and backscattering of the optically active components,

vi)   measures of transparency of water such as Secchi disk transparency, vertical attenuation of light and turbidity.

For optically shallow waters also:

vii)   estimates of the water column depth (bathymetry) and

viii) estimates of substratum type and cover (e.g. muds, sands, coral rubble, seagrasses, macro-algae, corals, etc.) as well as plants floating at or just above the water surface.

For residual sun glint correction (if sun glint mitigation measures are insufficient) and for estimating the atmospheric composition it is also required to have spectral bands to measure O_3, NO_2, water vapour and aerosols as well as have access to selected bands in the nearby infrared and/or SWIR for sun glint correction.

The results indicate that a dedicated sensor of (non-oceanic) aquatic ecosystems could be a multispectral sensor with ~26 bands in the 380-780 nm wavelength range for retrieving the aquatic ecosystem variables as well as another 15 spectral bands between 360-380 nm and 780-1400 nm for removing atmospheric and air-water interface effects. These requirements are very close to defining an imaging spectrometer with spectral bands between 360 and 1000 nm (suitable for Si based detectors), possibly augmented by a SWIR imaging spectrometer. In that case the spectral bands would ideally have 5 nm spacing and FWHM, although it may be necessary to go to 8 nm wide spectral bands (between 380 to 780nm where the fine spectral features occur -mainly due to photosynthetic or accessory pigments) to obtain enough signal to noise. The spatial resolution of such a global mapping mission would be between ~17 and ~33 m enabling imaging of the vast majority of water bodies (lakes, reservoirs, lagoons, estuaries etc.) larger than 0.2 ha and ~25% of river reaches globally (at ~17 m resolution) whilst maintaining sufficient radiometric resolution.

A cost-effective alternative solution of obtaining improved data over aquatic ecosystems could be to augment near future planned Earth observing sensors to make them significantly more useful for aquatic ecosystem Earth observation. Two spectral bands (one between ~615-625 nm and one between ~670-680 nm) would greatly enhance the capability of these terrestrial focused sensors to determine two important aspects of water quality in inland and coastal waters, respectively:

cyanobacterial (or blue-green algal) concentration and overall abundance of algae via the main photosynthesis pigment of chlorophyll-a.

As spectral and spatial resolution are the core sensor priorities the radiometric resolution and range and temporal resolution need to be as high as is technologically and financially possible. A high temporal resolution could be obtained by a constellation of Earth observing sensors e.g. in various low earth orbits augmented by high spatial resolution geostationary sensors.

Acknowledgements

CEOS, the Committee on Earth Observation Satellites, coordinates civil spaceborne observations of the Earth. Participating agencies strive to address critical scientific questions and to harmonise satellite mission planning to address gaps and overlaps. www.ceos.org

Acronyms and abbreviations

AI	Artificial Intelligence
ANN	Artificial neural network
AERONET-OC	AERONET - Ocean Colour
AOT	Aerosol optical thickness
AOP	Apparent optical property
BRDF	Bi-directional reflectance distribution function
BOA	Bottom of atmosphere
BOR	Bottom of Rayleigh
CDOM	Coloured dissolved organic matter
CEOS	Committee on Earth Observation Satellites
IVOS	The infrared and visible optical sensors subgroup
INFORM	Improved monitoring and forecasting of ecological status of European INland waters by combining Future earth ObseRvation data and Models
CHL	Chlorophyll
CPC	Cyano-phycocyanin
CPE	Cyano-phycoerythrin
CMOS	Complementary metal oxide semiconductor
COCI	Coastal Ocean Color Imager
CSIRO	Commonwealth Scientific and Industrial Research Organisation
CZCS	Coastal Zone Color Scanner
DLR	German Aerospace Center
DN	Digital number
EO	Earth observation
EnMAP	Environmental Mapping and Analysis Program
ET	Evapotranspiration
FLH	Fluorescence line height
FRM	Fiducial reference measurements
FOV	Field of view

FWHM	Full width half maximum
GEO	Group on Earth Observations
GEO	Geostationary orbit sensors
GEOSS	Group on Earth Observations System of Systems
GISAT-1	Geo Imaging Satellite-1
GLaSS	Global Lakes Sentinel Services
GLS	Global Landsat Survey
GLWD	Global Lakes and Wetlands Database
GOCI	Geostationary Ocean Colour Imager (Korea)
GOME	Global Ozone Monitoring Experiment
GOES-R	Geostationary Operational Environmental Satellite
GCP	Ground control point
GSD	Ground spatial distance
HAB	Harmful algal bloom
HEO	Highly elliptical orbit
HICO	Hyperspectral Imager for the Coastal Ocean
HPLC	High performance liquid chromatography
HyspIRI	Hyperspectral InfraRed Imager
IC	Influence coefficients
IOCCG	International Ocean-Colour Coordinating Group
IOP	Inherent optical properties
ISS	International Space Station
LEO	Low Earth Orbit
LIDAR	Light Detection and Ranging
MAA	Mycosporin-like amino acids
MODIS	Moderate Resolution Imaging Spectroradiometer (NASA)
MERIS	Medium Resolution Imaging Spectrometer (ESA)
MTF	Modulation transfer function
NAP	Non-algal pigmented particulate matter
NEΔL	Noise equivalent radiance differences

NIR	Near infrared
NTU	Nephelometric turbidity units
OBIA	Object-based image analysis
OCTS	Ocean Color and Temperature Scanner (Japan)
OCM-2	Ocean Colour Monitor
ODW	Optical Deep Waters
OLCI	Ocean and Land Colour Imager (ESA)
OLI	Operational Land Imager
OMI	Ozone Monitoring Instrument
OOB	Out-of-band
OSOAA	Ordres successifs océan-atmosphère - avancé
OSW	Optical shallow waters
PACE	Plankton Aerosol Cloud Ocean Ecosystem
PFT	Phytoplankton functional type
PRISMA	Prototype Research Instruments and Space Mission Technology Advancement
RadCalNet	Radiometric Calibration Network of Automated Instruments
RS	Remote sensing
RTF	Radiative transfer
RTE	Radiative transfer equation
SAR	Synthetic aperture radar
SCIAMACHY	Scanning Imaging Absorption Spectrometer for Atmospheric Chartography
SD	Secchi disc depth
SDG	Sustainable development goal
SEABASS	SeaWiFS Bio-optical Archive and Storage System
SeaWIFS	Sea-viewing Wide Field-of-view Sensor (NASA)
SGLI	Second Generation Global Imager
SI	International System of Units
SIOP	Specific inherent optical properties
SNR	Signal to noise ratio

SPOT	Satellite pour l'Observation de la Terre
TSM	Total suspended matter
TSS	Total suspended solids
TOA	Top of atmosphere
TOMS	Total Ozone Mapping Spectrometer
UN	United Nation
UV	Ultraviolet
VIS	Visible
VIIRS	Visible Infrared Imager Radiometer Suite
WASI	Water Colour Simulator
WV2	Worldview-2
WV3	Worldview-3

References

Adler-Golden, S. M., P. K. Acharya, A. Berk, M. W. Matthew, and D. Gorodetzky. (2005) Remote bathymetry of the littoral zone from AVIRIS, LASH, and QuickBird Imagery. IEEE Trans. Geosci. Remote Sens., 43, pp: 337-347. doi: /10.1109/TGRS.2004.841246

Ahmad, Z., Franz, B.A., McClain, C.R., Kwiatkowska, E.J., Werdell, J., Shettle, E.P., Holben, B.N. (2010) New aerosol models for the retrieval of aerosol optical thickness and normalized water-leaving radiances from the SeaWiFS and MODIS sensors over coastal regions and open oceans. Appl. Opt.; 49(29), pp: 5545-5560. doi: /10.1364/AO.49.005545

Albert, A., and Mobley, C. (2003) An analytical model for subsurface irradiance and remote sensing reflectance in deep and shallow case 2 waters, Opt. Express, 11(22), pp: 2873–2890. doi: /10.1364/OE.11.002873

Albert, A. (2004) Inversion technique for optical remote sensing in shallow water, Ph.D. dissertation, University of Hamburg, Dep. of Earth Sciences, http://www.sub.unihamburg.de/opus/volltexte/2005/2325/

Albert, A. and Gege, P. (2006) Inversion of irradiance and remote sensing reflectance in shallow water between 400 and 800 nm for calculations of water and bottom properties, Applied Optics, 45(10), pp: 2331-2343. doi: /10.1364/AO.45.002331

Alikas, K., Kratzer, S., Reinart, A., Kauer, T. and Paavel, B. (2015) Robust remote sensing algorithms to derive the diffuse attenuation coefficient for lakes and coastal waters. Limnol. Oceanogr. Methods, 13, pp: 402–415. doi: /10.1002/lom3.10033

Andreadis, K.M., Schumann, G. J-P. and Pavelsky, T. (2013) A simple global river bankfull width and depth database, Water Resources Res., 49, pp: 7164-7168, doi: /10.1002/wrcr.20440

Andrefouet, S., Kramer, P., Torres-Pulliza, D., Joyce, K. E., Hochberg, E. J., Garza-Perez, R., Mumby, P.J., Riegl, B., Yamano, H., White, W. H., Zubia, M., Brock, J. C., Phinn, S.R., Naseer, A., Hatcher, B.G. and Muller-Karger, F.E. (2003) Multi-site evaluation of IKONOS data for classification of tropical coral reef environments. Rem. Sens. of Environm., 88, pp: 128-143. doi: /10.1016/j.rse.2003.04.005

Astoreca, R., Rousseau, V., Ruddick, K., Knechciak, C., van Mol, B., Parent, Y-Y. and Lancelot, C. (2009) Development and application of an algorithm for detecting Phaeocystis globose blooms in the Case 2 Southern North Sea waters, J. of Plankton Res., (31) 3:pp 287-300.

Aurin, D. A., Dierssen, H. M., Twardowski, M., and Roesler, C. (2010) Optical complexity in Long Island Sound and implications for coastal ocean color remote sensing. J. of Geophysical Res., 115, C07011. doi: /10.1029/2009JC005837

Babin, M., D. Stramski, G.M. Ferrari, H. Claustre, A. Bricaud, G. Obolensky, and N. Hoepffner (2003) Variations in the light absorption coefficients of phytoplankton, non-algal particles, and dissolved organic matter in coastal waters around Europe, J. Geophys. Res., 108(C7), 3211. doi: /10.1029/2001JC000882

Bagheri, S., Peters, S., and Yu, T. (2005) Retrieval of marine water constituents from AVIRIS data in the Hudson/Raritan Estuary. International J. of Rem. Sens., 26(18), pp: 4013–4027. doi: /10.1080/0143116042000274023

Barbier, E.B., Hacker, S.D., Kennedy, C., Koch, E.W., Stier, A.C., and Silliman, B.R. (2011). The value of estuarine and coastal ecosystem services. Ecol. Monogr., 81(2), pp: 169–193.

Barnsley, M.J., Settle, J.J., Cutter, M.A., Lobb, D.R., and Teston, F. (2004) The PROBA/CHRIS mission: A low-cost smallsat for hyperspectral multiangle observations of the earth surface and atmosphere. IEEE Trans. on Geosci. and Rem. Sens. 42(7), pp: 1512-1520.

Barnes, R. A., A. W. Holmes, and W.E. Esaias (1995) Stray Light in the SeaWiFS Radiometer, NASA Tech. Memo. 104566, 31, S.B. Hooker, E.R. Firestone, and J.G. Acker, Eds., NASA Goddard Space Flight Center, Greenbelt, Maryland.

Bennett, S. and Wernberg, T. (2014) Canopy facilitates seaweed recruitment on subtidal temperate reefs. J. Ecol, 102, pp: 1462–1470. doi: /10.1111/1365-2745.12302

Blondeau-Patissier, D., Brando, V. E., Oubelkheir, K., Dekker, A.G., Clementson, L.A. and Daniel, P. (2009) Bio-optical variability of the absorption and scattering properties of the Queensland inshore and reef waters, Australia, J. of Geophysical Res., 114, C5. doi: /10.1029/2008JC005039

Blondeau-Patissier, D., Gower, J. F. R., Dekker, A. G., Phinn, S. R., and Brando, V. E. (2014) A review of ocean color remote sensing methods and statistical techniques for the detection, mapping and analysis of phytoplankton blooms in coastal and open oceans. Progr. in Oceanography. Elsevier Ltd. doi: /10.1016/j.pocean.2013.12.008

Botha, E.H., Brando, V.E., Anstee, J.M., Dekker, A.G. and Sagar, S. (2013) Increased spectral resolution enhances coral detection under varying water conditions, Rem. Sens. of Environm., 131, pp: 247–261. doi: 10.1016/j.rse.2012.12.021

Bourg, L. (Editor) (2012) OLCI Level 0, Level 1b Algorithm Theoretical Basis Document. S3-ACR-TN-007. Issue 4.0.

Bracher, A., Lamsal, L. N., Weber, M., Bramstedt, K., Coldewey-Egbers, M., and Burrows, J. P. (2005) Global satellite validation of SCIAMACHY O3 columns with GOME WFDOAS. Atmosph. Chem. and Physics, 5, pp: 2357–2368.

Bracher, A.; Vountas, M.; Dinter, T.; Burrows, J. P; Röttgers, R. and Peeken, I. (2009) Quantitative observation of cyanobacteria and diatoms from space using PhytoDOAS on SCIAMACHY data, Biogeosciences, 6(5), pp: 751-764. doi: /10.5194/bg-6-751-2009

Braga, F., Giardino, C., Bassani, C., Matta, E., Candiani, G.and Strömbeck, N. (2013) Assessing water quality in the northern Adriatic Sea from HICO data, Rem. Sens. Letters, Vol 4: pp: 1028-1037. doi: /10.1080/2150704X.2013.830203

Brando, V. E., and Dekker, A.G. (2003) Satellite hyperspectral remote sensing for estimating estuarine and coastal water quality. IEEE Trans. Geosci. Rem. Sens. 41, pp: 1378-1387. doi: /10.1109/TGRS.2003.812907

Brando, V.E; Anstee, J. M; Wettle, M.; Dekker, A.G; Phinn, S. R. and Roelfsema, C. (2009) A physics based retrieval and quality assessment of bathymetry from suboptimal hyperspectral data, Rem. Sens. of Environm.,113 (4), pp: 755-770, Elsevier.

Brando, V. E., Dekker, A. G., Park, Y. J., and Schroeder, T. (2012) Adaptive semianalytical inversion of ocean color radiometry in optically complex waters, Applied Optics, 51(15), pp: 2808–2833. doi: /10.1364/AO.51.002808

Brando, V. E., Braga, F., Zaggia, L., Giardino, C., Bresciani, M. , Matta, E., Bellafiore,D., Ferrarin, C., Maicu, F., Benetazzo, A., Bonaldo, D., Falcieri, F. M., Coluccelli,A., Russo, A. and Carniel., S. (2015) High-resolution satellite turbidity and sea surface temperature observations of river plume

interactions during a significant flood event. Ocean Science, 11, pp: 909–920. doi: /10.5194/os-11-909-2015

Brando, V. E., Lovell, J. L., King, E. A., Boadle, D., Scott, R., and Schroeder, T. (2016) The Potential of Autonomous Ship-Borne Hyperspectral Radiometers for the Validation of Ocean Color Radiometry Data, Remote Sensing, 8 (2), 150. doi: /10.3390/rs8020150

Bresciani, M., Stroppiana, D., Odermatt, D., Morabito, G. and Giardino, C. (2011) Assessing remotely sensed chlorophyll-a for the implementation of the Water Framework Directive in European perialpine lakes.,Science of the Total Environment, 409 (17), pp: 3083-3091.

Bresciani M., Rossini M., Morabito G., Matta E., Pinardi M., Cogliati S., Julitta T., Colombo R., Braga F. and Giardino C. (2013) Analysis of within- and between-day chlorophyll-a dynamics in Mantua Superior Lake, with a continuous spectroradiometric measurement. Marine and Freshwater Res. 64 (4), pp: 303-316. doi: /10.1071/MF12229

Briottet, X. ,Marion, R. ,Carrere, V., Jacquemoud, St., Chevrel, St. Prastault, P., d'Oria, M., Gilouppe, P., Hosford, S., Lubac, B. and Bourguignon A. (2011) HYPXIM: A new hyperspectral sensor combining science/defence applications, Whispers, 6-9 June 2011, Lisbon, Portugal.

Brondizio, E.S. Moran, E.F. and Wu, Y. (1994) Land use change in the Amazon estuary: patterns of Caboclo settlement and landscape management, Hum. Ecol., 22 (3) (1994), pp: 249-278.

Bulgarelli, B., Kiselev, V. and Zibordi, G. (2014) Simulation and analysis of adjacency effects in coastal waters: a case study, Applied Optics, 53 (8), pp: 1523-1545. doi: /10.1364/AO.53.001523

Byrd, K.B., O'Connell, J.L., Di Tommaso, S. and Kelly, M. (2014) Evaluation of sensor types and environmental controls on mapping biomass of coastal marsh emergent vegetation. Remote Sens. Environm. 149, pp: 166–180.

Byrnes, J., Reed, D., Cardinale, B., Cavanaugh, K., Holbrook, S. and Schmitt, R. (2011) Climate driven increases in storm frequency simplify kelp forest food webs. Glob. Change Biol., 17(8), pp: 2513-2524.

Carder, K.L., Chen, F.R., Cannizzaro, J.P., Campbell, J.W., and Mitchell, B.G. (2004), Performance of the MODIS semi-analytical ocean color algorithm for chlorophyll-a. Adv. Space Res., 33, pp: 1152-1159.

Caron, J., Bézy, J.-P., Courrèges-Lacoste G.B., Sierk, B., Meynart, R., Richert, M. and Loiseaux, D. (2012) Polarization scramblers in Earth observing spectrometers: lessons learned from Sentinel-4 and 5 phases A/B1, ESA.

Carvalho, L. C. McDonald, C. de Hoyos, U. Mischke, G. Phillips, G. Borics, S. Poikane, B. Skjelbred, A.L. Solheim, J. van Wichelen, A.C. Cardoso and M. Cadotte (2013) Sustaining recreational quality of European lakes: minimizing the health risks from algal blooms through phosphorus control, J. Appl. Ecol., 50 (2013), pp: 315-323. doi: /10.1111/1365-2664.12059

Cavanaugh, K., Siegel, D., Kinlan, B. and Reed, D. (2010) Scaling giant kelp field measurements to regional scales using satellite observations. Mar. Ecol. Prog. Ser. 403, pp: 13-27.

Casal, G., Sanchez-Carnero, N., Sanchez-Rodriguez, E.and Freire, J. (2011) Remote sensing with SPOT-4 for mapping kelp forests in turbid waters on the south European Atlantic Shelf, Estuarine, Coastal and Shelf Science, 91, pp: 371-378.

Chami M, Lafrance B, Fougnie B, Chowdhary J, Harmel T. and Waquet F. (2015) Opt Express.,23(21), pp: 27829-27852. doi: /10.1364/OE.23.027829

Chandrasekhar S., (1960) Radiative Transfer, Dover Publications, New-York, NY, 393 p.

Collett, E. (2005) Field Guide to Polarization. SPIE Press. 148 pp.

Concha, J.A. and Schott, J.R. (2016) Retrieval of color producing agents in Case 2 waters using Landsat 8, Rem. Sens. of Environm., 185, pp: 95–107.

Cox, C. and Munk, W. (1954) Measurement of the Roughness of the Sea Surface from Photographs of the Sun's Glitter., J. of the Opt. Soc. of America, 44 (11), pp: 838-850.

Cox, C. and Munk, W. (1954) Statistics of the Sea Surface Derived from Sun Glitter. J. Mar. Res., 13, pp: 198-227.

Corson, M.R., Korwan, D.R., Lucke, R.L., Snyder W.A. and Davis, C. O. (2008)The Hyperspectral Imager For The Coastal Ocean (HICO) On The International Space Station, IEEE Proceedings of the Int. Geosc. and Rem. Sens. Symp., 978-1-4244-2808-3/08.

Costa, M.P.F. (2004) Use of SAR satellites for mapping zonation of vegetation communities in the Amazon floodplain. International J. of Rem. Sens., 25 (10), pp: 1817-1835.

Costa, M.; Evans, T. and Silva, T.S.F. (2016) Remote Sensing of Wetland Types: Subtropical Wetlands of Southern Hemisphere. The Wetland Book. C.M, Finlayson et al., (eds.) Springer Science. doi: /10.1007/978-94-007-6172-8_307-2

Costanza, R., de Groot, R., Sutton, P., van der Ploeg, S., Anderson, S.J., Kubiszewski, I., Farber, S., and Turner, R.K. (2014) Changes in the global value of ecosystem services. Global Environ. Change, 26, pp: 152–158.

Cracknell, A. P. (1999) Remote sensing techniques in estuaries and coastal zones-an update, Int. J. Rem. Sens. 20, pp: 485-96.

Del Castillo, C. (2012) PACE Mission Science Definition Team Report. Del Castillo, Carlos (Chair). October 16th 2012, USA.

Dekker, A. G. (1993) Detection of water quality parameters for eutrophic waters by high resolution remote sensing. Ph.D. dissertation (Vrije Universiteit, Amsterdam, The Netherlands) Available from: dare.ubvu.vu.nl.

Dekker, A. G., Brando, V. E., Anstee, J. M., Pinnel, N., Kutser, T., Hoogenboom, H. J. , Peters, S. W. M., Pasterkamp, R., Vos, R. J., Olbert, C. and Malthus, T. J. (2001) Imaging spectrometry of water, Ch. 11 in: Imaging Spectrometry: Basic principles and prospective applications: Remote Sensing and Digital Image Processing, v. IV: Dordrecht, Kluwer Academic Publishers, pp: 307-359.

Dekker, A. G., Brando, V. E. and Anstee, J. M. (2005) Retrospective seagrass change detection in a shallow coastal tidal Australian lake, Rem. Sens. of Environm., 97, pp: 415-433.

Dekker, A. G., Brando, V.E., Anstee, J.M., Fyfe, S., Malthus, T.J.M. and Karpouzli, E. (2006) Remote sensing of seagrass ecosystems: use of spaceborne and airborne sensors, Chapter 15 in: Larkum, A., Orth, B. and Duarte, C. (eds) Seagrass Biology, Ecology and Conservation , Springer Verlag, Germany: 630 pp.

Dekker A.G., Phinn S.R., Anstee J.M., Bissett P., Brando V.E., Casey B., Fearns P., Hedley J., Klonowski, W., Lee Z.P., Lynch, M., Lyons, M., Mobley C. and Roelfsema C. (2011) Intercomparison of

shallow water bathymetry, hydro-optics and benthos mapping techniques in Australian and Caribbean coastal environments; Limn. & Ocean. Methods. 9: pp: 396-425. doi: /10.4319/lom.2011.9.396

Dekker, A.G. and Hestir, E. (2012) Evaluating the feasibility of systematic inland water quality monitoring with satellite remote sensing; Water for a Healthy Country Flagship, WIRADA Report to the National Plan for Environmental Information, CSIRO, Canberra, Australia, 105 pp.

Doerffer, R., and Schiller, H. (2007) The MERIS Case 2water algorithm. Intern. J. of Remote Sensing, 28(3–4), pp: 517–535.

Doerffer, R., (2008) MERIS Atmosphere and Glint Correction Algorithm Theoretical Basis Document (ATBD), GKSS Forschungszentrum Geesthacht GmbH, Germany.

Dogliotti, A. I., Ruddick, K. G., Nechad, B., Doxaran, D., and Knaeps, E. (2015) A single algorithm to retrieve turbidity from remotely-sensed data in all coastal and estuarine waters. Rem. Sens. of Environm., 156, pp: 157–168. doi: /10.1016/j.rse.2014.09.020

Dierssen, H., McManus, G.B., Chlus, A., Qiu, D., Gao, B_C. and Lina, S. (2015) Space station image captures a red tide ciliate bloom; Proc. National Academy of Sciences , 112 (48), pp: 14783–14787.

Doerffer, R. (2008) MERIS Atmosphere and Glint Correction Algorithm Theoretical Basis Document (ATBD), GKSS Forschungszentrum Geesthacht, GmbH, Germany.

Downing J. A., Prairie Y. T., Cole J. J. , Duarte C. M., Tranvik L. J., Striegl R. G., McDowell W. H., Kortelainen P , Caraco N. F., Melack J. M. and Middelburg J. J. (2006) The global abundance and size distribution of lakes, ponds, and impounds, Limn. and Ocean., 51 pp. doi: /10.4319/lo.2006.51.5.2388.

Dörnhöfer, K. and Oppelt, N. (2016) Remote sensing for lake research and monitoring – Recent Advances, Ecol. Indic., 64, pp: 105-122.

Dogliotti, A.I., Ruddick, K.G., Nechad, B., Doxaran, D. and Knaeps E. (2015) A single algorithm to retrieve turbidity from remotely-sensed data in all coastal and estuarine waters. Rem. Sens. of Environm., 156 pp: 157–168.

Duan, H., Ma, R., Zhang, Y., Loiselle, S.A. (2014) Are algal blooms occurring later in Lake Taihu? Climate local effects outcompete mitigation prevention, J. of Plankton Res., 36 (3), pp: 866–871. doi: /10.1093/plankt/fbt132.

Ebuchi, N.and Kizu, S. (2002) Probability Distribution of Surface Wave Slope Derived Using Sun Glitter Images from Geostationary Meteorological Satellite and Surface Vector Winds from Scatterometers, J. of Oceanography, 58 (477).

Eleveld, M.A., Ruescas, A.B., Hommersom, A., Moore, T.S., Peters, S.W.M., Brockmann, C. (2017) An Optical Classification Tool for Global Lake Waters. Remote Sens., 9, 420 pp.

Elliott M and Quintino V. (2007) The Estuarine Quality Paradox, Environmental Homeostasis and the difficulty of detecting anthropogenic stress in naturally stressed areas. Mar. Pollut. Bull., 54(6), pp: 640-645.

Elmendorf, S.C., Jones, K.D., Cook, B., Diez, J.M., Enquist, C.A. F., Hufft, R.A., Jones, M.O., Mazer, S. J., Miller-Rushing, A.J. Moore, D.J. P., Schwartz, M. D. and Weltzin J. F. (2016) The plant phenology monitoring design for The National Ecological Observatory Network. Ecosphere 7(4). doi: /10.1002/ecs2.1303.

Emberton, S., Chittka, L., Cavallaro, A. and Wang, M. (2016) Sensor capability and atmospheric correction in ocean colour remote sensing, Remote Sensing, 8(1), ISSN 2072-4292. doi: /10.3390/rs8010001.

Evans, T., Costa, M., Telmer, K. and Silva, T. (2010) Using ALOS/PALSAR and RADARSAT-2 to map land cover and seasonal inundation in the Brazilian Pantanal, J. of Selected Topics in Applied Earth Observations and Remote Sensing.

Fest, E.C. (2013) Stray light analysis and control. SPIE Press. 211 pp.

Ferwerda, J. G., Leeuw, J. Atzberger C. and Vekerdy Z. (2007) Satellite-based monitoring of tropical seagrass vegetation: current techniques and future developments. Hydrobiologia, 591, pp: 59-71.

Fox, D. et al., (2007) Near-surface wind speed retrieval from space-based multi-angle imaging of ocean sun glint patterns. Rem. Sens. of Environm., 107 (1-2), pp: 223-231.

Fraser, R.S., Matto, S., Yeh, E., McClain, C. (1997) Algorithm for atmospheric and glint corrections of satellite measurements of ocean pigment. J. of Geophysical Res., 102, pp: 17107–17118.

Fukushima, H. et al., (2009) Improvement of the ADEOS-II/GLI sun-glint algorithm using concomitant microwave scatterometer-derived wind data. Advances in Space Res., 43 (6) 6, pp: 941-947.

Gao, B.C., Montes, M.J. and Davis, C.O. (2004) Refinement of wavelength calibrations of hyperspectral imaging data using a spectrum matching technique, Rem. Sens. of Environm., 90 (4), pp: 424–433.

GaoB_C (2009); Bathymetric mapping by means of remote sensing: methods, accuracy and limitations, Prog. Phys. Geogr., 33, pp: 103-116. doi: /10.1177/0309133309105657

GCOS (2016) The Global observing systems for climate; implementation needs, WMO: www.gcos.wmo.int.

GEO (2007) Inland and Nearshore Coastal Water Quality Remote Sensing Workshop, 27-29th March 2007, Geneva, Switzerland, GEO. www.earthobservations.org/meetings/20070327_29_water_quality_workshop_report.pdf

GEO (2017) Earth Observations in support of the 2030 agenda for sustainable development: Japan Aerospace Exploration Agency (JAXA) on behalf of GEO under the EO4SDG Initiative. Design and Editing: Symbios Communications, JAXA.

GEOSS Water Strategy Report, ftp://ftp.earthobservations.org/TEMP/Water/GEOSS_WSR_Full_Report.pdf (accessed 07.08.2017)

Gege, P. (2014) WASI-2D: A software tool for regionally optimized analysis of imaging spectrometer data from deep and shallow waters. Computers and Geosciences, (62) , pp: 208-215. doi/10.1016/j.cageo.2013.07.022

Giardino, C., Pepe, M., Brivio, P.A. and Zillioli, E. (2001) Detecting chlorophyll, Secchi disk depth and surface temperature in a sub-alpine lake using Landsat imagery, Science of the Total Environment 268 (1),pp: 19-29.

Giardino, C., Brando, V. E., Dekker, A. G., Strömbeck, N., and Candiani, G. (2007) Assessment of water quality in Lake Garda (Italy) using Hyperion. Rem. Sens. of Environm., 109, pp: 183–195.

Giardino, C., Candiani, G., Bresciani, M., Lee, Z., Gagliano, S. and Pepe, M. (2012) BOMBER: a tool for estimating water quality and bottom properties from remote sensing images. Computers & Geosciences, 45, pp: 313–318.

Gilerson, A., Zhou, J. , Hlaing, S. , Ioannou, I. , Schalles, J. , Gross, B. , Moshary F , Ahmed S (2007) Fluorescence component in the reflectance spectra from coastal waters. Dependence on water composition. Optics Express ,15 (24), pp: 15702-15721. doi: / 10.1364/OE.15.015702

Gilerson, A., Zhou, J., Hlaing, S., Ioannou, I., Gross, B., Moshary, F., Ahmed S (2008) Fluorescence Component in the Reflectance Spectra from Coastal Waters. II. Performance of retrieval algorithms. Optics Express, 16, 2446–2460.

Gilerson,A.; Gitelson, A.; Zhou, .J, Gurlin, D., Moses, W.; Ioannou, I. and Ahmed, S. A., (2010) Algorithms for remote estimation of chlorophyll-a in coastal and inland waters using red and near infrared bands. Papers in Natural Resources. 286 pp.

Gitelson, A., Schalles, J., and Hladik, C. (2007) Remote chlorophyll-a retrieval in turbid, productive estuaries: Chesapeake Bay case study. Rem. Sens. of Environm., 109, pp: 464-472.

Gitelson, A.A., Gao, B.-C., Li, R.-R., Berdnikov, S., and Saprygin, V. (2011). Estimation of chlorophyll-a concentration in productive turbid waters using a Hyperspectral Imager for the Coastal Ocean—The Azov Sea case study. Environmental Res. Letters 6(2). doi: /10.1088/1748-9326/6/2/024023

Glaser, C., Groth, D. and Frauendorf, J. (2011) Monitoring of hydrochemical parameters of lignite mining lakes in Central Germany using airborne hyperspectral casi-scanner data; Int. J. of Coal Geology, 86 (1), pp: 40-53.

GLaSS project (2015): Technical report about measurement protocols. Available at: http://www.glass-project.eu/assets/Downloads/GLaSS-inland-waters-protocols-2015.pdfhttp://www.glass-project.eu/assets/Downloads/GLaSS-inland-waters-protocols-2015.pdf

Gong, P., Wang, J. Yu,L., Zhao,Y., Liang, L., Niu, Z., Huang, X., Fu, H., Liu,S., Li, C., Li, X., Fu, W., Liu, C., Xu, Y., Wang, X., Cheng, Q., Hu, L., Yao, W., Zhang, H., Zhu, P., Zhao, Z., Zhang, H., Zheng, Y., Ji, L., Zhang, Y., Chen, H., Yan, A., Guo, J., Yu,L., Wang, L., Liu, X., Shi, T., Zhu, M., Chen, Y., Yang, G., Tang, P., Xu, B., Giri, C., Clinton, N., Zhu, Z., Chen, J. and Chen, J. (2013) Finer resolution observation and monitoring of global land cover: first mapping results with Landsat TM and ETM+ data, International J. of Remote Sensing , 34(7), pp: 2607-2654. doi: /10.1080/01431161.2012.748992

Gons, H. J. (1999) Optical teledetection of chlorophyll a in turbid inland waters. Environmental Science & Technology, 33, pp: 1127–1132.

Goodman, J.; Ustin, S. (2007) Classification of Benthic Composition in a Coral Reef Environment Using Spectral Unmixing. J. Appl. Remote Sens. 1, pp: 011501:1-011501:17.

Gordon, H.R., Du, T., Zhang, T. (1997) Atmospheric correction of ocean color sensors: analysis of the effects of residual instrument polarization sensitivity. Applied Optics, 36, pp: 6938-6948.

Gordon, H. R., and Wang, M. (1994) Retrieval of water-leaving radiance and aerosol optical thickness over the oceans with SeaWiFS: A preliminary algorithm. Applied Optics, 33, pp: 443–452.

Gordon, H. R., Brown, O. B., and Jacobs, M.M. (1975) Computed relationships between the inherent and apparent optical properties of a flat homogeneous ocean. Applied Optics, 14, pp: 417–427.

Gorshelev, V., Serdyuchenko, A., Weber, M., Chehade, W. and Burrows J.P. (2014) High spectral resolution ozone absorption cross-sections – Part 1: Measurements, data analysis and comparison with previous measurements around 293 K V; Atmos. Meas. Tech., 7, pp: 609–624.

Gower, J.F.R. , R. Doerffer, G.A. Borstad ,(1999) Interpretation of the 685 nm peak in water-leaving radiance spectra in terms of fluorescence, absorption and scattering, and its observation by MERIS, International J. of Remote Sensing, 20 (9), pp: 1771-1786. doi: /10.1080/014311699212470

Gower, J.F.R., King, S., Borstad, G. and Brown, L. (2005) Detection of intense plankton blooms using the 709 nm band of the MERIS imaging spectrometer; International J. of Remote Sensing, 26 (9), pp: 2005-2012. doi: /10.1080/01431160500075857

Gower, J. and King, S. (2007) Validation of chlorophyll fluorescence derived from MERIS on the west coast of Canada. International J. of Remote Sensing, 28(3-4), pp: 625-635. doi: /10.1080/01431160600821010

Goyens, C., Jamet, C. and Schroeder, T. (2013) Evaluation of four atmospheric correction algorithms for MODIS-Aqua images over contrasted coastal waters. Rem. Sens. of Environm., 131, pp: 63-75. doi: / 10.1016/j.rse.2012.12.006.

Gregg, W.W., and F.S. Patt (1994) Assessment of tilt capability for spaceborne global ocean color sensors, IEEE Trans. Geosci. and Remote Sens., 33(4), pp: 866-877.

Groetsch, P. M. M., Simis, S. G. H., Eleveld, M. A., and Peters, S. W. M. (2014) Cyanobacterial bloom detection based on coherence between ferrybox observations. J. of Marine Systems, 140,pp: 50–58. doi: /10.1016/j.jmarsys.2014.05.015.

Groetsch, P.M.M., Gege, P., Simis, S.G.H., Eleveld, M.A., Peters, S.W.M. (2017) Validation of a spectral correction procedure for sun and sky reflections in above-water reflectance measurements. Optics Express, 25 (16), pp: A742 – A761.

Guanter, L., Ruiz-Verdu, A., Odermatt, D., Giardino, C., Simis, S., Estelles, V., et al., (2010) Atmospheric correction of ENVISAT/MERIS data over inland waters: Validation for European lakes. Rem. Sens. of Environm., 114, pp: 467–480.

Guanter, L.; Kaufmann, H.; Foerster, S.; Brosinsky, A.; Wulf, H.; Bochow, M.; Boesche, N.; Brell, M.; Buddenbaum, H.; Chabrillat, S.; Hank, T.; Heiden, U.; Heim, B.; Heldens, W.; Hill, J.; Hollstein, A.; Hostert, P.; Krasemann, H.; Leitão, P. J.; van der Linden, S.; Mauser, W.; Mielke, C.; Müller, A.; Oppelt, N.; Roessner, S.; Röttgers, R.; Schneiderhan, T.; Staenz, K.; Segl, K. (2016) EnMAP Science Plan. EnMAP Technical Report, GFZ Data Services. doi: /10.2312/enmap.2016.006.

Guerschman J.P., Donohue R.J., Van Niel T.G., Renzullo L.J., Dekker A.G., Malthus T.J., McVicar T.R., and van Dijk A.I.J.M. (2016) Earth Observations for Monitoring Water Resources. In L.E. García, D. J. Rodríguez, M. Wijnen and I. Pakulski, (Eds.), 'Earth Observation for Water Resources Management: Current Use and Future Opportunities for the Water Sector', the World Bank Group, Washington, USA, pp 78-143. ISBN: 978-1-4648-0475-5; e-ISBN: 978-1-4648-0476-2; doi: /10.1596/978-1-4648-0475-5

Harma P., Vepsalainen J., Hannonen T., Pyhalahti T., Kamari J., Kallio K., Eloheimo K. and Koponen S. (2001) Detection of water quality using simulated satellite data and semi-empirical algorithms in Finland. The Science of the Total Environment 268, pp: 107–121.

Hedley, J.D., Harborne, A.R., Mumby, P.J., (2005) Simple and robust removal of sun glint for mapping shallow-water benthos, International J. of Remote Sensing, 26 (10), pp: 2107–2112. doi: /10.1080/01431160500034086

Hedley, J., Roelfsema, C., and Phinn, S.R. (2009) Efficient radiative transfer model inversion for remote sensing applications. Rem. Sens. of Environm., 113(11), pp: 2527–2532.

Hedley, J., Roelfsema, C., Koetz, B. and Phinn, S. (2012) Capability of the Sentinel 2 mission for tropical coral reef mapping and coral bleaching detection. Rem. Sens. of Environm., 120, pp: 145-155. doi: / 10.1016/j.rse.2011.06.028

Hestir, E.L., Khanna, S., Andrew, M.E., Santos, M.J., Viers, J.H., Greenberg, J.A., Rajapakse, S.S., and Ustin, S.L. (2008) Identification of invasive vegetation using hyperspectral remote sensing in the California Delta ecosystem. Remote Sens. Environ., 112 (11), pp: 4034–4047. doi: /10.1016/j.rse.2008.01.022

Hestir, E., Greenberg, J. and Ustin, S. (2012) Classification trees for aquatic vegetation community prediction from imaging spectroscopy, IEEE J. of Selected Topics in Applied Earth Observations and Remote Sensing, 5 , pp: 1572-1584.

Hestir, E.L., V.E. Brando, M. Bresciani, C. Giardino, E. Matta, P. Villa, A.G. Dekker (2015) Measuring freshwater aquatic ecosystems: The need for a hyperspectral global mapping satellite mission. Rem. Sens. of Environm., 167, pp: 181-195.

Hmimina, G.; Dufrêne, E.; Pontailler, J.Y.; Delpierre, N.; Aubinet, M.; Caquet, B.; de Grandcourt, A.; Burban, B.; Flechard, C.; Granier, A. (2013) Evaluation of the potential of MODIS satellite data to predict vegetation phenology in different biomes: An investigation using ground-based NDVI measurements. Remote Sens. Environ., 132, pp: 145–158.

Hochberg, E. J., M. J. Atkinson and S. Andrefouet (2003) Spectral reflectance of coral reef bottom-types worldwide and implications for coral reef remote sensing. Rem. Sens. of Environm., 85, pp: 159-173.

Hunter, P.D., Tyler, A.N., Carvalho, L., Codd, G.A. and Maberly, S.C. (2010) Hyperspectral remote sensing of cyanobacterial pigments as indicators for cell populations and toxins in eutrophic lakes; Rem. Sens. of Environm., 114, pp: 2705–2718.

Hu C., Lee Z., Ma R., et al., (2010) Moderate Resolution Imaging Spectroradiometer (MODIS) observations of cyanobacteria blooms in Taihu Lake, China J. Geophys. Res. -Oceans , 115, C04002. doi: /10.1029/2009JC005511.

Hu, C., Feng, L., Lee, Z., Davis, C.O., Mannino, A., McClain, C.R. and Franz, B.A. (2012) Dynamic range and sensitivity requirements of satellite ocean color sensors: learning from the past, Applied Optics, 51, pp: 6045-6062.

Holben, B. N., Eck, T. F., Slutker, I., Tanré, D., Buis, J. P., Setzer, A., Vermote, E., Reagan, J. A., Kaufman, Y. J., Nakajima, T., Lavenu, F., Jankowiak, I. and Smirnov, A. (1998) AERONET—A federated instrument network and data archive for aerosol characterization. Rem. Sens. of Environm .,66(1), pp: 1–16.

Hommersom, A. (2012) Intercomparison in the field between the new WISP-3 and other radiometers (TriOS Ramses, ASD FieldSpec, and TACCS),J. of Applied Remote Sensing, 6(1), 63615. doi: /10.1117/1.JRS.6.063615

Hoogenboom, H. J., Dekker, A. G. (1998) Retrieval of chlorophyll and suspended matter in inland waters from CASI data by matrix inversion. Canadian J. of Remote Sensing 24(2), pp: 144-152.

IOCCG (2010) Atmospheric Correction for Remotely-Sensed Ocean-Colour Products. Wang, M. (ed.), Reports of the International Ocean-Colour Coordinating Group, No. 10, IOCCG, Dartmouth, Canada.

IOCCG (2012) Ocean-Colour Observations from a Geostationary Orbit. Ed. Antoine, D., IOCCG Report No. 12, Canada.

IOCCG (2013) In-flight Calibration of Satellite Ocean-Colour Sensors. Frouin, R. (ed.), Reports of the International Ocean-Colour Coordinating Group (IOCCG), No. 14, IOCCG, Dart-mouth, Canada.

IOCCG (2013) Software for Ocean-Colour Data, http://www.ioccg.org/data/soft ware.html).

IOCCG Report (in press) Earth Observation of global water quality, eds. Greb, S, Dekker, A.G., DiGiacomo, P., Binding, K and Stuart, V. IOCCG, Canada.

Jay, S., and M. Guillaume (2014) A novel maximum likelihood based method for mapping depth and water quality from hyperspectral remote-sensing data. Rem. Sens. of Environm. 147, pp: 121–132.

Jeppesen, E., Søndergaard, M., Søndergaard, M. and Christoffersen, K. (1998) The structuring role of submerged macrophytes in lakes. Ecological Series, Springer-Verlag 131, 423 pp.

Johnsen, G., Samset, O., Granskog, L. and Sakshaug, E. (1994) in vivo absorption characteristics in 10 classes of bloom-forming phytoplankton: taxonomic characteristics and responses to photo adaptation by means of discriminant and HPLC analysis; Marine Ecology Progress Series, 105, pp: 149-157.

Kay, S., Hedley, J. D., Lavender, S., (2009) Sun glint correction of high and low spatial resolution images of aquatic scenes: a review of methods for visible and near-Infrared wavelengths. Remote Sens. 1, pp: 697-730.

Kallio, K., Kutser, T., Hannonen, T., Koponen, S., Pulliainen, J., Vepsäläinen, J. and Pyhälahti, T. (2001) Retrieval of water quality variables from airborne spectrometer in various lake types at different seasons. The Science of the Total Environment, 268 (1 – 3), pp: 59 – 77. doi: /10.1016/S0048-9697(00)00685-9

Keddy, P.A. (2010) Wetland Ecology. Cambridge Studies in Ecology. Cambridge Univ. Press, Cambridge, UK.

Kirk, J. T. O. (2011) Light and photosynthesis in aquatic ecosystems (3rd ed.). Cambridge: Cambridge University Press.UK.

Kiselev, V., Bulgarelli, B. and Heege, T. (2015) Sensor independent adjacency correction algorithm for coastal and inland water systems Rem. Sens. of Environm., 157, pp: 85-95

Klemas, V. (2013) Remote sensing of emergent and submerged wetlands: An overview. International J. of Remote Sensing, 34, pp: 6286-6320.

Klonowski, W. M., Fearns, P. R. C. S. and Lynch, M.J. (2007) Retrieving key benthic cover types and bathymetry from hyperspectral imagery. J. of Applied Remote Sensing, 1 (1),011505. doi: /10.1117/1.2816113.

Knaeps, E., Dogliotti, A., Raymaekers, D., Ruddick, K., and Sterckx, S. (2012) In situ evidence of non-zero reflectance in the OLCI 1020nmband for a turbid estuary. Rem. Sens. of Environm., 120, pp: 133–144

Kuchinke, C. P., Gordon, H. R., and Franz, B. A. (2009) Spectral optimization for constituent retrieval in case 2 waters I: Implementation and performance. Rem. Sens. of Environm., 113, pp: 571–587.

Kuenzer, C., Bluemel, A., Gebhardt, S., Quoc, T.V., Dech, S. (2011) Remote sensing of mangrove ecosystems: A review, Remote Sensing, 3 (5), pp: 878-928.

Kuenzer, C., Renaud, F. G. (2012) Climate and Environmental Change in River Deltas Globally: Expected Impacts, Resilience, and Adaptation. In: The Mekong Delta System - Interdisciplinary Analyses of a River Delta. pp: 7—46, Springer, ISBN: 978-94-007-3961-1.

Kuenzer, C., Leinenkugel, P., Dech, S. (2017) Remote sensing the Mekong. 978-0-415-30638-6 (ISBN), 192 pp.

Kutser, T., Dekker A. G. and Skirving W. (2003) Modelling spectral discrimination of Great Barrier Reef benthic communities by remote sensing instruments. Limn. & Oceanogr., 48, pp: 497-510.

Kutser, T.; Vahtmäe, E.; Praks, J.A. (2009) Sun Glint Correction Method for Hyperspectral Imagery Containing Areas with Non-Negligible Water Leaving NIR Signal. Rem. Sens. of Environm. 113, pp: 2267-2274.

LeDrew, E. F., Wulder M. and Holden H. (2000) Change detection of satellite imagery for reconnaissance of stressed tropical corals. IGARSS 2000: IEEE 2000 International Geoscience and Remote Sensing Symposium, Vol I - Vi, Proceedings, pp: 2678-2680.

Lee, Z. P., Carder ,K.L., Mobley, C.D., Steward, R.G. and Patch, J.S. (1998) Hyperspectral remote sensing for shallow waters. 1. A semi-analytical model, Appl. Opt. 37, pp: 6329-6338. doi: /10.1364/AO.37.006329

Lee, Z. P., Carder, K. L., Mobley, C. D., Steward, R. G., and Patch, J. S. (1999) Hyperspectral remote sensing for shallow waters: 2. Deriving bottom depths and water properties by optimization. Applied Optics, 38, pp: 3831–3843. doi: /10.1364/AO.38.003831

Lee, Z. P.; Carder, K.L.; Arnone, R.A (2002) Deriving inherent optical properties from water color: A multiband quasi-analytical algorithm for optically deep waters. Applied Optics, 41, pp: 5755-5772. doi: /10.1364/AO.41.005755

Lee, Z. P., and and Carder, K. L. (2002) Effect of spectral band numbers on the retrieval of water column and bottom properties from ocean color data. Applied Optics, 41, pp: 2191–2201. doi: /10.1364/AO.41.002191

Lee, Z.P., Du, K. P., Arnone, R., Liew, S. C., and Penta, B. (2005) Penetration of solar radiation in the upper ocean: A numerical model for oceanic and coastal waters. J. of Geophysical Res. C: Oceans, 110(9), pp: 1–12. doi: /10.1029/2004JC002780.

Lee, Z. P., Carder, K., Arnone, R., and He, M. (2007) Determination of primary spectral bands for remote sensing of aquatic environments. Sensors, 7, pp: 3428–3441. doi: /10.3390/s7123428

Lee, Z. P. Ahn, Y.H. Mobley, C. and Arnone, R. (2010) Removal of surface-reflected light for the measurement of remote-sensing reflectance from an above-surface platform, Opt. Express, 18, pp: 26313–26342. doi: /10.1364/OE.18.026313

Lee, Z. P., Du, K., Voss, K. J., Zibordi, G., Lubac, B., Arnone, R. A. and Weidemann, A. (2011) An inherent-optical-property-centered approach to correct the angular effects in water-leaving radiance. Applied Optics, 50, pp: 3155–3167. doi: /10.1364/AO.50.003155

Lee, Z. P., Shang, L., Hu, C. and Zibordi, G. (2014) Spectral interdependence of remote-sensing reflectance and its implications on the design of ocean color satellite sensors, Applied Optics, 53, pp: 3301-3310. doi: /10.1364/AO.53.003301

Lehner, B. and Döll, P. (2004) Development and validation of a global database of lakes, reservoirs and wetlands, In J. of Hydrology, 296 (1–4), pp: 1-22, ISSN 0022-1694. doi: /10.1016/j.jhydrol.2004.03.028.

Leiper, I., S. Phinn and A. G. Dekker (2012) Spectral reflectance of coral reef benthos and substrate assemblages on Heron Reef, Australia. International J. of Remote Sensing, 33, pp: 3946-3965.

Leiper, I. A., Phinn, S.R., Roelfsema, C.M., Joyce, K.E. and Dekker, A.G.(2014) Mapping Coral Reef Benthos, Substrates, and Bathymetry, Using Compact Airborne Spectrographic Imager (CASI) Data, Remote Sensing 2014, 6(7), pp: 6423-6445; doi: /10.3390/rs6076423.

Lim, A., J. D. Hedley, E. LeDrew, P. J. Mumby and C. Roelfsema (2009) The effects of ecologically determined spatial complexity on the classification accuracy of simulated coral reef images. Rem. Sens. of Environm., 113, pp: 965-978.

Liu, X., Zhang, Y., Yin, Y., Wang, M., and Qin, B. (2013) Wind and submerged aquatic vegetation influence bio-optical properties in large shallow Lake Taihu, China. J. of Geophysical Res., Biogeosciences, 118, pp: 713–727.

Lobo, F.L. Costa, M.P. Novo E.M. (2015), Time-series analysis of Landsat-MSS/TM/OLI images over Amazonian waters impacted by gold mining activities, Remote Sens. Environ., 157, pp: 170-184. doi: /10.1016/j.rse.2014.04.030.

Louchard, E.M.; Reid, R.P.; Stephens, F.C.; Davis, C.O.; Leathers, R.A.; Downes, T.V. (2003) Optical remote sensing of benthic habitats and bathymetry in coastal environments at Lee Stocking Island, Bahamas: A comparative spectral classification approach. Limnol. Oceanogr. , 48, pp: 511-521.

Lodhi, M. A. and Rundquist, D. C. (2001) A spectral analysis of bottom-induced variation in the colour of Sand Hills lakes, Nebraska, USA, International J. of Remote Sensing, 22 (9), pp: 1665-1682. doi: /10.1080/01431160117495

Lucke, R.L., Corson, M., McGlothlin, N.R., Butcher, S.D., Wood, D.L., Korwan, D.R., Li R.R., Snyder, W.A., ,Davis, C.O., Chen, D.T., (2011) Hyperspectral Imager for the Coastal Ocean: instrument description and first images. Applied Optics, 50, pp: 1501-1516. doi: /10.1364/AO.50.001501

Lyzenga, D.; Malinas, N.; Tanis, F. (2006) Multispectral bathymetry using a simple physically based algorithm. IEEE Trans. Geosci. Remote Sens., 44, pp: 2251-2259.

Lymburner, L., Botha, E., Hestir, E., Anstee, J., Sagar, S., Dekker, A.G., and Malthus, T.J., (2016) Landsat 8: Providing continuity and increased precision for measuring multi-decadal time series of total suspended matter. Rem. Sens. of Environm., 185, pp: 108-118. doi: /10.1016/j.rse.2016.04.011.

MEA (Millennium Ecosystem Assessment) (2005) Ecosystems and Human Well-being: Synthesis. A Report of the Millennium Ecosystem Assessment, Island Press, Washington, DC, USA.

Malthus, T.J., and George, D.G. (1997) Airborne remote sensing of macrophytes in Cefni Reservoir, Anglesey, UK. Aquatic Botany, 58(3-4), pp: 317-332.

Mannino, A., Novak, M.G., Hooker, S.B. Hyde, K. and Aurin D. (2014) Algorithm development and validation of CDOM properties for estuarine and continental shelf waters along the northeastern U.S. coast; Rem. Sens. of Environm., 152; pp: 576–602. doi: /10.1016/j.rse.2014.06.027

Maritorena, S., Morel, A. and Gentili, B. (1994) Diffuse reflectance of oceanic shallow waters: Influence of water depth and bottom albedo, Limnology and Oceanography, 39 , pp: 1689-1703.

Martinez-Vicente, V., Simis, S. G. H., Alegre, R., Land, P. E. and Groom, S. B. (2013) Above-water reflectance for the evaluation of adjacency effects in earth observation data: Initial results and methods comparison for near coastal waters in the western channel, UK. J. of the European Optical Society, 8.

Matthews, M.W. (2011) A current review of empirical procedures of remote sensing in inland and near-coastal transitional waters, Int. J. Remote Sens., 32 (2011), pp: 6855-6899. doi: /10.1080/01431161.2010.512947

Matthews, M.W., Bernard, S., and Robertson, L. (2012) An algorithm for detecting trophic status (chlorophyll-a), cyanobacterial-dominance, surface scums and floating vegetation in inland and coastal waters. Rem. Sens. of Environm., 124, pp : 637–652.

Matthews, M. W., and Bernard, S. (2013) Characterizing the absorption properties for remote sensing of three small optically-diverse south-african reservoirs. Remote Sensing, 5(9), pp: 4370–4404. doi: /10.3390/rs5094370

Mazeran, C. (2012), Kalicotier, SAABIO processing, Tech. Note Ref. A1037-TN-010-ACR.

Meerhoff, M., Mazzeo, N., Moss, B., and Rodríguez-Gallego, L. (2003) The structuring role of free-floating versus submerged plants in a subtropical shallow lake. Aquatic Ecology, 37, pp: 377-391.

Meister, G. and C. R. McClain (2010) Point-spread function of the ocean color bands of the Moderate Resolution Imaging Spectroradiometer on Aqua. Applied Optics, 49, pp: 6276–6285.

Meister, G., McClain C.R., Ahmad, Z., Bailey, S.W., Barnes, R.A., Brown, S., Eplee, R.E., Franz, B., Holmes, A., Monosmith, W.B., Patt, F.S., Stumpf, R.P., Turpie, K.R., Werdell, P.J. (2011) Requirements for an Advanced Ocean Radiometer. NASA/TM—2011-215883.

Melin, F., Vantrepotte, V., Chuprin, A., Grant, M., Jackson, T. and Sathyendranath, S. (2016) Global Trends in Chlorophyll Concentration Observed with the Satellite Ocean Colour Data Record. ESA Living Planet Symposium 2016, 9-13 May 2016, Prague, Czech Republic.

Miesch, C. Poutier, L., Achard, V., Briottet, X., Lenot, X. Boucher Y. (2005) . Direct and inverse radiative transfer solutions for visible and near-infrared hyperspectral imagery. IEEE Transactions on Geoscience and Remote Sensing, 3 (7), pp: 1552-1562.

Minu, S., and Shetty, A. (2015) Atmospheric Correction Algorithms for Hyperspectral Imageries : A Review, (2015) International Res. J. of Earth Sciences, ISSN 2321–2527, 3(5), pp: 14-18.

MODIS Level 3 Data User Guide. (2015) Document #D-96147, JPL URS CL#15-5550Version 5.0, 29 pp.

Mobley, C.D. (1994) Light and Water, San Diego, CA: Academic Press.

Mobley, C. D. (1999) Estimation of the remote-sensing reflectance from above-surface measurements. Applied Optics, 38, pp: 7442–7455.

Mobley, C.D., Sundman, L.K., Davis, C.O., Bowles, J.H., Downes, T.V., Leathers, R.A., Montes, M.J., Bissett, W.P., Kohler, D.D.R., and Reid, R.P. (2005) Interpretation of hyperspectral remote-sensing imagery by spectrum matching and look-up tables. Applied Optics, 44(17), pp: 3576–3592.

Mobley, Curtis D. (2011) Fast light calculations for ocean ecosystem and inverse models, Opt. Express, 19, pp: 18927-18944.

Mobley, C. D., P. J. Werdell, B. Franz, Z. Ahmad, and S. Bailey (2016) Atmospheric Correction for Satellite Ocean Color Radiometry: A Tutorial and Documentation of the Algorithms Used by the NASA Ocean Biology Processing Group. Sequoia Scientific, Inc. USA.

Montagner, F., Billat, V. and Belanger, S. (2003) MERIS ATBD 2.13 Sun Glint Flag Algorithm. Available at: http://envisat.esa.int/instruments/meris/atbd/atbd_2_13.pdfhttp://envisat.esa.int/instruments/meris/atbd/atbd_2_13.pdf

Moore, G., and S. J. Lavender (2011), Case 2 (sediment) bright water atmospheric correction, MERIS ATBD 2.6 Issue 5.0.

Moore, G., and Lavender, S. (2011) Case II.S bright pixel atmospheric correction. Tech. Rep., MERIS ATBD 2.7, issue 5, 2011 (URL http://envisat.esa.int/instruments/meris/atbd/ atbd_2.6.pdf).

Moses, W.J.; Bowles, J.H.; Lucke, R.L. and Corson, M.R. (2012) Impact of signal-to-noise ratio in a hyperspectral sensor on the accuracy of biophysical parameter estimation in case II waters. Opt. Express, 20, pp: 4309–4330.

Moses, W.J.; Bowles, J.H. and Corson, M.R. (2015) Expected improvements in the quantitative remote sensing of optically complex waters with the use of an optically fast hyperspectral spectrometer—a modeling study. Sensors, 15, pp: 6152-6173.

Moss, B. (2012) Cogs in the endless machine: lakes, climate change and nutrient cycles: a review, Sci. Total Environ., 434, pp: 130-142. doi: /10.1016/j.scitotenv.2011.07.069

Mumby, P. J., E. P. Green, A. J. Edwards and C. D. Clark (1997) Coral reef habitat-mapping: how much detail can remote sensing provide? Marine Biology, 130, pp: 193-202.

Mumby, P. J. and A. R. Harborne (1999) Development of a systematic classification scheme of marine habitats to facilitate regional management and mapping of Caribbean coral reefs. Biological Conservation, 88, pp: 155-163.

Nechad, B., Ruddick, K. G., and Park, Y. (2010) Calibration and validation of a generic multisensor algorithm for mapping of total suspended matter in turbid waters. Rem. Sens. of Environm., 114(4), pp: 854–866. doi: /10.1016/j.rse.2009.11.022

Nechad, B. , Ruddick, K., Schroeder, T., Oubelkheir, K. Blondeau-Patissier, D. Cherukuru, N., Brando, V.E., Dekker, A.G., Clementson, L., Banks, A.C., Maritorena, S., Werdell, P.J., Sá, C. Brotas, V., Caballero de Frutos, I., Ahn, Y.-H., Salama, S., Tilstone, G., Martinez-Vicente, V., Foley, D., McKibben, M., Nahorniak, J., Peterson, T., Siliò-Calzada, A., Röttgers, R., Lee, Z., Peters, S.W.M and Brockmann, C. (2015) CoastColour Round Robin data sets: a database to evaluate the performance of algorithms for the retrieval of water quality parameters in coastal waters, Earth Syst. Sci. Data, 7 (2), pp: 319-348. doi: /10.5194/essd-7-319-2015

Newton, A. and Mudge, S. (2005) Lagoon-sea exchanges, nutrient dynamics and water quality management of the Ria Formosa (Portugal), Estuarine, Coastal and Shelf Science 62 (2005), pp: 405–414.

Odermatt, D., Gitelson, A., Brando, V. E., and Schaepman, M. (2012) Review of constituent retrieval in optically deep and complex waters from satellite imagery. Remote Sens. Environ., 118, pp: 116-126. doi: /10.1016/j.rse.2011.11.013

OLCI Level 2 ATBD (2010), Glint Correction. Sentinel-3 Optical Products and Algorithm Definition Ref: S3-L2-SD-03-C09-ARG- ATBD, Issue: 2.0, 24 pp.

Olmanson, L.G. , Bauer, M.E. and Brezonik, P.L. (2008) A 20-year Landsat water clarity census of Minnesota's 10,000 lakes. Rem. Sens. of Environm., 112 (11), pp: 4086-4097.

Olmanson, L., Brezonik, P.L. and Bauer, M.E. (2011) Evaluation of medium to low resolution satellite imagery for regional lake water quality assessments, Water Resources Res., 47 (9). doi: /10.1029/2011WR011005

O'Neil, J.D. and Costa, M. (2015) Spatial temporal extent of bull kelp (Nereocystis leutkeana) floating canopy area on the west coast of Canada, Final Report Salish Sea Marine Survival Project. 30pp.

Oudrari, H., Schwarting, T., Chiang, K-F., McIntire, J., Pan, C., Xiong, X. and Butler, J. (2010) A methodology to assess the impact of optical and electronic crosstalk in a new generation of sensors using heritage data, IGARSS, 2010, 978-1-4244-9566-5.

Ozesmi, S.L. and Bauer, M.E. (2002) Satellite remote sensing of wetlands. Wetlands Ecology and Management 10, pp: 381-402. doi: /10.1023/A:1020908432489

PACE SDT. (2012) Pre-Aerosol, Clouds, and ocean Ecosystem (PACE) Mission Science Definition Team Report, http://decadal.gsfc.nasa.gov/PACE/PACE_SDT_Report_final.pdf.

Palmer, S.C.J., Odermatt, D., Hunter, P.D., Brockmann, C., Présing, M., Balzter, H., and Tóth, V.R. (2015) Satellite remote sensing of phytoplankton phenology in Lake Balaton using 10 years of MERIS observations. Remote Sens. Environ., 158, pp: 441–452.

Park,E. and Latrubesse, A.M. (2014) Surface water types and sediment distribution patterns at the confluence of mega rivers: The Solimões-Amazon and Negro Rivers junction, Water Resources Res., 51 (8), pp: 6197-6213.

Park, Y.-J., and Ruddick, K. (2005) Model of remote-sensing reflectance including bidirectional effects for case 1 and case 2 waters. Applied Optics, 44, pp: 1236–1249. doi: /0003-6935/05/071236-14

Pavelsky, T.M., Durand, M.T. (2012) Developing new algorithms for estimating river discharge from space. EOS Trans. AGU 93 (45), 457.

Pearlman, J., Barry, P., Segal, C., Shepanski, J., Beiso, D., Carman, S., (2003) Hyperion, a Space-Based Imaging Spectrometer, IEEE Transactions on Geoscience and Remote Sensing, 41(6)6, pp: 1160–1173.

Peters, S. Hommersom, A, Alikas, K., Latt, S., Reinart, A., Giardino, C. ,Bresciani, M. Philipson, P.,Ruescas, A. ,Stelzer, K., Schenk, K. ,Heege, T. ,Gege, P.,Koponen, S., Kallio, K., Zhang, Y. (2015): Global Lakes Sentinel Services: Water quality parameters retrieval in lakes using the MERIS and S3-OLCI band sets. Sentinel-3 for Science Workshop, 2-5 June 2015, Venice, Italy.

Peters, S. W. M., Verhoef, W., Laanen, M., and Van Swol, R. (2008) Sentimers: Towards operational processing of inland waters MERIS FR and Sentinel-3 data. In European Space Agency, (Special Publication) ESA SP.

Pinnel, N. (2007) A method for mapping submerged macrophytes in lakes using hyperspectral remote sensing, PhD Dissertation, Technical University of Munich, Germany, 164 pp.

Pflug, B., (2013) Ground based measurements of aerosol properties using Microtops instruments, AIP Conf. Proc. 1531, 588; doi: /10.1063/1.4804838

Phinn, S., C. Roelfsema, A. Dekker, V. Brando and J. Anstee (2008) Mapping seagrass species, cover and biomass in shallow waters: An assessment of satellite multi-spectral and airborne hyper-spectral imaging systems in Moreton Bay (Australia). Rem. Sens. of Environm., 112, pp: 3413-3425.

Pleskachevsky, A., M. Dobrynin, A.V. Babanin, H. Günther, and E. Stanev, (2011) Turbulent Mixing due to Surface Waves Indicated by Remote Sensing of Suspended Particulate Matter and Its implementation into Coupled Modeling of Waves, Turbulence, and Circulation. J. Phys. Oceanogr., 41, 708–724, doi: /10.1175/2010JPO4328.1

Pons, X., Pesquer, L.,Cristóbal, J. and González-Guerreroa, O. (2014) Automatic and improved radiometric correction of Landsat imagery using reference values from MODIS surface reflectance images, International J. of Applied Earth Observation and Geoinformation, 33, pp: 243-254.

Proctor, C, and Y. He. (2013) Estimation of foliar pigment concentration in floating Macrophytes using hyperspectral vegetation indices. International J. of Remote Sensing. 34(22), pp: 8011-8027.

Purkis, S.J., and Pasterkamp, R. (2004) Integrating in situ reef-top reflectance spectra with Landsat TM imagery to aid shallow-tropical benthic habitat mapping. Coral Reefs, 23, pp: 5-20

Purkis, S. J. (2005) A "Reef-Up" approach to classifying coral habitats from IKONOS imagery. Geoscience and Remote Sensing, IEEE Transactions on, 43, pp: 1375-1390.

QGIS Development Team, (2009) QGIS Geographic Information System. Open Source Geospatial Foundation. URL http://qgis.osgeo.org, Qian, S.E. (Editor) (2016) Optical Payloads for Space Missions. Wiley. 975 pp.

Razinkovas, A., Gasiunaite Z. , Viaroli, P. and Zaldívar J. M. (2008), Preface: European lagoons—Need for further comparison across spatial and temporal scales, Hydrobiologia, 611(1), pp: 1–4, doi: /10.1007/s10750-008-9463-4.

Remer, L.A., Kaufman, Y.J., Tanré, D., Mattoo, S., Chu, D.A., Martins, J.V., Li, R.-R., Ichoku, C., Levy, R.C., Kleidman, R.G., Eck, T.F., Vermote, E., and Holben, B.N. (2005) The MODIS aerosol algorithm, products, and validation. J. Atmos. Sci., 62, pp: 947–973. doi: /10.1175/JAS3385.1.

Reyjol, Y., Argillier, Bonne, Borja, A. Buijse, A.D. Cardoso, A.C. et al. (2014) Assessing the ecological status in the context of the European Water Framework Directive: where do we go now? Sci. Total Environ., 497-498, pp: 332-344. doi: /10.1016/j.scitotenv.2014.07.119

Richter, R., Wang, X., Bachmann, M. and Schläpfer, D. C (2011) Correction of cirrus effects in Sentinel-2 type of imagery , International J. of Remote Sensing, 32(10), pp: 2931-2941.

Riegl, B., A. Bruckner, S. L. Coles, P. Renaud and R. E. Dodge (2009) Coral Reefs Threats and Conservation in an Era of Global Change. Year in Ecology and Conservation Biology 2009, 1162, pp: 136-186.

Robertson Lain, L., Bernard and Matthews, M. (2017) Understanding the contribution of phytoplankton phase functions to uncertainties in the water colour signal; Optics Express, 25 (4), pp: A151-A165. doi: /10.1364/OE.25.00A151

Rodger, A., and Lynch, M. J. (2001) Determining atmospheric column water vapour in the 0.4–2.5 µm spectral region. In: Proceedings of the AVIRIS Workshop 2001. Pasadena, CA.

Ruddick, K. G., Ovidio, F., and Rijkeboer, M. (2000) Atmospheric correction of SeaWiFS imagery for turbid coastal and inland waters. Applied Optics, 39, pp: 897–912.

Ruddick, K. G., De Cauwer, V., Park, Y.-J., and Moore, G. F. (2006) Seaborne measurements of near infrared water-leaving reflectance: The similarity spectrum for turbid waters. Limnology and Oceanography, 51(2), pp: 1167–1179. doi: /10.4319/lo.2006.51.2.1167

Ruddick, K., Brockmann, C., Doerffer, R., Lee, Z., Brotas, V., Fomferra, N., Groom, S., Krasemann, H., Martinez-Vicente, V., Sa, C., Santer, R., Sathyendranath, S., Stelzer, K., Pinnock, S. (2010) The Coastcolour project regional algorithm round robin exercise Remote Sensing of the Coastal Ocean, Land, and Atmosphere Environment, edited by Robert J. Frouin, Hong Rhyong Yoo, Joong-Sun Won, Aiping Feng, Proc. of SPIE ,Vol. 7858. doi: /10.1117/12.869506

Ruescas, A., Brockmann, C., Stelzer, K., Tilstone, G., Beltran, J. (2014) DUE Coastcolour Validation Report, Deliverable DEL-27, version 1.0, Brockmann Consult, Geesthacht, 06-05-2014. http://www.coastcolour.org/documents/DEL-27%20Validation%20Report_v1.pdf.

Ryan A. Vandermeulen, R.A., Mannino, A., Neeley, A., Werdell, J. and Arnone, R. (2017) Determining the optimal spectral sampling frequency and uncertainty thresholds for hyperspectral remote sensing of ocean color; Optics Express, 25(16)pp: A785-A797. doi: /10.1364/OE.25.00A785

Sabbah, S., Shashar, N. (2007) The polarization of light under water near sunrise. J. of the Optical Society of America A. Optics and Image Science, 24, pp: 2049–2056.

Salama, S. (2012) Current Advances in Uncertainty Estimation of Earth Observation Products of Water Quality, Earth Observation, Dr. Rustam Rustamov (Ed.), ISBN: 978-953-307-973-8.

Santer R., Schmechtig, C. (2000) Adjacency effects on water surfaces: primary scattering approximation and sensitivity study. Applied Optics, 39, pp: 361-375. doi: /10.1364/AO.39.000361

Santini,F., Alberotanza, L.,Cavalli. R.M. and Pignatti, S. (2010) A two-step optimization procedure for assessing water constituent concentrations by hyperspectral remote sensing techniques: An application to the highly turbid Venice lagoon waters, Rem. Sens. of Environm. 114, pp: 887–898.

Santos, M., Anderson, L., and Ustin, S. (2011) Effects of invasive species on plant communities: an example using submersed aquatic plants at the regional scale. Biological Invasions, 13, pp: 443-457.

Santos, M.J., Hestir, E.L., Khanna, S., and Ustin, S.L. (2012) Image spectroscopy and stable isotopes elucidate functional dissimilarity between native and non native plant species in the aquatic environment. New Phytol., 193, pp: 683–695.

Schaefer, M.,Goldman,E., Bartuska,A.M.,Sutton-Grier, A. and Lubchenco, J. (2015) Nature as capital: Advancing and incorporating ecosystem services in United States federal policies and programs., PNAS , 112(24), pp: 7383–7389.

Schaeffer, B., Schaeffer, K., Keith, D., Lunetta, R., Conmy, R., and Gould, R. (2013) Barriers to adopting satellite remote sensing forwater qualitymanagement. International J. of Remote Sensing, 34, pp: 7534–7544.

Schaepman, M., Itten, K. , Schlaepfer, D. , Kaiser, J. , Brazile, J., DeBruyn, W. , Neukom, A., Feusi, H. , Adolph, P., Moser, R. ,Schilliger ,T. ,Vos, L. d., Brandt, G. , Kohler, P., Meng, M., Piesbergen, J. , Strobl, P., Gavira, J., Ulbrich, G. ,and Meynart ,R. (2004) Apex: current status of the airborne dispersive pushbroom imaging spectrometer, in Sensors, Systems, and Next-Generation Satellites VII, SPIE Remote Sensing Conference, Barcelona.

Schläpfer, D., C. C. Borel, J. Keller, and K. I. Itten. (1998) Atmospheric precorrected differential absorption technique to retrieve columnar water vapor. Rem. Sens. of Environm., 65, pp: 353-366.

Schroeder, Th., Schaale, M., and Fischer, J. (2007) Retrieval of atmospheric and oceanic properties from MERIS measurements: A new Case-2 water processor for BEAM. International J. of Remote Sensing, 28(24), pp: 5627–5632.

Short, F. T. and H. A. Neckles (1999) The effects of global climate change on seagrasses. Aquatic Botany, 63, pp: 169-196.

Simis, S. G. H., Peters, S. W. M., and Gons, H. J. (2005) Remote sensing of the cyanobacterial pigment phycocyanin in turbid inland water. Limnology and Oceanography, 50(1), pp: 237–245. doi: /10.4319/lo.2005.50.1.0237

Simis, S.G.H., Ruiz-Verdú, A., Domínguez-Gómez, J.A., Peña-Martinez, R., Peters, S.W.M. , Gons, H.J. (2007) Influence of phytoplankton pigment composition on remote sensing of cyanobacterial biomass, Rem. Sens. of Environm., 106(4), pp: 414-427, ISSN 0034-4257, doi: /10.1016/j.rse.2006.09.008.

Simis, S. G. H., and Kauko, H. M. (2012) In vivo mass-specific absorption spectra of phycobilipigments through selective bleaching. Limnology and Oceanography: Methods, 10(2), pp: 214–226. doi: /10.4319/lom.2012.10.214

Simis, S. G. H., and Olsson, J. (2013) Unattended processing of shipborne hyperspectral reflectance measurements. Rem. Sens. of Environm., 135, pp: 202–212. doi: /10.1016/j.rse.2013.04.001

Sondergaard, M., Johansson, L.S., Lauridsen, T.L., Jorgensen, T.B., Liboriussen, L., Jeppesen, E. (2010) Submerged macrophytes as indicators of the ecological quality of lakes. Freshwat. Biol., 55, pp: 893-908.

Sørensen, K., Grung, M. and Roettgers, R., (2003) An inter-comparison of chlorophyll a determinations within the MERIS validation team. Proceedings, MAVT Validation Workshop, 2003a, CD-ROM.

Steinmetz, F., Deschamps, P.-Y. and Ramon, D. (2011) Atmospheric correction in presence of sun glint: application to MERIS, Optics Express, 19 (10), pp: 9783-9800.

Stendera, S., Adrian, R. Bonada, N., Cañedo-Argüelles, M., Hugueny, B., Januschke, K., Pletterbauer, F. and Hering D. (2012) Drivers and stressors of freshwater biodiversity patterns across different ecosystems and scales: a review, Hydrobiologia, 696, pp: 1-28. doi: /10.1007/s10750-012-1183-0

Sterckx, S., and Debruyn, W. (2004) A hyperspectral view of the North Sea. In Proceedings of the Airborne Imaging Spectroscopy Workshop. 2004, Bruges, Belgium.

Sterckx, S., Knaeps, E., and Ruddick, K. (2010) Detection and correction of adjacency effects in hyperspectral airborne data of coastal and inland waters: The use of the near infrared similarity spectrum. International J. of Remote Sensing, 32(21), pp: 6479–6505.

Sterckx S., Knaeps E., Kratzer, S. and Ruddick, K. (2015) SIMilarity Environment Correction (SIMEC) applied to MERIS data over inland and coastal waters, Rem. Sens. of Environm. 157, pp: 96–110. doi: /10.1016/j.rse.2014.06.017.

Stomp, M., Huisman, J., Stal, L. J., and Matthijs, H. C. P. (2007) Colorful niches of phototrophic microorganisms shaped by vibrations of the water molecule. The ISME J., 1(4), pp: 271–282. doi: /10.1038/ismej.2007.59.

Srebotnjak, T., Carr, G., de Sherbinin, A. and Rickwood, C. (2012) A global Water Quality Index and hot-deck imputation of missing data, Ecological Indicators, 17, pp: 108-119. doi: /10.1016/j.ecolind.2011.04.023.

Salama, S. (2012) Current Advances in Uncertainty Estimation of Earth Observation Products of Water Quality, Earth Observation, R. Rustamov (Ed.), ISBN: 978-953-307-973-8, InTech, Available from: http://www.intechopen.com/books/earth-observation/current-advances-in-uncertainty-estimation-ofearth-observation-products-of-water-quality.

Sun, D., Hu, C., Qiu, Z and Wang, S. (2015) Reconstruction of hyperspectral reflectance for optically complex turbid inland lakes: test of a new scheme and implications for inversion algorithms; Optics Express, 23 (11),pp: A718-A740. doi: /10.1364/OE.23.00A718.

Tagliapietra, D., Sigovini, M., and Ghirardini, A. V. (2009) A review of terms and definitions to categorise estuaries, lagoons and associated environments. Marine and Freshwater Res., 60(6), pp: 497-509.

Takashima, T. and Masuda, K. (1985) Degree of radiance and polarization of the upwelling radiation from an atmosphere-ocean system. Applied Optics,24(15), pp: 2423-2429.

Tian, Y. Q., Yu, Q., Zimmermann, M. J., Flint, S. and Waldron, M. C. (2010) Differentiating aquatic plant communities in a eutrophic river using hyperspectral and multispectral remote sensing, Freshwater Biology, 55, pp: 1658–1673. doi: /10.1111/j.1365-2427.2010.02400.x.

Tilstone, G. H., Peters, S. W. M., van der Woerd, H. J., Eleveld, M. A., Ruddick, K., Schoenfeld, W. and Shutler, J. D. (2012) Variability in specific-absorption properties and their use in a semi-analytical ocean colour algorithm for MERIS in North Sea and Western English Channel Coastal Waters, Rem. Sens. of Environm., 118, pp: 320–338. doi: /10.1016/j.rse.2011.11.019

Toming, K., Kutser, T., Laas, A., Sepp, M., Paavel, B. and Nõges, T. (2016) First experiences in mapping lake water quality parameters with Sentinel-2 MSI imagery, Remote Sensing 8, 640. doi: /10.3390/rs8080640.

Turpie, K.R., Klemas, V.V., Kelly, M., Jo, Y.-H. and Byrd, K. (2015) Prospective HyspIRI global observations of tidal wetlands (HyspIRI), Rem. Sens. of Environm., 167, pp: 206-217.

Turpie, K. R., Allen, D. W., Ackelson, S., Bell, T., Dierssen, H., Cavanaugh, K., Fisher, J. B., Goodman, J., Guild, L., Hochberg, E., Klemas, V. V., Lavender, S., Lee, C., Muller-Karger, F., Ortiz, J. D., Palacios, S., Thompson, D. R. and Zimmerman, R. (2015) New need to understand changing coastal and inland aquatic ecosystem services (pp. 11) Decadal Survey for Earth Science and Applications from Space - Request for Information. doi: /10.13140/RG.2.1.5162.6007

Tyler, A. N., Svab, E., Preston, T., Presing, M., and Kovacs, W. A. (2006) Remote sensing of the water quality of shallow lakes: A mixture modelling approach to quantifying phytoplankton in water characterized by high-suspended sediment. International J. of Remote Sensing, 27, pp: 1521-1537.

Tyler, A.N. Hunter, P.D. Spyrakos, E., Groom, S., Constantinescu, A.M. and Kitchen, J. (2016) Developments in Earth observation for the assessment and monitoring of inland, transitional, coastal and shelf-sea waters, Sci. Total Environ. doi: /10.1016/j.scitotenv.2016.01.020

UNEP-WCMC: Millennium Ecosystem Assessment (2005a) Coastal vector digital data. Washington DC, USA, Island Press.

UNEP-WCMC: Millennium Ecosystem Assessment (2005b) Inland water raster digital data. Washington DC, USA, Island Press.

UNEP (2012) Global environment outlook (geo) 5, Tech. Rep., United Nations Environment Programme.

Ungar, S., Pearlman, J., Mendenhall, J. and Reuter, D. (2003) Overview of the Earth Observing One (EO-1) Mission, IEEE Transactions on Geoscience and Remote Sensing, 41(6), pp: 1149 -1159.

USFWS (2014) National Wetlands Inventory website. U.S. Department of the Interior, Fish and Wildlife Service, Washington, D.C., US, (http://www.fws.gov/wetlands/).http://www.fws.gov/wetlands/

Ustin, S.L. Roberts, D.A., Gamon, J.A., Asner, G.P. , Green, R.O. (2004) Using Imaging Spectroscopy to Study Ecosystem Processes and Properties, BioScience, 54 (6), pp: 523–534, doi: /10.1641/0006-3568

Vandermeulen, R.A., Mannino, A., Neeley, A., Werdell, J. and Arnone, R. (2017) Determining the optimal spectral sampling frequency and uncertainty thresholds for hyperspectral remote sensing of ocean color, Optics Express 25(16), pp: A785-A797. doi: /10.1364/OE.25.00A785

Vanderstukken, M., Declerck, S., Decaestecker, E., and Muylaert, K. (2014) Long-term allelopathic control of phytoplankton by the submerged macrophyte Elodea nuttallii, Freshwater Biology, 59, pp: 930–941.

Van der Woerd, H. J., & Pasterkamp, R. (2008) HYDROPT: A fast and flexible method to retrieve chlorophyll-a from multispectral satellite observations of optically complex coastal waters. Rem. Sens. of Environm., 112, pp: 1795-1807. doi: /10.1016/j.rse.2007.09.001

Vanhellemont, Q. and Ruddick, K. (2014) Turbid wakes associated with offshore wind turbines observed with Landsat 8, Rem. Sens. of Environm., 145, pp: 105–115. doi: /10.1016/j.rse.2014.01.009.

Vanhellemont, Q. and Ruddick, K. (2015) Advantages of high quality SWIR bands for ocean colour processing: Examples from Landsat-8; Rem. Sens. of Environm. 161, pp: 89–106.

Van Gorp, B., Mouroulis, P., Wilson, D. and Balasubramanian K. (2010) Polarization and Stray Light Considerations for the Portable Remote Imaging Spectrometer (PRISM). Proc. of SPIE ,Vol. 7812.

Van Puijenbroek, P., Evers, C. and van Gaalen, F.W. (2015) Evaluation of Water Framework Directive metrics to analyse trends in water quality in the Netherlands, Sustain. Water Qual. Ecol. doi: /10.1016/j.swaqe.2015.02.004

Verpoorter, C., Kutser, T., Seekell and D.A., Tranvik, L.J., (2014) A global inventory of lakes based on high-resolution satellite imagery, Geophysical Res. Letters, 41, pp 6396-6402, doi: /10.1002/2014GL060641.

Verrelst, J., Geerling, G.W., Sykora, K.V. and Clevers, J.G.W.P. (2009) Mapping of aggregated floodplain plant communities using image fusion of CASI and LiDAR data. International J. of Applied Earth Observation and Geoinformation, 11(1), pp: 83-94. doi: /10.1016/j.jag.2008.09.001

Viaroli, P., Lasserre, P. and Campostrini, P. (2007) Lagoons and coastal wetland in the global change context: Impacts and management issues, Hydrobiologia, 577.

Vilas, L.G., Spyrakos, E. and Palenzuela, J.M.T. (2011) Neural network estimation of chlorophyll afrom MERIS full resolution data for the coastal waters of Galician Rias (NW Spain). Rem. Sens. of Environm. , 115 (2),pp: 524-535.

Villa, P., Bresciani, M., Bolpagni, R., Pinardi, M. and Giardino, C. (2015) A rule-based approach for mapping macrophyte communities using multi-temporal aquatic vegetation indices . Rem. Sens. of Environm., 171, pp: 218-233.

Wabnitz, C. C., Andrefouet, S., Torres-Pulliza, D., Muller-Karger, F.e. and Kramer, P.A. (2008) Regional-scale seagrass habitat mapping in the Wider Caribbean region using Landsat sensors: Applications to conservation and ecology. Rem. Sens. of Environm., 112, pp: 3455-3467.

Wang, M. and Bailey, S. W. (2001) Correction of sun glint contamination on the SeaWiFS ocean and atmosphere products, Applied Optics, 40, pp: 4790–4798. doi: /10.1364/AO.40.004790

Wang, X.J., et al., (2009) Regulation of phytoplankton carbon to chlorophyll ratio by light, nutrients and temperature in the Equatorial Pacific Ocean: a basin-scale model. Biogeosciences 6, 13.

Wang, X. and Veizer, J. (2000) Respiration–photosynthesis balance of terrestrial aquatic ecosystems, Ottawa area, Canada, Geochimica et Cosmochimica Acta, 64 (22), pp:3775-3786. doi: /10.1016/S0016-7037(00)00477-4

Wettle, M., Brando, V. E. and Dekker, A.G. (2004) A methodology for retrieval of environmental noise equivalent spectra applied to four Hyperion scenes of the same tropical coral reef. Rem. Sens. Environm. (93), pp: 188 – 197.

Wollschläger, J. Grunwald, M. Röttgers, R. and Petersen W. (2013) Flow-through PSICAM: a new approach for determining water constituents absorption continuously, Ocean Dyn. 63(7), pp: 761–775.

Wolanin, A., Soppa, M.A. and Bracher, A. (2016) Investigation of spectral band requirements for improving retrievals of phytoplankton functional types, Remote Sensing 2016, (8) 871. doi: /10.3390/rs8100871

Xu, F., Dubovik, O., Zhai, P-W., Diner, D.J., Kalashnikova, O.V., Seidel, F.C., Litvinov, P., Bovchaliuk, A., Garay, M.J., van Harten, G., and Davis, A.D, (2016) Joint retrieval of aerosol and water-leaving radiance from multispectral, multiangular and polarimetric measurements over ocean, Atmos. Meas. Tech., 9, pp: 2877–2907.www.atmos-meas-tech.net. doi: /10.5194/amt-9-2877-2016

Yang, W., Matsushita, B., Chen, J. and Fukushima, T. (2011) Estimating constituent concentrations in case II waters from MERIS satellite data by semi-analytical model optimizing and look-up tables. Rem. Sens. of Environm., 115(5), pp: 1247–1259. doi: /10.1016/j.rse.2011.01.007

Yamano, H. and Tamura, M. (2004) Detection limits of coral reef bleaching by satellite remote sensing: Simulation and data analysis. Rem. Sens. of Environm., 90, pp: 86-103.

Yeh, E-N., Barnes, R.A. Darzi, M. Kumar, L. Early, E.A. Johnson, B.C. Mueller, J.L. and Trees, C.C. (1997) Case Studies for SeaWiFS Calibration and Validation, Part 4, NASA Tech. Memo 104566, 41, S.B. Hooker and E.R. Firestone, Eds., NASA Goddard Space Flight Center, Greenbelt, Maryland, USA.

Zappalà. G. and Azzaro, F. (2004) A new generation of coastal monitoring platforms. Chem. Ecol., 20(5), pp: 387–398.

Zhang, M., Kong, F.X., Wu, X.D. and Xing, P. (2008) Different photochemical responses of phytoplankters from the large shallow Taihu Lake of subtropical China in relation to light and mixing. Hydrobiologia 603 (1), pp: 267-278.

Zhang, Y., Yin, Y., Wang, M. and Liu, X. (2012) Effect of phytoplankton community composition and cell size on absorption properties in eutrophic shallow lakes: field and experimental evidence. Optics Express, 20(11),pp: 11882-11898.

Zhou, L., and Zhou, G. (2009) Measurement and modelling of evapotranspiration over a reed (Phragmites australis) marsh in Northeast China. J. of Hydrology, 372, pp: 41-47.

Zibordi, G., Ruddick, K., Ansko, I., Moore, G., Kratzer, S., Icely, J. and Reinart, A. (2012) In situ determination of the remote sensing reflectance: An inter-comparison. Ocean Science, 8(4), pp: 567–586. doi: /10.5194/os-8-567-2012

Appendices

A.1   Science Traceability Matrix (Inland waters & Wetlands, Estuarine, Delta's and Lagoon, Seagrasses and Coral Reef, Macro-algae, Shallow Water Bathymetry)

ARNOLD G. DEKKER, NICOLE PINNEL, KEVIN R. TURPIE, STEEF PETERS, CLAUDIA GIARDINO, VITTORIO E. BRANDO

A.2   Sensitivity analysis

PETER GEGE , SINDY STERCKX, ARNOLD G. DEKKER

A.1 Science Traceability Matrix (Inland waters & Wetlands, Estuarine, Delta's and Lagoon, Seagrasses and Coral Reef, Macro-algae, Shallow Water Bathymetry)

ARNOLD G. DEKKER, NICOLE PINNEL, KEVIN R. TURPIE, STEEF PETERS, CLAUDIA GIARDINO, VITTORIO E. BRANDO

This matrix summarizes our applications and scientific requirements findings for the entire range of (non-ocean) aquatic ecosystems. It is based on the expertise of the writing team, the results of the simulations and the literature review results in the main report. The level of scientific and aquatic ecosystem management end user requirements varies across each application area, preventing specific requirements for each habitat to be established. Therefore this SATM is indicative of what needs to be considered – it is recommended to be improved in future as relevant research gets published.

									spatial resolution of 5 m =~ 25 m²
		What management or science relevant information is needed for this aquatic ecosystem component (integrating information from multiple sources such as Earth Observation and.....)	**directly measureable from Earth observation: management relevant aquatic ecosystem variables (by applying a form of inversion algorithm)**	**What variable needs to be measured from Earth observation for quantitative assessment of these variables**	**What variable needs to be measured *in situ* for quantitative assessment or validation of these variables**	**Temporal resolution: Scientific**	**Temporal resolution: Management relevant**	**Spatial resolution Scientific**	**Spatial resolution: Management relevant**
1	Habitats- optically deep								
1.1	Inland waters	phytoplankton primary production, presence and physiological state, eutrophication, PFTs, pHABs, short term bloom phenology, underwater light climate, transparency,(river) plumes of high concentration flowing into lower concentration waters;	Concentrations of chlorophyll-a, CPC, CPE, light attenuation (Kd) , euphotic depth, Secchi Disk transparency, turbidity, TSM, NAP, CDOM, temperature	Spectral Rrs, concentrations of chlorophyll-a, CPC, CPE, Kd, euphotic depth, Secchi Disk transparency, turbidity, TSM, NAP, CDOM, IOPs, SIOPs, temperature	Chl, CPC, CPE using Fluorescence or spectrophotometric or HPLC techniques; Rrs, Kd, Secchi Disk transparency, turbidity, NAP, SPIM + SPOM, CDOM, IOPs, SIOPs.	Hourly (TSM and pHAB's) to daily to weekly to monthly	Bi-monthly (EU Water Framework Directive - water quality), Daily (EU Bathing Directive - HABs),[EU UrbanWaste eWater Treatment Directive]	5-10 m; 100 m for the whole lake surface	pelagic, emissaries/tributaries, up to 300 m from the coastline 10 m resolution - to 50 m
1.2	Estuarine, lagoon, delta and coastal waters	Same as inland waters PLUS: TSM plumes due to dredging activities, wind-induced TSM resuspension from the seafloor, salinity/saltwater intrusions;	same as inland waters PLUS: Oceanic vs freshwater CDOM	Same as inland waters PLUS: CDOM (as proxy for salt water/fresh water dynamics- plume extent etc.)		Hourly to weekly; tidal waters quarter- to half-hourly: (to be achieved through constellation or combination of different sensors)	Bi-Monthly EU-WFD, MSFD (EU- Marine Strategy Framework Directive), MPS (EU Maritime Spatial Planning), BWD (EU- Bathing Water Directive); daily-weekly	20-100 m; Coastal: 1000; Harbours/ estuarine: high spatial variability; lagoons and deltas: 10-30 m	lagoons and deltas: 10-20m ; up to 25m-50m for harbours and near shore applications; Coastal : 100 - 300m

Table A1.1 Habitat- optically deep 1a – temporal and spatial requirement

		Measurement Requirement B=Baseline; T = Threshold				Platform /Ancillary requirements
		Levels/ranges	Spatial	Spectral	Radiometric	**Geometric requirements and geolocational accuracy Sunglint avoidance Polarisation sensitivity**
1	Habitats-optically deep					
1.1	Inland waters	CHL: 0.1-500; TSM: 0.1-1000; CDOM 0.01-20;	T=Spatial resolution 30 m (nominal, nadir) B= 10m	Spectral range from 400 nm to 1100 nm Spectral cal accuracy ±3 nm Spectral sampling 5 nm (FWHM 5nm)	NedL=0.1; NedR=0.0001	Sunglint avoidance, geolocation 10 m
1.2	Estuarine, lagoon, delta and coastal waters	Same as inland waters	T= Spatial resolution 100 m B= Spatial resolution 25 m	Spectral range from 400 nm to 1100 nm Spectral cal accuracy ±3 nm Spectral sampling <10 nm (FWHM <10nm) TSM/Turbidity : 600-850 nm (T requirement) ; Extremely turbid waters: up to 1080 nm (B - Requirement); coarse spectral sampling sufficient (~40 nm)	NedL; NedR	Sunglint avoidance, geolocation 10 m

Table A1.2 Habitat-optically deep 1b – measurement and platform requirement

		What management or science relevant information is needed for this aquatic ecosystem component (integrating information from multiple sources such as Earth Observation and…..)	directly measureable from Earth observation: management relevant aquatic ecosystem variables (by applying a form of inversion algorithm)	What variable needs to be measured from Earth observation for quantitative assessment of these variables	What variable needs to be measured *in situ* for quantitative assessment or validation of these variables	Temporal resolution: Scientific	Temporal resolution: Management relevant	Spatial resolution Scientific	spatial resolution of 5 m =~ 25 m^2
									Spatial resolution: Management relevant
2	Habitats-optically shallow								
2.1	Inland water & submerged macrophytes	primary productivity, eutrophication, biodiversity	Species, extent, density, condition, nascence, scenescence	Spectral Rrs, species reflectance+ depth in water column + background substratum reflectance	Spectral libraries of macrophytes	Monthly to Seasonal	Monthly to Seasonal	5 to 10 m	10 m (from coastline down to the maximum depth of growth)
2.2	Seagrasses, macro-algae & coral reefs	energy environment, eutrophication, temperature effects; seagrass-specific: epibionts; corals-specific: disease, bleaching and COTS damage & recovery;	Type or species, extent, density, biodiversity, condition, nascence, scenescence and coral bleaching	Spectral Rrs, species reflectance + depth in water column + background substratum reflectance	Spectral libraries of seagrasses, macro-algae & corals, rocky reefs, encrusting algae, seagrass and macro-algae wrack, coral rubble, algal overgrowth, epibionts, sands, silts, muds	Weekly to Monthly (except for bleaching and COTS events then weekly)	Weekly to Monthly (except for bleaching and COTS events then weekly)	5 to 10 m	10 m (from coastline down to the maximum depth of growth)
2.3	Shallow water bathymetry	sedimentation, erosion	Shallow water bathymetry for hydrographic, extreme events and environmental applications	all variables for optically deep aquatic habitats PLUS Spectral Rrs, species reflectance PLUS Depth to substratum	Spectral libraries of macrophytes, seagrasses, macro-algae & corals, rocky reefs, encrusting algae, seagrass and macro-algae wrack, coral rubble, algal overgrowth, epibionts, sands, silts, muds	Monthly to yearly	yearly or after extreme event (e.g. tsunami)	5 m	5 m

Table A1.3 Habitats-optically shallow 2a – temporal and spatial requirement

		Measurement Requirement B=Baseline; T = Threshold				Platform /Ancillary requirements
		Levels/ranges	Spatial	Spectral	Radiometric	Geometric requirements and geolocational accuracy Sunglint avoidance Polarisation sensitivity
2	Habitats-optically shallow					
2.1	Inland water & submerged macrophytes		T= spatial resolution 30 m; B= spatial resolution 10 m	Spectral range from 400 nm to 1100 nm Spectral cal accuracy ± 5 Nm Spectral sampling 8 nm (FWHM 8nm)	NedL=0.1; NedR=0.0001	Sunglint avoidance, geolocation 5 m
2.2	Seagrasses, macro-algae & coral reefs		T= spatial resolution 30 m; B= spatial resolution 10 m	Spectral range from 400 nm to 1100 nm Spectral cal accuracy ± 5 Nm Spectral sampling 8nm nm (FWHM 8 nm)	NedL=0.1; NedR=0.0001	Sunglint avoidance, geolocation 5 m
2.3	Shallow water bathymetry		T= spatial resolution 10 m; B= spatial resolution 5 m	Spectral range from … nm to ….. nm Spectral cal accuracy ± ….. Nm Spectral sampling ….. nm (FWHM …nm)	NedL=0.3; NedR=0.001	

Table A1.4 Habitats – optically shallow 2b - measurement and platform requirement

		What management or science relevant information is needed for this aquatic ecosystem component (integrating information from multiple sources such as Earth Observation and…..)	directly measureable from Earth observation: management relevant aquatic ecosystem variables (by applying a form of inversion algorithm)	What variable needs to be measured from Earth observation for quantitative assessment of these variables	What variable needs to be measured *in situ* for quantitative assessment or validation of these variables	Temporal resolution: Scientific	Temporal resolution: Management relevant	Spatial resolution Scientific	Spatial resolution: Management relevant spatial resolution of 5 m =~ 25 m^2
3	Habitats-emersed								
3.1	Macrophytes	Extent and distribution, productivity, biodiversity, condition, invasive species, material flux, dieback	Type or species, extent, density, inflorescence, nascence, scenescence, Vegetation Indices (VI), PRI or photosynthetic pigment fluorescence, CDOM fluorescence	Spectral Rrs, Kd, IOPs (for depth of macrophyte calculations)	Spectral libraries of macrophytes; water depth, tidal range, salinity, water temperature, pH, nutrients, DOx, CDOM, TSM, drainage conditions, canopy height, LAI, LAD, above and below ground biomass, plant stress, photosynthetic efficiency and yield, CO2/O2 flux, microtopology, biodiversity	Tidal fluxes: hours Phenology: 2-3 Days - Monthly Secular trends and peak growth: Weekly to seasonal	Secular trends and peak growth: Weekly to monthly	1 to 30 m	1 to 30 m
3.2	Macro-algae (e.g. kelp)	Extent and distribution, productivity, biodiversity, condition,invasive species, material flux, dieback, eutrophication, temperature	Type or species, extent, density, biodiversity, condition, nascence, scenescence	Spectral Rrs, Kd, IOPs (for depth of macrophyte calculations)	Spectral library of macro-algae	Weekly to monthly			
3.3	Floating layers (algal scum, coral spawning, oil etc)	eutrophication, coral spawning timing, range and extent oil pollution or natural oil slicks	pHAB floating layer, sargassum and ulva, sea grass wracks, oil layers	Spectral Rrs	Spectral library of algal scum, coral spawn, oil types and thicknesses	Hourly to daily	Weekly	5 m	5 m
3.4	Intertidal exposed areas	Extent and distribution, productivity, biodiversity, condition, invasive species, material flux, dieback, energy environment, sedimentation, erosion, eutrophication, temperature effects	Species, extent, density, biodiversity, condition, nascence, scenescence	Spectral Rrs	Spectral library of intertidal seagrasses, macro-algae, benthic micro-algae, muds, silts, sands	Weekly to monthly			

Table A1.5 Habitat – emersed 3a - temporal and spatial requirement

		Measurement Requirement B=Baseline; T = Threshold				Platform /Ancillary requirements
		Levels/ranges	Spatial	Spectral	Radiometric	Geometric requirements and geolocational accuracy Sunglint avoidance Polarisation sensitivity
3	Habitats-emersed					
3.1	Macrophytes	B: 5 days T: 15 days	Spatial resolution B: 10 m (nominal, nadir) T: 30 m (nominal, nadir)	B: Spectral range from 400 nm to 1000 nm Spectral cal accuracy ± 5 Nm Spectral sampling 5 nm (FWHM 10 nm) T: Spectral range from 400 nm to 1000 nm Spectral cal accuracy ± 10 Nm Spectral sampling 10 nm (FWHM 10 nm)	NedL=0.3; NedR=0.001	Glint avoidance, Hot spot avoidance, geolocation 5 m
3.2	Macro-algae (e.g. kelp)		Spatial resolution …. m (nominal, nadir)	Spectral range from … nm to ….. nm Spectral cal accuracy ± ….. Nm Spectral sampling ….. nm (FWHM …nm)	NedL; NedR	Hot spot avoidance, geolocation 5 m
3.3	Floating layers (algal scum, coral spawning, oil etc)	from 1 to 7 days	Spatial resolution 10 m (nominal, nadir)	Spectral range from 400 nm to 2500 nm Spectral cal accuracy ± 5 Nm Spectral sampling 10 nm (FWHM 10 nm)	NedL=0.6; NedR=0.01	Geolocation 10 m
3.4	Intertidal exposed areas		Spatial resolution …. m (nominal, nadir)	Spectral coverage VIS-NIR ….. nm; SWIR … and ….nm Spectral cal accuracy ± ….. Nm Spectral sampling ….. nm (FWHM …nm)	NedL; NedR	

Table A1.6 Habitats – emersed 3b – measurement and platform requirement

		What management or science relevant information is needed for this aquatic ecosystem component (integrating information from multiple sources such as Earth Observation and…..)	directly measureable from Earth observation: management relevant aquatic ecosystem variables (by applying a form of inversion algorithm)	What variable needs to be measured from Earth observation for quantitative assessment of these variables	What variable needs to be measured *in situ* for quantitative assessment or validation of these variables	Temporal resolution : Scientific	Temporal resolution: Management relevant	Spatial resolution Scientific	Spatial resolution: Management relevant
									spatial resolution of 5 m =~ 25 m^2
4	Atmospheric correction			Directly measureable from Earth observation	Required from other sources				
4.1	Atmosphere above coral reef, coastal and inland environments (incl rural and urban) and adjacency effect correction;	NA		H_2O, O_3, NO_2,CO, CH_4, CO_2-vertical column content; aerosol optical (thickness@550nm and aerosol type) or (optical thickness spectrum and aerosol single scattering albedo); vertical distribution of aerosols; Cloud cover and cloud detection (cloud mask); polarisation, atm pressure	TOA solar irradiation; *in-situ* to support validation: aerosol optical thickness spectrum, aerosol type; anthropogenic organic and inorganic compounds with relevant optical signatures; atm. Pressure; H_2O, O_3, NO_2,CO, CH_4, CO_2-vertical column content	Each image	NA	each lake	NA
4.2	Sun and sky glint	NA	sun and skyglint characterisation (like slope distribution of wave normals over ocean), reflectance of foam and area covered by whitecaps, wind speed and direction	specular reflectance (i.e., sky and sun glint characterisation), wind speed	specular reflectance (i.e., sky and sun glint); in-situ to support atm. correction : wind speed; from models: reflectance of foam and area covered by whitecaps	Each image	NA	Each lake	NA

Table A1.7 Atmospheric correction - temporal and spatial resolution requirement

		Measurement Requirement B=Baseline; T = Threshold				Platform /Ancillary requirements
		Levels/ranges	Spatial	Spectral	Radiometric	**Geometric requirements and geolocational accuracy Sunglint avoidance Polarisation sensitivity**
4	Atmospheric correction		Spatial resolution …. m (nominal, nadir): e.g. spatial resolution of 5m =~ 25m²	Spectral range from … nm to ….. nm Spectral cal accuracy ± ….. Nm Spectral sampling ….. nm (FWHM …nm)	NedL; NedR	
4.1	Atmosphere above coral reef, coastal and inland environments (incl rural and urban) and adjacency effect correction;	Each image	low spatial resolution sufficient : 300 - 1km (nominal, nadir)	B: At least the spectral range as for the observations of water properties, optimal spectral range from 360 nm to 2400 nm T: • One or two bands in UV, around 360 and 368 nm for absorbing aerosols • Spectral range: 400-950 nm; Spectral resolution (FWHM) : 6-10nm; Spectral calibration accuracy: +/-0.3 nm • SWIR bands at least at 1.6 and 2.2 µm for aerosol retrieval • Cirrus band 1.38µm • Oxygen B and A band spectra: Spectral range: (B) 675 nm-710 nm and (A) 757 nm - 780 nm, bandwidth <0.3 nm; spectral cal accuracy 0.1 nm; T: • Polarisation……..	NedL: 0.1 - 0.5 mW/(m² sr nm)	two or better multi-directional observation for improved aerosol retrieval; polarized observations at one wavelength in the VIS would be nice to have for estimation of aerosol characteristics
4.2	Sun and sky glint	Each image	Same as each image	Spectral Range 730 to 1000 nm (temporally and spatially coregistered with VIS bands)- no preference for band width. Just need one spectral band to use solely for sunglint correction	NedL; NedR (needs to avoid saturation if possible - else sunglint correction impossible)	tilted (off nadir) observation for sunglint avoidance

Table A1.8 Atmospheric correction -measurement and platform requirement

Appendix A.2 Sensitivity analysis

PETER GEGE , SINDY STERCKX, ARNOLD G.DEKKER

Goal of this study is to derive sensor requirements for measuring the spectral and radiometric properties of different water and benthic cover types that are relevant for extracting information from optically deep and shallow inland, coastal and coral reef waters. For this purpose forward simulations of hyperspectral measurements are made. Using an analytical model, a large number of reflectance spectra are calculated for bottom of atmosphere (BOA) to study the expected spectral and radiometric variability. These simulated measurements are first analyzed for the information bearing wavelengths and reflectance signals to derive sensor requirements concerning spectral range and spectral resolution. In a second step a representative subset is converted to top of atmosphere (TOA) radiances in order to determine the required radiometric sensitivity.

The retrieval of parameters from measurements is addressed in the main report.

A2.1. Scenarios

The (non-oceanic) aquatic ecosystem waters on Earth are as variable and wide ranging as their surrounding ecosystems and catchment areas: water constituents and bottom substrates differ considerably in type, concentration and optical properties. This makes the reflectance spectra more variable than for the open ocean and many optically deep coastal waters. To define reasonable requirements for a sensor, the spectral variety is described by scenarios covering a relevant part of these aquatic ecosystems.

A2.1.1 Deep water

As the concentrations of water constituents are not completely independent from each other, the choice of scenarios is oriented on certain types of lakes. Scenarios for typical lakes are defined in Table 1.

These scenarios are also representative of coastal waters. Each scenario represents a typical concentration and a representative range of total suspended matter (TSM), colored dissolved organic matter (CDOM) or chlorophyll-a (CHL). The concentrations of TSM and CHL are expressed in terms of mass per water volume, [g m^{-3}] and [mg m^{-3}], while CDOM is specified by its absorption coefficient at 440 nm (a_{CDOM}) in units of m^{-1} and its spectral slope (S_{CDOM}) in units of nm^{-1}. The concentrations and ranges for scenarios X+ (low TSM), Y- (low a_{CDOM}), Y+ (High a_{CDOM}) and C- (low CHL) are based on Table 1 in Peters et al., (2015), while scenario C+ (high CHL) is based on the two Finnish lakes Tuusulanjärvi and Hiidenvesi (Ylöstalo et al., 2014).

Table 1: Standard scenarios for optically deep water. A scenario is defined by the value of a parameter marked as bold. The other parameters are specified by a typical value and a range in the notation typical (min-max).

Scenario	X-	X+	Y-	Y+	C-	C+
Represents	low TSM	high TSM	low a_{CDOM}	high a_{CDOM}	low CHL	high CHL
Example	L. Constance	Lake Peipsi	L. Maggiore	Lake Peipsi	Lake Garda	2 Finnish l.
TSM [g m^{-3}]	**1**	**5**	1(0.2-10.0)	5(1-10)	1(0.2-20.0)	10(5-15)
a_{CDOM} [m^{-1}]	0.5(0.2-2.0)	2.5(1-5)	**0.2**	**2.5**	0.1(0.04-2.00)	2.5(1.5-4.5)
CHL[mg m^{-3}]	2(0.5-15.0)	5(1-20)	1(0.2-5.0)	5(1-20)	**1**	**40**
S_{CDOM}[nm^{-1}]	0.014 (0.01-0.02)	0.014 (0.01-0.02)	0.014 (0.01-0.02)	0.014 (0.01-0.02)	0.014 (0.01-0.02)	0.014 (0.01-0.02)

Of particular relevance for defining sensor requirements are the extreme cases of the measurements of interest; if a sensor is suitable for the extremes, it should provide even better data in the intermediate ranges. This concept of extremes defines the scenarios of Table 2. The choice of extreme values is based on Table 1 in Peters et al., (2015), as it covers a large range of conditions. The extreme concentrations of TSM, CDOM and CHL are chosen close to a minimum or maximum of Table 1 in Peters et al., (2015).

Table 2: Extreme scenarios for optically deep water. The notation is the same as in Table 1.

Scenario	X--	X++	Y--	Y++	C--	C++
Extreme for	low TSM	high TSM	low a_{CDOM}	high a_{CDOM}	low CHL	high CHL
Example	Lake Garda	Lake Taihu	Lake Garda	Finnish lakes	Italian lakes	Lake Taihu
TSM [g m^{-3}]	**0.1**	**300**	1(0.2-20.0)	2(0.5-5.0)	1(0.2-20.0)	50(10-300)
a_{CDOM} [m^{-1}]	0.1(0.04-2.00)	1(0.2-3.0)	**0.04**	**10**	0.1(0.04-2.00)	1(0.2-3.0)
CHL [mg m^{-3}]	1(0.1-10.0)	20(1-1000)	1(0.1-10.0)	5(1-10)	**0.2**	**1000**
S_{CDOM} [nm^{-1}]	0.014 (0.01-0.02)	0.014 (0.01-0.02)	0.014 (0.01-0.02)	0.014 (0.01-0.02)	0.014 (0.01-0.02)	0.014 (0.01-0.02)

A sensitivity analysis for a scenario consists of three simulation runs. Each run calculates N spectra at different values of TSM, a_{CDOM}, CHL, or the slope of CDOM absorption (S_{CDOM}), while the other parameters are kept constant. For example, a CDOM run of scenario X-- changes a_{CDOM} in N steps from 0.04 to 2.00 m^{-1} and sets TSM = 0.1 g m^{-3}, CHL = 1 mg m^{-3} and S_{CDOM} = 0.014 nm^{-1}. N = 50 is chosen, hence 150 reflectance spectra are calculated for all three runs of a deep water scenario.

A2.1.2 Shallow water

The scenarios of shallow water are defined by the irradiance reflectance spectra of bottom substrate and the water column composition. The water is represented by scenario Y- in this study, as its low concentrations of TSM, CDOM and CHL represent relatively clear water. The bottom substrate spectra were provided by N. Pinnel (#0, #1), E. Botha (#2 to #12) (Botha et al., 2013), and D. Rogge (#13). A plot of these spectra is shown in Figure 1. The labeling is as follows:

0   Chara contraria (macrophyte)

1   Potamogeton perfoliatus (macrophyte)

2   Rock

3   Bleached coral

4   Dark silt

5   Bright sand

6   Yellow *porites* sp. (coral)

7   Purple encrusting coralline algae

8   Brown *porites* sp. (coral)

9   Posidonia australia (seagrass)

10   Detritus (sea-grass wrack)

11   Ecklonia radiata (kelp)

12   Coarse coral rubble

13   Dark sand
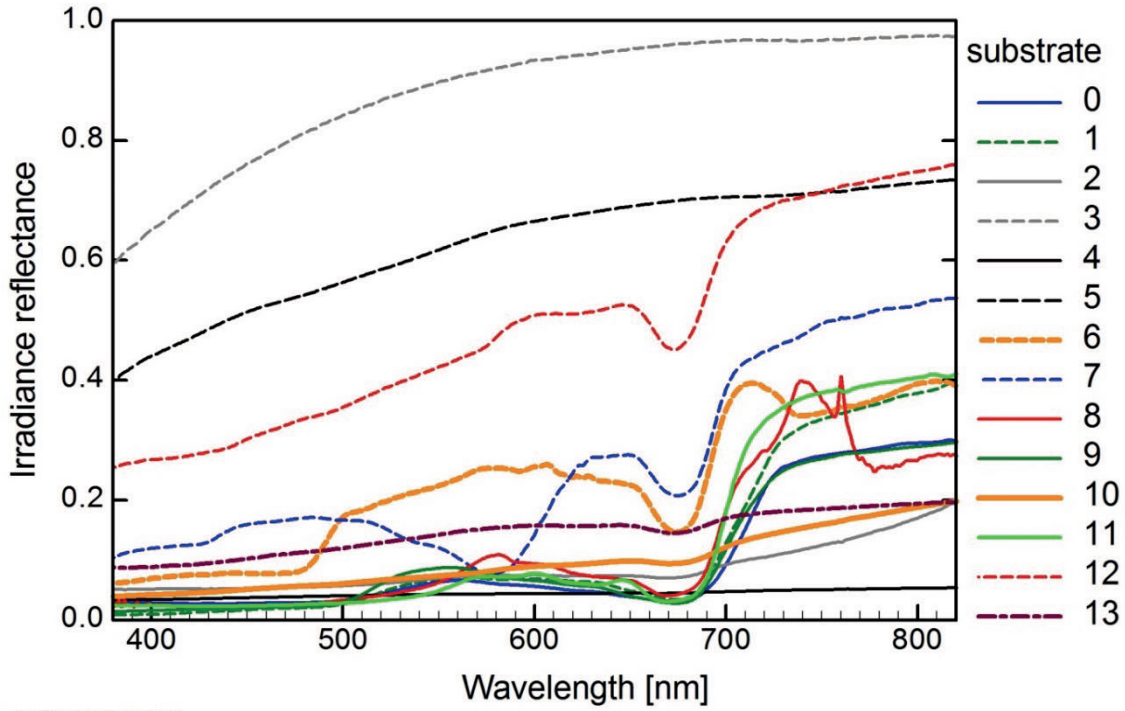
BOTTOM | 7.12.2016

Figure 1: Bottom substrate spectra used for the simulations.

A2.2 Model

The reflectance of water depends on the spectral absorption coefficient, $a(\lambda)$, and spectral backscattering coefficient, $b_b(\lambda)$, of the water layer. The most relevant components contributing to $a(\lambda)$ and $b_b(\lambda)$ are: pure water (index "W"), phytoplankton (index "p"), coloured dissolved organic matter (index "CDOM") and non-algal particles (index "NAP"). Their absorption and backscattering coefficients are *inherent optical properties* (IOPs), which are additive:

$$a(\lambda) = a_w(\lambda) + C_p \cdot a_p^*(\lambda) + C_{CDOM} \cdot a_{CDOM}^*(\lambda) + C_{NAP} \cdot a_{NAP}^*(\lambda), \tag{1}$$

$$b_b(\lambda) = b_{b,w}(\lambda) + C_p \cdot b_{b,p}^*(\lambda) + C_{NAP} \cdot b_{b,NAP}^*(555) \cdot \left(\frac{\lambda}{555}\right)^{-n}. \tag{2}$$

The C's are the concentrations, and the star symbol indicates normalization to concentration (for phytoplankton and NAP) or wavelength (for CDOM). The normalized IOPs are called *specific inherent optical properties* (SIOPs).

All calculations are made with the software WASI (Gege, 2004; Gege and Albert, 2006). These simulate measurements of remote sensing reflectance R$_{rs}$, which is the ratio of upwelling radiance to downwelling irradiance, both above the water surface and excluding specular reflections at the surface. The model of Albert (Albert and Mobley 2003, Albert 2004) is used for the simulations, which expresses R$_{rs}$ as a polynomial of fourth order of the quantity

148

$$u(\lambda) = \frac{b_b(\lambda)}{a(\lambda) + b_b(\lambda)} \tag{3}$$

The model can be used for optically deep and shallow waters and accounts for the sun zenith angle and the viewing angle. Its coefficients have been derived using Hydrolight simulations covering wide ranges of environmental parameters, including most of the high concentrations observed in inland waters. A similar model has been developed by Lee et al., (1998, 1999); see Gege (2017) for a comparison of the equations and parameter ranges.

The simulations assume, for each band, a Gaussian shaped spectral response with a full width at half maximum (FWHM) of 5 nm. The SIOPs are chosen as follows:

- $a_p^*(\lambda)$: two specific absorption spectra of green algae (from the WASI database) and cyanobacteria (S. Peters, personal communication) (Figure 2).
- $a_{CDOM}^*(\lambda)$ is approximated by an exponential equation with slope SCDOM = 0.014 nm-1 (Figure 2).
- $a_{NAP}^*(\lambda)$ is approximated by an exponential equation with a slope SNAP = 0.011 nm-1 (D'Sa et al. 2006; also average of GLASS data) and a specific absorption coefficient of 0.027 m2 g-1 at 440 nm (Babin et al., 2003) (Figure 2).
- $b_{b,p}^*(\lambda)$: two specific backscattering coefficients from Lake Garda; for green algae from normal clear water, for cyanobacteria from water with Anabaena (both spectra provided by C. Giardino, personal communication) (Figure 3).
- b_b,NAP*(555) = 0.011 $m^2\,g^{-1}$ and n = 0.75 (result from GLASS).
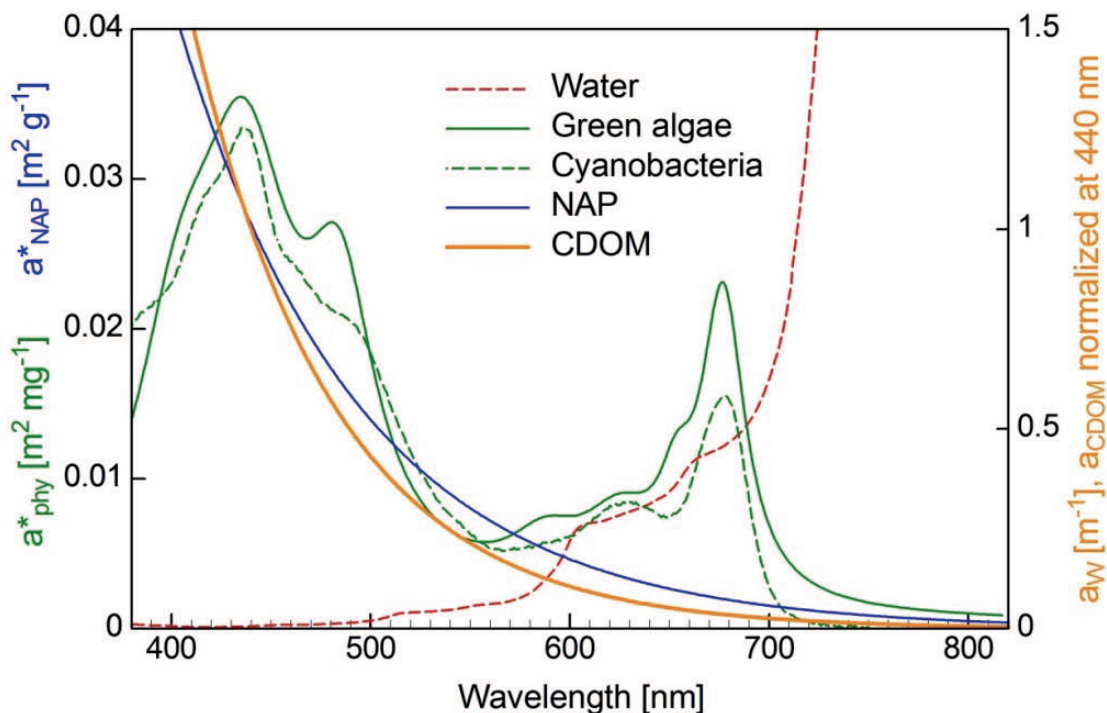
SIOPS | 24.11.2016

Figure 2: Specific absorption coefficients used for the simulations.
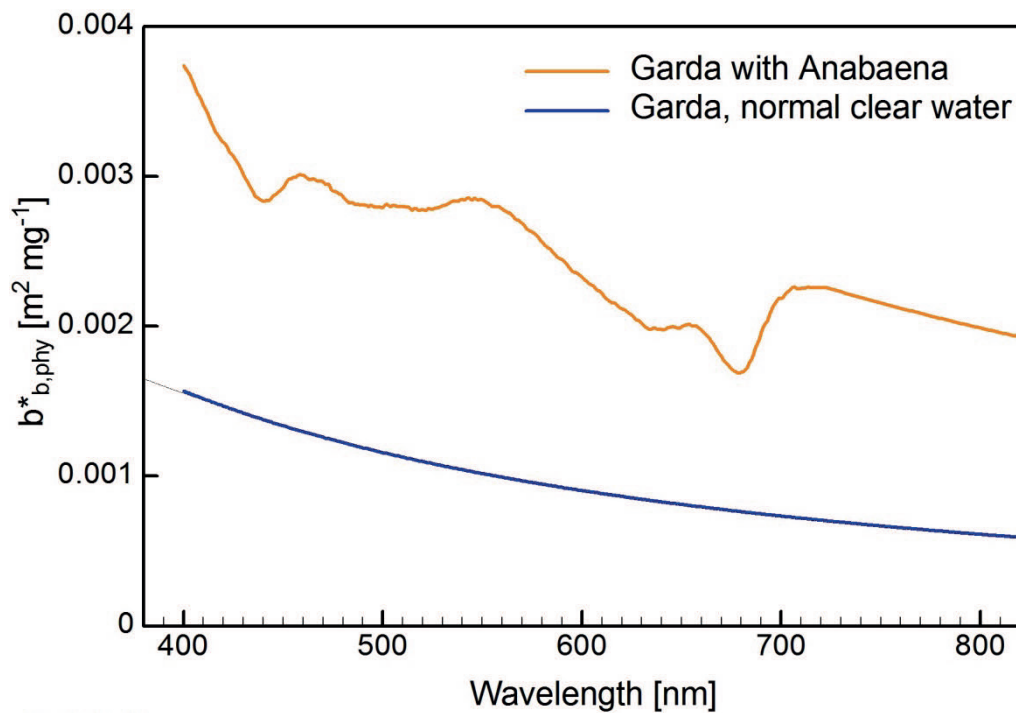
BB | 22.12.2016

Figure 3: Specific backscattering coefficients of phytoplankton used for the simulations.

A note of caution in interpreting these results is due as our simulations are based on a small selection of possible specific inherent optical properties and substratum types. E.g. our phytoplankton SIOPs are quite specific to where they were measured and the species present in these natural waters at that time of sampling. This has consequences for e.g. the ratio of spectral backscattering of the phytoplankton to the pigment absorption of the same phytoplankton. The spectral absorption efficiency and the location of accessory pigments will vary significantly with species and their growing (and stress) conditions. If we were to have simulated e.g. Microcystis species (cyanobacteria) with high refractive indices and gas vacuoles we would get different simulation results than for an algal species with lower refractive indices and higher or lower specific absorption values. In a similar manner the suspended matter may be composed of mainly mineral matter or mainly detrital organic matter of anything in between. In the tropics it is possible that the suspended matter is mainly composed of very weathered fine clays scattering light very efficiently. In glacial lakes fine fresh glacial clays may be similar in being highly scattering. In lakes in peat areas the suspended sediment may be mostly very dark brown and mainly organic. The substratum types (rocks, pebbles, coarse sand, fine sand, silts and clays as well as biogenic reefs) may vary as will its cover type (micro-algae, macro-algae, algal mats, seagrasses, freshwater plants, coralline algae, encrusting algae, sponges, corals etc.). The simulations presented here are not exhaustive-they are indicative. In chapter 2 of the main report we also discuss other spectral information that needs to be considered for determining the specifications of a generic globally valid (non-oceanic) aquatic ecosystem Earth observing system.

A2.3 Methods

A2.3.1 Determination of the most relevant wavelengths

The following figures illustrate using the example of scenario Y- the simulations that were made to determine the spectral sensor requirements. Scenario Y- is defined by a low CDOM concentration of $a_{CDOM}(440) = 0.2$ m^{-1} and associated conditions of TSM = 1 mg/l, CHL = 1 µg/l, and $S_{CDOM} = 0.014$ nm^{-1}. Analogous spectra, plots and associated tables are generated for all the scenarios.

Figure 4 illustrates the changes induced to $R_{rs}(\lambda)$ by altering TSM from 0.2 to 10 mg/l (panel A), CHL from 0.2 to 5 µg/l (panel B) and S_{CDOM} from 0.010 to 0.020 nm^{-1} (panel C). A shallow water simulation shows Panel D. It illustrates the changes of the reflectance spectrum when the bottom substrate "Posidonia australia" is submerged in water of different depth ranging from 1 mm to 50 cm. In each case, the altered parameter was changed in 50 equidistant steps, while all other parameters were kept constant.
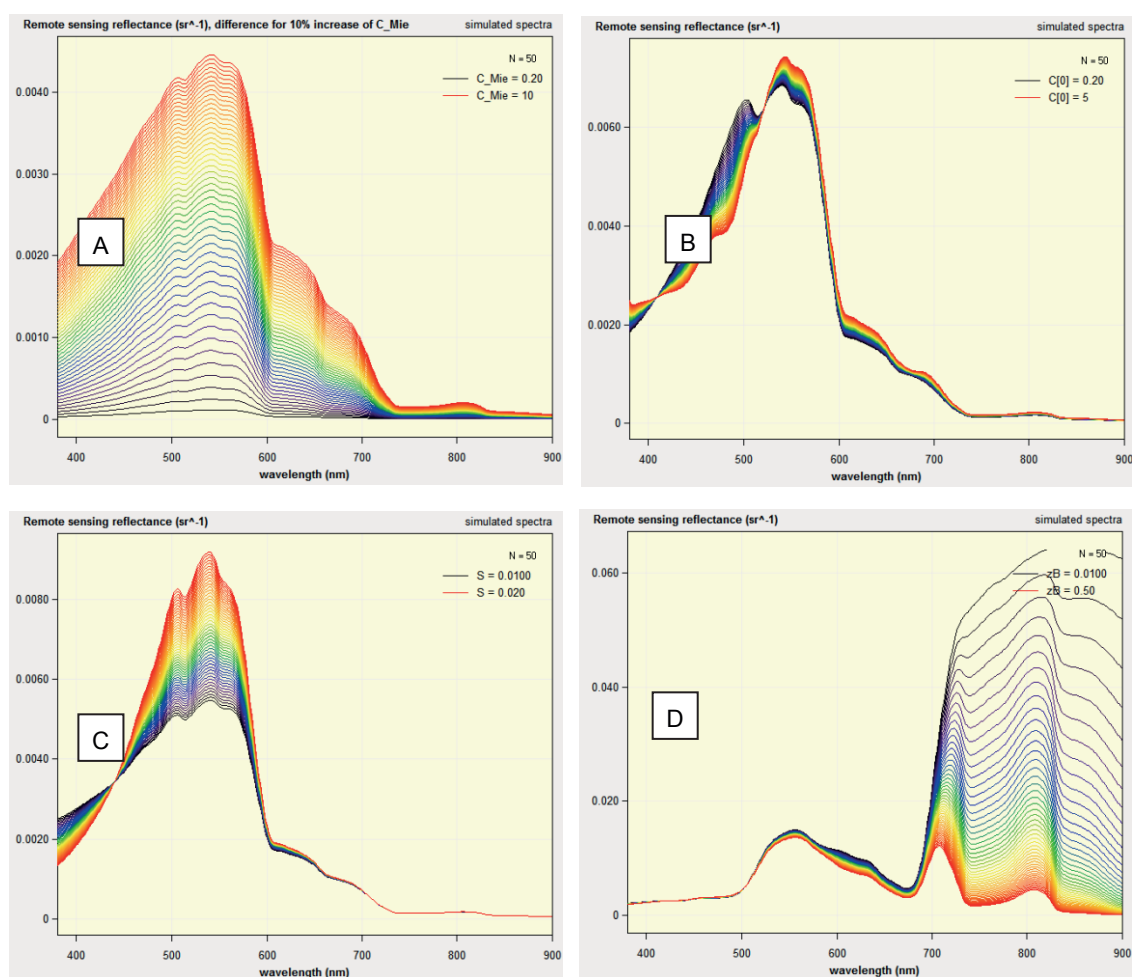

Figure 4: Remote sensing reflectance for (A) TSM range 0.2 – 10.0 mg/l, (B) CHL range 0.2 – 5.0 µg/l, (C) S$_{CDOM}$ range 0.010 – 0.020 nm^{-1}, (D) depth range 0.01 – 0.50 m.

The largest changes in the amplitudes of $R_{rs}(\lambda)$ are obviously introduced by changes of TSM (panel A) and water depth (panel D), but the spectral changes are difficult to recognize in this kind of representation. The spectral changes are more easily visualized after normalization. The spectra $R_{rs}(\lambda)$ normalized in the range from 400 to 800 nm are shown in Figure 5.
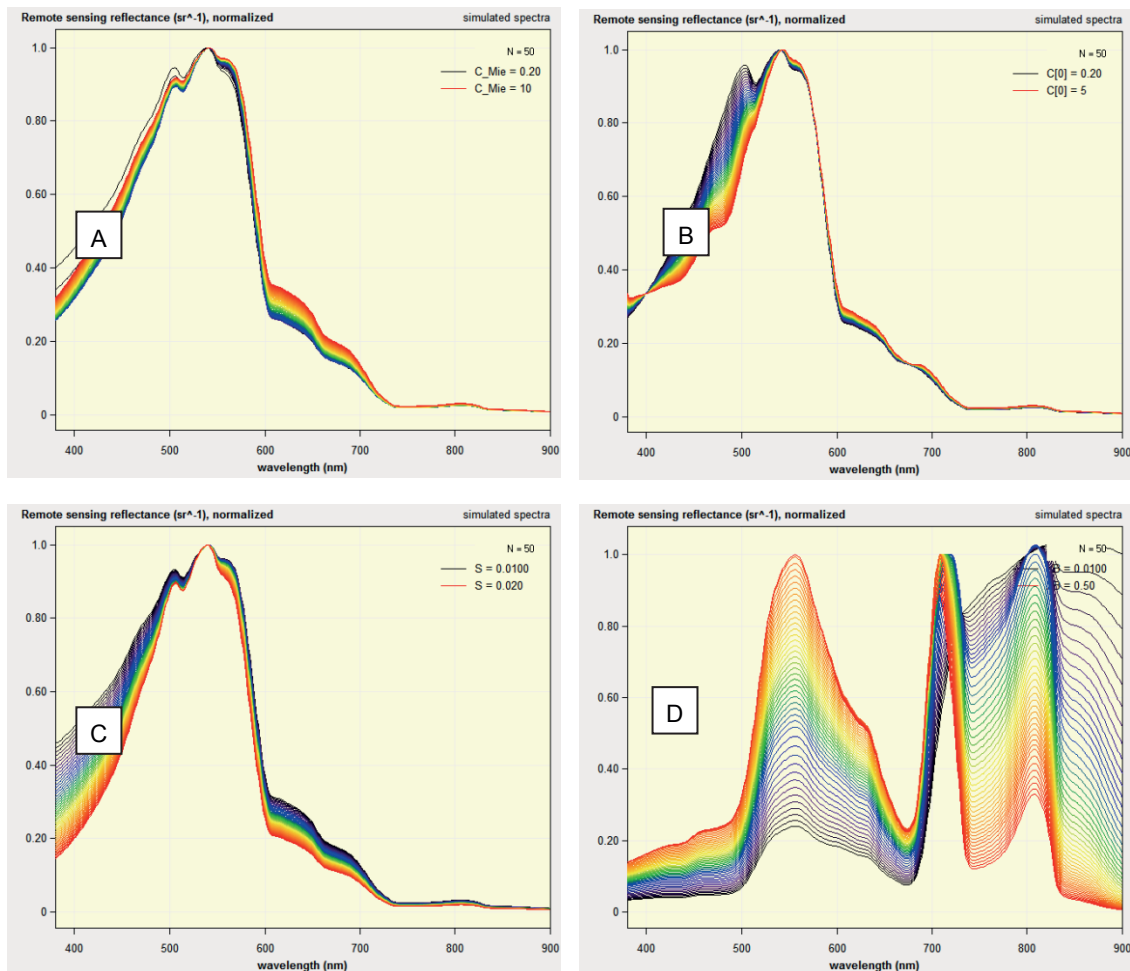
Figure 5: Normalized remote sensing reflectance for (A) TSM range 0.2 – 10.0 mg/l, (B) CHL range 0.2 – 5.0 µg/l, (C) S$_{CDOM}$ range 0.010 – 0.020 nm^{-1}, (D) depth range 0.01 – 0.50 m.

For optically deep waters (panels A, B, C), the normalized spectra show little spectral variability , which is more pronounced for changes of S$_{CDOM}$ (panel C) and CHL (panel B) than for changes of TSM (panel A). The reflectance maximum remains near 540 nm for all studied conditions, but the spectral shape undergoes systematic modifications.

For shallow water, Panel D illustrates the large spectral changes of remote sensing reflectance for water layer thicknesses between 1 mm (black) and 50 cm (red). The 1 mm case represents almost no water (a water depth of zero cannot be simulated). The difference between any two curves corresponds to a water layer difference of 1 cm. The water not only decreases the amplitude of R$_{rs}$ (panel D of Figure 4), but also changes the spectral shape with e.g. a shift of the minima and maxima of the R$_{rs}$ spectra.

In order to highlight the changes of spectral shape, the first and second derivatives, $\partial R_{rs}/\partial \lambda$ and $\partial^2 R_{rs}/\partial \lambda^2$, are shown in Figure 6. The most useful information of the derivative spectra are the positions of the zeros and their changes, as these indicate the wavelengths and wavelength changes of the local minima, maxima and shoulders. These are shown in Figure 7 as histograms summing up the zeros of the plots of Figure 6.
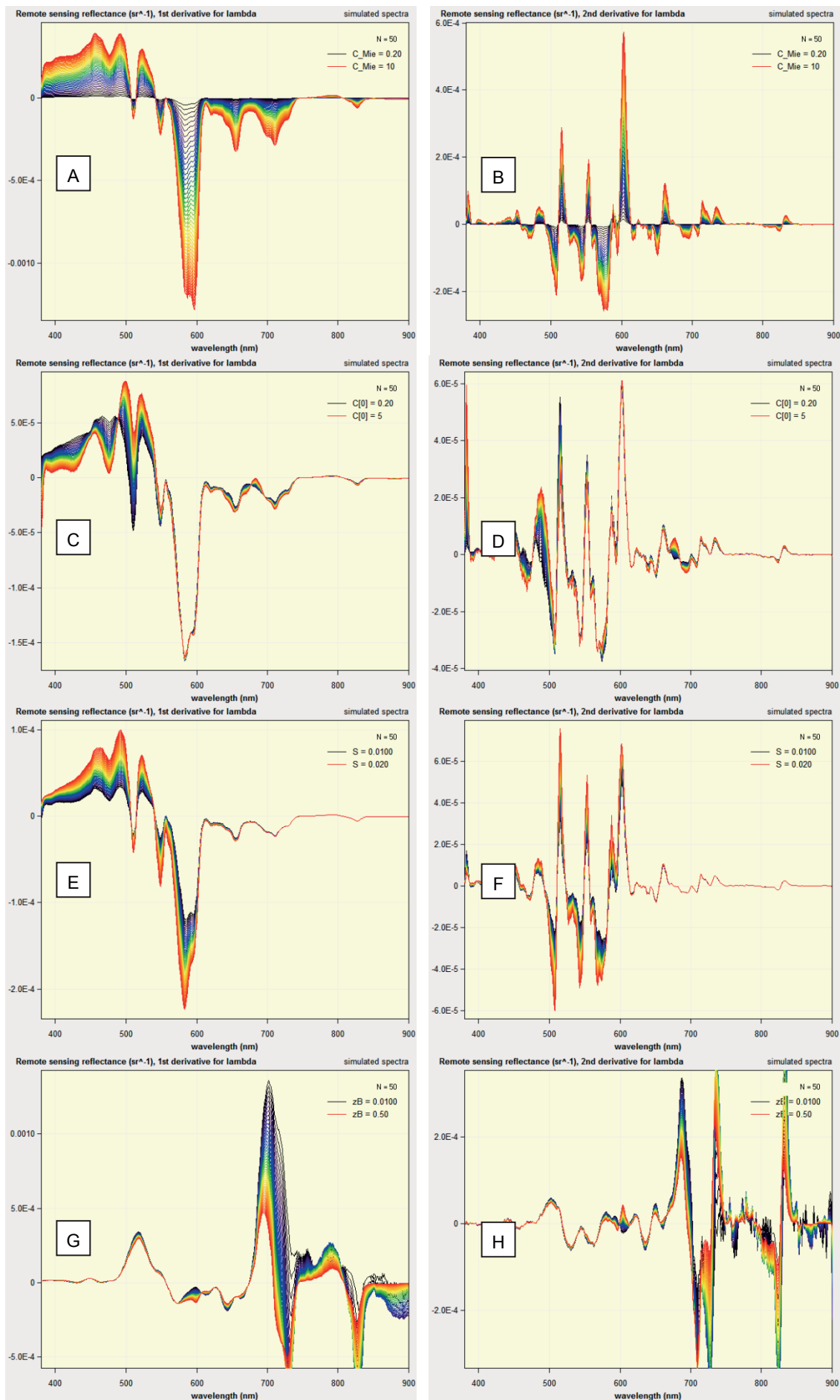
Figure 6: First (left column) and second (right column) derivatives of remote sensing reflectance for (A, B) TSM range 0.2 – 10.0 mg/l, (C, D) CHL range 0.2 – 5.0 µg/l, (E, F) S_{CDOM} range 0.010 – 0.020 nm^{-1}, (G, H) water depth range 0.01 – 0.50 m.
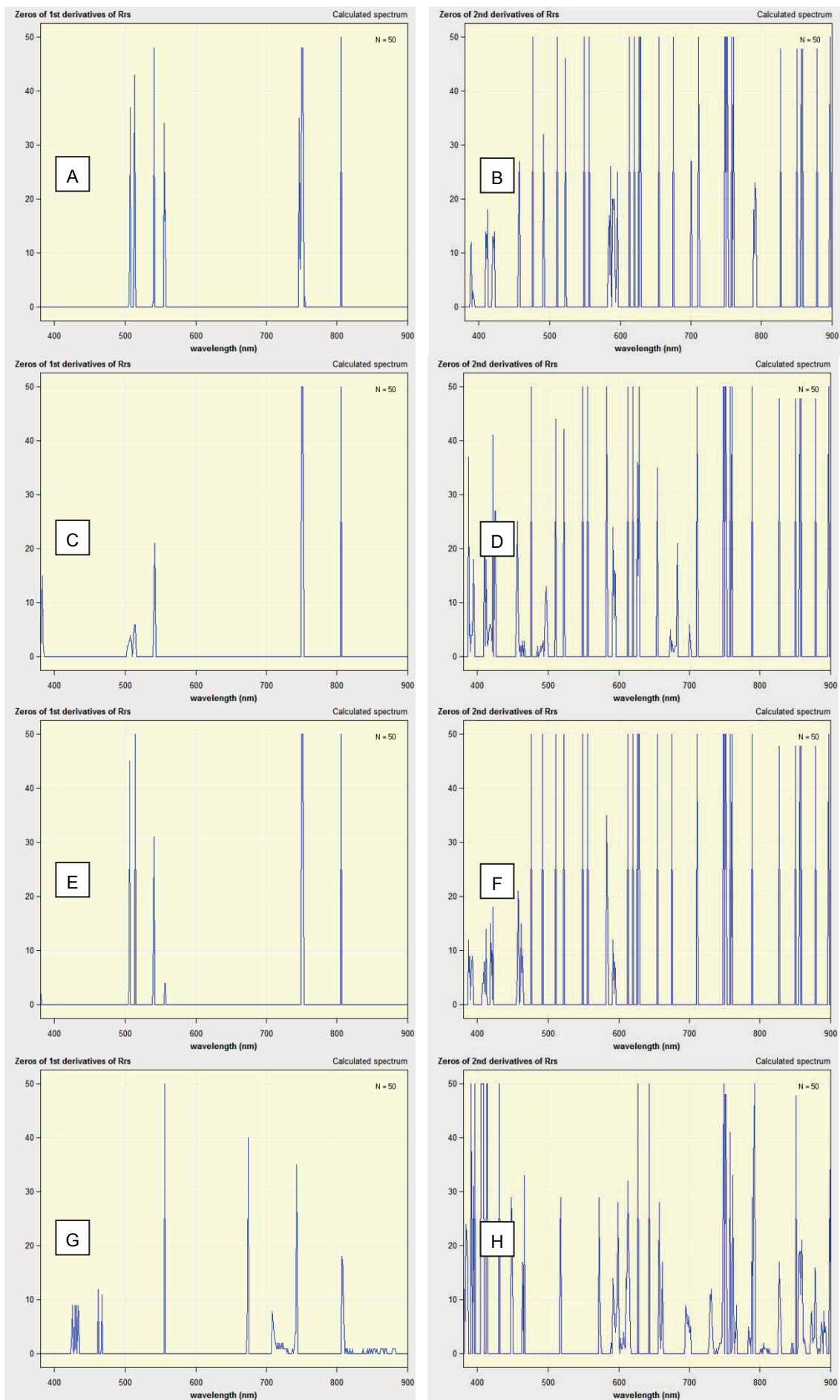
Figure 7: Zeros of first (left column) and second (right column) derivatives of remote sensing reflectance for (A, B) TSM range 0.2 – 10.0 mg/l, (C, D) CHL range 0.2 – 5.0 µg/l, (E, F) S_{CDOM} range 0.010 – 0.020 nm^{-1}, (G, H) water depth range 0.01 – 0.50 m.

Histogram values of 50 (= number of simulation runs) represent R_{rs} extrema that remain at the same wavelength. For the chosen example, only the reflectance minimum at 751 nm and the reflectance maximum at 806 nm remain stable, while all other peaks and troughs change their wavelength, in particular for changes of CHL (panel C).

In order to make the spectral changes induced by TSM, CHL, S_{CDOM} and water depth comparable, the zeros of the first derivatives are shown in Figure 8 for all parameter values used in the simulations.
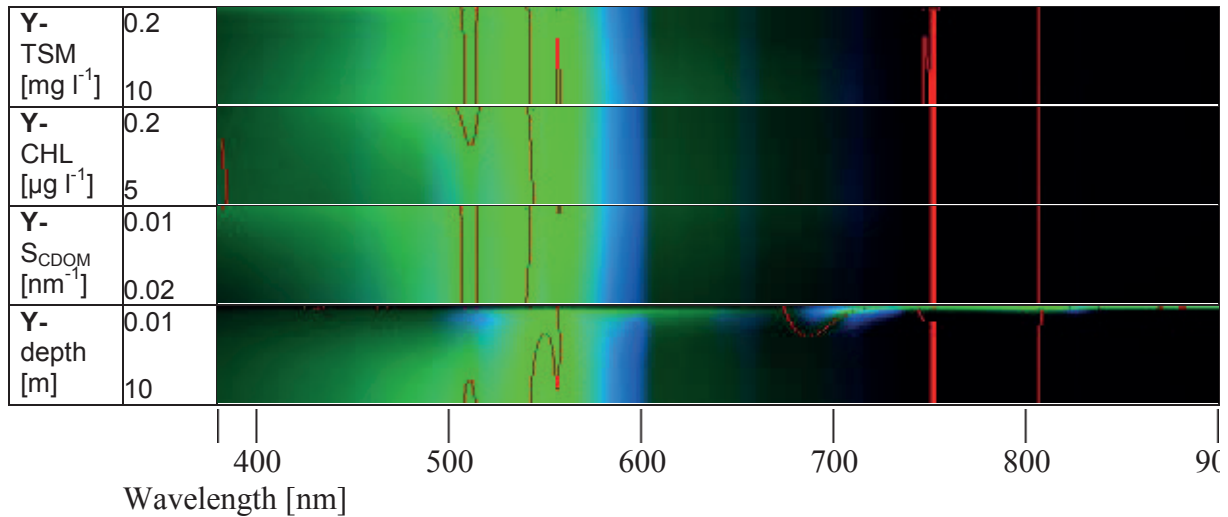

Figure 8: Red lines: Zeros of first derivatives of remote sensing reflectance for TSM range 0.2 – 10.0 mg/l (first row), CHL range 0.2 – 5.0 µg/l (second row), S_{CDOM} range 0.010 – 0.020 nm^{-1} (third row) and water depth range 0.01 – 10.0 m (third row). Background: normalized R_{rs} (green), normalized first derivative of R_{rs} (blue).

The background color of Figure 8 codes the amplitude of the normalized reflectance spectrum in green and the normalized first derivative in blue in order to give an indication of the relative radiometric sensitivity required to resolve the spectral feature of interest. The bright colors from 500 to 600 nm for deep water represent high reflectance, suggesting that it might be easier to measure the reflectance maxima at 507 nm and 541 nm and the minima at 513 nm and 555 nm than the reflectance minimum at 751 nm and the maximum at 806 nm. For very shallow water, the bright regions and maxima of the reflectance spectra are very different from those of optically deep water, but approach these above approximately 9 m depth in this example.

Figure 9 shows the first derivatives (red) and the second derivatives (green). Such plots are used to compare the relevant wavelengths for the different scenarios.
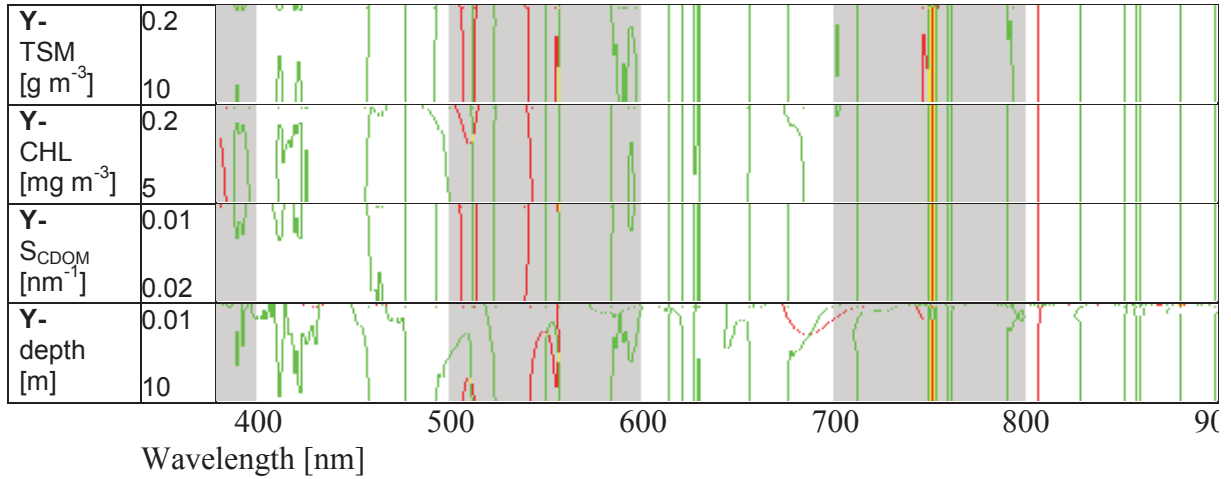
		400	500	600	700	800	9(
Y- TSM [g m^{-3}]	0.2 10						
Y- CHL [mg m^{-3}]	0.2 5						
Y- S$_{CDOM}$ [nm^{-1}]	0.01 0.02						
Y- depth [m]	0.01 10						

Wavelength [nm]

Figure 9: Zeros of first derivatives (red) and zeros of second derivatives (green) of remote sensing reflectance for scenario Y-.

A2.3.2 Determination of the optimal spectral resolution

To capture the information content of a reflectance spectrum, the sensor has to resolve the spectral features of the spectrum, in particular the peaks, dips and shoulders. These changes of steepness are given by the first derivative $\partial R_{rs}(\lambda)/\partial\lambda$. It can be measured by a real sensor only approximately, depending on the sensor's radiometric resolution ΔR_{rs} and spectral resolution $\Delta\lambda$: $\Delta R_{rs}/\Delta\lambda \approx \partial R_{rs}(\lambda)/\partial\lambda$. For given ΔR_{rs}, the ideal spectral resolution is thus:

$$\Delta\lambda = \frac{\Delta R_{rs}}{\partial R_{rs}/\partial\lambda} \qquad (4)$$

At wavelength regions of large reflectance changes, the spectrum must be sampled more frequently than at regions of small gradients, hence $\Delta\lambda$ is inversely related to $\partial R_{rs}(\lambda)/\partial\lambda$. Eq. (4) defines the optimal spectral resolution for a sensor with a noise-equivalent reflectance of ΔR_{rs}. Higher (or finer) spectral resolution increases sensor noise (due to a decreased sensitivity-thus decreasing the signal to noise ration SNR), while lower (or coarser) spectral resolution decreases the information content of the reflectance measurement and increases the signal to noise ratio (SNR).

Since the measurement of gradients requires adjacent channels, ΔR_{rs} is taken from the requirement for hyperspectral sensors, i.e. $NE\Delta R_{rs,1}$ from eq. (5) is used to calculate $\Delta\lambda$. Figure 10 and Figure 11 illustrate the results of $\Delta\lambda$ calculations for scenario Y-.

It does need to be realized that these results are for the chosen parameterisation (see tables 1and 2 as well as figures 1 to 3) and if other parameterisations are run (different algal species, other particulate matter, CDOM substratum etc.) some of these results will vary. We caution against interpreting these results as being absolute for all non-oceanic aquatic ecosystems. Indeed our advice is that in the case of determining a specific sensor for a specific aquatic environment to perform more of these simulations with appropriate parameterisations.
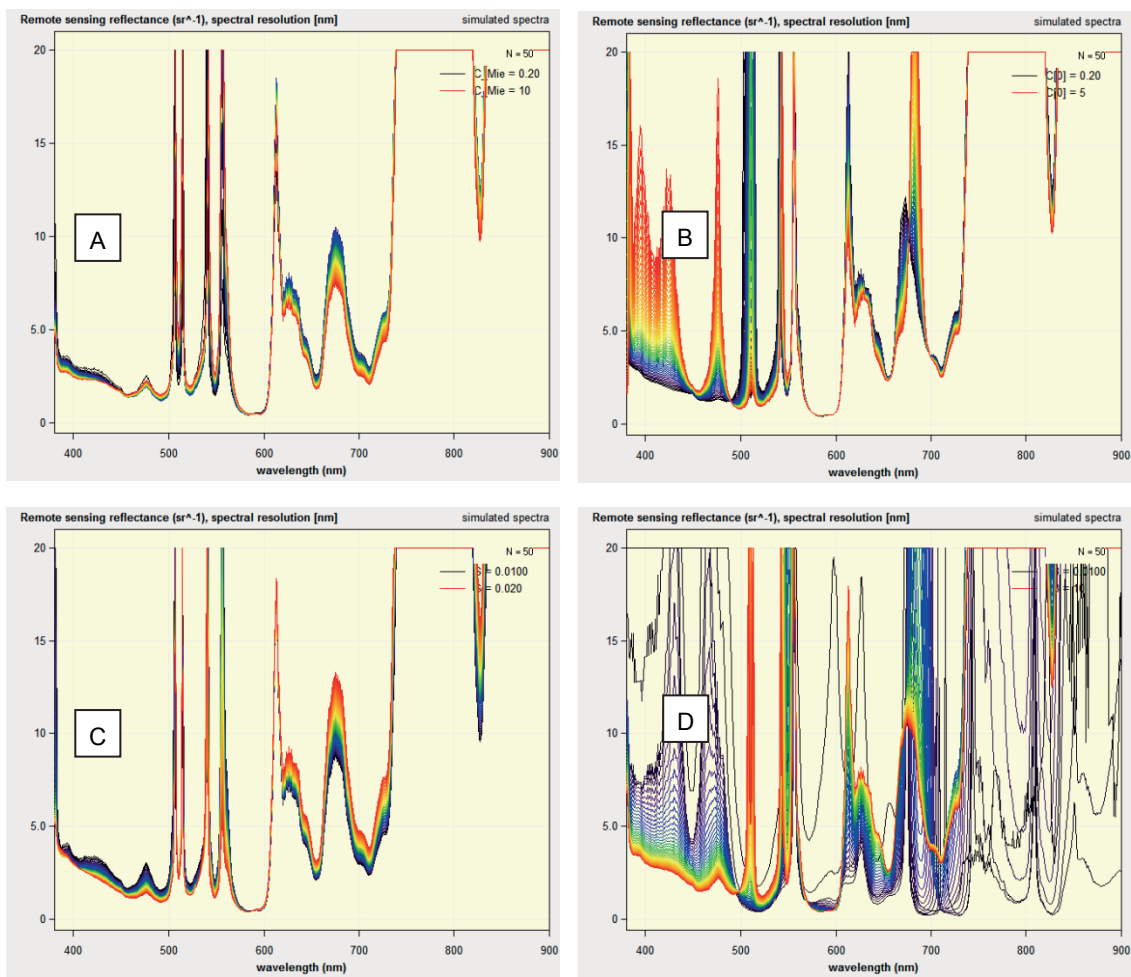
Figure 10: Spectral resolution for (A) TSM range 0.2 – 10.0 mg/l, (B) CHL range 0.2 – 5.0 µg/l, (C) S$_{CDOM}$ range 0.010 – 0.020 nm^{-1}, (D) depth range 0.01 – 10.0 m.
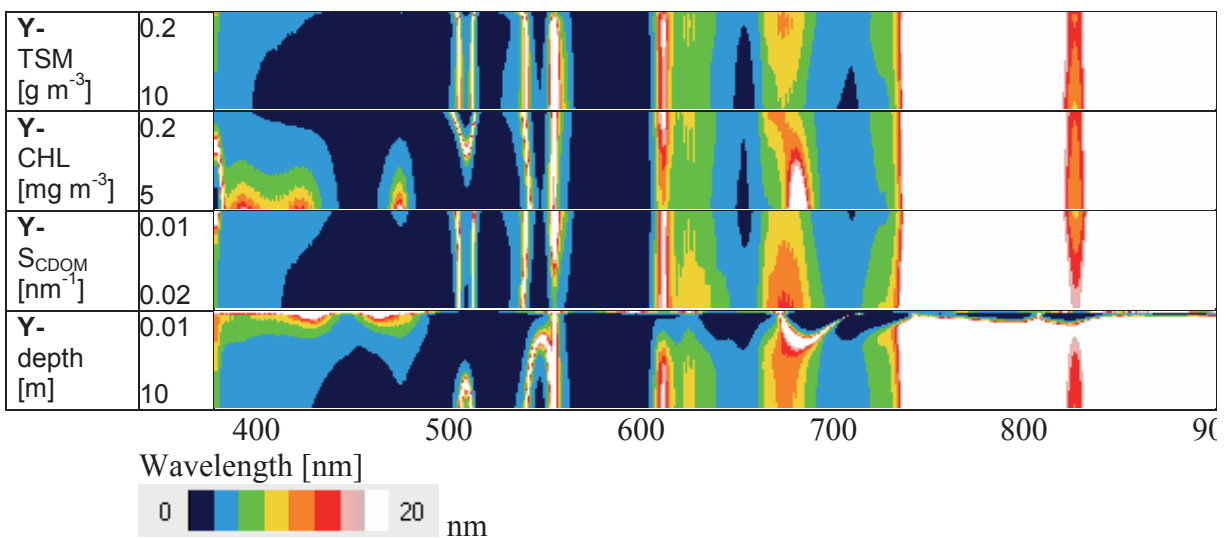

Figure 11: Spectral resolution required to resolve changes in reflectance (using $NE\Delta R_{rs,1}$) due to varying concentrations for scenario Y- .

A2.3.3 Determination of the required radiometric resolution

The requirement concerning radiometric resolution is derived using two approaches.

The first approach is based on the assumption that the dynamics of a spectrum $R_{rs}(\lambda)$ should be sampled at a typical resolution of 1%. Hence, the noise-equivalent remote sensing reflectance difference, $NE\Delta R_{rs}$, is calculated as 1% of the difference between the reflectance maximum, $R_{rs,max}$, and the reflectance minimum $R_{rs,min}$:

$$NE\Delta R_{rs,1} = 0.01 \left| R_{rs,max} - R_{rs,min} \right|. \tag{5}$$

The subscript "1" refers to approach number 1. The wavelength interval from 400 to 800 nm is taken to determine $R_{rs,min}$ and $R_{rs,max}$.

The second approach is oriented on the assumption that a measurement should be sensitive to parameter changes in the order of 10%. It determines first the wavelength λ_{max} which is most sensitive to changes of $R_{rs}(\lambda)$ induced by parameter x. The reflectance change at λ_{max} induced by a 10% change of x is then taken to define the noise-equivalent remote sensing difference:

$$NE\Delta R_{rs,2} = \left| R_{rs}(\lambda_{max}, 1.1x) - R_{rs}(\lambda_{max}, x) \right|. \tag{6}$$

The subscript "2" refers to approach number 2. Figure 12 illustrates the spectra $R_{rs}(\lambda, 1.1x) - R_{rs}(\lambda, x)$ for scenario Y- and x representing TSM, a_{CDOM}, CHL, and water depth.

Both approaches are applied to all spectra simulated for all scenarios. The recommendation for $NE\Delta R_{rs}$ is derived from a comparison of the results. A value which is close to the minimum of $NE\Delta R_{rs,1}$ and $NE\Delta R_{rs,2}$ of the majority of the standard scenarios is selected.
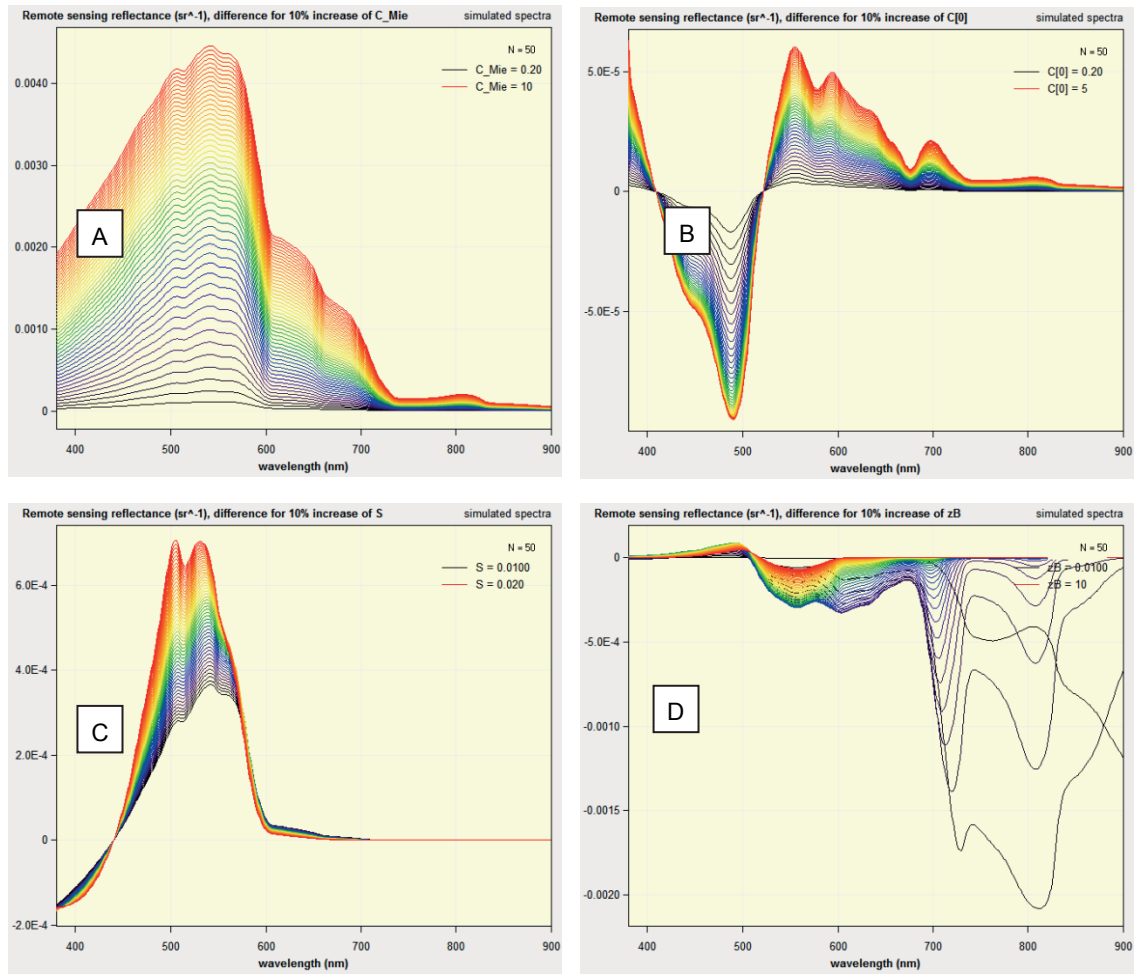
Figure 12: Changes of R_{rs} for 10% increase of (A) TSM in the range 0.2 – 10.0 mg/l, (B) CHL in the range 0.2 – 5.0 µg/l, (C) S_{CDOM} in the range 0.010 – 0.020 nm^{-1}, (D) depth in the range 0.01 – 10.0 m for bottom substrate of the seagrass *Posidonia australia*.

A2.3.4 Determination of radiometric sensor requirements

In order to derive radiometric sensor requirements, top of atmosphere (TOA) simulations of radiance, $L^{TOA}(\lambda)$, are made for a few water types representing a wide range of aquatic ecosystems. The considered combinations of water constituents are summarized in Table 3.

**Table 3: Concentration combinations for top of atmosphere simulations.**

No.	TSM [g m^{-3}]	a$_{CDOM}$ [m^{-1}]	CHL [mg m^{-3}]	Remark
01	0.5	1	1	
02	0.5	1	10	
03	0.5	1	100	
04	0.5	3.16	1	
05	0.5	3.16	10	
06	0.5	3.16	100	largest $\Delta R_{rs}(\lambda)$ in NIR
07	0.5	10	1	darkest $R_{rs}(\lambda)$, used for a reference spectrum $L^{TOA}(\lambda)$
08	0.5	10	10	
09	0.5	10	100	
10	1.58	1	1	
11	1.58	1	10	
12	1.58	1	100	
13	1.58	3.16	1	
14	1.58	3.16	10	
15	1.58	3.16	100	
16	1.58	10	1	
17	1.58	10	10	
18	1.58	10	100	
19	5	1	1	brightest $R_{rs}(\lambda)$
20	5	1	10	largest $\Delta R_{rs}(\lambda)$ in VIS
21	5	1	100	
22	5	3.16	1	
23	5	3.16	10	
24	5	3.16	100	
25	5	10	1	
26	5	10	10	
27	5	10	100	

The 27 R_{rs} spectra resulting from the settings of Table 3 are shown in Figure 13. Some of the challenging water types have R_{rs} maxima below 0.005 sr^{-1} and minima in the order of 10^{-4} sr^{-1} in the range from 400 to 800 nm.

Each of the R_{rs} spectra shown in Figure 13 is converted to top of atmosphere (TOA) spectral radiance, $L^{TOA}(\lambda)$, using Modtran-5 (Berk et al., 2005). The sun zenith angle (SZA) is set to 10° and 70° (representing low and high latitude sun angles occurring in late spring, summer and early autumn), and horizontal visibilities (VIS) of 10 km and 80 km are chosen to represent turbid and very clear atmospheres. The aerosol type is set to maritime, and all calculations are made for a relative sun-earth distance of 1. All simulations assume a Lambertian surface and exclude sun glint and sky glint. The Modtran-5 calculations are made at a spectral resolution of 5 cm^{-1}. For adjusting the resolution to the R_{rs} simulations, a moving Gaussian filter with a full width at half maximum (FWHM) of 5 nm was applied.

In order to investigate the changes of L^{TOA} induced by ecologically relevant concentration differences in dark waters, the R_{rs} differences induced by chlorophyll-a concentration changes of 10%, 20%, 30%, 40% and 50% are calculated for the 27 parameter combinations of Table 3. Figure 14 shows the

resulting ΔR_{rs} spectra for 10% and 50% changes of CHL. All these ΔR_{rs} spectra are then converted to L^{TOA} differences, $\Delta L^{TOA}(\lambda)$, using Modtran-5.
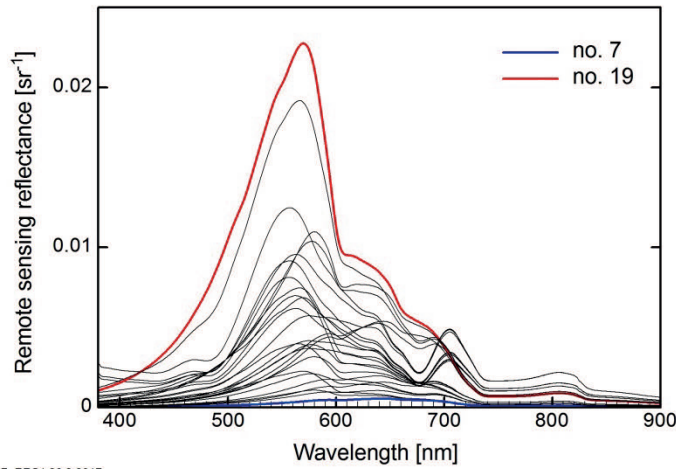
Figure 13: Remote sensing reflectance spectra used to simulate TOA radiances. No. 7 represents the darkest spectrum, no. 19 the brightest.
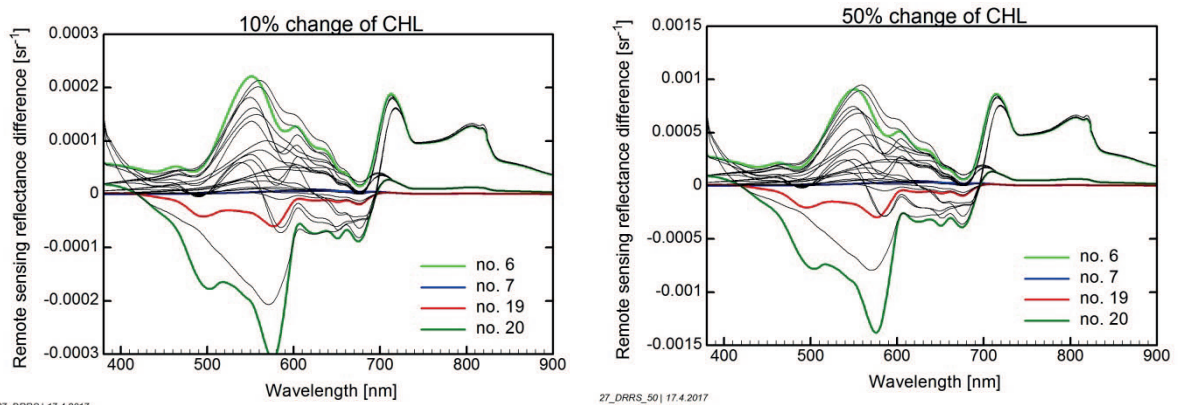
Figure 14: BOA remote sensing reflectance differences used to determine TOA radiance differences. The darkest spectrum (no. 7) induces the lowest change in reflectance, but the brightest spectrum (no. 19) not the highest. The highest reflectance differences are attributed to spectra no. 6 (in the NIR) and no. 20 (in the VIS).

If a sensor is able to measure the induced radiance differences, its noise is below $\Delta L^{TOA}(\lambda)$, hence the ratio

$$SNR(\lambda) \geq \frac{L^{TOA}(\lambda)}{\Delta L^{TOA}(\lambda)} \tag{7}$$

defines the necessary signal-to-noise ratio of a measurement $L^{TOA}(\lambda)$ for resolving CHL changes at wavelength λ. If a sensor fulfills equation (7) for at least one wavelength λ_m, it bears the potential to derive CHL changes:

$$SNR(\lambda_m) \geq \frac{L^{TOA}(\lambda_m)}{\Delta L^{TOA}(\lambda_m)}. \tag{8}$$

161

The minimum requirement to a sensor is derived from the plot of $SNR(\lambda_m)$ vs. λ_m for the 27 water types defined by Table 3.

To derive a realistic range of TOA radiances, a dark and two bright TOA radiance spectra are calculated. The dark spectrum is obtained by converting the darkest R_{rs} spectrum from Table 3 (no. 7) to $L^{TOA}(\lambda)$ for low sun elevation (SZA = 70°) and clear atmosphere (VIS = 80 km).

The two bright spectra represent optically deep water with high reflectance in the blue-green, and optically shallow water with high reflectance in the red-NIR spectral region. For deep water, a simulated spectrum R_{rs} from scenario Y-- is selected which combines very low absorption (a_{CDOM} = 0.04 m^{-1}, CHL = 1 mg m^{-3}) with very high backscattering (TSM = 20 g m^{-3}). For shallow water, the simulated spectrum R_{rs} for bottom substrate no. 7 (purple encrusting coralline algae) is used as this substrate has very high reflectance in the near infrared (~40%, see Figure 1). The water depth is set to 1 cm to minimize attenuation by water and to obtain high R_{rs} even in the infrared. Once a dedicated aquatic ecosystem sensor application is well defined (preferably both science and end-user driven) it is advised to run more of these type of simulations with more varying conditions and parameterisations. This study focuses on generic considerations across a variety of aquatic ecosystems.

A2.4. Results

A2.4.1 Most relevant wavelengths

A2.4.1.1 Reconstruction of reflectance spectra

If a spectrum should be sampled with a minimum number of spectral bands, but as accurate as possible with a reduced set of bands (such as for a multispectral band sensor), the bands must be centered at the wavelengths at which the spectrum has minima and maxima. These wavelengths are given by the zeros of the first derivatives of remote sensing reflectance, i.e., $\partial R_{rs}/\partial \lambda$ = 0. If the major spectral features of a spectrum should be captured, the number of bands must be increased to measure the reflectance shoulders as well. These are given by the zeros of the second derivatives of remote sensing reflectance, i.e., $\partial^2 R_{rs}/\partial \lambda^2$ = 0. This chapter investigates the spectral locations of $\partial R_{rs}/\partial \lambda$ = 0 and $\partial^2 R_{rs}/\partial \lambda^2$ = 0 that allow reconstruction of the reflectance spectra of the scenarios presented in chapter 1 with a limited number of spectral bands.

Figure 15 shows the results for the standard scenarios. The red lines indicate the positions of maxima and minima in R$_{rs}(\lambda)$, i.e. the spectral locations of $\partial R_{rs}/\partial \lambda$ = 0, and their shifts induced by changing a single parameter. The green lines show the positions of shoulders, i.e. the wavelengths of $\partial^2 R_{rs}/\partial \lambda^2$ = 0, as a function of a model parameter. Figure 16 shows the analog results for extreme scenarios. The subsequent Figures show the relevant wavelengths of reflectance spectra for different substrate types of optically shallow water as a function of water depth: Figure 17 for the depth range from 0 to 0.5 m, and Figure 18 for the range from 0 to 10 m.
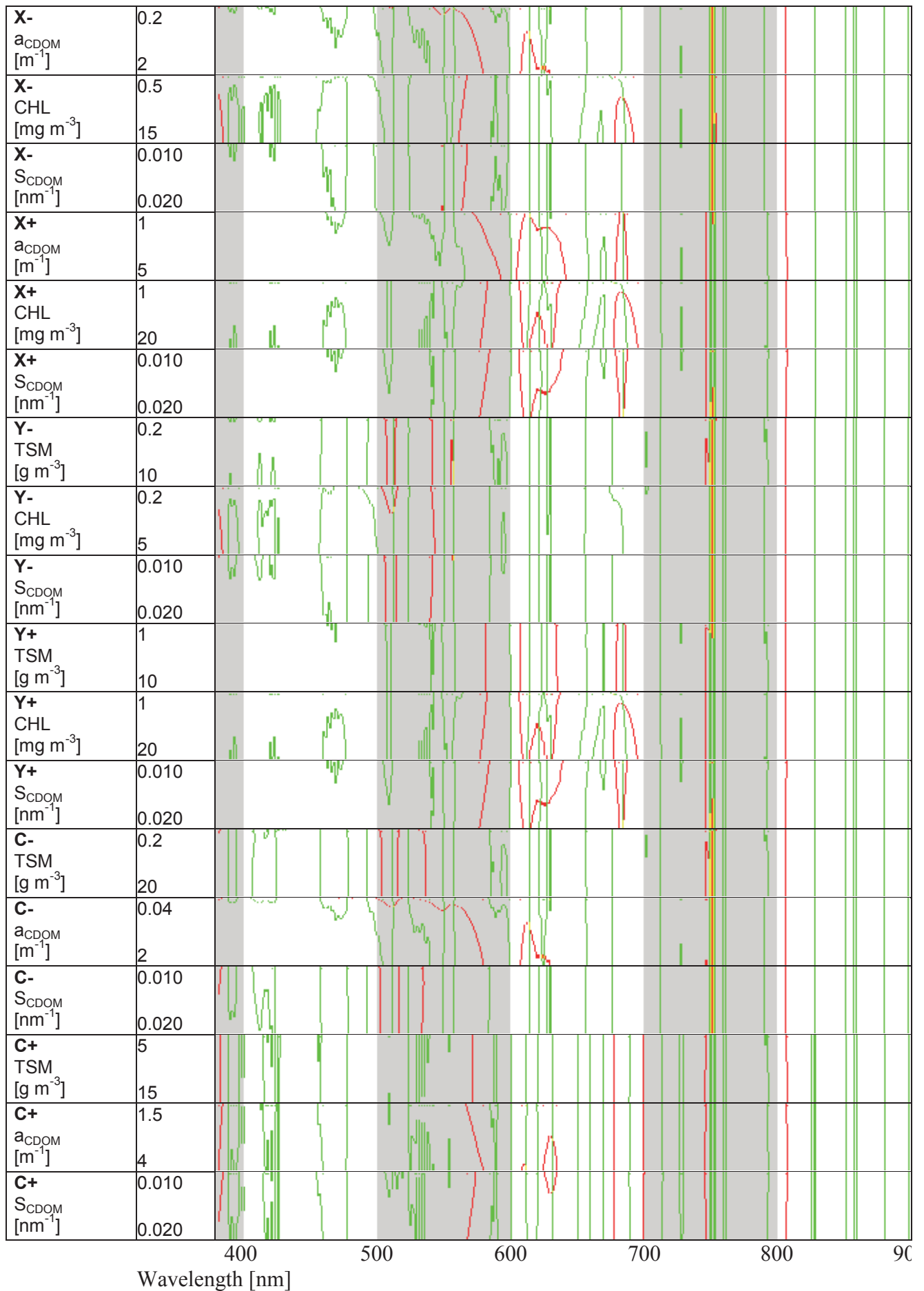
Figure 15: Zeros of first (red) and second derivatives (green) of standard scenarios.
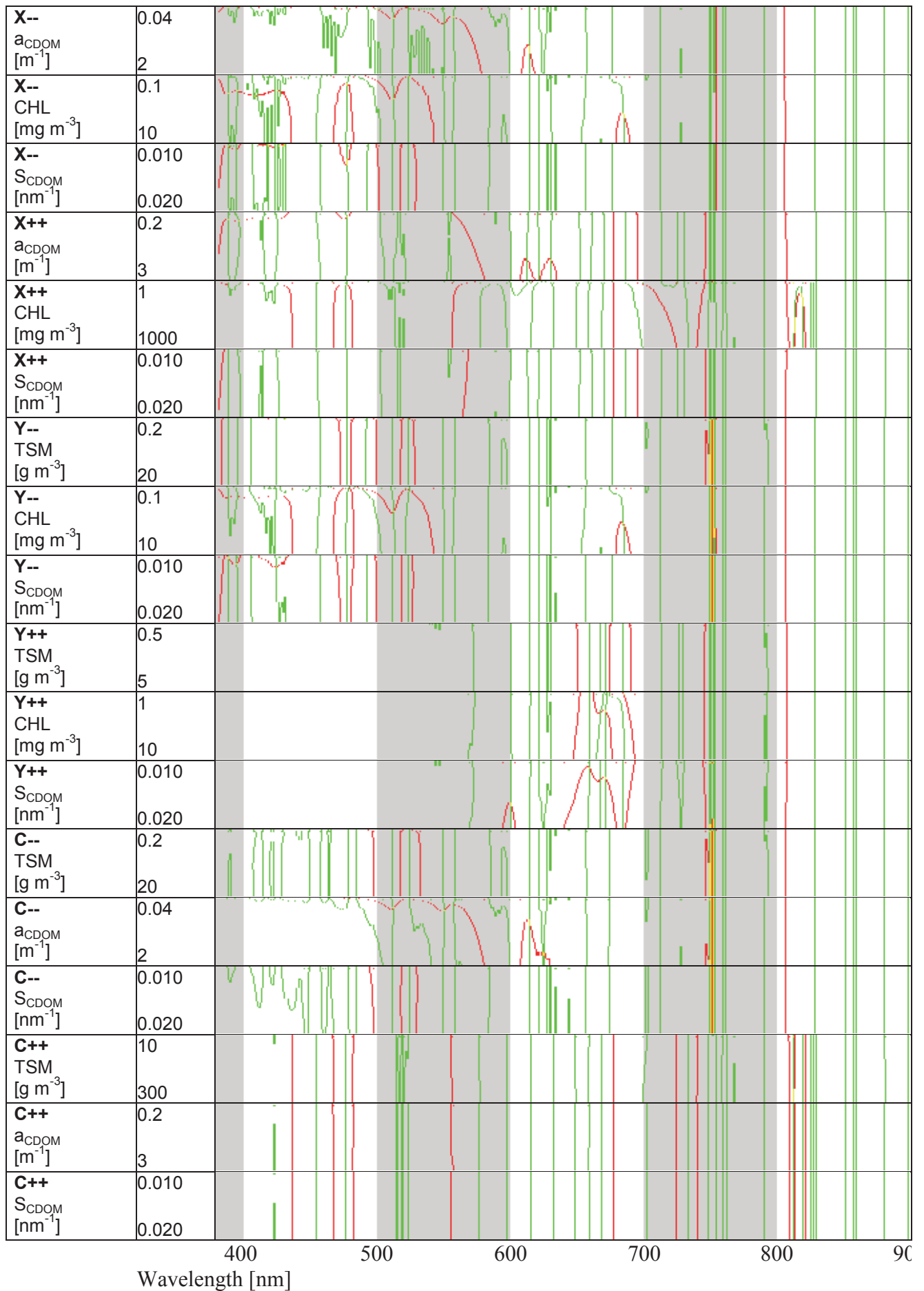
The table/figure rows, from top to bottom, carry the following labels:

Label	Value (top)	Value (bottom)
X-- a_{CDOM} [m^{-1}]	0.04	2
X-- CHL [mg m^{-3}]	0.1	10
X-- S_{CDOM} [nm^{-1}]	0.010	0.020
X++ a_{CDOM} [m^{-1}]	0.2	3
X++ CHL [mg m^{-3}]	1	1000
X++ S_{CDOM} [nm^{-1}]	0.010	0.020
Y-- TSM [g m^{-3}]	0.2	20
Y-- CHL [mg m^{-3}]	0.1	10
Y-- S_{CDOM} [nm^{-1}]	0.010	0.020
Y++ TSM [g m^{-3}]	0.5	5
Y++ CHL [mg m^{-3}]	1	10
Y++ S_{CDOM} [nm^{-1}]	0.010	0.020
C-- TSM [g m^{-3}]	0.2	20
C-- a_{CDOM} [m^{-1}]	0.04	2
C-- S_{CDOM} [nm^{-1}]	0.010	0.020
C++ TSM [g m^{-3}]	10	300
C++ a_{CDOM} [m^{-1}]	0.2	3
C++ S_{CDOM} [nm^{-1}]	0.010	0.020

Wavelength [nm]

Figure 16: Zeros of first (red) and second derivatives (green) of extreme scenarios.

164

0 Chara contraria	0 — 0.5 m	
1 Potamogeton perfoliatus	0 — 0.5 m	
2 Rock	0 — 0.5 m	
3 Bleached coral	0 — 0.5 m	
4 dark silt	0 — 0.5 m	
5 bright sand	0 — 0.5 m	
6 yellow Poirites sp.	0 — 0.5 m	
7 purple encr. corr. algae	0 — 0.5 m	
8 brown Poirites sp.	0 — 0.5 m	
9 Posidonia australia	0 — 0.5 m	
10 detritus (sea-grass wrack)	0 — 0.5 m	
11 Ecklonia radiata	0 — 0.5 m	
12 coarse coral rubble	0 — 0.5 m	
13 dark sand	0 — 0.5 m	

Wavelength [nm]
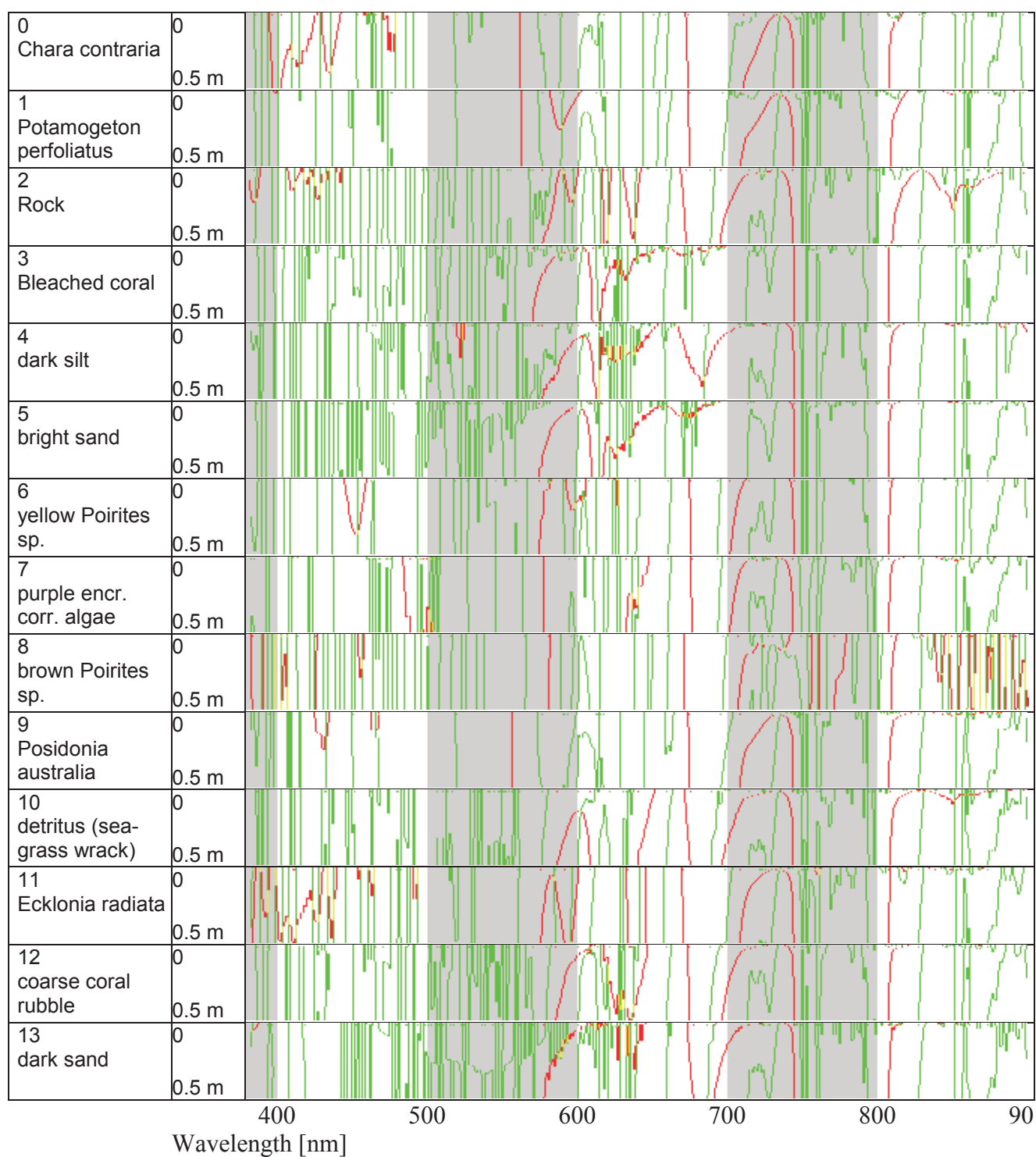
Figure 17: Zeros of first (red) and second derivatives (green) of very shallow waters.
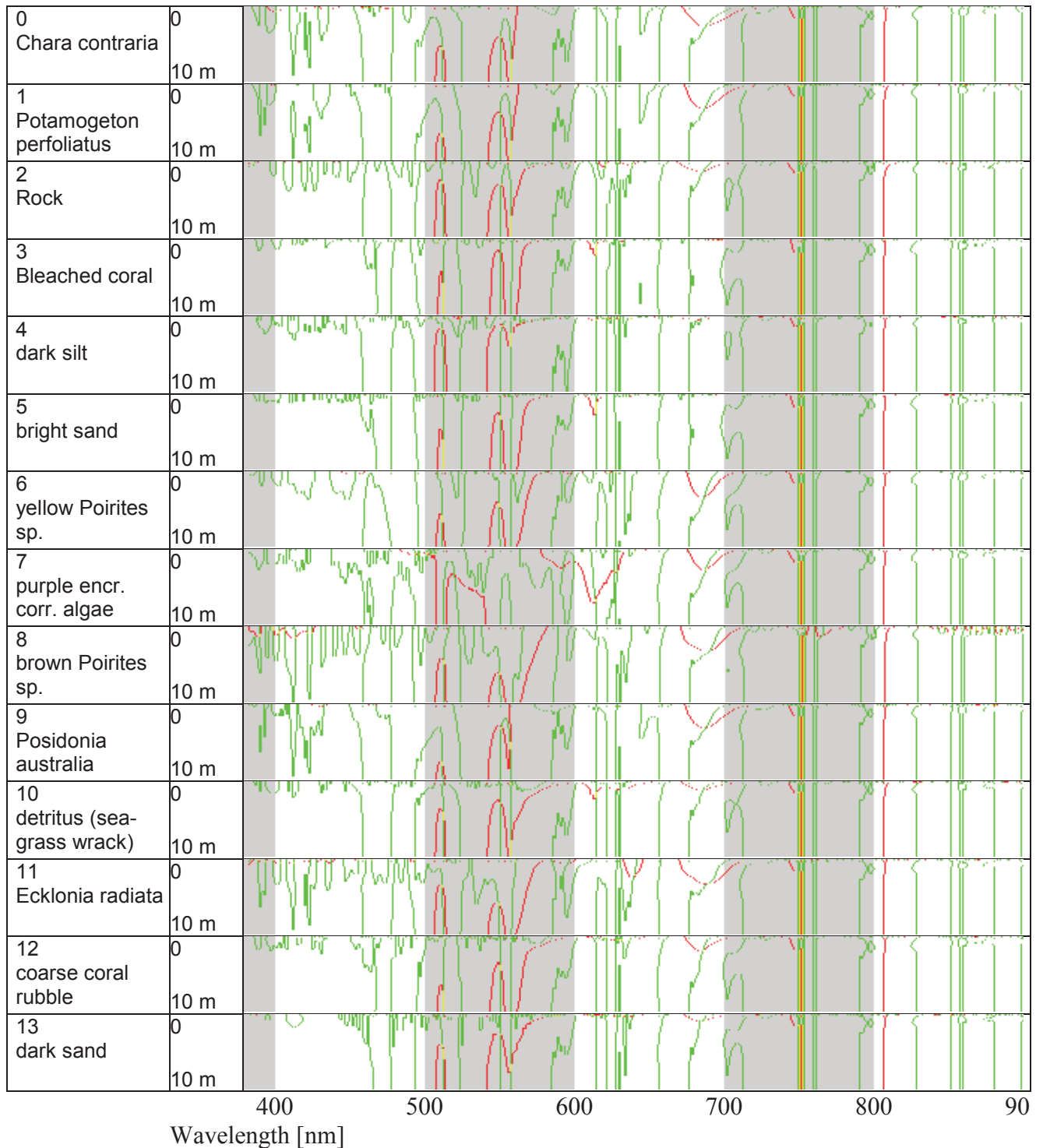
Figure 18: Zeros of first (red) and second derivatives (green) of shallow waters.

In order to cover the variability within a scenario more completely, three parameters were iterated simultaneously, and the zeros of $\partial R_{rs}/\partial\lambda$ were calculated for all parameters. For each scenario, three parameters were changed in 10 steps, resulting in $10^3 = 1000$ spectra. A histogram of the resulting spectral locations of the minima and maxima is shown in Figure 19 for the standard scenarios.
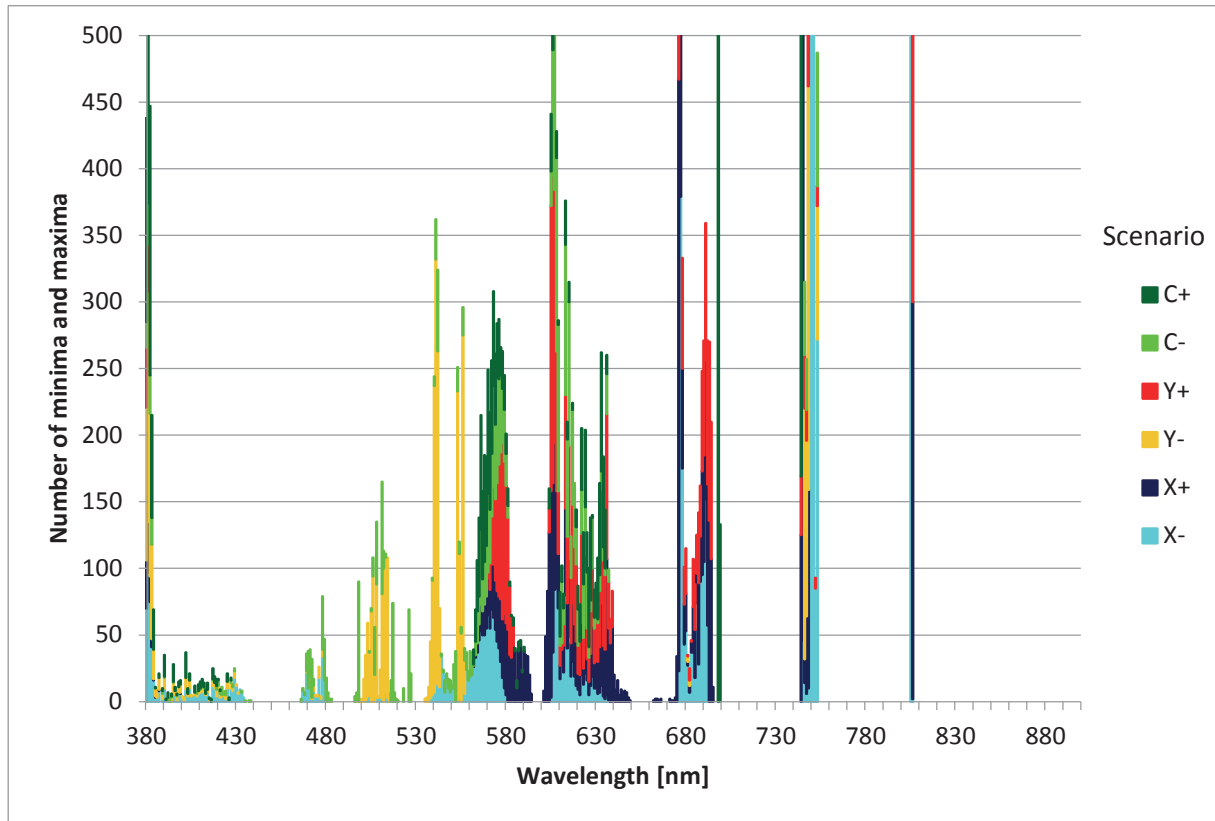
Figure 19: Cumulative histogram of the minima and maxima ($\partial R_{rs}/\partial\lambda = 0$) for the standard scenarios. The most prominent wavelengths are labeled on top of the diagram.

In the spectral range from 380 to 700 nm, the position of minima and maxima of R_{rs} changes significantly from one scenario to the next. This strong dependency of characteristic wavelengths on the water type is a strong argument for a hyperspectral sensor in that range. Multispectral sensors are of most benefit if these have bands centered at 382, 608, 677 and 699 nm, where many scenarios have a peak or dip in the reflectance spectrum. The scenarios C- and Y- have in addition six characteristic wavelengths between 470 and 550 nm (green and orange peaks at 472, 479, 499, 507-515, 527 and 542 nm).

The spectral range beyond 700 nm is characterized by just three extrema at 746, 751 and 806 nm, which don't depend much on the scenario.

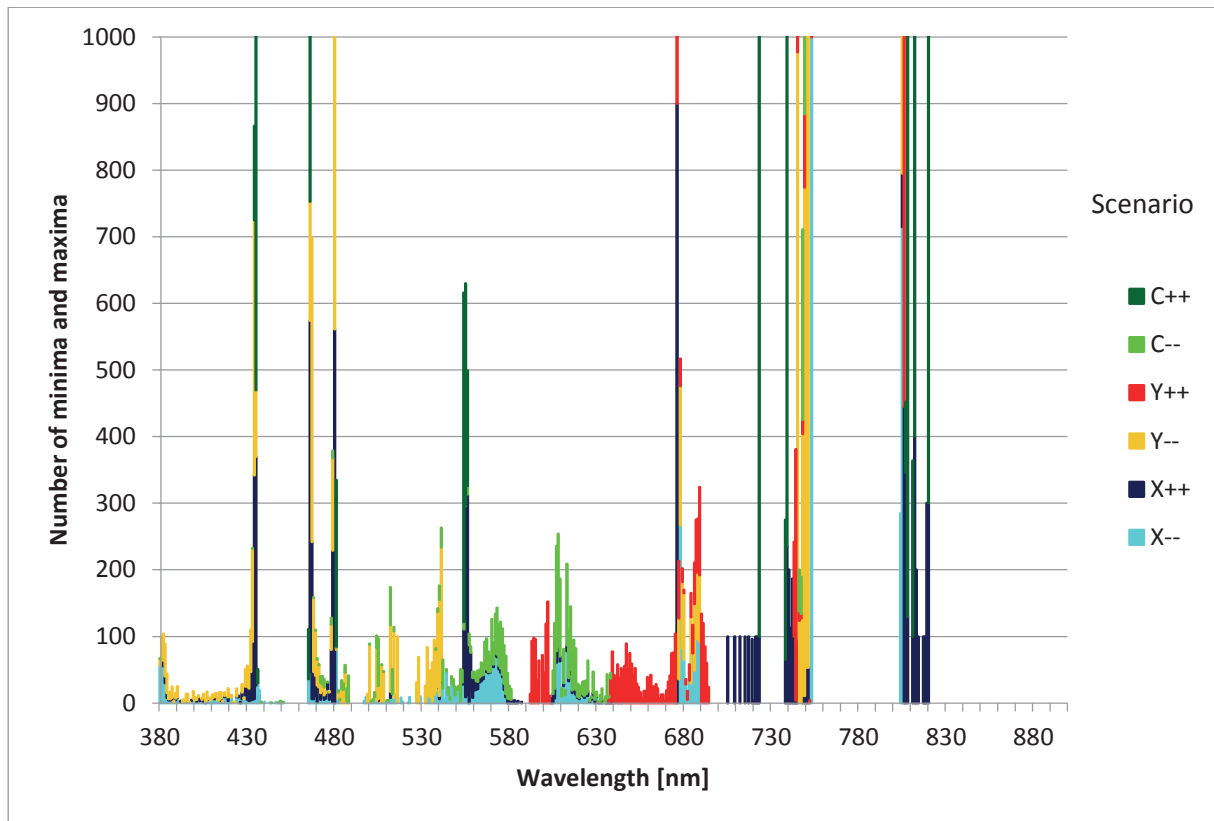Figure 20 shows the histogram of the zeros of the first derivatives of the extreme scenarios.

Figure 20: Cumulative histogram of the minima and maxima ($\partial R_{rs}/\partial \lambda = 0$) for the extreme scenarios. The most prominent wavelengths are labeled on top of the diagram.

The positions of the reflectance minima and maxima of extreme scenarios are more variable than for the standard scenarios, and the range of large variability extends now up to 725 nm. The spectral features of such water types can be monitored best using a hyperspectral sensor in the range from 380 to 725 nm.

For multispectral sensors, the outstanding wavelengths of extreme scenarios are at 436, 467, 481, 677 and 724 nm. The characteristic wavelengths above 700 nm depend now also slightly on the scenario. If these are not resolved by a hyperspectral sensor, the ideal multispectral sensor has 15 nm wide bands ranging from 740 to 754 nm and 806 to 821 nm.

Figure 21 shows a histogram of the zeros of the first derivatives of very shallow waters from 0 – 0.5 m depth.
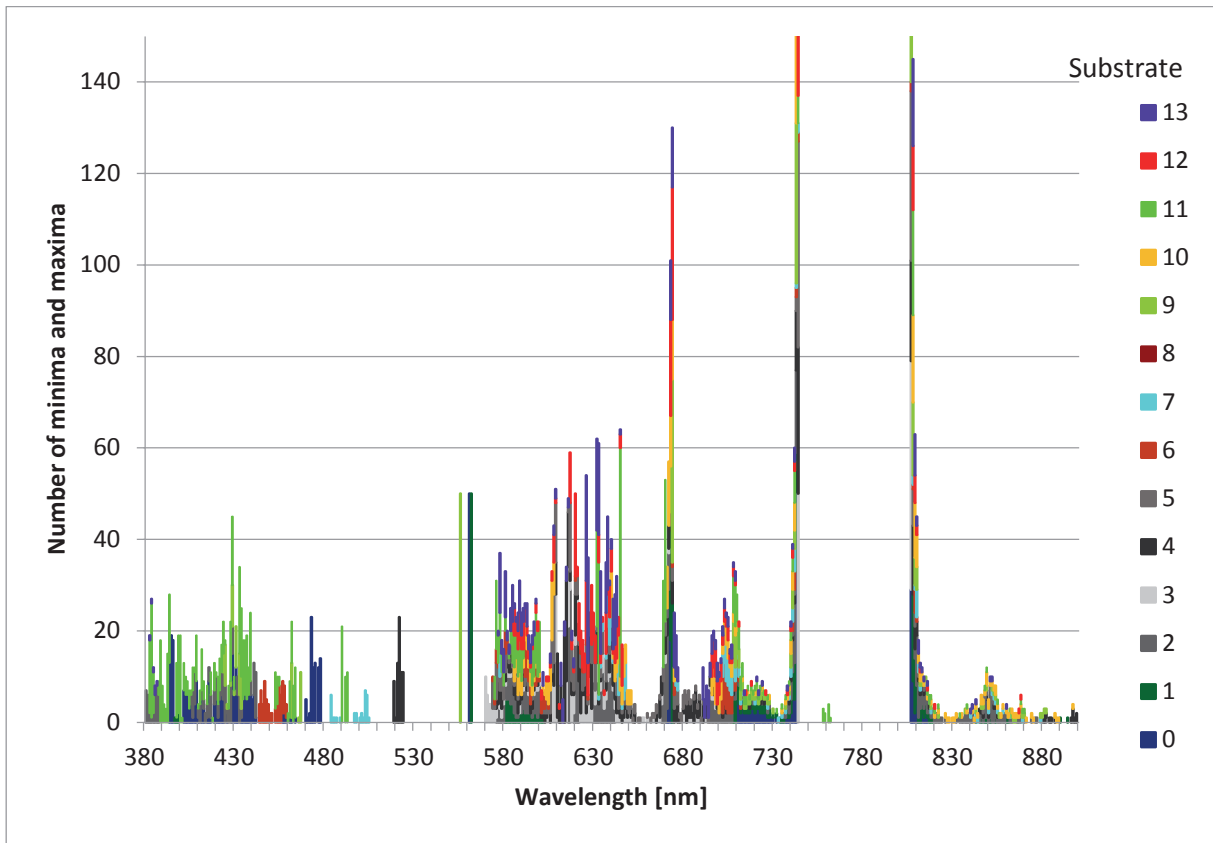
Figure 21: Cumulative histogram of the minima and maxima ($\partial R_{rs}/\partial \lambda = 0$) for very shallow water of $0 - 0.5$ m depth.

The location of minima and maxima is highly variable from 380 to 730 nm, thus accurate substrate classification requires a hyperspectral sensor in that range. The many peaks in the histogram from 750 to 780 nm and from 830 to 900 nm, caused by substrate no. 8, can be attributed to noise of the substrate spectrum (cf. Figure 1). Useful for a multispectral sensor are mainly the extrema at 743 and 807 nm.

Figure 22 shows a histogram of the zeros of the first derivatives of shallow waters from $0 – 10$ m depth.
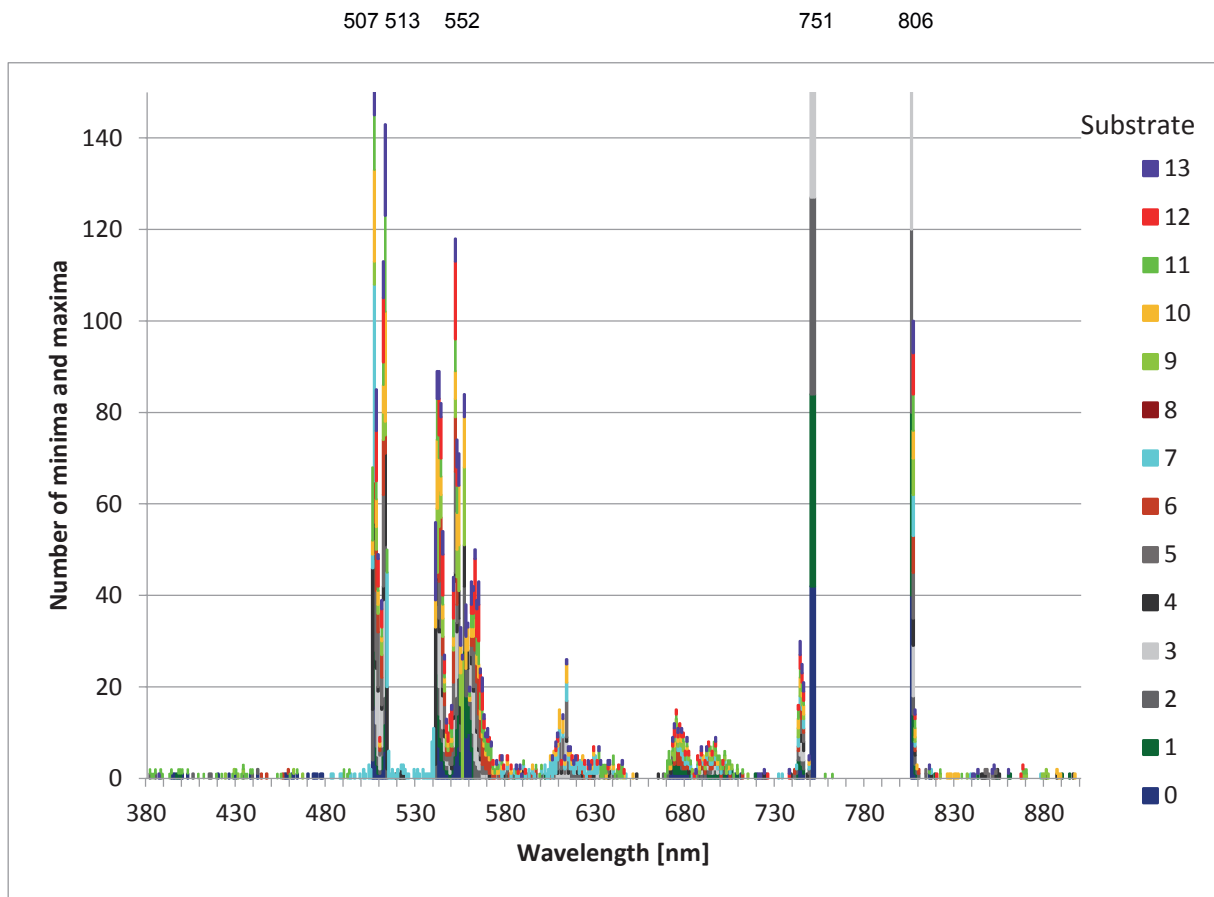

Figure 22: Cumulative histogram of the minima and maxima ($\partial R_{rs}/\partial\lambda = 0$) for shallow water of $0 – 10$ m depth.

Compared to the very shallow depths from 0 to 0.5 m, the histogram of the $0 – 10$ m depth range reveals more clear features, i.e. the information from the bottom substrates is now more confined to specific wavelengths or wavelength intervals. Characteristic wavelengths can be identified at 507, 513, 552, 751 and 806 nm. Significant variability, best monitored by a hyperspectral sensor, occurs between 540 and 680 nm. Most of the many extrema with low frequency outside these wavelength ranges can be attributed to the very shallow waters from Figure 21.

Figure 23 shows a histogram of the zeros of the second derivatives for the standard scenarios.
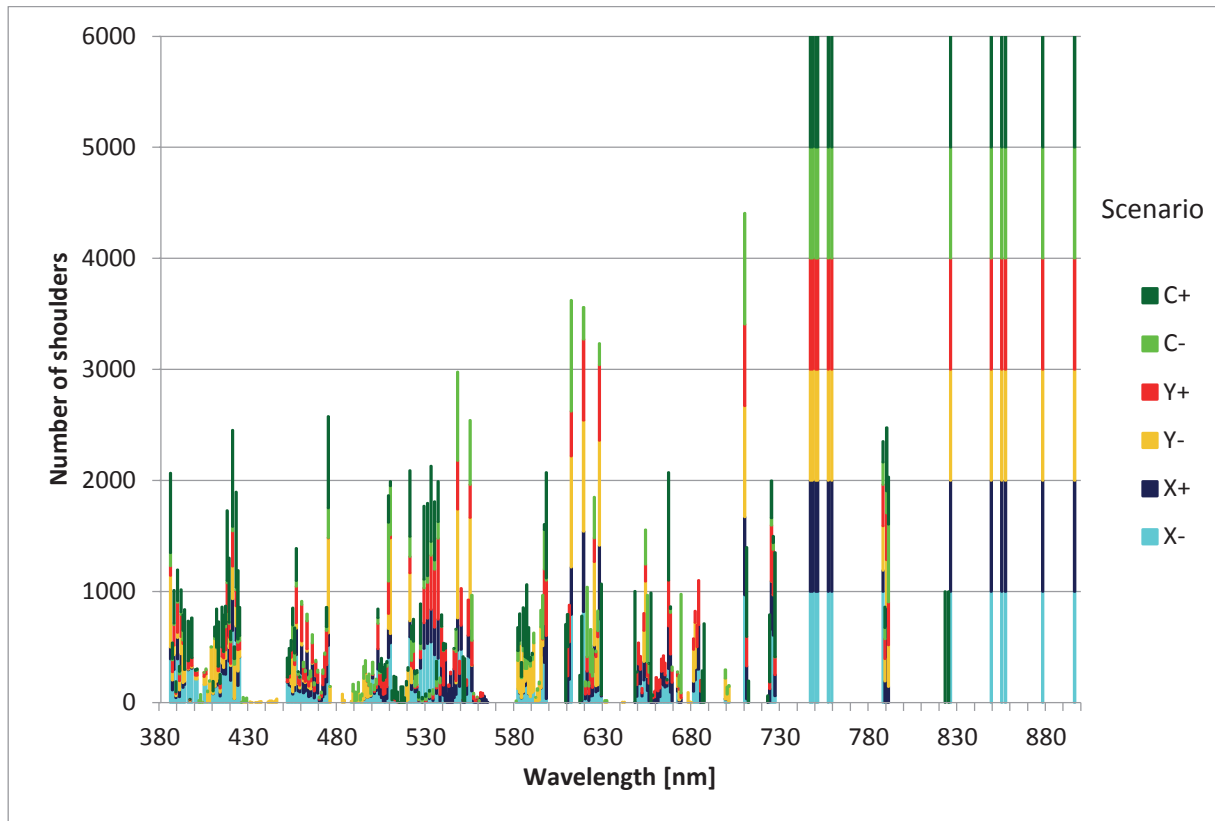

Figure 23: Cumulative histogram of the shoulders ($\partial^2 R_{rs}/\partial\lambda^2 = 0$) for the standard scenarios.

In the spectral range from 380 to 690 nm, the position of R_{rs} shoulders changes significantly from one scenario to the next. Outside this range, characteristic wavelengths for most of the scenarios are observed at 711, 748-760, 791, 827, 850-858, 879 and 897 nm.

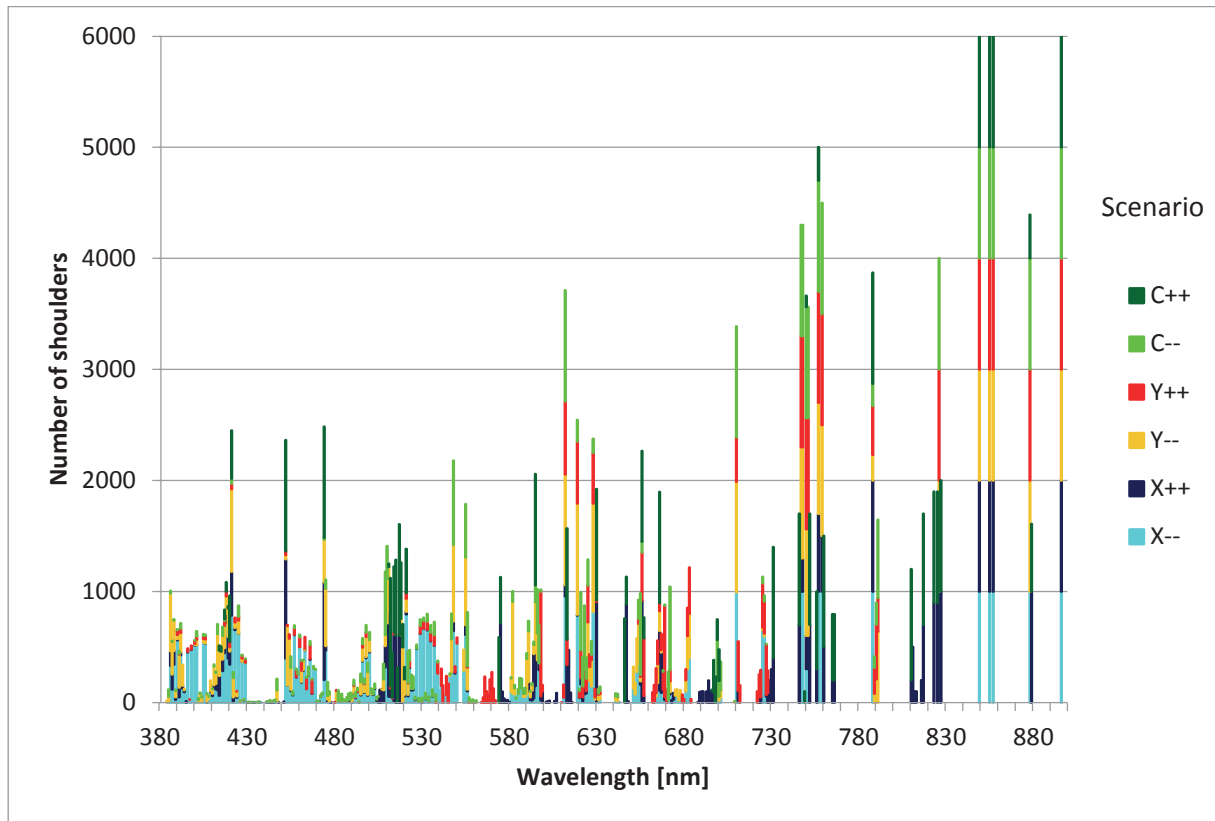Figure 24 shows a histogram of the zeros of the second derivatives for the standard scenarios.

Figure 24: Cumulative histogram of the shoulders ($\partial^2 R_{rs}/\partial\lambda^2 = 0$) for the extreme scenarios.

Similar as before, the position of R_{rs} shoulders changes significantly from one scenario to the next from 380 to 700 nm. The characteristic wavelengths outside this range are almost identical to the standard scenarios: 711, 748-760, 789, 827, 850-858, 879 and 897 nm.

Figure 25 shows a histogram of the zeros of the second derivatives for very shallow water of 0.01 – 0.50 m depth.
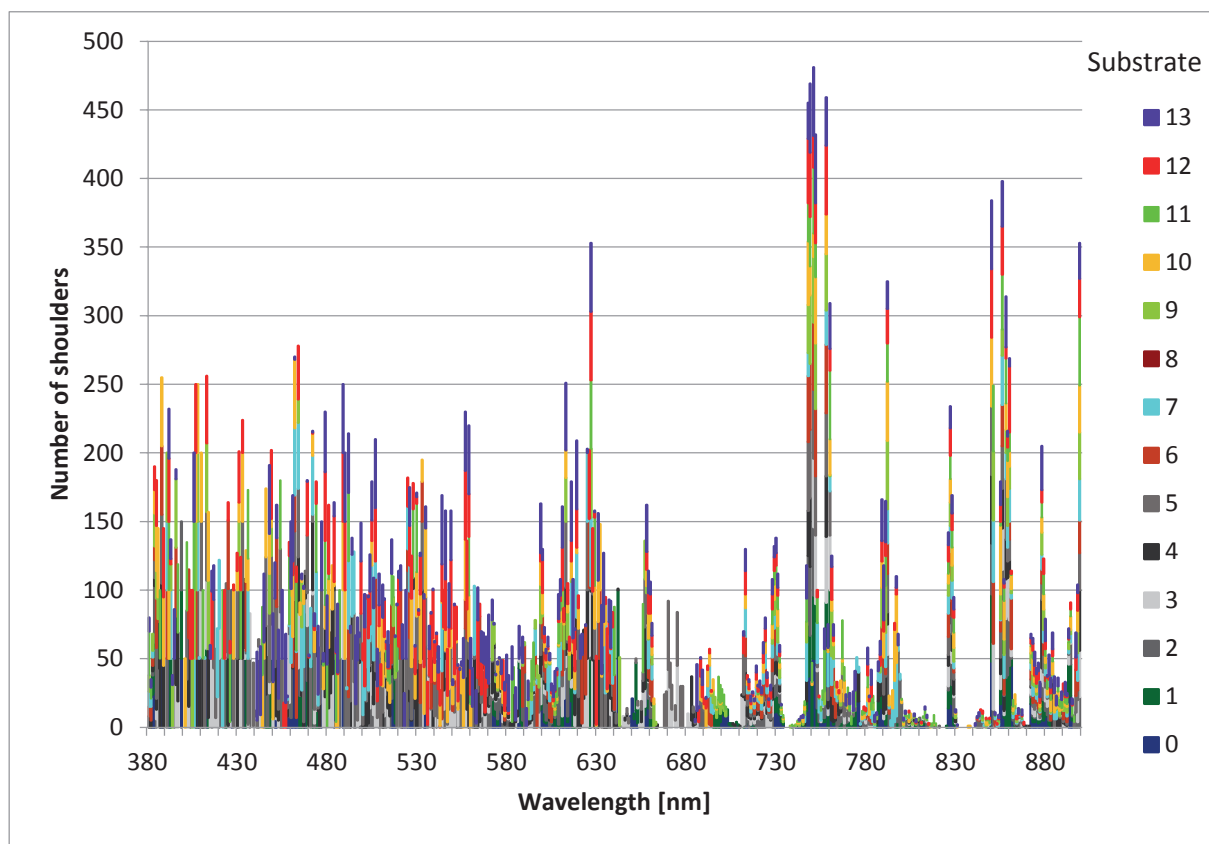
748-760 792   827,850-858,878,899

Figure 25: Cumulative histogram of the shoulders ($\partial^2 R_{rs}/\partial \lambda^2 = 0$) for very shallow water of 0.01 – 0.50 m depth.

The wavelengths where the second derivatives are zero, i.e. the position of the shoulders of the reflectance spectrum, show a huge variability for optically very shallow water (0.01 – 0.50 m). Remarkably, the characteristic wavelengths above 700 nm, which were observed for deep water, are also present here: 748-760, 792, 827, 850-858, 878 and 899 nm.

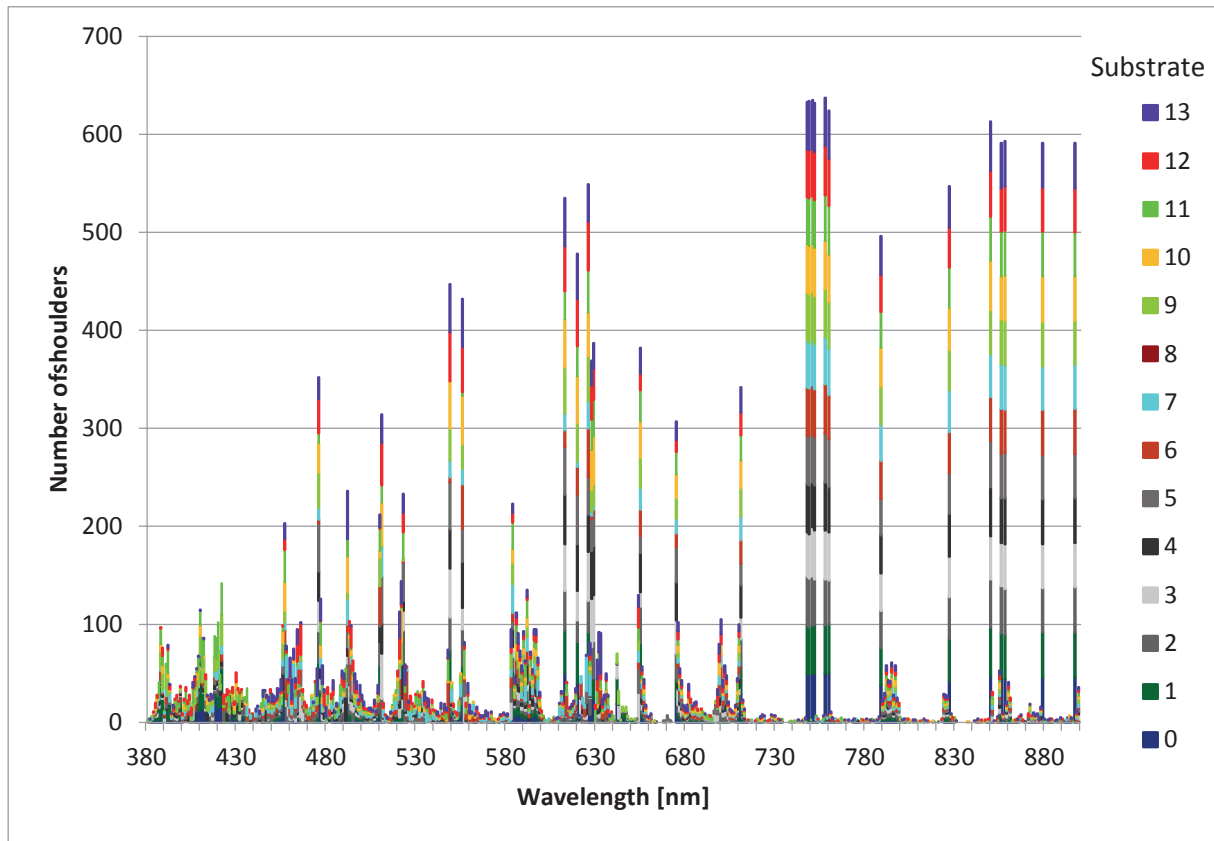Figure 26 shows a histogram of the zeros of the second derivatives for shallow water of 0 – 10 m depth.

Figure 26: Cumulative histogram of the shoulders ($\partial^2 R_{rs}/\partial\lambda^2 = 0$) for shallow water of 0 – 10 m depth.

Compared to the histogram of Figure 25, which is not much structured for very shallow waters below 730 nm, the entire spectral range from 380 to 900 nm is now characterized by distinct peaks at certain wavelengths. If histogram peaks above a threshold of N=200 are counted (total number of runs: N=700), 23 prominent peaks can be identified, located at 457, 476, 492, 511, 523, 549, 556, 584, 613, 620, 626, 629, 655, 675, 711, 748-752, 758-760, 789, 827, 850, 856-858, 879 and 897 nm. The histogram peaks above 700 nm are almost identical to those observed in the second derivatives of deep water and very shallow water.

A graphical summary of the eight histograms (Figure 19 to Figure 26) is provided in Figure 27. It shows a wide spread of minima and maxima for different water types, and even more of the shoulders. The spectral shift of characteristic wavelengths is most pronounced in the range from 380 to 730 nm, while the infrared region above approximately 730 nm is spectrally more stable. Consequently, the ideal sensor for capturing the characteristic features of reflectance spectra is hyperspectral in the visible, but could be multispectral in the infrared.
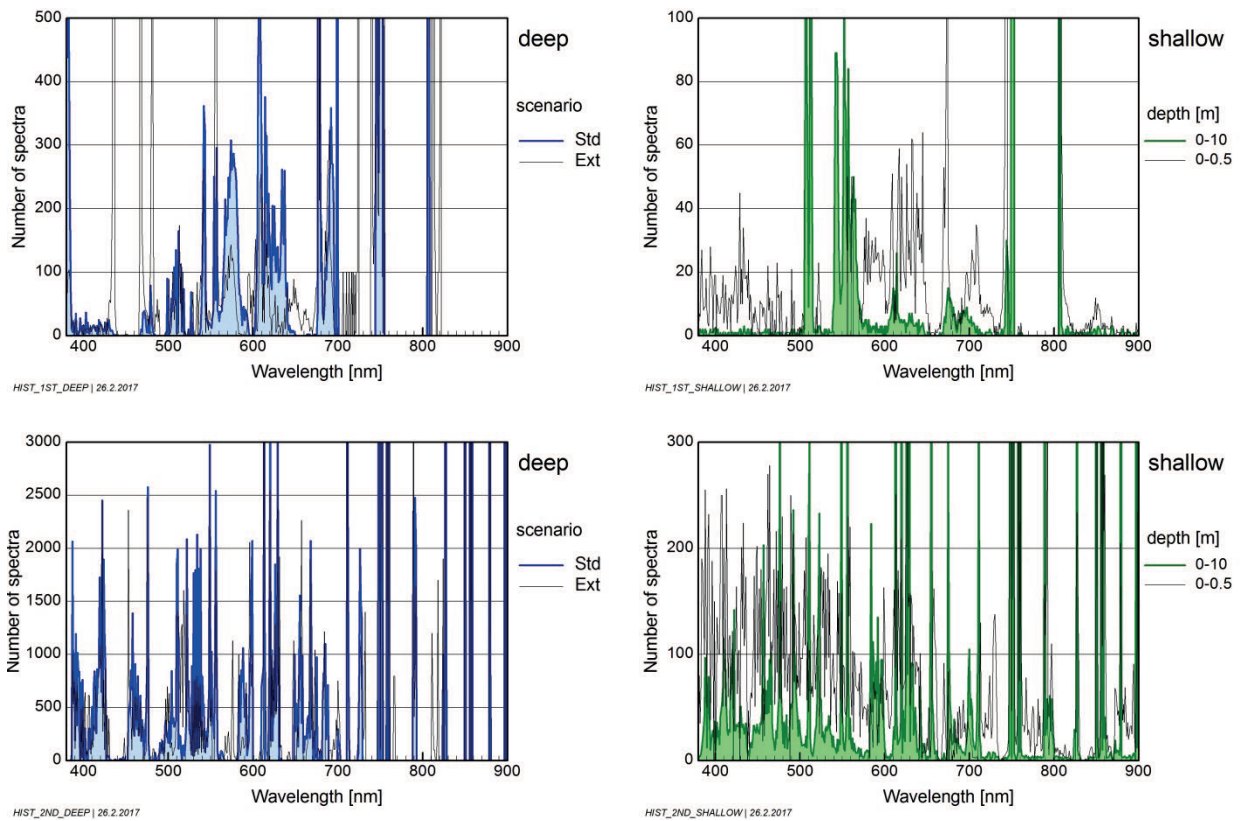
Figure 27: Histograms of wavelengths of extremes (upper row, $\partial R_{rs}/\partial\lambda$ =0) and shoulders (lower row, $\partial^2 R_{rs}/\partial\lambda^2$ =0) of reflectance spectra in deep (left column) and shallow waters (right column).

A list of the most relevant wavelengths is given in Table 4. It has been compiled using the first derivatives, i.e. the most frequent peaks and dips of reflectance spectra, and summarizes the major spectral features for reconstructing the reflectance spectra of the simulated scenarios. This table can be considered a compromise for multispectral sensors, which can cover a significant amount of the natural variability, albeit for the parameterisations as chosen for this study.

Table 4: Characteristic wavelengths for which a significant number of the simulated reflectance spectra have a maximum, minimum or shoulder. Std = standard scenarios, Ext = extreme scenarios, Shore = very shallow water of depths 0 – 0.5 m, Shallow = shallow water of depths 0 – 10 m.

No	Wavelength [nm]	Std	Ext	Shore	Shallow	Std	Ext	Shore	Shallow
		Zeros of 1st derivative				Zeros of 2nd derivative			
1	382-387	x				x			
2	422					x	x		
3	436		x						
4	453-457						x		x
5	467		x						
6	475-481		x			x	x		x
7	492								x
8	507-513				x	x			
9	522-523					x			x
10	534-538					x			
11	549-556				x	x	x		x
12	584								x
13	596-599						x		
14	608	x							
15	613					x	x		x
16	620					x	x		x
17	626-631					x	x		x
18	655-657						x		x
19	668-674	x	x	x		x		x	x
20	699	x							
21	711					x	x		x
22	724-726		x			x			
23	742-743		x	x					
24	746-754	x	x		x	x	x	x	x
25	758-760					x	x	x	x
26	789-792					x	x	x	x
27	806-807	x	x	x	x				
28	813		x						
29	821		x						
30	827					x	x	x	x
31	850					x	x	x	x
31	856-858					x	x	x	x
32	878-879							x	x
33	897-899							x	x

A2.4.1.2 Wavelengths of maximum sensitivity

The wavelengths of maxima, minima and shoulders in reflectance spectra, which have been determined inAppendix A.2.3.1 are not necessarily identical to the wavelengths of maximum sensitivity to a parameter of interest. These spectral regions where changes of a certain parameter

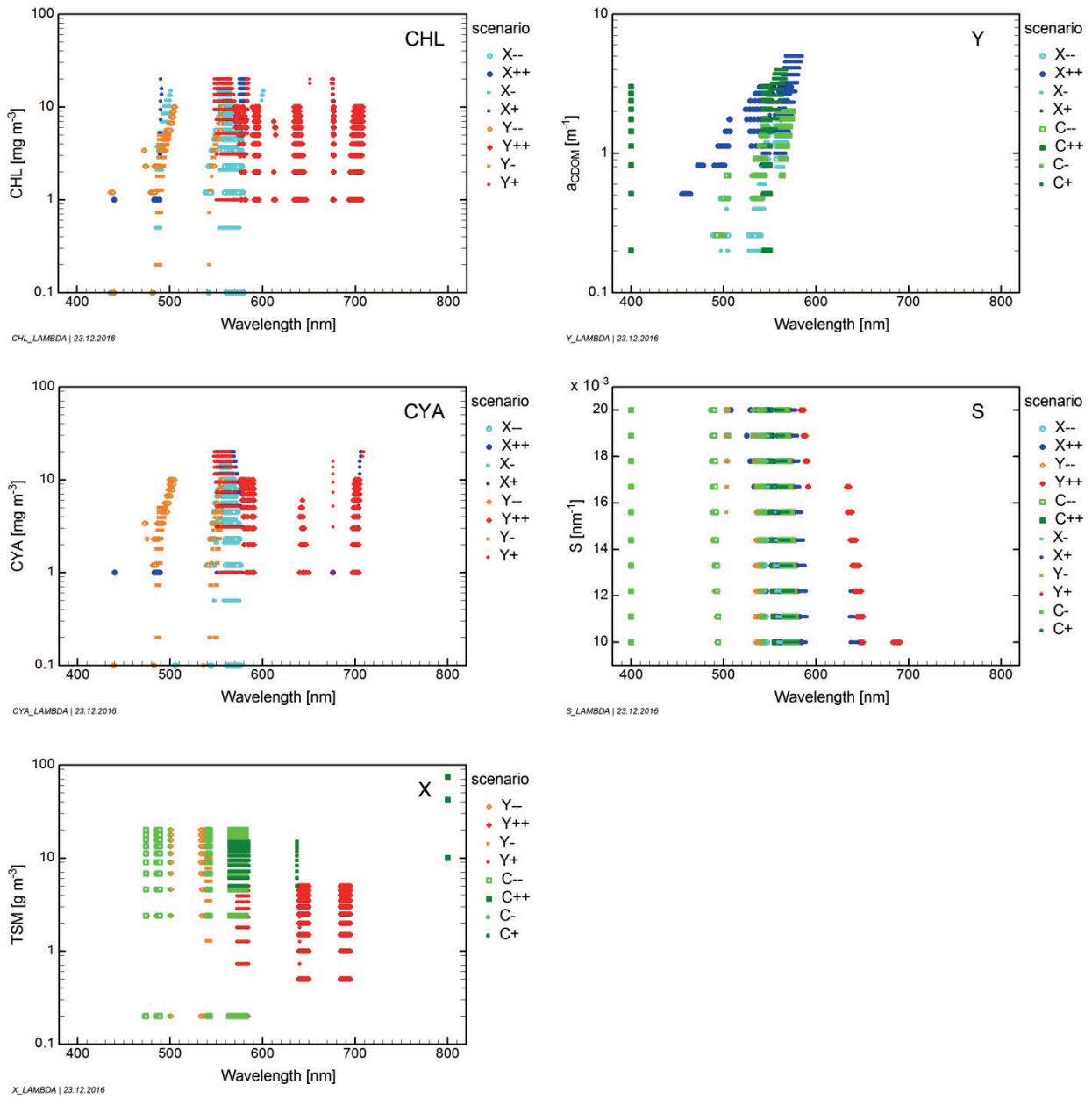induce the largest reflectance change are determined by applying Eq. (6). The results are shown in Figure 28.

Figure 28: Wavelengths of maximum sensitivity to the parameter indicated top right.
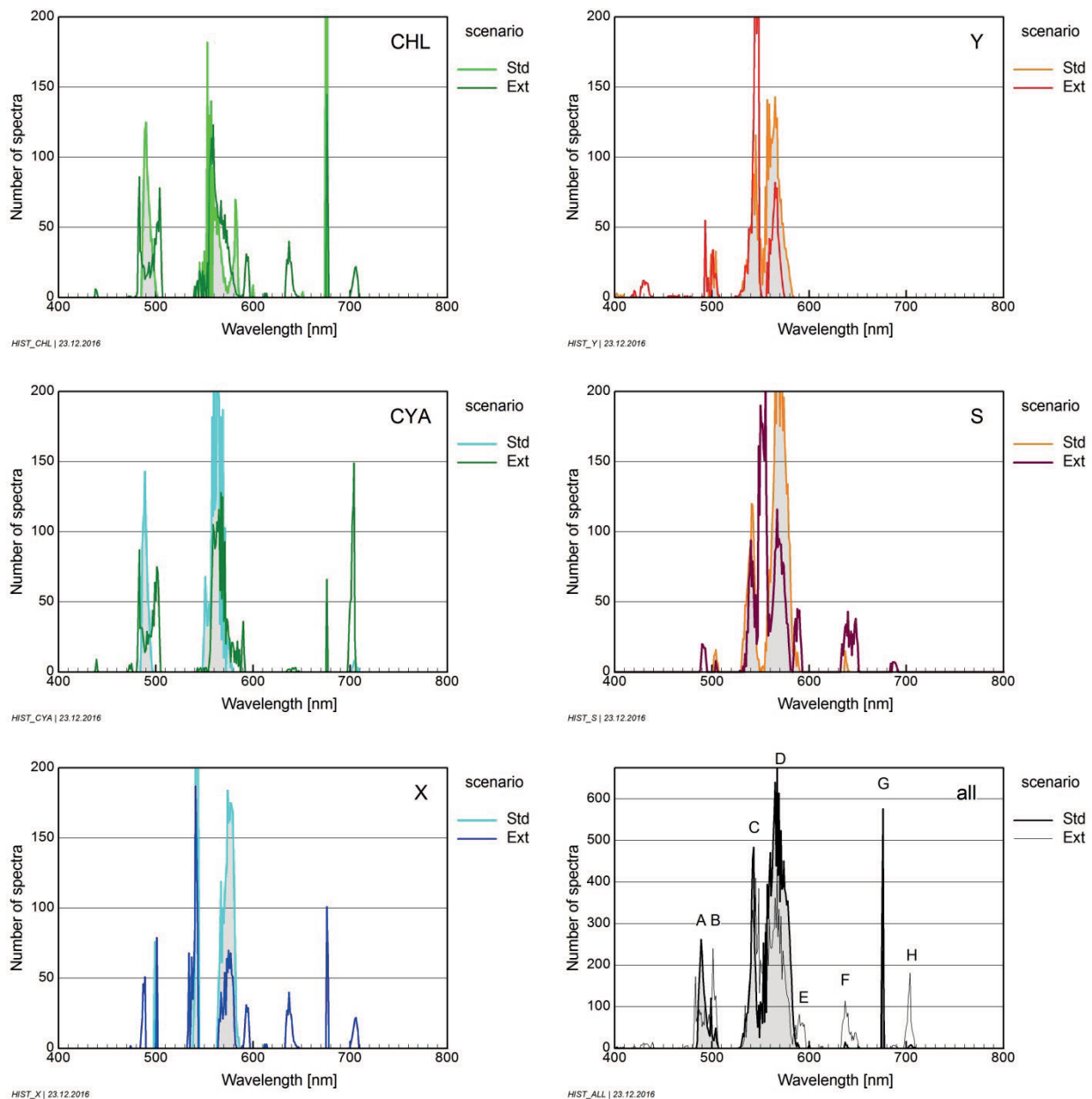
Figure 29: Histograms of wavelengths of maximum sensitivity to the parameter indicated top right. The histogram "all" is the sum of the histograms for CHL, CYA, X, Y and S. The labels A to H indicate the most sensitive spectral regions.

The frequency distributions of the most sensitive wavelengths are shown in Figure 29. These histograms indicate the most sensitive spectral regions for measuring CHL, CYA, TSM, a_{CDOM} and S_{CDOM}. The label "Std" refers to the standard scenarios of Table 1, the label "Ext" to the extreme scenarios of Table 2. Figure 29 shows that the wavelengths of maximum sensitivity are concentrated in eight spectral regions, labeled A to H.

Table 5 summarizes the center wavelengths and spectral widths of these regions. Most regions are spectrally narrow with widths of 8 nm or below (±1, ±3, ±4 nm); only the regions at 565 nm (±15 nm) and 641 nm (±8 nm) are much broader.

A comparison with the results from Table 4 and with the center wavelengths suggested by IOCCG (2012) for ocean colour satellites is given in Table 6. IOCCG recommendations focused on atmospheric correction are omitted, as well as the characteristic wavelengths no. 25 to 33 from Table 4 as these have no correspondence from the other methods. Remarkably, just two sensitive regions (A, C) coincide with prominent features of reflectance (7, 10). Hence, derivative analysis is not the

178

method of first choice for identifying the best suited wavelengths for monitoring of CHL, CYA, TSM, a_{CDOM} or S_{CDOM} in optically deep water.

Table 5: Spectral regions most sensitive to concentration changes of chlorophyll-a (CHL), cyanobacteria (CYA), total suspended matter (X), colored dissolved organic matter (Y), and to the spectral slope of CDOM absorption (S). Bold: standard scenarios, normal: extreme scenarios.

Region	Center [nm]	+/- [nm]	sensitive
A	490	4	**CHL, CYA,** X, Y
B	502	3	CHL, CYA, **X, Y**
C	542	4	**X, Y, S**
D	565	15	**all**
E	592	4	**CHL,** CYA, **X**
F	641	8	CHL, X, S
G	676	1	CHL, **CYA,** X
H	703	1	CHL, CYA, X

Table 6: Comparison of wavelengths relevant for measurements of optically deep water at bottom of atmosphere. IOCCG: recommended by IOCCG (2012) for ocean colour satellites; Reflectance: prominent features of reflectance spectra (see Table 4); Sensitive: high sensitivity to water constituents (see Table 5). Wavelengths common to independent methods or highly sensitive for many scenarios are marked in bold; recommended wavelengths are marked in yellow.

IOCCG	Reflectance		Sensitive		Application
385	1	**382-387**			CDOM-CHL separation
400					CDOM-CHL separation
425	2	**422**			CDOM-CHL separation
	3	436			
443					Chl-a absorption peak
	4	453-457			
460					Accessory pigments & Chl
	5	467			
475	6	**475-481**			Accessory pigments & Chl
490	7	**492**	A	**490**	CHL band-ratio algorithm
			B	502	
510	8	**507-513**			CHL band-ratio algorithm
	9	522-523			
532					MODIS band (10 nm)
	10	534-538	C	542	Bio-optical algorithms
555	11	**549-556**			Bio-optical algorithms
			D	565	Bio-optical algorithms
583	12	**584**			Phycoerythrin
			E	592	Bio-optical algorithms
	13	596-599			
	14	608			
	15	613			
620	16	**620**			Cyanobacteria, suspended sediment, phycocyanin
	17	626-631			
640			F	**641**	Particulate backscatter
655	18	**655-657**			CHL-b
670	19	**668-674**			Fluorescence line height baseline; chlorophyll in highly turbid water
678			G	676	Fluorescence line height
	20	699			
			H	703	Particles; phytoplankton at high concentrations
710	21	**711**			FLH baseline; HABs detection; CHL in highly turbid water; turbid water atmosphere correction
	22	724-726			
	23	742-743			
748	24	**746-754**			Atmospheric correction open ocean; CHL in highly turbid water

A2.4.2 Optimal spectral resolution

A2.4.2.1 Deep water

The optimal spectral resolution for resolving all radiometric details with a relative radiometric resolution of 1% was calculated using Eq. (4). Figure 30 shows the results for the standard scenarios, and Figure 31 for the extreme scenarios. The legend for the colors is shown in Figure 11. The color changes in steps of 2.5 nm, i.e. dark blue is 0 to 2.5 nm, light blue 2.5 to 5.0 nm, and so on.

With the exception of the extreme scenarios X++ and C++, the optimal spectral resolution changes significantly at 730 nm: a resolution of 5 nm or better (light blue, dark blue) can be used to resolve spectral details below 730 nm, while a resolution of 10 nm or less (orange, red, pink, white) is favourable for most scenarios above 730 nm to minimize the noise of these bands, which are characterized by very low reflectance values. Frequently a spectral resolution of 20 nm or more (white) is sufficient above 730 nm.
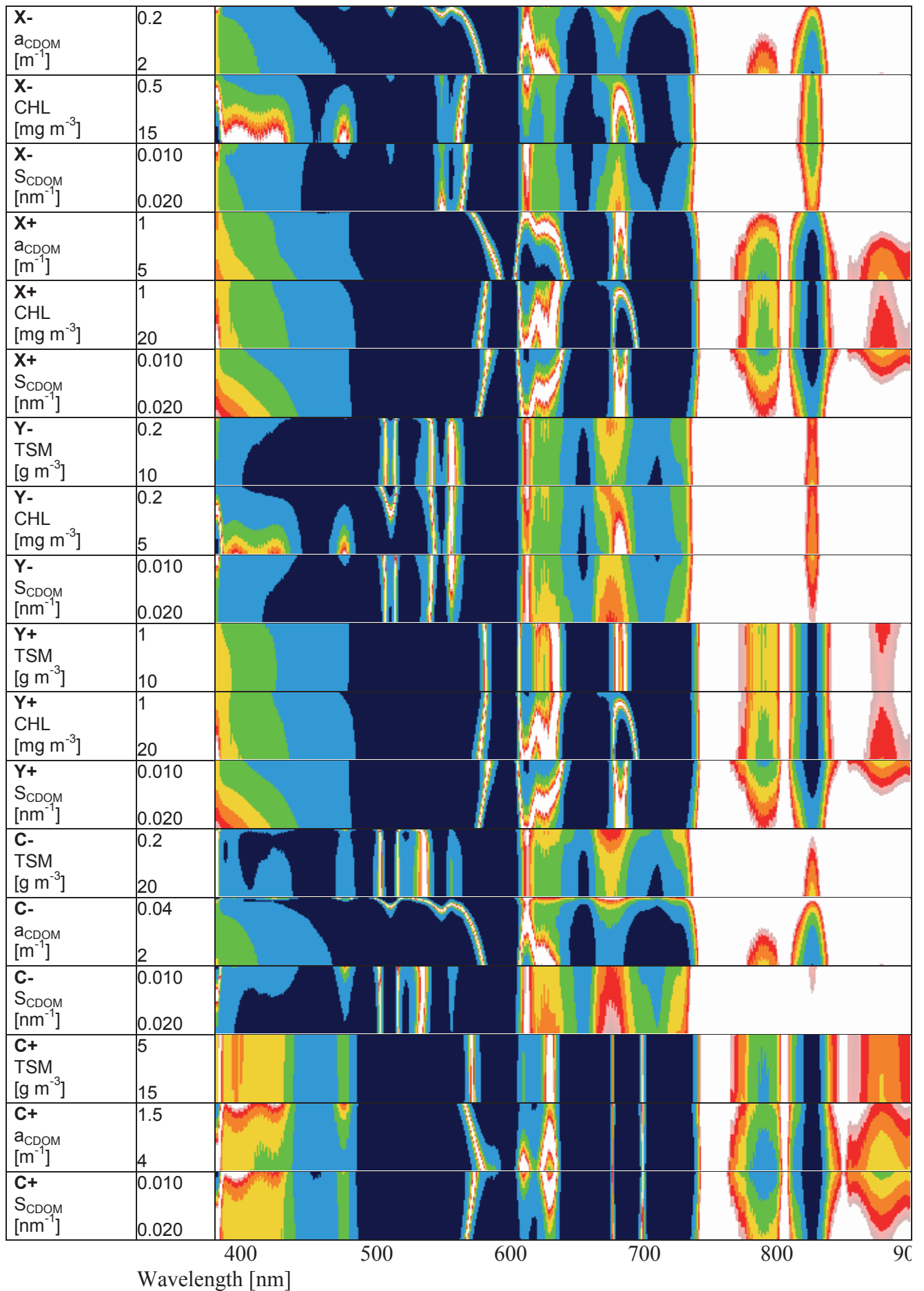
X- a_{CDOM} [m^{-1}]	0.2 — 2	
X- CHL [mg m^{-3}]	0.5 — 15	
X- S_{CDOM} [nm^{-1}]	0.010 — 0.020	
X+ a_{CDOM} [m^{-1}]	1 — 5	
X+ CHL [mg m^{-3}]	1 — 20	
X+ S_{CDOM} [nm^{-1}]	0.010 — 0.020	
Y- TSM [g m^{-3}]	0.2 — 10	
Y- CHL [mg m^{-3}]	0.2 — 5	
Y- S_{CDOM} [nm^{-1}]	0.010 — 0.020	
Y+ TSM [g m^{-3}]	1 — 10	
Y+ CHL [mg m^{-3}]	1 — 20	
Y+ S_{CDOM} [nm^{-1}]	0.010 — 0.020	
C- TSM [g m^{-3}]	0.2 — 20	
C- a_{CDOM} [m^{-1}]	0.04 — 2	
C- S_{CDOM} [nm^{-1}]	0.010 — 0.020	
C+ TSM [g m^{-3}]	5 — 15	
C+ a_{CDOM} [m^{-1}]	1.5 — 4	
C+ S_{CDOM} [nm^{-1}]	0.010 — 0.020	

Wavelength [nm]

400   500   600   700   800   90

Figure 30: Optimal spectral resolution for the standard scenarios of optically deep water.

182

X-- a_{CDOM} [m^{-1}]	0.04 2		
X-- CHL [mg m^{-3}]	0.1 10		
X-- S_{CDOM} [nm^{-1}]	0.010 0.020		
X++ a_{CDOM} [m^{-1}]	0.2 3		
X++ CHL [mg m^{-3}]	1 1000		
X++ S_{CDOM} [nm^{-1}]	0.010 0.020		
Y-- TSM [g m^{-3}]	0.2 20		
Y-- CHL [mg m^{-3}]	0.1 10		
Y-- S_{CDOM} [nm^{-1}]	0.010 0.020		
Y++ TSM [g m^{-3}]	0.5 5		
Y++ CHL [mg m^{-3}]	1 10		
Y++ S_{CDOM} [nm^{-1}]	0.010 0.020		
C-- TSM [g m^{-3}]	0.2 20		
C-- a_{CDOM} [m^{-1}]	0.04 2		
C-- S_{CDOM} [nm^{-1}]	0.010 0.020		
C++ TSM [g m^{-3}]	10 300		
C++ a_{CDOM} [m^{-1}]	0.2 3		
C++ S_{CDOM} [nm^{-1}]	0.010 0.020		

Wavelength [nm]
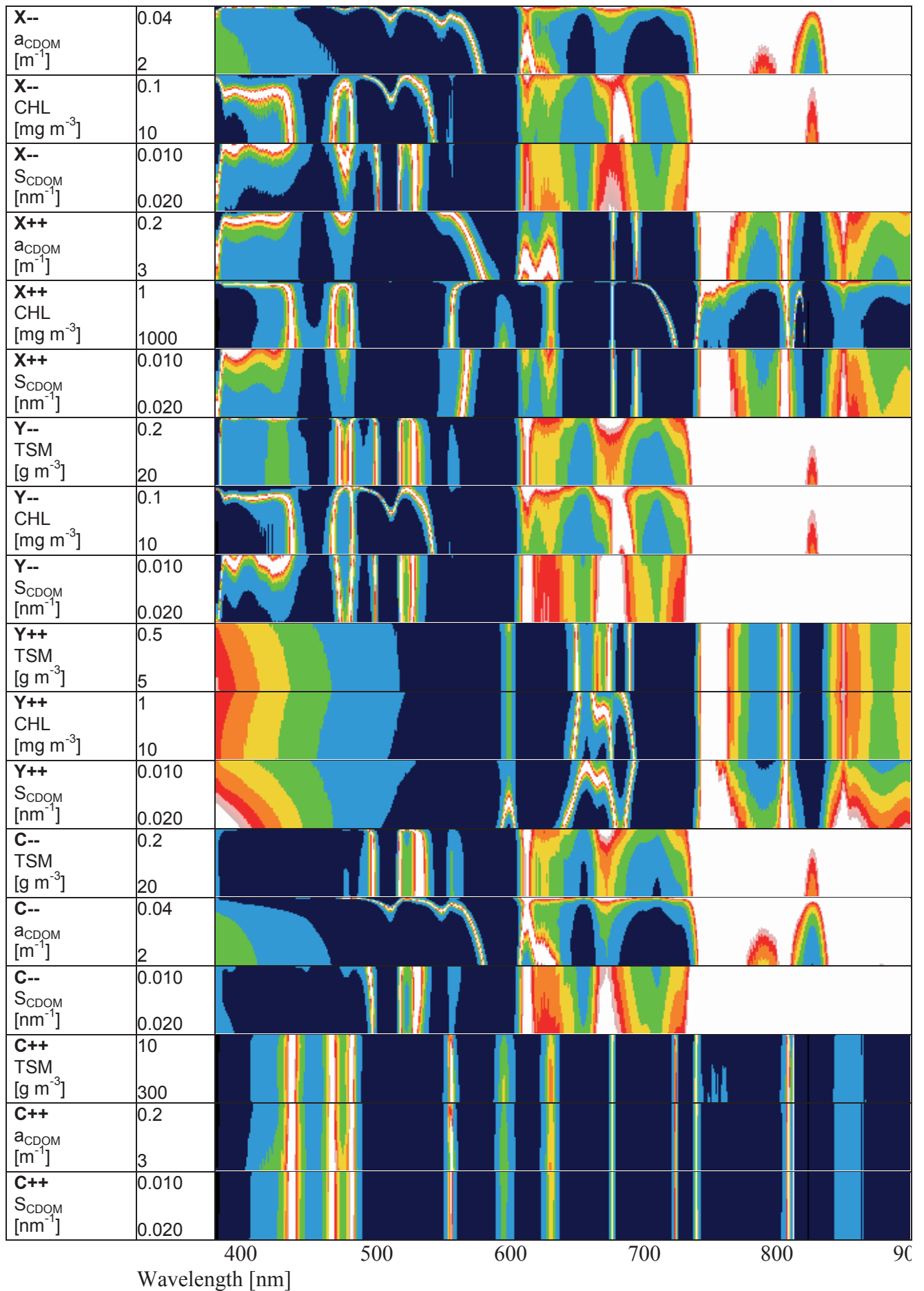
Figure 31: Optimal spectral resolution for the extreme scenarios of optically deep water.

A2.4.2.2 Optically shallow water

The optimal spectral resolution for very shallow water (0 to 0.5 m) is shown in Figure 32, and for shallow water (0 to 10 m) in Figure 33.
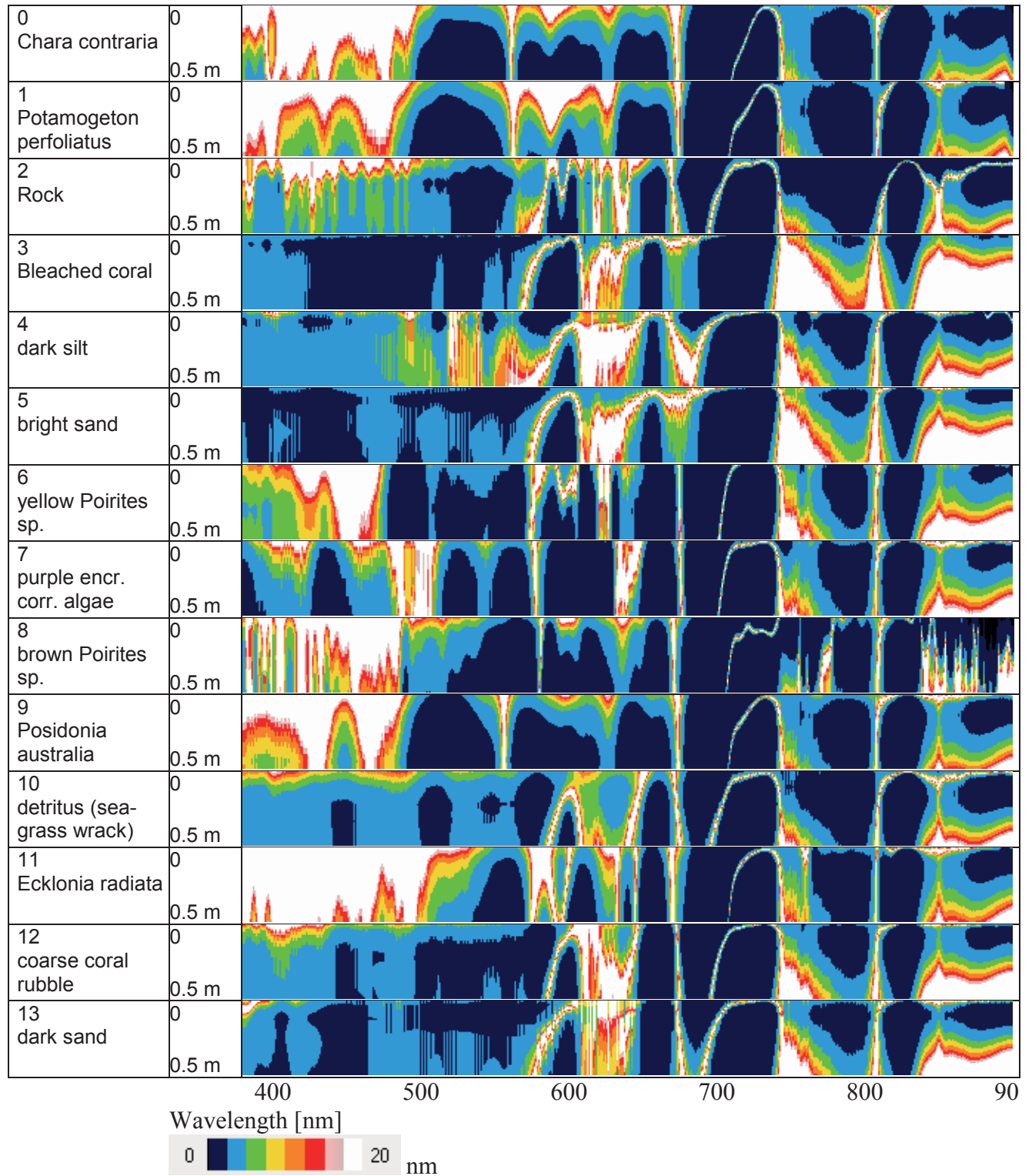
Figure 32: Optimal spectral resolution for very shallow waters of 0.01 – 0.5 m depth.
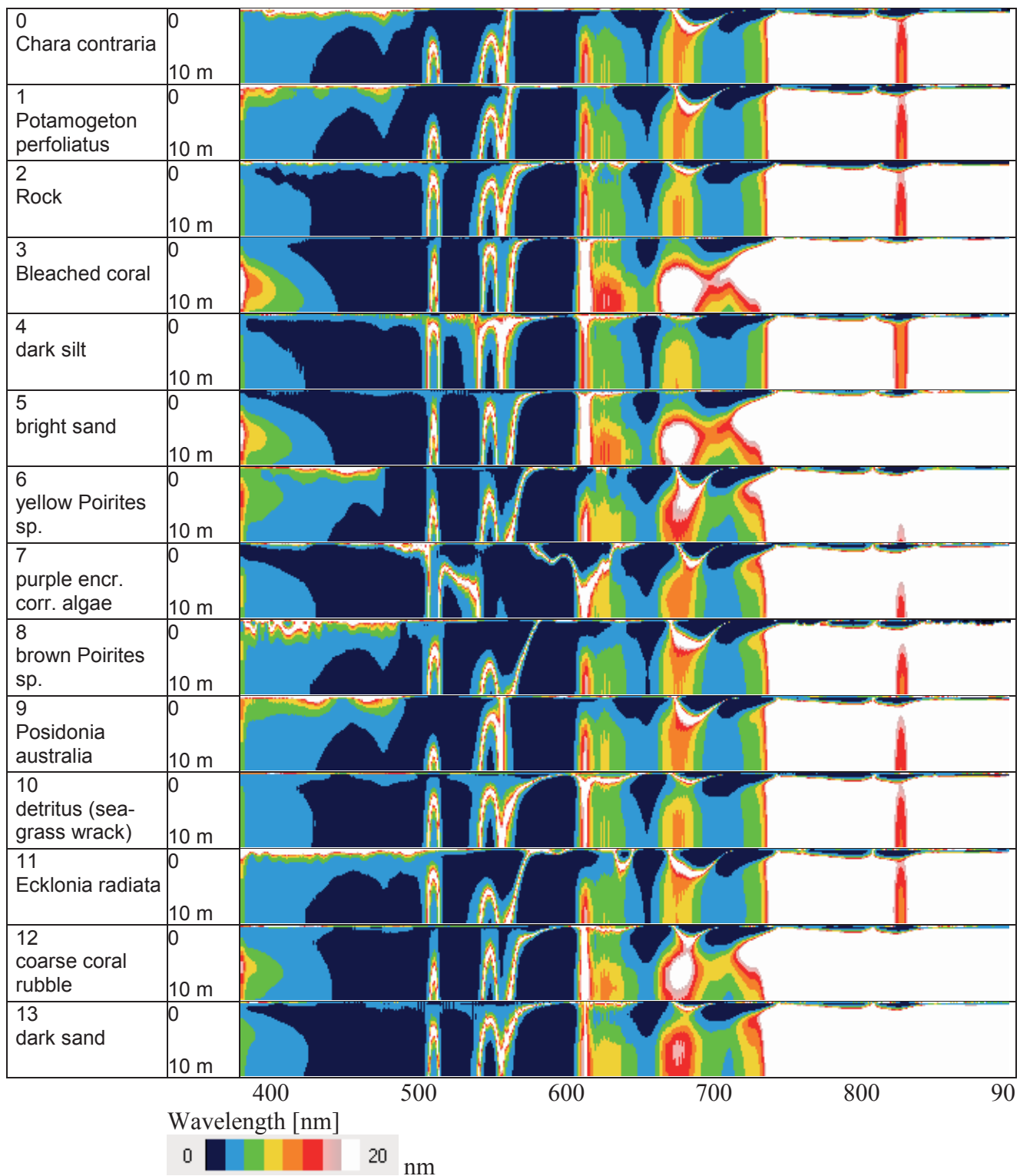
Figure 33: Optimal spectral resolution for shallow waters of 0.01 – 10 m depth.

A2.4.2.3 Recommended spectral resolution

The previous sections show that the optimal spectral resolution depends on the water type. To obtain a sensor recommendation, the resolutions were averaged for all water types of the standard

scenarios (Figure 30), extreme scenarios (Figure 31), very shallow waters from 0.01 to 0.5 m depth (Figure 32) and shallow waters from 0.01 to 10 m depth (Figure 33). The result is shown in Figure 34.
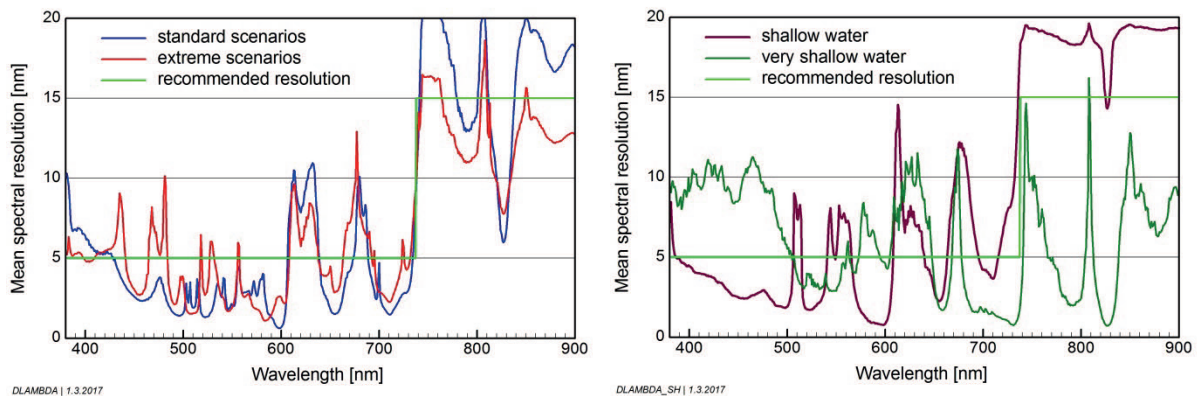
Figure 34: Averages of optimal spectral resolutions. Left: for optically deep water. Right: for optically shallow water.

It can be seen in Figure 34 left that the average of the optimal spectral resolutions of the optically deep water scenarios is in the order of 5 nm from 380 to 737 nm, and around 15 nm above 737 nm (green line). Figure 34 right shows a similar result for shallow waters in the range from 0.01 to 10 m, while for very shallow waters (0.01 to 0.5 m), which are more representative of land surfaces than of water, a resolution of 5 nm is also appropriate in the near infrared.

The strong spectral variations of the averages are caused by the dependencies of the optimum resolution on wavelength and water type. In other words, the spectral properties of the optimal sensor depend on the water type. The green line is a fair compromise for all considered water types and wavelengths. Thus, the recommended spectral resolution of a hyperspectral sensor is 5 nm from 380 to 737 nm, and 15 nm from 737 to 900 nm.

A2.4.3 Radiometric resolution

The optically deep water scenarios are used to derive a recommendation for radiometric resolution since these encompass the dark targets driving the requirement for radiometric sensitivity. Shallow waters are generally much brighter and thus not considered here.

The required radiometric resolution is estimated using two approaches. The first specifies the noise-equivalent remote sensing reflectance $NE\Delta R_{rs,1}$ in terms of 1% of the remote sensing reflectance difference between 400 and 800 nm according to Eq. (5). The results are shown in Figure 35.
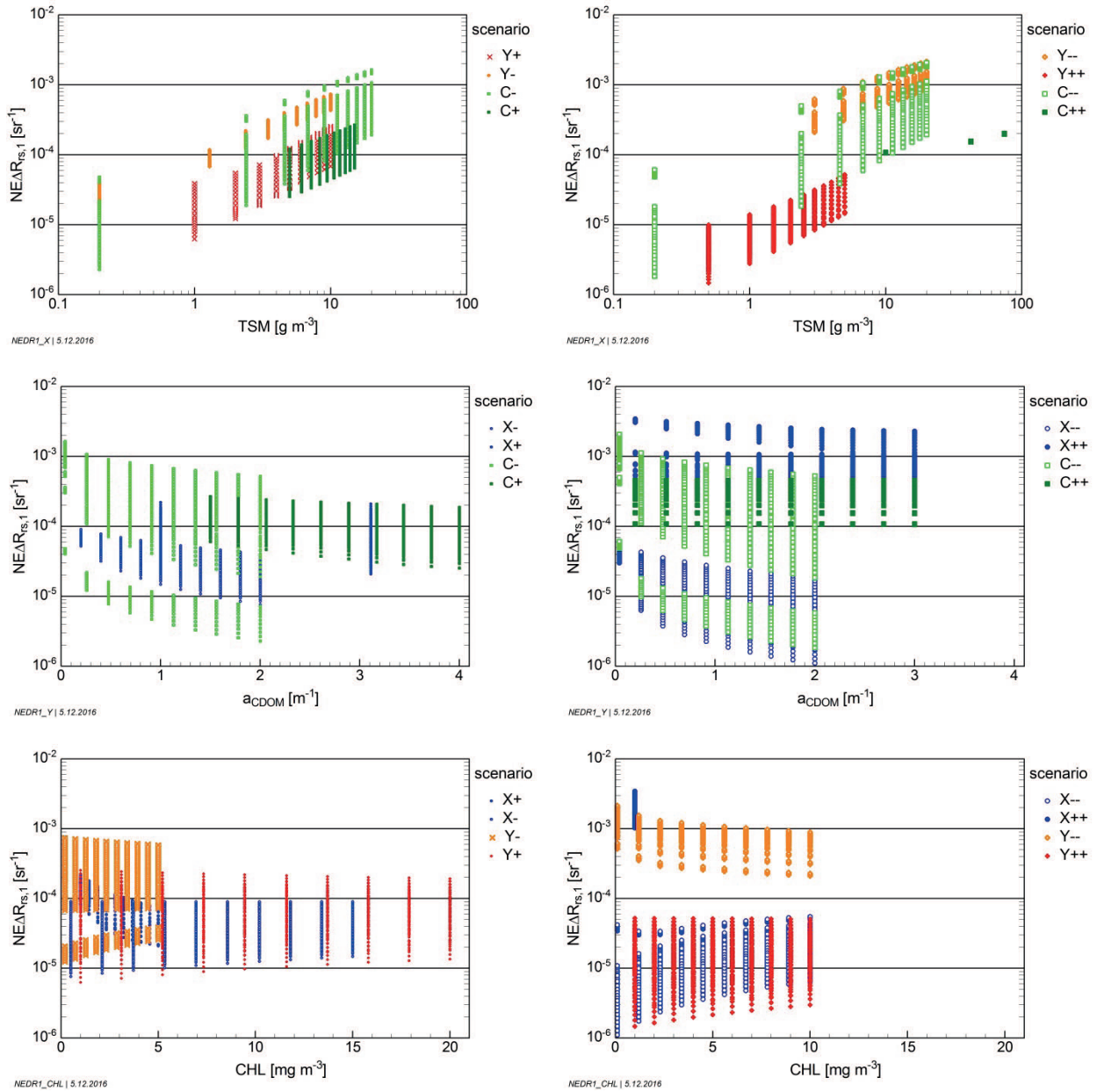
Figure 35: R$_{rs}$ difference corresponding to 1% of the dynamic range of R$_{rs}$. Left column: standard scenarios, right column: extreme scenarios.

Figure 35 summarizes the results for three parameters of interest, i.e. total suspended matter (TSM), colored dissolved organic matter (a$_{CDOM}$) and chlorophyll-a (CHL). In each plot, the parameter of interest was kept constant at the scenario-specific values given in Table 1 and Table 2, and the other parameters of interest and the slope of CDOM absorption (S$_{CDOM}$) were iterated in 10 steps in the ranges given also in Table 1 and Table 2. Thus, for each parameter of interest, 10^3 = 1000 spectra were simulated for each scenario. Applying Eq. (5) resulted in the 24,000 values of NEΔR$_{rs,1}$ of Figure 35.

Figure 35 quantifies the known fact that the required radiometric sensitivity decreases with increasing TSM and decreasing CDOM, and depends not much on CHL. The reflectance spectra of all considered scenarios can be sampled at a radiometric resolution of 1% or better for NEΔR$_{rs}$ = 10^{-6} sr^{-1}, which is technically very demanding. A NEΔR$_{rs}$ of 10^{-5} sr^{-1} is sufficient for most parameter combinations of the standard scenarios, except scenarios Y+ and C- for TSM < 1 g m^{-3}, scenario C- for

$a_{CDOM} > 0.4$ m^{-1}, and scenario X- for $a_{CDOM} > 2$ m^{-1}. The extreme scenarios require more frequently a NEΔR$_{rs}$ between 10^{-5} and 10^{-6} sr^{-1}.

The second approach is given by Eq. (6). It specifies the noise-equivalent remote sensing reflectance NEΔR$_{rs,2}$ as the maximum change of R$_{rs}$ in the wavelength range 400 to 800 nm induced by a 10% change of the parameter of interest. The results are shown in Figure 36 for the standard scenarios and in Figure 37 for the extreme scenarios as a function of the wavelength of maximum sensitivity.
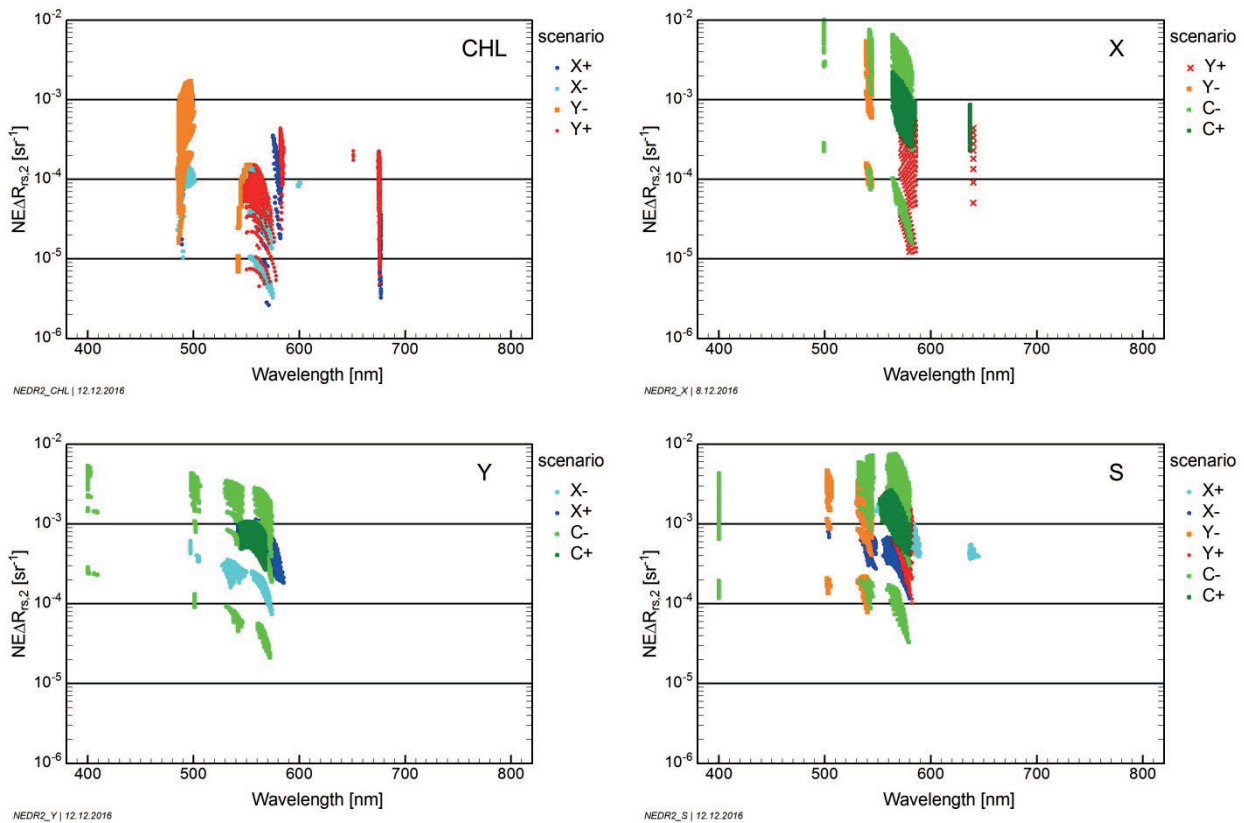
Figure 36: Maximum change of R$_{rs}$ for a 10% change of the parameter indicated top right for the standard scenarios.

Similar as before, each plot summarizes the natural variability within a number of scenarios. CHL, TSM, a_{CDOM} and S_{CDOM} were now treated as parameters of interest. Each of these was iterated for each scenario in 10 steps in the ranges given in Table 1 and Table 2. Simultaneously to the parameter of interest, two other parameters from the set (CHL, TSM, a_{CDOM}, S_{CDOM}) were iterated in 10 steps each in order to capture the variability. For example, the required sensitivity for CHL in scenario X- was calculated by setting TSM = 1 g m^{-3} and iterating CHL from 0.5 to 15 mg m^{-3} in 10 steps, and for each step, iterating a_{CDOM} from 0.2 to 2 m^{-1} and S_{CDOM} from 0.010 to 0.020 nm^{-1}. In this way 36,000 values of NEΔR$_{rs,2}$ were calculated.
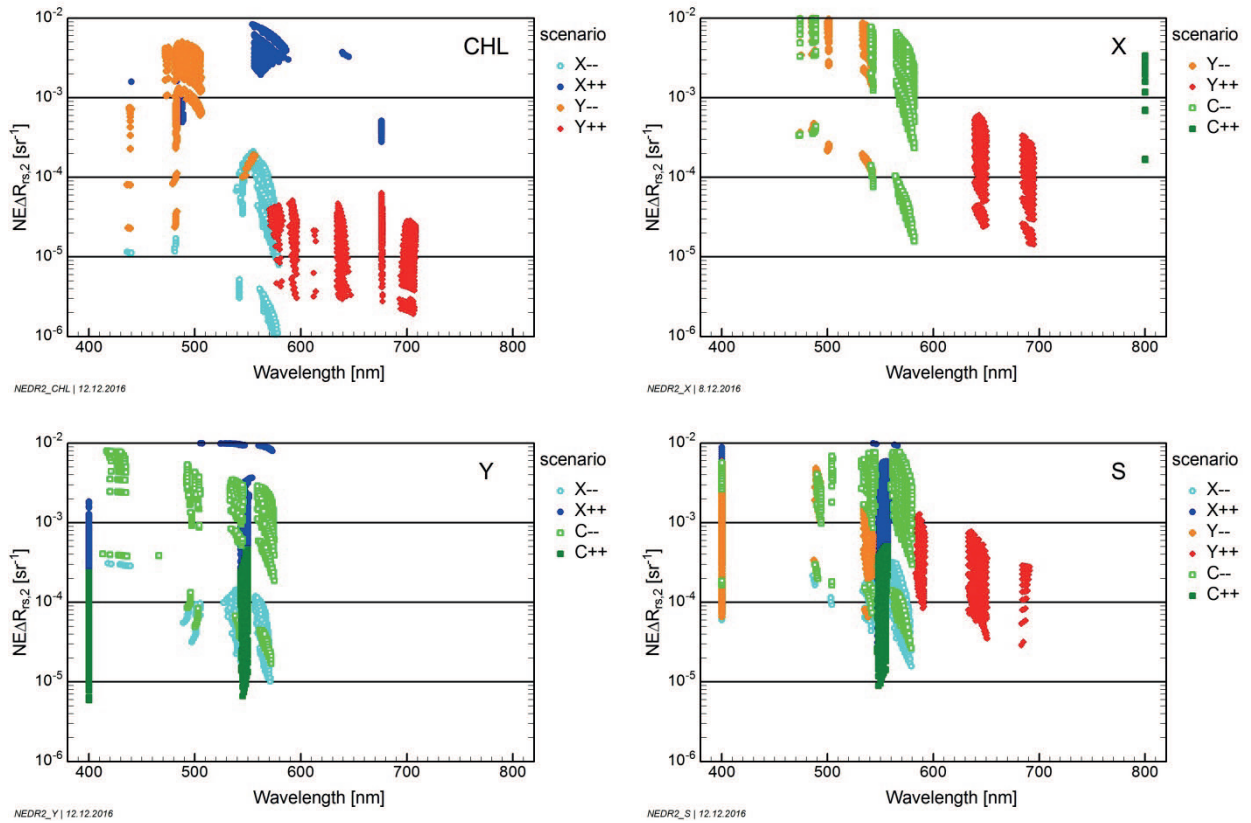
Figure 37: Maximum change of R_rs for a 10% change of the parameter indicated top right for the extreme scenarios.

Figure 36 and Figure 37 show that a $NE\Delta R_{rs}$ of 10^{-5} sr^{-1} is sufficient to resolve 10% changes of TSM, a_{CDOM} and S for all standard scenarios and for the majority of the conditions studied for the extreme scenarios. However, CHL requires $NE\Delta R_{rs}$ down to 3×10^{-6} sr^{-1} for the standard scenarios, and even below 1×10^{-6} sr^{-1} for the extreme scenarios. High sensitivity is particularly required for retrieval of low CHL concentrations in dark waters with low TSM or high CDOM concentration (scenarios X-, X--, Y++). This dependency on CHL concentration is illustrated in Figure 38.
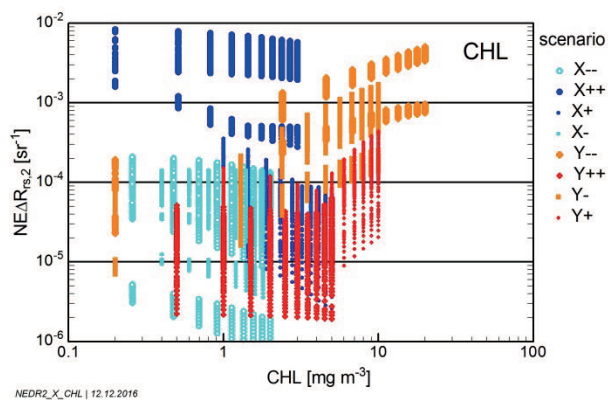
Figure 38: Dependence of $NE\Delta R_{rs,2}$ required to discriminate a 10% change of chlorophyll-a concentration on CHL.

Both approaches lead to the same conclusion that a noise-equivalent remote sensing reflectance of $NE\Delta R_{rs} = 1 \times 10^{-5}$ sr^{-1} should be targeted. It is sufficient for most considered scenarios, except for detection of chlorophyll-a differences in dark waters. The ideal sensor, which is also sensitive to CHL differences under difficult conditions, should be able to resolve a $NE\Delta R_{rs}$ of 1×10^{-6} sr^{-1}.

189

The derived NEΔR$_{rs}$ values are the *maximum* changes of R$_{rs}$ in the range from 400 to 800 nm. These make 10% changes of the considered parameter principally detectable, but this does not necessarily mean that the parameter can be identified and distinguished from other parameters. Figure 36 and Figure 37 show that CHL, TSM, a$_{CDOM}$ and S have no specific spectral region which could be attributed uniquely to one of them, but each can induce strong changes to R$_{rs}$ almost anywhere in the visible. Thus, classification requires in most of the considered water types spectral information from other wavelengths with less pronounced R$_{rs}$ changes, i.e. the radiometric resolution must be even higher for quantitative data analysis.

A2.4.4 Radiometric sensor requirements

The TOA radiance spectra with the lowest and highest intensities are of particular interest for sensor design. These are shown Figure 39. The spectra are presented in two spectral resolutions: 5 cm^{-1} and resampled to a full width at half maximum (FWHM) of 5 nm.
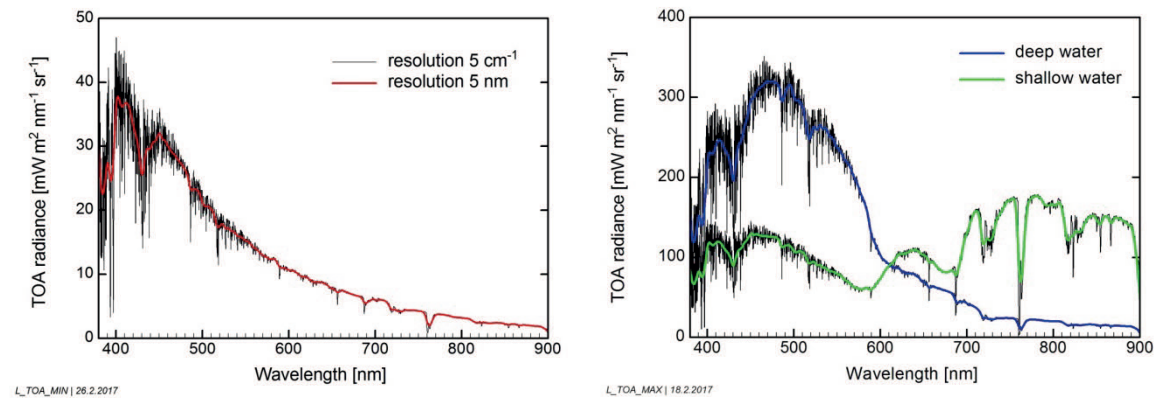

Figure 39: Darkest (left) and brightest (right) radiance spectra at top of atmosphere

As shown in section 4.3, most challenging for remote sensing are dark waters with low concentration of TSM or high concentration of CDOM. In order to derive radiometric sensor requirements, top of atmosphere (TOA) simulations were made for these critical water types as described in section 3.4.

Figure 40 shows as example the TOA simulations for the darkest (no. 7 of Table 3) and brightest R$_{rs}$ spectra (no. 19). Compared to the large differences of R_{rs}, the L^{TOA} spectra do not differ much, demonstrating that TOA radiance is dominated by the atmosphere, while the water leaving radiance contributes only little to the signal at the satellite.
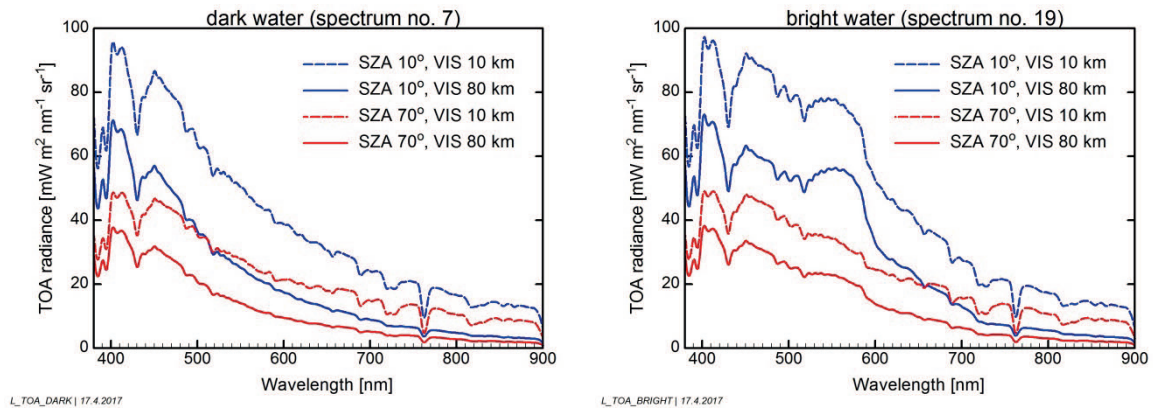
Figure 40: At-sensor radiances for the darkest and brightest spectra of Table 3 for different combinations of sun zenith angle (SZA) and visibility (VIS).

To investigate the changes of L^{TOA} induced by ecologically relevant concentration differences in dark waters, the R_{rs} differences induced by 10% changes of chlorophyll-a (Figure 14) were converted to radiance differences, $\Delta L^{TOA}(\lambda)$, using Modtran-5. Two examples are shown in Figure 41.
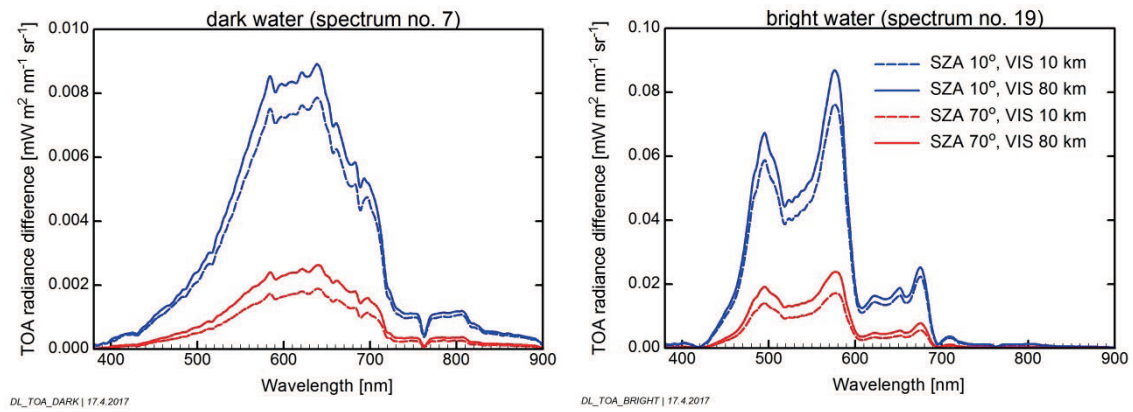

Figure 41: At-sensor radiance differences for 10% changes of chlorophyll-a concentration.

The comparison of Figure 40 with Figure 41 shows that ΔL^{TOA} is around 4 orders of magnitude lower than L^{TOA}. Examples of their ratio are shown in Figure 42.
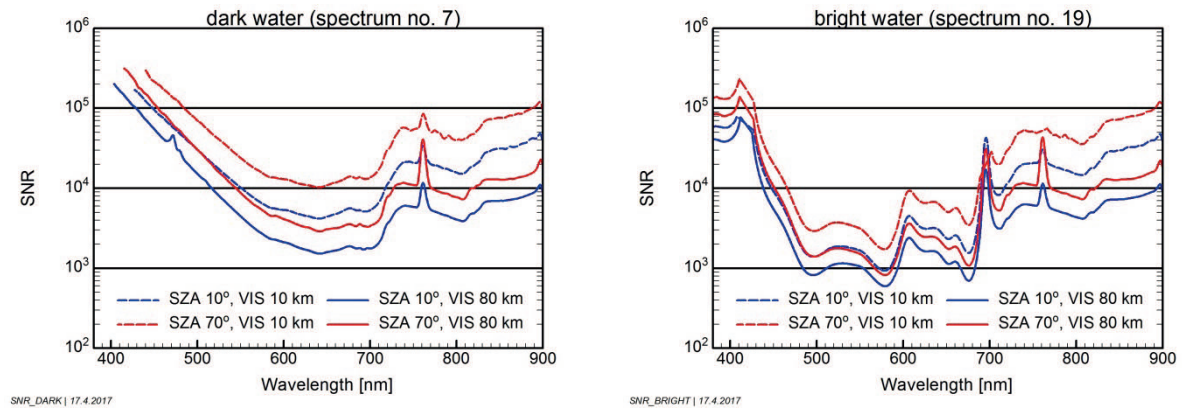

Figure 42: SNR required to detect 10% changes of chlorophyll-a concentration.

The ratios $\frac{L^{TOA}(\lambda)}{\Delta L^{TOA}(\lambda)}$ are strongly dependent on wavelength. Their minima define the minimum sensor requirements according to Equation (8), and the wavelengths of the minima (λ_m) specify the spectral regions of maximum sensitivity of L^{TOA}. Figure 43 shows these minima for the considered water types, atmospheric conditions and sun zenith angles.
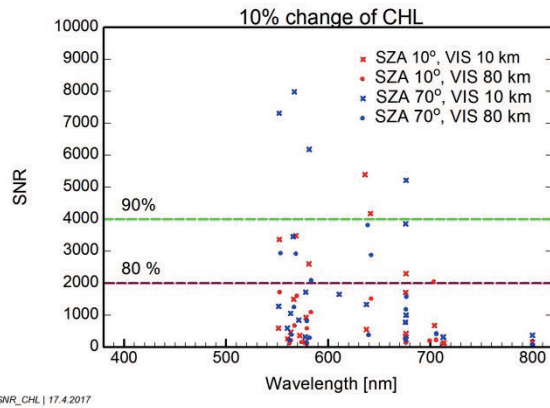

Figure 43: Minimum SNR required to detect 10% changes of CHL. One value is outside the shown SNR range (SNR 12,192 for SZA 70°, VIS 10 km). The dashed horizontal lines show the SNRs that cover more than 80% (red) and more than 90% of the studied cases (green).

The most sensitive wavelengths λ_m are in the yellow-red spectral region between 550 and 715 nm. They are not in the blue-green as for the open ocean since the water types chosen for the simulations are dominated by CDOM, which absorbs strongly at short wavelengths.

A SNR statistics is presented in Table 7. It can be concluded that a SNR of at least 2000:1 from 550 to 715 nm should be targeted. It produces, for more than 80% of the studied cases, a detectable signal at top of atmosphere. To cover more than 90% of the cases, a SNR of 4000:1 is required. A low sun elevation (70° SZA) in combination with a turbid atmosphere (10 km VIS) constitutes most of the critical cases.

Table 7: SNR statistics specifying the relative number of cases in which 10% changes of chlorophyll-a produce a detectable signal at top of atmosphere.

SNR	cases [%]
10,000	98.1
4,000	92.6
3,000	88.0
2,000	81.5
1,500	74.1
1,000	67.6

It should be noted that the SNR is frequently used in a misleading and confusing way. Since the SNR depends on the signal and the measurement noise, it specifies the quality of a measurement, but not of a sensor. Confusion is caused by the fact that it is common practice to use the SNR for comparing

192

or specifying optical sensors, even though no common definition of the underlying signal exists. To mention a few, the saturating signal is sometimes taken, sometimes a 30% or 5% bottom albedo in combination with a certain sun zenith angle and atmosphere condition, and sometimes a given TOA radiance spectrum. This inconsistent usage of SNR makes the comparison of sensors difficult (see Hu et al., 2012 for a method to compare sensors with varying SNR definitions).

A suitable parameter for comparing or specifying the radiometric sensitivity of sensors is the noise-equivalent radiance difference, $NE\Delta L$, which is a sensor property. It can be compared directly with observed or expected radiance differences ΔL at top of atmosphere. Such a comparison is shown in Figure 44 for the TOA simulations and the sensor MERIS.
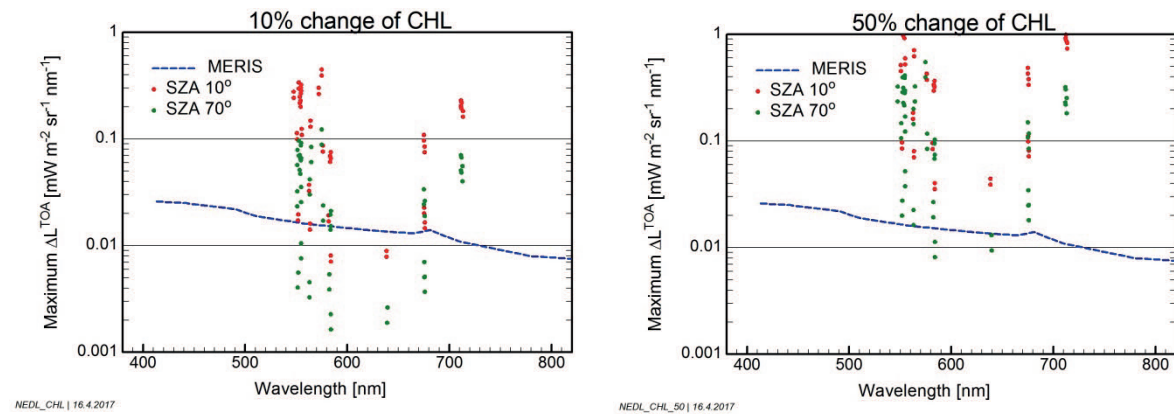

Figure 44: Maximum radiance differences induced at top of atmosphere by 10% changes of CHL (left) and by 50% changes of CHL (right). The noise-equivalent radiance difference of MERIS is shown for comparison.

Low sun elevation produces lower radiance differences than high sun elevation. A ΔL statistic is presented in Table 8. 10% changes of CHL produce, in more than 80% of the studied cases, radiance differences above 0.010 mW m^{-2} sr^{-1} nm^{-1} at top of atmosphere, and in more than 90% the induced radiance changes are above 0.005 mW m^{-2} sr^{-1} nm^{-1}. The radiance changes are proportional to the CHL changes, thus a sensitivity of 0.010 mW m^{-2} sr^{-1} nm^{-1} is almost always (98.1% of the cases) sufficient to detect 50% changes of CHL. Table 8 thus leads to the recommendation that the sensor should be able to resolve radiance differences NEΔL of at least 0.010 mW m^{-2} sr^{-1} nm^{-1} in the range from 550 to 715 nm.

Table 8: Statistics specifying the relative number of scenarios (# in %) in which certain changes of chlorophyll-a produce a radiance difference larger than ΔL at top of atmosphere. Note that the number of scenarios cannot be related to numbers or areas of the lakes on Earth.

CHL change	10%	20%	30%	40%	50%
ΔL [mW m^{-2} sr^{-1} nm^{-1}]	#	#	#	#	#
0.005	91.7	97.2	100	100	100
0.010	82.4	91.7	95.4	97.2	98.1
0.015	78.7	86.1	91.7	94.4	96.3
0.020	69.4	82.4	88.0	90.7	92.6

It should be noted that such sensitivity is required for the sensor reacting to CHL induced differences, but this does not imply that data analysis is able to detect or quantify the CHL changes. Data analysis is always difficult close to the sensitivity limit of a measurement device, thus a significantly higher sensitivity may be desirable from the perspective of measurement interpretation. Specifying a methodologic sensitivity add-on is however difficult since it depends on the inversion algorithms, which are numerous.

A2.5. References

Albert, A. and Mobley, C. D. (2003) An analytical model for subsurface irradiance and remote sensing reflectance in deep and shallow case-2 waters, Opt. Express 11, pp: 2873-2890.

Albert, A. (2004) Inversion technique for optical remote sensing in shallow water. Ph.D. Dissertation, Universität Hamburg, Hamburg, Germany, 188 pp.

Antoine, D., Siegel, D. A., Kostadinov, T., Maritorena, S., Nelson, N.B., Gentili, B., Vellucci, V. and Guillocheau, N. (2011) Variability in optical particle backscattering in three contrasting bio-optical oceanic regimes. Limnol. Oceanogr. 56(3), pp: 955-973.

Babin, M., Morel, A., Fournier-Sicre, V., Fell, F. and Stramski, D. (2003a) Light scattering properties of marine particles in coastal and open ocean waters as related to the particle mass concentration. Limnol. Oceanogr. 48, pp: 843-859.

Babin, M., Stramski, D., Ferrari, G. M., Claustre, H., Bricaud, A., Obolensky, G., et al., (2003b) Variations in the light absorption coefficients of phytoplankton, nonalgal particles, and dissolved organic matter in coastal waters around Europe, J. Geophys. Res., 108, C7.

Berk, A. and coauthors, (2005) MODTRAN5: A reformulated atmospheric band model with auxiliary species and practical multiple scattering options. Multispectral and Hyperspectral Remote Sensing Instruments and Applications II, A. M. Larar, M. Suzuki, and Q. Tong, Eds., International Society for Optical Engineering (SPIE Proceedings, Vol. 5655.) doi: /10.1117/12.578758.

Botha, E.J., Brando, V.E., Anstee, J.M., Dekker, A.G. and Sagar, S. (2013) Increased spectral resolution enhances coral detection under varying water conditions. Remote Sens. Environ. 131, pp:247-261.

Chami, M., Shybanov, E. B., Churilova, T. Y., Khomenko, G. A., Lee, M. E.-G., Martynov, O. V., Berseneva, G. A. and Korotaev, G. K. (2005) Optical properties of the particles in the Crimea coastal waters (Black Sea). J. Geophys. Res. 110, C11020.

Gege, P. (2004) The water colour simulator WASI: An integrating software tool for analysis and simulation of optical in-situ spectra. Comput. Geosci. 30, pp: 523-532.

Gege, P.and Albert, A. (2006) A tool for inverse modeling of spectral measurements in deep and shallow waters. In: L.L. Richardson and E.F. LeDrew (Eds): "Remote Sensing of Aquatic Coastal Ecosystem Processes: Science and Management Applications", Kluwer book series: Remote Sensing and Digital Image Processing, Springer, ISBN 1-4020-3967-0, pp: 81-109.

Gege, P. (2017) Radiative transfer theory for inland waters. In: Mishra D.R., Ogashawara I. and Gitelson., A.A. (Eds.), Bio-Optical Modelling and Remote Sensing of Inland Waters, Elsevier, ISBN 9780128046449, 332 pp.

D'Sa, E.J., Miller, R. L. and Del Castillo, C. (2006) Bio-optical properties and ocean color algorithms for coastal waters influenced by the Mississippi River during a cold front. Appl. Opt. 45, pp: 7410-7428.

Heege, T. (2000) Flugzeuggestützte Fernerkundung von Wasserinhaltsstoffen am Bodensee. PhD thesis. DLR-Forschungsbericht 2000-40, 134 pp.

IOCCG (2012) Mission Requirements for Future Ocean-Colour Sensors. McClain, C. R. and Meister, G. (eds.), Reports of the International Ocean-Colour Coordinating Group,No. 13, IOCCG, Dartmouth, Canada.

Lee, Z.-P., Carder, K. L., Mobley, C. D., Steward, R. G. and Patch J. S. (1998) Hyperspectral remote sensing for shallow waters: 1. A semi-analytical model. Appl. Opt. 37, pp: 6329-6338.

Lee, Z.-P., Carder, K. L., Mobley, C. D., Steward, R. G. and Patch, J. S., (1999) Hyperspectral remote sensing for shallow waters: 2. Deriving bottom depths and water properties by optimization. Appl. Opt. 38, pp: 3831-3843.

Peters, S., Hommersom, A., Alikas, K., Latt, S., Reinart, A. , Giardino, C. , Bresciani, M., Philipson, P., Ruescas, A. , Stelzer, K., Schenk, K. , Heege, T. ,Gege, P., Koponen, S. , Kallio K., and Zhang Y. (2015) Global Lakes Sentinel Services: Water quality parameters retrieval in lakes using the MERIS and S3-OLCI band sets. SENTINEL-3 for Science Workshop, 2-5 June 2015, Venice, Italy.

Ylöstalo, P. ,Kallio K. and Seppälä J. (2014) Absorption properties of in-water constituents and their variation among various lake types in the boreal region. Remote Sens. Environ. 148, pp: 190–205.